Tina Treude

Anaerobic oxidation of methane in marine sediments

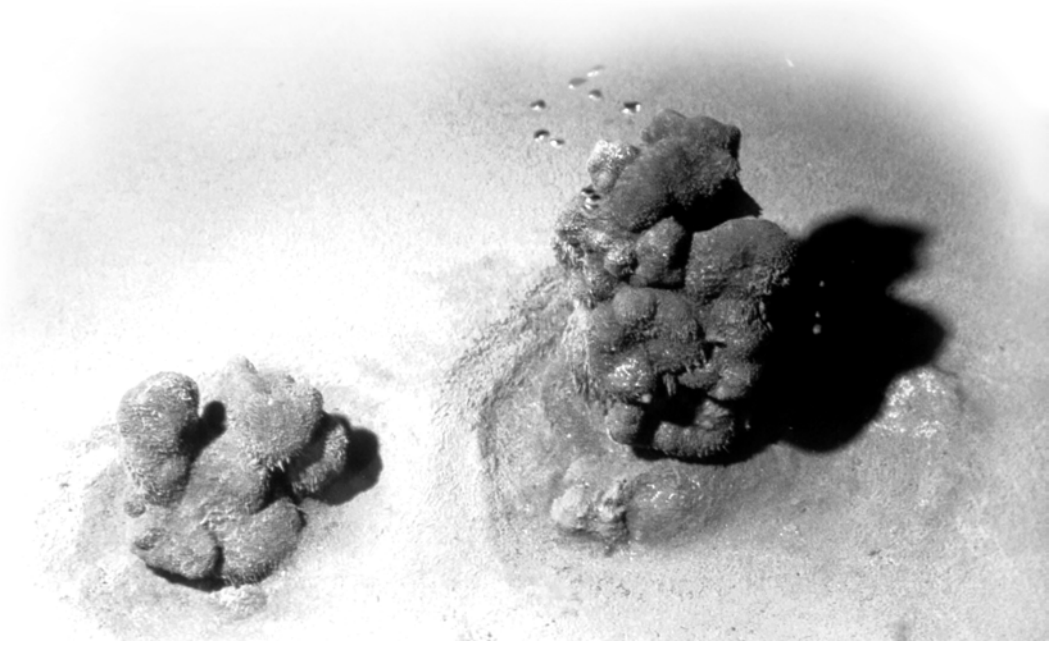

Anaerobic oxidation of methane in marine sediments

Dissertation

zur Erlangung des Doktorgrades
der Naturwissenschaften

-Dr. rer. nat.-

dem Fachbereich Biologie/Chemie der

Universität Bremen vorgelegt von

Tina Treude

Bremen
Dezember 2003

Die vorliegende Arbeit wurde in der Zeit vom Juli 2000 bis Dezember 2003 am Max-Planck-Institut für Marine Mikrobiologie in Bremen angefertigt.

1. Gutachterin: Prof. Dr. Antje Boetius
2. Gutachter: Prof. Dr. Bo Barker Jørgensen

Weitere Prüfer:
Prof. Dr. Gunter Kirst
Dr. Martin Krüger

Tag des Promotionskolloquiums: 23. Januar 2004

Imagination is more important than knowledge

—Albert Einstein

Diese Arbeit widme ich meinen Großeltern,
Hanna und Richard Treude,
die beide das Ende meiner Doktorarbeit
nicht mehr miterleben konnten.
Ich denke an Euch, wo immer ihr seid.

Zusammenfassung

Die anaerobe Oxidation von Methan (AOM) ist ein mikrobieller Prozess in anoxischen marinen Sedimenten, bei dem im Gegensatz zur aeroben Methanoxidation Sulfat zur Oxidation des Methans verwendet wird. AOM wird nach heutigen Kenntnissen von einem mikrobiellen Konsortium aus methanotrophen Archaea und sulfatreduzierenden Bakterien durchgeführt. Untersuchungen der letzten 20 Jahre zeigen, dass AOM einen Austritt von Methan aus dem Meeresboden in die Wassersäule fast vollständig verhindert, und dieser Prozess damit für die geringe Methanemission der Ozeane verantwortlich sein könnte. Die Umsetzung von Methan mit Sulfat ist erst vor weniger als 30 Jahren entdeckt worden und ist bis heute nicht vollständig erklärt. Weltweit existieren nur relativ wenige Messungen von AOM in marinen Sedimenten. In der vorliegenden Arbeit wurde das Vorkommen und die Bedeutung von AOM in marinen Habitaten mit unterschiedlichen Methanflüssen untersucht. Zum anderen wurde die Steuerung von AOM in Sedimenten und mikrobiellen Matten ausgewählter Habitate durch verschiedene Umweltfaktoren untersucht. Die Untersuchungen zeigten Folgendes:

1. Am Hydratrücken vor Oregon, wo fossile Gase aufsteigen und Gashydrate sich im Oberflächensediment zersetzen, wurden einige der höchsten jemals gemessenen Umsatzraten von Methan (maximal 5 μmol cm^{-3} d^{-1}) festgestellt. AOM und Sulfatreduktion zeigen ein Verhältnis von ca. 1:1. Die Oberflächen der Sedimente sind durch chemoautotrophe Bakterien und Muscheln besiedelt, welche das aus der AOM entstehende Sulfid als Energiequelle nutzen. Peripher zu diesen advektiven Stellen sind AOM Raten stark reduziert und kaum nachweisbar. Die AOM-Messungen am Hydratrücken zeigten, dass selbst bei höchsten Methanflüssen von ca. 200 mmol m^{-2} d^{-1} zwischen 50 und 90% des aufsteigenden Methans konsumiert wird, bevor es in die Wassersäule gelangt. Insgesamt zeichnet sich AOM in den Oberflächensedimenten des Hydratrückens durch eine extrem hohe Heterogenität aus, welche vermutlich durch ungleichmäßig aufsteigende Gase und Fluide, Carbonatausfällungen und Bioturbation hervorgerufen wird.
2. Die Sedimente der Eckernförder Bucht sind reich an Methan auf Grund hoher Raten rezenter Methanbildung im Organik-reichen Meeresboden. Die Methankonzentration übersteigt die Sättigungsgrenze von 6–7 mM, wodurch es zum Aufsteigen von Gasblasen kommt. Es konnte gezeigt werden, dass AOM in den oberen 20 cm des Sedimentes jahreszeitlichen Veränderungen unterworfen ist, welche durch die

Eindringtiefe von Sauerstoff und Sulfat, der Produktionszone von Methan sowie der Temperatur bedingt sind. Im Spätsommer/Herbst reicht die Zone erhöhter AOM-Aktivität bis zur Sediment-Wasser Grenze, während sie im Winter in die Tiefe verschoben wird. Neben jahreszeitlichen Einflüssen wurden auch kurzzeitige Veränderungen in der Zonierung von AOM beobachtet, welche vermutlich im Zusammenhang mit aufsteigenden Gasblasen stehen. In der Eckernförder Bucht wird die Emission von Methan in die Wassersäule effektiv durch AOM verhindert. Einzig durch das Austreten von Gasblasen kann Methan der mikrobiellen Umsetzung entkommen. Die in der Eckernförder Bucht für AOM verantwortlichen Mikroorganismen gehören wahrscheinlich zur ANME-2 Gruppe der Archaea und bilden Aggregate ohne direkt assoziierten bakteriellen Partner.

3. Das Auftriebsgebiet vor der peruanisch-chilenischen Küste wird als die produktivste marine Region der Welt angesehen. An drei untersuchten Stationen entlang des chilenischen Kontinentalhanges (Wassertiefen 800 – 3000 m) konnte gezeigt werden, dass Methan in Sedimenttiefen von 110 bis 360 cm vollständig durch AOM gezehrt wird. Alle drei Stationen zeichnen sich durch einen rein diffusiven Charakter aus, d.h. Methan wird nur durch molekulare Diffusion und nicht durch advektive Prozesse transportiert. An einer der Stationen wurde die Ausbildung von authigenen Karbonaten mit niedrigen δ^{13}C-Werten (–14.6 ‰ VPDB) in der AOM Zone nachgewiesen. Letzteres ist ein Hinweis auf Methan als Quelle für den Kohlenstoff in den Karbonaten.
4. In der anoxischen Zone des Schwarzen Meeres wurden von methanotrophen Mikroben gebildete Riffe untersucht. Diese Riffe befinden sich direkt über Methanquellen und erreichen eine Höhe von bis zu 4 m und einen Durchmesser von ca. 1 m. Sie sind im Inneren stabilisiert durch poröse Karbonatausfällungen und tragen außen eine bis zu mehreren Zentimetern dicke Matte aus anaeroben methanotrophen Mikroorganismen. Es wurde nachgewiesen, dass sich diese Organismen von dem ausströmenden Methan ernähren. Unter anderem wurde mittels Zusatz radioaktiver Substrate gezeigt, dass die Mikroben Methan und Sulfat in einem Verhältnis von 1:1 umsetzen und der aus dem Methan stammende Kohlenstoff sowohl in Biomasse wie auch in Karbonate eingelagert wird. Das methanotrophe Konsortium setzt sich aus der Archaea Gruppe ANME-1 und der sulfatreduzierenden bakteriellen Gruppe *Desulfococcus/ Desulfosarcina* zusammen. Diese Untersuchungen zeigen, dass AOM-Organismen enorme Biomassen aufbauen können.

5. Weitere Untersuchungen an den methanotrophen Riffen des Schwarzen Meeres zeigten, dass neben AOM auch Methanogenese, basierend auf CO_2-Reduktion, in der mikrobiellen Matte von Bedeutung ist. Methanogenese-Raten erreichen in der Matte die Größenordnung von AOM und beide Prozesse scheinen gekoppelt zu sein, wobei die Art der Kopplung nicht geklärt werden konnte. Es wird vermutet, dass die methanotrophe ANME-1 Gruppe in der Lage ist, sowohl AOM wie auch Methanogenese durchzuführen. Des weiteren lassen Experimente mit radioaktiven Substraten vermuten, dass CO_2-Fixierung einen wichtigen Weg der Kohlenstoffassimilation von ANME-1 darstellt. Eine Kombination zwischen Beta-Imaging von assimiliertem ^{14}C aus Methan und Fluoreszenz-in situ-Hybridisierung (FISH) an Mattenschnitten zeigte, dass methanotrophe Aktivität und ANME-1-Biomasse hauptsächlich in einer schmalen Zone nahe der Mattenoberfläche lokalisiert sind. Oberhalb und unterhalb dieser Zone konnten verschiedene sulfatreduzierende Bakterien identifiziert werden, deren Rolle noch unklar ist. Der Nachweis von AOM in einer mikrobiellen Matte im Sediment weist darauf hin, dass die Entwicklung der Riffe im Sediment beginnen könnte.
6. Aktuelle Fragen zur AOM-Physiologie sind auch die Verwendung alternativer Elektronenakzeptoren sowie der mögliche Austausch von Elektronen zwischen den syntrophen Partnern. In $^{14}CH_4$-Inkubationen mit Sedimenten vom Hydratrücken konnte keine AOM-Aktivität mit alternativen Elektronenakzeptoren (u.a. Nitrat, Mn^{4+}, Fe^{3+}) nachgewiesen werden. $^{14}CH_4$-Inkubationen mit Elektronen-bindenden Substanzen zeigten keinen positiven Effekt auf den Methanumsatz.

Der Vergleich verschiedener Habitate zeigt, dass AOM ein in den marinen Sedimenten weltweit verbreiteter Prozess ist, der in rein diffusiven Systemen zu einer vollständigen Rückhaltung des Methans im Meeresboden führt. Als Quelle für eine Methanemission aus dem Ozean sind daher eher Systeme mit advektiven Transportmechanismen, vor allem aufsteigende Gasblasen, zu vermuten. Wichtige Steuerungsmechanismen für den anaeroben Umsatz von Methan im Meeresboden sind: (1) der Methan- und Sulfatfluss, (2) die daran gekoppelte Größe der AOM-Gemeinschaft, (3) die Methansättigungskonzentration, vornehmlich bedingt durch den hydrostatischen Druck, (4) die Entfernung der AOM-Produkte H_2S und CO_2.

Abstract

Anaerobic oxidation of methane (AOM) is a microbial process in anoxic marine sediments. Unlike aerobic oxidation of methane, sulfate is used as electron acceptor. The current hypothesis is that AOM is mediated by a microbial consortium of methanotrophic archaea and sulfate-reducing bacteria. Research over the past 20 years has shown that AOM retains most of the methane in the sediment. AOM is thus most likely responsible for the low methane emission from the oceans, despite high methane production rates in marine sediments. The oxidation of methane via sulfate was discovered 30 years ago, but its biochemistry is still not well understood. Only few data on AOM in marine sediments are available. In this study, the distribution and relevance of AOM in marine habitats with different methane fluxes was investigated. Selected sediments and microbial mats were investigated to explain some of the factors regulating AOM in the environment. Investigations showed the following:

1. Hydrate Ridge, off Oregon, USA, where fossil gases rise and gas hydrates dissociate in the surface sediment, has some of the highest AOM rates (max. 5 μmol cm^{-3} d^{-1}) ever measured in marine sediments. AOM and sulfate reduction have a ratio of approx. 1:1. The surface sediments at theses fluid impacted sites are covered by chemoautotrophic bacteria and clams, which use sulfide, a product of AOM, as energy source. At the periphery of theses sites, AOM is strongly reduced and hardly detectable. AOM measurements at Hydrate Ridge demonstrated that even at highest methane fluxes of approx. 200 mmol m^{-2} d^{-1}, between 50 and 90% of the rising methane is consumed by AOM before it reaches the sediment-water interface. AOM in the surface sediments of Hydrate Ridge is characterized by high heterogeneity, probably due to transient gas injection, carbonate precipitation, and bioturbation.
2. The sediments of Eckernförde Bay are characterized by high methane concentrations due to in situ methane production in the organic-rich sediment. Methane concentrations exceed the saturation level of 6–7 mM, thereby leading to the rise of gas bubbles. We were able to demonstrate that AOM of the upper 20 cm is subject to seasonal changes caused by the penetration depth of oxygen and sulfate, the depth of methane production, as well as temperature. In late summer/early autumn the AOM zone reaches the sediment-water interface, whereas during winter it takes place deeper in the sediment. In addition to seasonal variations, short-term changes occur in the distribution of AOM, most likely associated with rising gas bubbles. AOM in the sediments of Eckernförde Bay effectively inhibits the emission of methane into the

hydrosphere. Only gas bubbles enable methane to escape from microbial turnover in the sediment. The organisms that mediate AOM in Eckernförde Bay apparently belong to the archaeal ANME-2 cluster and form aggregates without a bacterial partner.

3. The upwelling system off the Peruvian/Chilean coast is considered to be the most productive marine region. We demonstrated in investigations at three sites along the Chilean continental margin (water depth 800 – 3000 m) that methane is completely depleted by AOM in sediment depths between 110 and 360 cm. All stations had a diffusive character, i.e. the only mechanism of methane transport was molecular diffusion. We also found that authigenic carbonates with low δ^{13}C-values (-14.6 ‰ VPDB) were formed within the zone of AOM. This indicates that methane is a source of carbonate carbon.
4. In the anoxic zone of the Black Sea, we investigated unique reefs of methanotrophic microbes. These reefs are situated immediately above methane seeps and reach a height of 4 m and a diameter up to 1 m. The inner parts of the reefs are stabilized by porous precipitated carbonates. The outer sides are covered by methanotrophic microbial mats that may attain a thickness of several centimeters. We found that the organisms feed on the emanating methane. By radiotracer experiments we showed that methane and sulfate are consumed at a 1:1 ratio and that methane-derived carbon is assimilated into mat biomass and precipitated as carbonate. The methanotrophic consortium consists of archaea of the ANME-1 cluster and sulfate-reducing bacteria of the *Desulfococcus/Desulfosarcina* cluster. Our investigations demonstrated that AOM enables the buildup of a large biomass.
5. Further investigations on the methanotrophic reefs of the Black Sea demonstrated that methanogenesis of the CO_2 reduction pathway plays a major role in the mat in addition to AOM. Rates of methane production were of the same magnitude as for AOM; both processes appear to be coupled but the nature of coupling could not be clarified. It is thought that methanotrophs of the ANME-1 cluster are able to mediate both AOM and methanogenesis. Further experiments with radiotracers revealed that CO_2 fixation is an important pathway of carbon assimilation in ANME-1. Combining beta-imager micrographs of methane-derived ^{14}C assimilation and fluorescence in situ hybridization (FISH) of mat sections showed that major AOM activity and ANME-1 biomass were located in a narrow zone close to the mat-water interface. Above and below that zone, various sulfate-reducing bacteria were identified. Their role in the

mat is currently unknown. The evidence of AOM in microbial mats within the sediments indicates that reef development may be initiated in the sediment.

6. Current questions on AOM physiology concern the use of alternative electron acceptors and a possible electron exchange between the syntrophic partners. $^{14}CH_4$ incubations with sediments from Hydrate Ridge revealed no AOM activity with alternative electron acceptors (e.g. nitrate, Mn^{4+}, Fe^{3+}). $^{14}CH_4$ incubations with electron-binding substances showed no positive effect on methane turnover.

The comparison between different habitats shows that AOM is an ubiquitous process in marine sediments, leading in diffusive systems to a complete retention of methane in the sediment. The sources of oceanic methane emission are most likely systems with advective methane transport mechanisms, especially rising gases bubbles and methane-rich fluids. The principal factors controlling the turnover of methane in marine habitats are: (1) methane and sulfate fluxes, (2) the resulting size of the AOM community, (3) the methane saturation concentration, which is mainly determined by hydrostatic pressure, (4) the removal of the AOM products H_2S und CO_2.

TABLE OF CONTENTS

Chapter 1

General Introduction

1. Chapters outline

The oxidation of methane by anaerobic microbes is a significant process in the global carbon cycle and a major sink for methane on earth. The anaerobic oxidation of methane (AOM) effectively controls the emission of methane to the hydrosphere by converting more than 90% of the methane produced in marine sediments before it enters the hydrosphere and atmosphere. AOM therefore plays an important role in the regulation of the greenhouse gas methane. During AOM, methane is oxidized with sulfate as the terminal electron acceptor, mediated by a consortium of methane-oxidizing archaea and sulfate-reducing bacteria. These microorganisms were identified for the first time in 1999 in methane rich sediments above gas hydrate. Hence, the biochemical pathways, controlling mechanisms, and mediating organisms of the process still bear many unknowns. This study was planned to investigate the diversity of marine environments with methane turnover, to find the hot spots of AOM, to quantify the local AOM rates, and to analyze the main factors controlling AOM rates in different environmental settings. Chapter 1 gives an introduction into the current knowledge on global methane cycling and the process of AOM. Chapter 2 to 7 present the results of the present study "Anaerobic oxidation of methane in marine sediments". Each chapter 2-7 consists of a manuscript already published, submitted or in preparation for submission.

Chapter 2 represents a study of AOM above gas hydrates. Hydrate Ridge (Oregon) is a special marine habitat characterized by gas discharges and rising fluids forming gas hydrates close to the sediment surface . It is shown that AOM at this location exhibit some of the highest rates ever measured in marine systems. The study focuses on small-scale differences in methane turnover rates depending on methane supply, and shows the high dynamics of habitats influenced by methane seepage.

Chapter 3 deals with the environmental control on AOM in the gassy sediments of Eckernförde Bay (German Baltic). In this high-productive coastal sediment of the temperate zone, enhanced organic matter degradation and thus methanogenesis leads to methane oversaturation resulting in gas bubble formation. Seasonal changes of different environmental parameters influence the amount and distribution of AOM in the surface sediment. Beside seasonal parameters, the study showed that rising gas bubbles lead to short-term increases of

AOM. Furthermore, the organisms apparently responsible for AOM in Eckernförde Bay sediments have been identified.

Chapter 4 looks at AOM in the sulfate-methane transition zone along the Chilean continental margin. This study focuses on AOM in a diffusive system, i.e. without the impact of rising gases bubbles or fluids. The investigated sites are located along the continental margin (between 800 and 3000 m water depth) in the coastal-upwelling region off Chile. The methane originates from in situ degradation of deposited organic matter. AOM in this diffusive system forms an efficient barrier against upward diffusing methane. The results show that methane turnover is relatively high for these water depths caused by enhanced organic matter deposition from the high-productive upwelling system. Furthermore, AOM leads to the formation of distinct layers of authigenic carbonates.

Chapter 5, "Microbial reefs in the Black Sea fueled by anaerobic oxidation of methane", presents a –so far- unique methanotrophic microbial community forming reef structures above methane seeps in the anoxic part of the Black Sea. The results show that archaea and sulfate reducing bacteria, which gain their energy from AOM, are able to build up an immense biomass on precipitated carbonate. With different microbiological, molecular and geochemical methods it is shown how AOM is fueling these reefs.

Chapter 6, " Distribution of methane-oxidizers and methanotrophy in microbial mats from the anoxic Black Sea", is a study following up on the results shown in Chapter 5. The metabolic pathways and microbial diversity in the methanotrophic reefs of the Black Sea was studied in detail. High rates of AOM and sulfate reduction rates were measured and evidence is provided for potential methanogenesis possibly coupled to AOM in the mat. We further showed that methanotrophs are only abundant and active in a distinct layer of the mat and that other zones of the mat are dominated by different sulfate-reducing bacteria. Carbon assimilation experiments revealed CO_2-fixation as an important pathway. At the end, a hypothetical model of the reef development is provided.

Chapter 7 deals with the environmental regulation of AOM mediated by ANME-I and ANME-II communities. The methanotrophic communities of Hydrate Ridge (Chapter 2) and the Black Sea (Chapter 5 and 6) are compared. The study shows that, although different phylogenetic groups of methanotrophs dominate the respective habitat, the communities

reveal many physiological similarities, meaning that both groups may occupy the same ecological niche. In a set of experiments, the use of alternative electron acceptors and the impact of different electron captures on AOM was tested for Hydrate Ridge sediments. The results show that no other electron acceptor beside sulfate is used and that electrons are not exchanged between methanotrophs and sulfate reducers.

Chapter 8 discusses the results from chapter 2 to 7 and provides summary conclusions as to the quantification, diversity and environmental regulation of AOM.

2. Introduction

The following introduction gives an overview on the knowledge on methane, its production and consumption relevant to this study. It is important to understand the sinks and sources of methane in the marine environment in order to understand the significance of AOM. An introduction into the current knowledge on the microbiology of aerobic and anaerobic methane oxidation, methanogenesis and sulfate reduction is also provided.

2.1 Methane – its properties, sources and sinks

Methane is the simplest molecule of all organic compounds and the most reduced form of carbon (Beyer and Walter, 1991). It is a hydrocarbon and contains four hydrogen atoms covalently bond to carbon as a tetrahedron (Fig. 1). Methane belongs to the alkane family. Further important homologous in natural environments are e.g. ethane, propane, and butane.

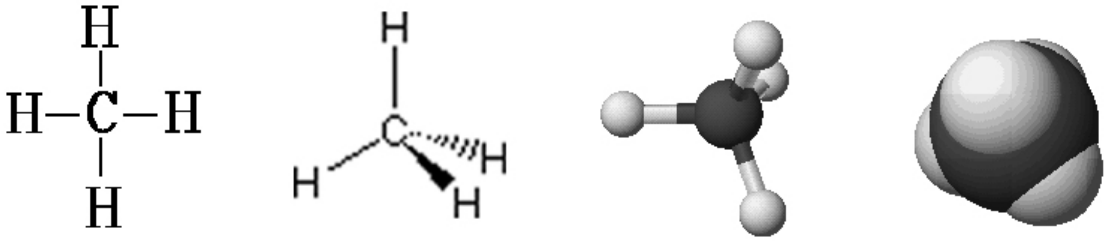

Figure 1. Different representations of the methane molecule.

The melting and boiling point of methane are -183 and –161.5°C, respectively, explaining why methane is gaseous at room temperatures. Methane is a non-polar molecule und therefore only slightly soluble in water (ca. 1.4 mM in seawater at atmospheric pressure (Yamamoto et al., 1976)). Its solubility depends on salinity, temperature and hydrostatic pressure (Yamamoto et al., 1976). One of the basic reactions involving methane is the formation of carbon dioxide and water with oxygen. This process is mediated by aerobic microbes, or requires a substantial activation energy from ignition or through photooxidation.

$$CH_4 + 2\,O_2 \rightarrow CO_2 + 2\,H_2O \qquad (1)$$

Methane is the main component in the atmosphere of Jupiter, Saturn, Uranus and Neptune (Beyer and Walter, 1991). The methane concentration of the Earth's atmosphere is on average 1.7 ppmv (Nakaya et al., 2000). The concentrations have increased by 145% since 1800 (ARM, 2001). This increase coincides with the onset of industrialization and roughly parallels world population growth, pointing to anthropogenic sources as the cause. Methane has the ability to trap and re-emit infrared radiation. It therefore belongs to the greenhouse gases and is jointly responsible for global warming (Fig. 2). Methane is 21 times more effective at trapping heat in the atmosphere than carbon dioxide. Today, its contribution to global warming is about 20%.

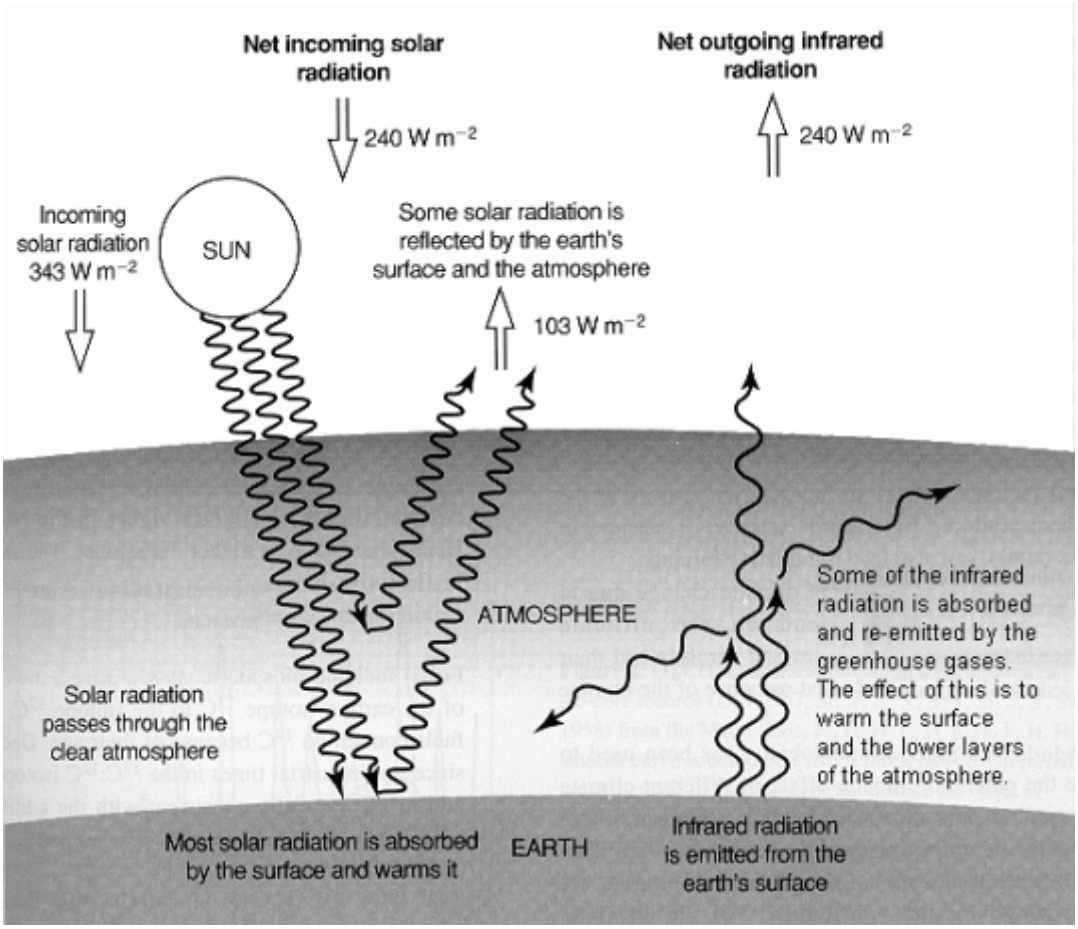

Figure 2. A simplified diagram illustrating the effect of greenhouse gases on global long-term radiative balance of the atmosphere. Scheme by Hong Kong Observatory.

Next to petroleum and coal, gas is one of the main energy sources of human society. Methane makes up to 95% of natural gas from fossil fuel reservoirs, and is used for cooking, heating, or driving a car. The largest reservoirs of methane are located in natural gas, gas hydrates and petroleum deposits (Heyer, 1990). These fossil fuels were formed over millions of years from deposits of organic matter in aquatic systems. However, beside old methane

deposits, there are many recent sources of methane on earth. The most important sources are listed in Table 1.

Table 1. Global methane production, consumption and emission (after Reeburgh, 1996). Production was calculated from the sum of emission and consumption. Gray rows indicate poorly investigated terms. The terms are sorted by the amount of net emission.

	Tg CH_4 a^{-1}		
Source/Sink term	**Gross production**	**Consumption**	**Net emission**
Wetlands	142	27	115
- bogs, tundra	50	15	35
- swamp, alluvial	92	12	80
Rice production	577	477	100
Ruminants	80	-	80
Biomass burning	55	-	55
Landfills	62	22	40
Gas production	58	18	40
- venting, flaring	10	-	10
- distribution leaks	48	18	30
Coal production	35	-	35
Termites	44	24	20
Ocean, freshwater	85	75	10
Hydrates	10	5	5
Soil consumption	40	50	-10
Chemical destruction	-	450	-450
Total production	*1388*		
Total consumption		*1193*	
Total emission			*195*

The majority of recent methane production is biogenic, i.e. produced by thermogenic transformation of organic material or by methanogenesis as the final step in fermentation of organic matter by methanogenic archaea in anoxic habitats (Reeburgh, 1996). There are also abiotic sources of methane e.g. at mid oceanic ridges where serpentinization takes place. The following sections will give an overview over global methane sources and sinks:

Wetlands- The sum of all wetlands such as bogs, tundra, swamps, and ponds represent the strongest natural methane emitters on Earth (Table 1, Reeburgh, 1996). However, estimations of emission rates are difficult in these complex and diverse ecosystems. Swamps are

characterized by an imbalance of organic matter production from plants and organic matter degradation. As a result, organic matter accumulates leading to the formation of peat. Due to the high water content, anoxic conditions develop and methane is formed during the degradation of organic matter by methanogens (Svensson, 1976). Hereby, methane concentrations often exceed saturation. The formed gas bubbles rise to the surface causing the typical bubbling surface of swamps. Through diffusion of methane into the upper oxic zone of the swamp, a part of the methane is oxidized to carbon dioxide by aerobic methanotrophic bacteria before it reaches the atmosphere. Methane emission from swamps was recognized already many centuries ago, better known as "swamp gas" or "marsh gas". Its mysterious spontaneous ignition was named "ghost light" and became famous in the legend of "Will O' The Wisp" (Page and Ingpen, 1985). Today we know that methane is ignited by traces of hydrogen phosphide.

Rice paddies- From a global view, rice paddies are the most important man-made habitats of methane emission into the atmosphere (Furukawa and Inubushi, 2002). The paddies are flooded with water to provide optimum conditions for the grow of the rice plants. As a consequence, anoxic conditions develop, leading to strong microbial methanogenesis upon the degradation of organic matter. The rice plants play a major role in the emission of methane from the paddies as about 90% of the methane leaves the soil via the aerenchyma of the plants (Seiler, 1984). Furthermore, the plants are suggested to stimulate methanogenesis due to the excretion of exudates, i.e. organic substances, from the roots (Seiler, 1984). However, the aerenchyma not only enables enhanced methane emission from the paddies but also leads to an increase in oxygen penetration into the sediment. The oxygen is utilized by methanotrophic bacteria to mediate aerobic oxidation of methane (Krüger et al., 2001; Krüger et al., 2002). This explains relatively high methane consumption rates during concurrent methane production leading to a lowered net methane emission from the paddies (Table. 1). As rice paddies are anthropogenic, many efforts are attempted today to reduce the methane emission from this environment (Furukawa and Inubushi, 2002).

Ruminants- After wetlands and rice paddies, the intestines of ruminants, especially of cattle, are the next large source of atmospheric methane (Table 1, Reeburgh, 1996). Different to other ecosystems, the methane produced by ruminants is not partly re-oxidized by microbes and hence completely emitted into the atmosphere (Heyer, 1990). The volumetric rates of methanogenesis in the intestines of a cattle are about 100-1000 times higher compared to

aquatic systems (Wolin, 1979). The reason for such a high methane production is the digestive system of a ruminant. Without microbial help, the ruminant is unable to utilize a major part of the incorporated polymeric substances from plants, especially cellulose, as it is lacking the essential degrading enzymes (Heyer, 1990). Therefore its intestine is inhabited by a diverse community of symbiotic microbial organisms which mediate (1) the enzymatic decomposition of polymeric substances like cellulose, hemi-cellulose, pectin, and amylum, (2) the fermentative transformation of the hydrolytic products into low-molecular weight fatty acids that can be resorbed by the host to gain energy and to synthesize cells, (3) the synthesis of microbial protein to meet the protein requirements of the host, and (4) the formation of vitamins. The specific role of methanogens in the process is the consumption of the large amounts of hydrogen that are formed during the fermentative processes (Heyer, 1990). Without removal of hydrogen, the fermentative products would change in an energetically unfavorable manner for the symbionts, and thus for the host. The hydrogen is directly transferred from the hydrogen producing bacteria to the methanogens by "interspecies hydrogen transfer". About 800 L hydrogen are produced in a cattle intestine per day (Wolin, 1979) and are transformed into 200 L methane by the methanogens. The methane is then released via the esophagus as a "burp". For the host, methanogenesis means a lost of 10-15% of the total energy of its food (Heyer, 1990). However, hydrogen consumption leads to an increase of the fermentative community and therefore to an increase in microbial protein usable for the host. Similar to rice paddies, most of the methane emission by cattle is caused by humans due to animal husbandry.

Biomass burning- Methane emissions arising from biomass burning are a result of incomplete combustion (Bertschi et al., 2003). Huge amounts can be produced during large scale burning of woodlands, savanna and agricultural waste. In savanna regions, burning is often performed to promote regeneration of the vegetation.

Landfills- Landfilling is becoming a common practice worldwide to dispose waste. The emission of methane from landfills due to organic matter degradation already represents an important contribution to the global methane budget (Augenstein, 1992). Today many efforts are made to collect the emitted methane and to utilize it. A consumption of methane prior to its release into the atmosphere by aerobic methanotrophic bacteria appears to be very weak (about 10%, Mancinelli and McKay, 1985).

Gas and coal production- Oil and coal deposits always contain methane (Heyer, 1990). During production of oil, gas or coal, large amounts of methane can be released into the atmosphere. In coal mines, the released methane is called firedamp. In an explosive mixture with air it can cause devastating pit explosions. Today, industrial production units are built to minimize loss of gas into the atmosphere.

Termites- Most strikingly, termites have a significant contribution to the global atmospheric methane (Table 1). Termites are xylophagous, i.e. they feed on wood (Rasmussen and Khalil, 1983). Like cattle, they do not comprise the enzymes to hydrolyze the cellulose-rich food and are therefore dependent on microbes that inhabit their intestines. This complex microbial consortium includes also methanogens. Laboratory studies on methane emission from termites revealed higher emission rates compared to in situ measurements at termite hills. This is explained by an intensive methane oxidation in the hills and the surrounding soil (Seiler et al., 1984).

Ocean and freshwater- The bulk of methane in marine environments is produced in shelf and near-shore sediments receiving a high deposition of organic matter, covering about 3.5% of the ocean area (Reeburgh, 1996). In most of the deeper continental margin zones, primary production of organic matter is comparatively low and only 1-5% of the surface primary production reaches the bathyal and abyssal seabed due to degradation processes in the water column (Gage and Tyler, 1996). Exceptions are the upwelling zones of continental margins, as well as the river fans receiving high amounts of organic matter. Because of the low accumulation rate in open ocean sediments, most of the organic matter is decomposed by aerobic processes in deep sea sediments (Wenzhöfer and Glud, 2002). However, considering that the total annual methane production of the oceans is similar to ruminants or swamps, their contribution to the atmospheric methane appears rather low (Table 1). In general, areal methane emission rates from the oceans are lower compared to freshwater systems (Heyer, 1990). The crucial reason for the difference between these two aquatic environments is the presence of sulfate in marine systems. Sulfate is an electron acceptor used for the degradation of organic matter by sulfate-reducing bacteria (Jørgensen and Fenchel, 1974; Jørgensen, 1982). As long as sulfate is present in the sediment, major methanogenesis is inhibited caused by substrate competition between sulfate-reducing bacteria and methanogens (Zehnder, 1988). Bulk methanogenesis in marine sediments is usually banished into deeper parts of the sediment. This shift might be centimeters (Martens et al., 1986) to meters (Fossing et al.,

2000) depending on methane and sulfate fluxes. Methane diffusing upwards towards the sediment-water interface has consequently a longer passage in marine compared to freshwater sediments, in which methanogenesis begins right below the penetration depth of oxygen (Heyer, 1990). In freshwater sediments, methane is consumed solely in the very thin oxic sediment surface layer by aerobic methanotrophic bacteria. Methane passing this small barrier is emitted to the hydrosphere and finally, if not consumed in the water column, to the atmosphere. In the oceans, there are two pathways of methane consumption: aerobic and anaerobic oxidation of methane. In the latter process, AOM, methane is oxidized with sulfate instead of oxygen (Zehnder and Brock, 1980; Hoehler et al., 1994; Reeburgh, 1996; Valentine and Reeburgh, 2000; Hinrichs and Boetius, 2002). This process will be explained in detail in the following chapters of this introduction. The high availability of sulfate enables a methane consumption far below the sediment-water interface. However, if any methane passes this first barrier, there is a second sink caused by aerobic oxidation close to the sediment surface and in the water column retaining methane in the ocean. This interlocking of two consumption processes explains the low methane emission from ocean systems despite the high methane production rates.

Hydrates- Gas hydrates represent the world largest methane reservoir (Kvenvolden, 1988; Kvenvolden, 1993). Their properties, occurrence, and role in the global methane cycling will be presented in a separate section of this introduction.

Soil consumption- Only little is known on the regulation of methane production and consumption in soil. Its magnitude might vary strongly depending on water content, oxygen ventilation, organic matter content and temperature. Considering net emission from soils into the atmosphere, soil represent a sink for methane (King, 1992; King, 1996). Indeed, many investigations on soils from tropical savanna, agriculture, grasslands, and forests confirmed substantial rates of atmospheric methane consumption by methanotrophic bacteria (King, 1992 and references therein). Recent studies show that the consumption underlies seasonal changes in temperate climates (Henckel et al., 2000) and is sensitive to disturbances of the soil structure (Roslev et al., 1997). In many studies, aerobic methanotrophic bacteria in soil seem to be different from known groups of methanotrophs (Roslev et al., 1997; Holmes et al., 1999; Henckel et al., 2000; Ragajewski et al., 2002).

Chemical destruction- The atmosphere represents the largest sink for methane (Table 1, Wuebbles and Hayhoe, 2002). In a chemical reaction, methane reacts with hydroxyl (OH) radicals, forming water and carbon dioxide. The break up of methane is much stronger in the troposphere compared to the stratosphere (about 12:1). The consumption of hydroxyl radicals indirectly magnifies the effects of other pollutants due to the reduced oxidizing power in the atmosphere as a whole.

Other sources of methane- Beside the methane sources mentioned in Table 1, there are many other sources, however, their contribution to the atmospheric methane is either negligible or has not been quantified globally. Some examples are hydrothermal vents/hot springs, wastewater treatment, livestock manure, and trees.

At *hydrothermal vents and hot springs*, methane is produced both thermogenic and microbial. Thermogenic methane is formed by water-rock reactions with hydrogen and CO_2 (Westgate et al., 2001) or by pyrolysis of complex organic substances (Teske et al., 2002). Microbial methanogenesis is facilitated by the low solubility of oxygen in hot water and the low redox potentials given by the volcanic exhalations of the vents (H_2S, H_2, CO, CO_2) (Heyer, 1990). Methanogens in these habitats tolerate very high temperature optima (80-100°C) and live exclusively autotrophic using volcanic hydrogen and CO_2 (Stetter et al., 1981).

Wastewater treatment and *livestock manure* bear the problem of high concentrations of feces and manure in relatively small areas, which would usually be spread out over a wide area and decompose aerobically in the natural environment. Accumulation of feces and manure lead to anoxic conditions and therefore to a predominance of methane producing anaerobic decomposition (Heyer, 1990; Ginting et al., 2003).

Methanogens were also found in the wood of living *trees* (Heyer, 1990). Methane can build up a high pressure in cottonwood, elm, willow, oak, and maple. It is suggested that wood degrading microbes immigrate into dead xylem through injured roots. The high water content and anaerobic conditions in the dead xylem (wetwood) facilitate the microbial degradation of pectin and other substances. Like in other ecosystems, methane is formed by methanogens at the end of the anaerobic degradation process.

2.2 Gas hydrates – the largest methane reservoir on Earth

Gas hydrates are known since the 19th century from experiments performed by Sir Humphrey Davy using chloric gas and water. However, they were considered as chemical curiosities until they caused major problems to the petroleum industry in the 1930´s (Hammerschmidt, 1934). Unintentional formation of gas hydrates blocked the transport in oil pipelines. Today many natural sources of gas hydrates are known from permafrost and the deep oceans (e.g. Makogon, 1981; Kvenvolden, 1993; Egorov et al., 1999; Suess et al., 1999; Borowski et al., 2000).

Gas hydrates, also called gas clathrates, are non-stoichiometric compounds of carbon gases, water and other molecules (Kvenvolden, 1993). The gas, e.g. methane, is enclosed in a rigid lattice of cages formed by water molecules (Fig. 3). Three structures of the isomeric (cubic) lattice were found in nature: structure I, II and H (www.gashydrate.de, Fig. 3). Structure I comprises only small gas molecules like methane, ethane, CO_2 and H_2S. Structure II includes also larger gas molecules like propane and isobutane. Structure H comprises cage types that need very large gas molecules, like methylcyclohexane, for their formation. In a fully saturated structure I methane hydrate, one molecule of methane is present compared to six molecules of water (Kvenvolden, 1993). When methane hydrate decomposes, 164 m^3 methane is released from 1 m^3 gas hydrate due to gas expansion. The remaining water has a volume of 0.8 m^3. Thus, gas hydrates contain more gas than an equivalent volume of free gas, which attracts a lot of attention especially from the gas and petroleum industry. Possibilities to commercially exploit gas hydrates as a future energy source are debated but the respective technology has not been developed yet.

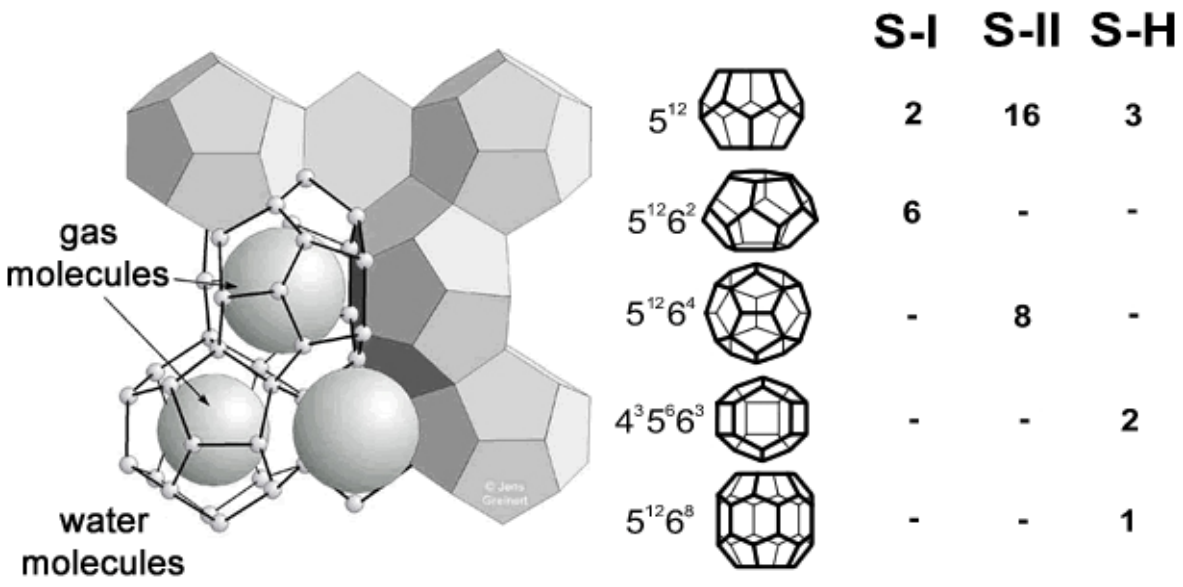

Figure 3. Left: Schematic design of gas hydrate structure I. Right: Different forms of water cages present in structure I, II, and H. Pictures by GEOMAR.

The formation of gas hydrates is controlled by temperature, hydrostatic pressure, the presence of water and high concentrations of gases (Kvenvolden, 1993). At atmospheric pressure, gas hydrates form only in very cold regions, i.e. permafrost. In the oceans, gas hydrates are stable at high hydrostatic pressure and/or low temperature. In Fig. 4 the stability conditions for gas hydrates are given. The lower boundary of their occurrence in marine sediments is determined by the geothermal gradient. Below this zone, free gas occurs. The phase change from solid to gas causes the so-called bottom-simulating reflector (BSR) in seismic profiles that is used to identify gas hydrate locations. A BSR marks the interface between higher sonic velocity, hydrate-cemented sediment above and lower sonic velocity, free gas sediment below (Fig. 4).

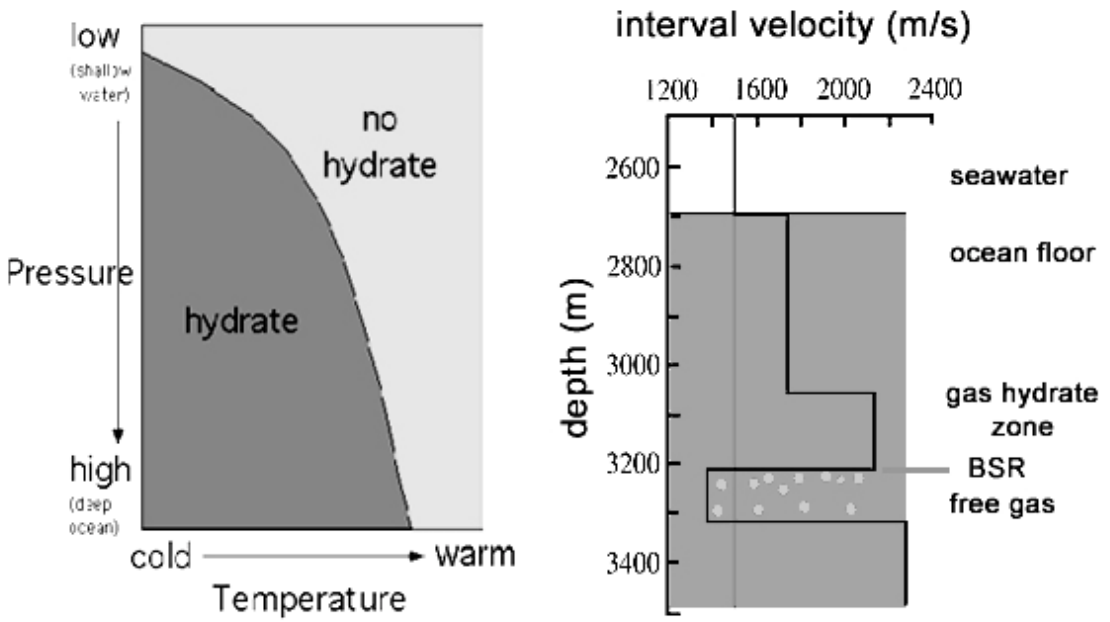

Figure 4. Left: Gas hydrate stability dependent on hydrostatic pressure and temperature. Right: Change of seismic velocity at the border between gas hydrate and free gas causing the so-called bottom simulating reflector (BSR). Pictures by GEOMAR.

Marine gas hydrates mostly occur as structure I type with methane as the most important gas component (Kvenvolden, 1993). At oil seepage locations, like the Gulf of Mexico, the formation of structure II type hydrates with methane and higher hydrocarbons has been observed (Sassen et al., 1998; Joye et al., accepted). Because methane hydrate formation in the oceans is favored by high pressure, low temperature and huge amounts of methane, most methane hydrates are found in outer continental margins (Kvenvolden, 1993). Here, the bottom water has low temperatures and the supply of organic matter from the shelf areas and the euphotic zone is still high enough to sustain the build up of large methane reservoirs. Global estimations of methane resources stored in gas hydrates are highly speculative due to incomplete knowledge about gas hydrate distribution and poor methods to quantify subsurface gas hydrate reservoirs (Kvenvolden, 1988). However, it is believed that the amount of carbon stored in gas hydrates (approx. 1 x 10^4 GT) strongly exceeds the amount of carbon of known conventional gas deposits (40 GT) and recoverable fossil fuel reserves (130 GT) (Potential Gas Commitee, 1981; Kvenvolden, 1988). Beside utilization of methane from gas hydrates, many speculations have been made about possible influences and reactions of gas hydrate reservoirs on global climate. Two scenarios are hypothesized for both global cooling and global warming, both controlled by positive and negative feedback mechanism factors (Judd

et al., 2002): During global cooling, gas hydrates of permafrost would remain stable because of low temperatures (negative feedback), whereas the reduction in hydrostatic pressure that is accompanied with the lowering of sea-level (increase of ice on poles) could cause a downslope migration of the gas hydrate stability zone in the world oceans. Gas hydrates in shallow areas could dissociate and significant volumes of methane could be released in such a scenario (positive feedback). During global warming, permafrost would melt and significant amounts of methane could be released from the dissociating gas hydrates (positive feedback). A consequent sea-level rise may stabilize gas hydrates and enables their formation in lower levels of the oceans (negative feedback). It was also hypothesized that a warming of deep ocean currents during global warming could cause a destabilization of gas hydrates in the deep ocean despite the stabilizing effect of the rising sealevel (Bice and Marotzke, 2002).

2.3 Microbial methanogenesis – the main source of methane in the ocean

Methanogenic archaea are very widespread and can be found in all habitats with anaerobic degradation of organic matter. Their occurrence was described in detail in section 2.1. As they are not able to directly consume polymeric organic substances, methanogens are always found in facultative or obligate syntrophic associations with microbial communities of the anaerobic degradation pathways (Heyer, 1990).The ability to form methane is restricted to a small group of archaea including the phylogenetic groups *Methanobacteriales*, *Methanococcales*, *Methanomicrobiales*, *Methanosarcinales*, and *Methanopyrales* (Madigan et al., 2000).

After the discovery of biological methanogenesis by A. Volta 1776 and the clarification of the chemical nature of methane by W. Henry 1806 it still took 100 years to recognize that methane is a product of microbial metabolism. The morphology of methanogens is manifold, including rod-like and spiral-shaped cells, coccid and sarcina-like aggregates (Heyer, 1990). However, there are some characteristics that all methanogens have in common: (1) they all belong to the archaeal kingdom of *Euryarchaeota*, (2) they are all obligate anaerobes, and (3) they grow and form methane only at redox potentials below -300 mV.

The substrates of methanogenesis can be H_2/CO_2, acetate, formate, methanol, methylamines and CO (Daniels et al., 1984; Zehnder, 1988; Heyer, 1990):

$$4\,H_2 + CO_2 \rightarrow CH_4 + 2\,H_2O \quad (2)$$

$$4\,HCOOH \rightarrow CH_4 + 3\,CO_2 + 2\,H_2O \quad (3)$$

$$4\,CH_3OH \rightarrow 3\,CH_4 + CO_2 + 2\,H_2O \quad (4)$$

$$CH_3COOH \rightarrow CH_4 + CO_2 \quad (5)$$

$$4\,CO + 2\,H_2O \rightarrow CH_4 + 3\,CO_2 \quad (6)$$

$$4\,CH_3NH_2 + 2\,H_2O \rightarrow 3\,CH_4 + CO_2 + 4\,NH_3 \quad (7)$$

$$2\,(CH_3)_2NH + 2\,H_2O \rightarrow 3\,CH_4 + CO_2 + 2\,NH_3 \quad (8)$$

$$4\,(CH_3)_3N + 6\,H_2O \rightarrow 9\,CH_4 + 3\,CO_2 + 4\,NH_3 \quad (9)$$

The formation of methane from H_2/CO_2 or acetate are the most common pathways. Hydrogen and acetate are competitive substrates in marine sediments as they are also used by sulfate-reducing bacteria (Zehnder, 1988). Methanogens using these pathways are usually outcompeted by sulfate reducers. Other substrates like methylamines, methanol are non-competitive, i.e. methanogenesis proceeds despite the presence of sulfate reduction (Oremland et al., 1982).

The process of methanogenesis is mediated in several enzymatic steps. The last step is common for all methanogenic substrates (Thauer, 1998):

$$\underset{methyl-coenzyme\ M}{CH_3-S-CoM} + H-S-CoB \rightarrow CH_4 + \underset{heterodisulfide}{HS-CoM-S-S-CoB} \quad (10)$$

Methyl-coenzyme M is the central intermediate in this oxidative reaction and is unique for methanogens. It is formed from coenzyme M, the smallest coenzyme known to date, and the substrate (e.g. CO_2, acetate). Methyl-coenzyme-M is subsequently reduced with coenzyme B to methane with the concurrent formation of heterodisulfide of co-enzyme M and co-enzyme B (Thauer, 1998 and references therein). The key enzyme of this reaction is Methyl-coenzyme M reductase. This last step in methane formation is, as far as known, not coupled with energy conservation. The energy required for growth must be generated in the reductive part, i.e. the exergonic reduction of the heterodisulfide.

2.4 Aerobic oxidation of methane - A sink for methane in oxic habitats

Where methane reaches the oxic biosphere it is consumed by aerobic microbial oxidation (see Eq. 1). Especially in aquatic systems and soils, aerobic methanotrophs reduce the release of methane into the atmosphere (King, 1992; Reeburgh, 1996). The ability to oxidize methane with oxygen is restricted to a diverse group of specialized alpha and gamma proteobacteria (Madigan et al., 2000). Their existence is known from the beginning of the 20th century. The first isolated methanotrophic organism was named *Bacillus methanicus* (Söhngen, 1906), although the isolate turned out to be not a pure culture. Some of the most important properties that characterizes typical aerobic methanotrophs are (Heyer, 1990): (1) they are gram negativ, (2) they are aerobic, (3) they are obligate methylotrophs, i.e. they use methane and methyl-groups as their sole carbon and energy source and do not grow on substrates with C-C-bonds, (4) they use ammonium as nitrogen source, (5) they show co-oxidations of ammonium, carbon monoxide, dimethylether and other organic compounds, (6) they form different kind of resting stages like cysts or exospores. Beside the here characterized obligate methylotrophic bacteria, there are some others, i.e. facultative methylotrophs that are able to utilize also organic substances with C-C-bonds. It is important to mention that not all methylotrophic bacteria are consequently methanotrophs, however, all methanotrophic bacteria are methylotrophs. The initial catabolic enzyme in aerobic methane oxidation is methane monooxygenase (King, 1992).

Aerobic methanotrophs are very widespread (Heyer, 1990; King, 1992; Reeburgh, 1996). Basically they can be found in every oxic habitat that contains methane. They are able to metabolize methane even at very low oxygen concentrations down to 6.3 x 10^{-3} mM (Heyer, 1990) (for comparison: the average oxygen concentration of oxygenated deep-sea bottom water is around 0.43 mM (Wenzhöfer and Glud, 2002)). This enables them to inhabit oxic-anoxic transition zones. A special characteristic of aerobic methanotrophs is their ability to form resting stages (Heyer, 1990). They are able to survive even long periods of anoxia or without methane. The resistance of many spores against drying is important for soil bacteria or spreading through the air.

It was observed that aerobic oxidation of methane is inhibited by the addition of ammonium (King, 1996). This is explained by a competition between ammonium and methane for methane monooxygenase. Thus, anthropogenic ammonium fertilization of soil effects the release of methane into the atmosphere.

2.5 Sulfate reduction – the main oxidative pathway in anoxic marine habitats

In marine sediments, sulfate reduction, and in particular organoclastic sulfate reduction, is the most important degradation process of organic matter (Jørgensen, 1982). Although other electron acceptors such as oxygen, nitrate, iron and manganese yield higher energy outputs compared to sulfate, their combined concentration at the sediment-water interface are more than 50 times lower compared to the total sulfate concentration (D´Hondt et al., 2002). The general reaction of organoclastic sulfate reduction is (Jørgensen, 1982):

$$2\,CH_2O + SO_4^{2-} \rightarrow 2\,HCO_3^- + H_2S \qquad (11)$$

Sulfate reduction is mainly performed by groups of the delta proteobacteria (Madigan et al., 2000). They use a large variety of electron donators like hydrogen, acetate, lactate, pyruvate, formate, methanol. Some groups, e.g. *Desulfosarcina*, *Desulfonema*, *Desulfococcus*, are able to live chemoautolithotrophic with hydrogen as the electron donor, sulfate as electron acceptor and CO_2 as the solely carbon source. Among the sulfate reducers there are obligate anaerobic forms, however, some also tolerate oxygen in small amounts or even use it as electron acceptor (Madigan et al., 2000).

Beside the degradation of organic matter, sulfate reduction is also the oxidative pathway driving AOM. In this case, we call the process methanotrophic sulfate reduction. Its pathways will be explained in detail in the next section.

2.6 Anaerobic oxidation of methane – the main methane sink in anoxic marine habitats

AOM is a microbial process in anoxic marine sediments whereby methane is oxidized with sulfate as the terminal electron acceptor (Barnes and Goldberg, 1976):

$$CH_4 + SO_4^{2-} \rightarrow HCO_3^- + HS^- + H_2O \qquad (12)$$

According to current knowledge, AOM is mediated by a syntrophic consortium of methanotrophic archaea and sulfate-reducing bacteria (Zehnder and Brock, 1980; Hoehler et al., 1994; Boetius et al., 2000; Orphan et al., 2001).

The first investigation of AOM dates back to the year of 1974, when Martens and Berner (1974) speculated about the cause for conspicuous *methane and sulfate profiles* in organic rich sediments (Fig. 5). The scientists observed that methane was not accumulating before sulfate was exhausted. From the decrease of methane concentrations in the sulfate-reducing zone, they concluded that methane must be consumed with sulfate.

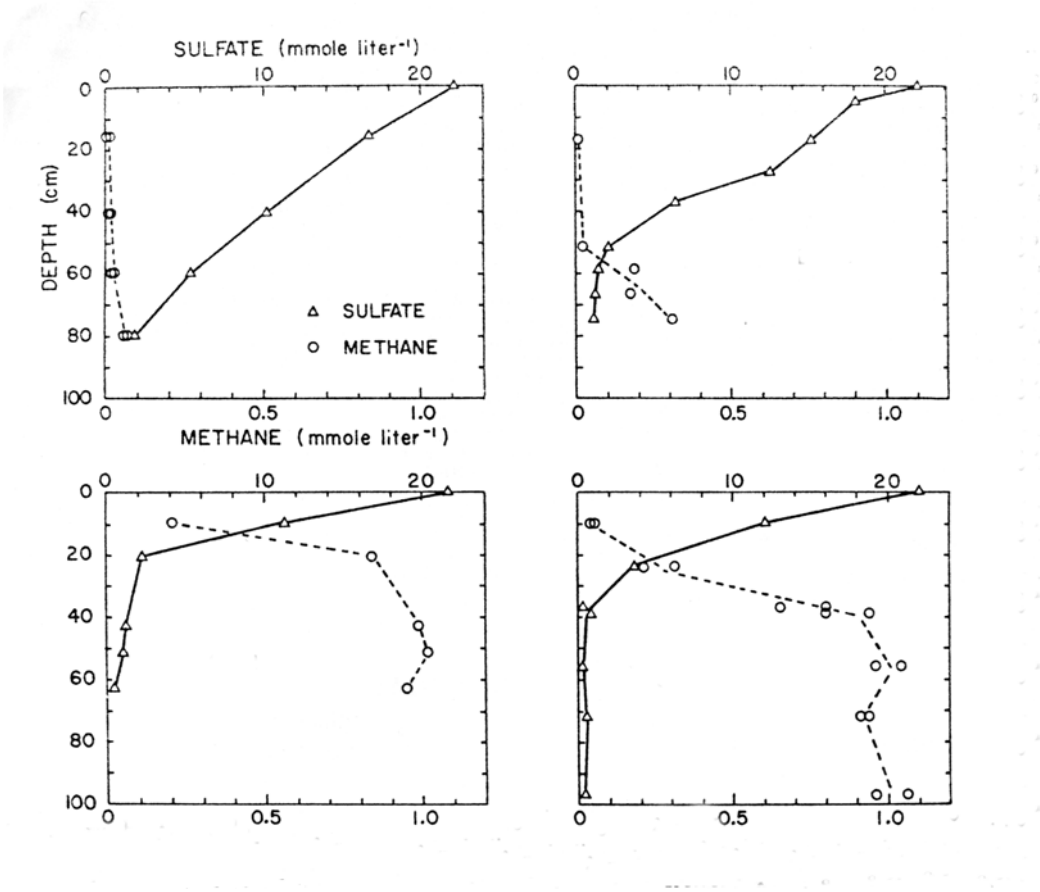

Figure 5. Methane and sulfate profiles in the sediments of Long Island Sound that stimulated the first discussions about methane oxidation with sulfate (Martens and Berner, 1974).

Zehnder and Brock (1979 and 1980) were the first who demonstrated methane oxidation under anoxic conditions and hypothesized a *coupled two-step mechanisms* of AOM. They postulated that methane is first activated by methanogenic archaea, working in reverse, leading to the formation of intermediates, e.g. acetate or methanol. In a second step, the intermediates are oxidized to CO_2 under concurrent sulfate reduction by other non-methanogenic members of the microbial community (Fig. 6).

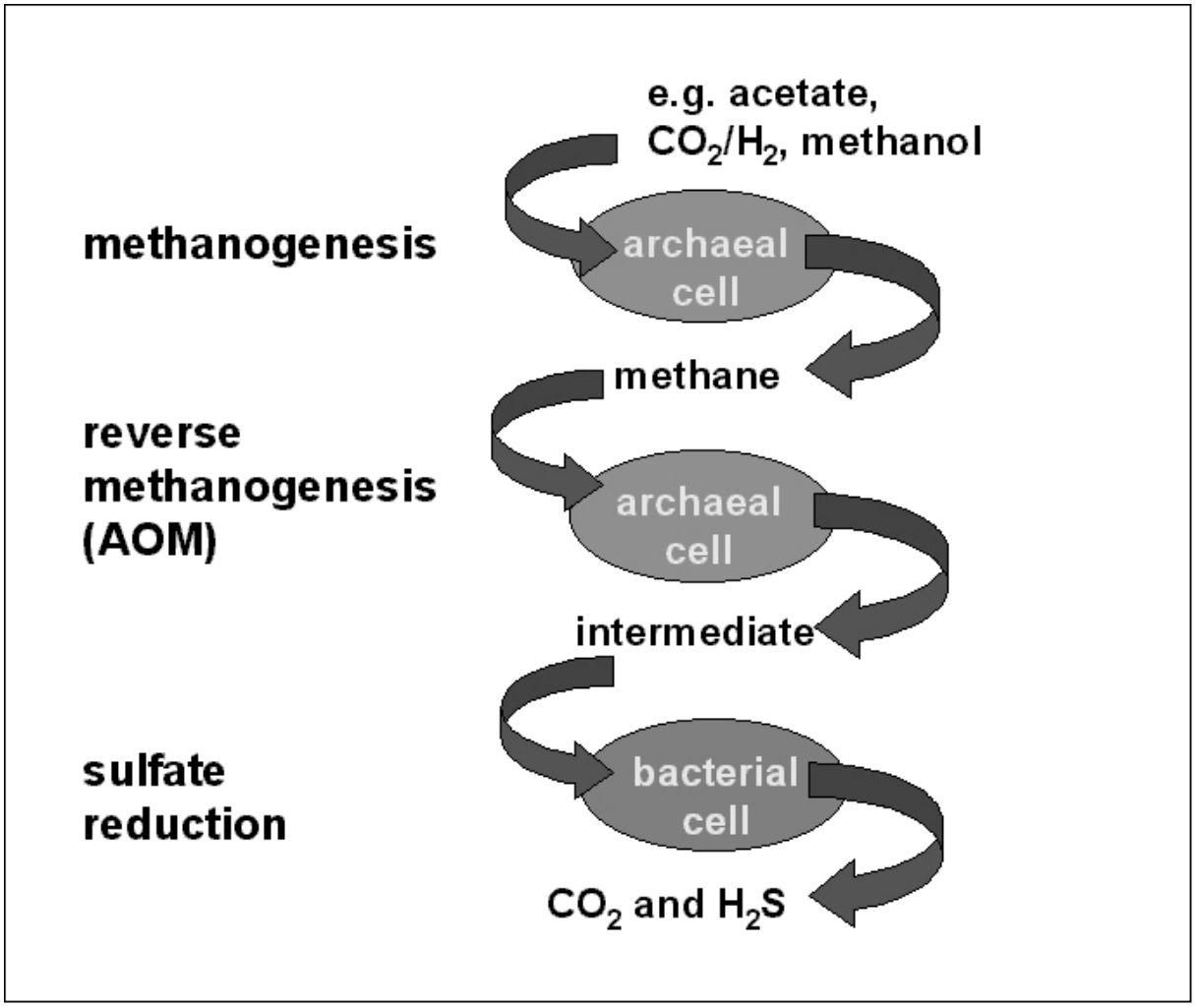

Figure 6. Interactions between methanotrophic archaea and sulfate-reducing bacteria according to the hypothesis of Zehnder and Brock (1980).

Since then, the knowledge of AOM increased substantially involving biogeochemical, microbiological, and molecular methods adding one peace after the other to the big puzzle. *Radiotracer measurements* enabled the first direct quantification of AOM and concurrent sulfate reduction rates in anoxic marine sediments (Reeburgh, 1976; Iversen and Blackburn, 1981; Devol, 1983). By this technique, traces of $^{14}CH_4$ and $^{35}SO_4^{-2}$ are added to the sediment and their conversion into $^{14}CO_2$ and $H_2{}^{35}S$ are determined. Including the total methane and sulfate concentration of the sediment, turnover rates can be calculated. Iversen and Blackburn (1981) measured a 1:1 ratio of AOM and sulfate reduction in the sulfate-methane transition zone of Danish sediments, demonstrating the close coupling between these processes.

In 1994, Hoehler et al. confirmed by *thermodynamic modelling* that a consortium of methanogenic archaea and sulfate-reducing bacteria could gain energy from AOM. The hypothetical pathway involves hydrogen and CO_2 production from methane by methanogens.

The hydrogen is than consumed by sulfate-reducing bacteria, thereby maintaining hydrogen partial pressure low enough for favourable free energy yields.

Further evidences were gained by *inhibition experiments* (Hoehler et al., 1994; Hansen et al., 1998). Chemical substances were added to anoxic methanotrophic sediments with the purpose of inhibiting the activity of either methanogens or sulfate reducers. For methanogens, 2-bromoethanesulfonic acid (BES) was used (Hoehler et al., 1994). This inhibitor is an analog to coenzyme M (Gunsalus et al., 1978), an enzyme cofactor present only in methanogens (see section 2.3). The enzymatic pathway of sulfate reduction was inhibited by the addition of molybdate (Hansen et al., 1998). In both experiments, AOM was strongly reduced. When sulfate was removed from the sediment, AOM was completely inhibited (Hoehler et al., 1994). Again, a close coupling between AOM and sulfate reduction was demonstrated.

The search for the microorganisms involved in AOM was advanced by investigations of *lipid biomarkers* in sediments from methane seeps. Biomarkers are specific biologically produced molecules that allow identifications of organisms on the level of kingdoms or sometimes orders (Peters and Moldowan, 1993). Biomarkers used for the differentiation between archaeal and bacterial cells originate from the phospholipid bilayer of the cell membrane. Typical archaeal biomarkers are characterized by isoprenoid chains and ether linkages, whereas bacterial cells are charakterized by fatty acids and ester linkages (Fig. 7). Not only the type of biomarker is informative but also its carbon isotopic composition. It bears diagnostic information on the carbon source and/or metabolic carbon fixation pathways utilized by its producer. When methane is produced, the microbes discriminate against the heavier ^{13}C-substrate, due to a slower reactivity of the heavier molecule, resulting in an enrichment of ^{12}C in the produced methane (Whiticar, 1999). This process is called *kinetic isotope fractionation.* The isotope ratio of ^{12}C and ^{13}C is expressed as the δ^{13}C-value, giving the magnitude of discrimination relative to a known standard (Vienna Peedee belemnite; VPDB). During consumption of the isotopically light methane by methanotrophs, a second step of carbon fractionation is involved. Thus, the methane-derived carbon that is incorporated into methanotrophic biomass reveals a very light signal. In search for the organisms involved in AOM, scientists found methanogen-specific lipids, named crocetane, archaeol and hydroxyarchaeol, in active methane seeps (Elvert and Suess, 1999; Hinrichs et al., 1999; Pancost et al., 2000; Thiel et al., 2001). Hinrichs et al. (1999) were able to show that archaeol and hydroxyarchaeol were absent in close-by non-seep sediments. Furthermore, the carbon isotopic signature of these lipids from the methane seep was extremely light, revealing δ^{13}C values of -100 and -110 ‰, respectively. The methane at this location had a δ^{13}C value

of -49.5 ‰ . The extremely light lipids gave an unequivocal evidence for an involvement of archaea in methane consumption. These archaeal lipids were also found in association with isotopic light bacterial lipids, although the δ^{13}C-values of the latter were somewhat heavier (-50 to -100 ‰ , Hinrichs et al., 2000; Hinrichs and Boetius, 2002). Similar to archaeal lipids, this relative enrichment in ^{12}C indicates the incorporation of methane-derived carbon into bacterial cells. The respective bacterial lipids (e.g. Di-*n*-pentadecylglycerolether and a C_{17}-cyclopropyl fatty acid) are not specific for certain phylogenetic clades, but have been commonly found in sulfate-reducing bacteria

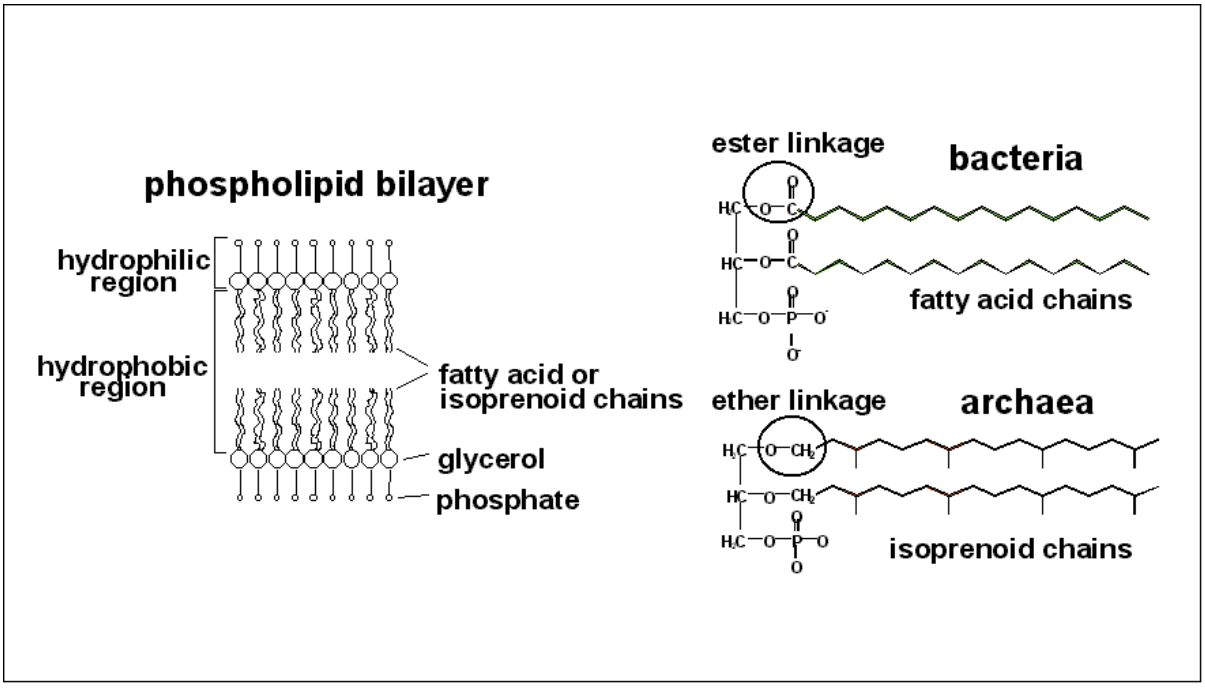

Figure 7. Left: Lipid biomarker in the phospholipid bilayer of cell membranes. Right: Simplified structure of typical archaeal and bacterial lipid biomarker. Figures provided by M. Elvert.

Although convincing evidences for the involvement of methanogenic archaea and sulfate reducing bacteria were found by rate measurements, inhibition experiments and lipid biomarkers, still the organisms themselves were not visualized. Finally a molecular method, called *fluorescence in situ hybridisation* (FISH), revealed a first consortium of microbes involved in AOM. The FISH technique allows the identification and quantification of individual microbial cells in environmental samples (Amann et al., 1990; Amann et al., 1990). Probes (nucleic acid strands) that are complementary to rRNA sequences unique to different phylogenetic groups or even species bind to ribosomes in intact fixed cells of the appropriate species by complementary base pairing. The probes carry different fluorescent dyes enabling

a visual identification of the targeted cells by fluorescence microscopy. In 2000 Boetius et al. presented the first microscopic pictures of an AOM-consortium, visualized by FISH, showing aggregates of archaeal cells surrounded by a shell of sulfate reducing bacteria (Fig. 8). The aggregates grow to a size of about 6-10 µm before they break apart into subaggregates implicating the need to keep short distances between cells during substrate exchange. The aggregates were discovered in surface sediment overlying methane hydrates where they made up more than 90% of the microbial biomass.

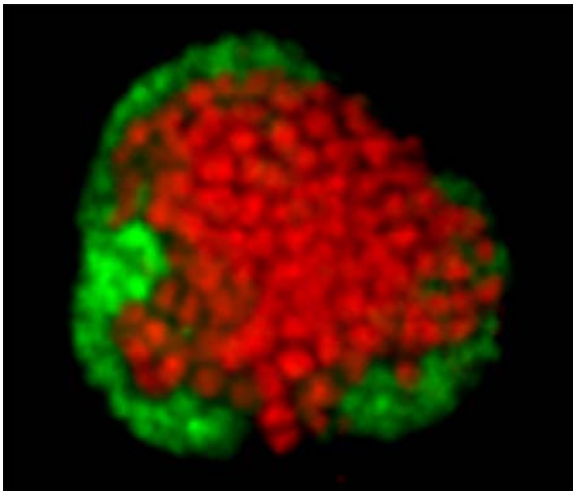

Figure 8. Aggregate of methane-oxidizing archaea (inner core, stained red) and sulfate-reducing bacteria (outer shell, stained green) found in sediments overlying gas hydrates (Boetius et al., 2000).

After revealing the conspicuous morphology of the AOM consortium, further methods were involved to obtain a direct evidence for the methanotrophy of the AOM consortium. A combination of FISH and *secondary ion mass spectrometry* (SIMS) allowed the measurement of δ^{13}C-profiles of the biomass of single aggregates (Orphan et al., 2001). A high depletion in ^{13}C in the archaeal cells with values down to -96‰ and of -62‰ in the bacterial cells was found. The results confirmed the assimilation of isotopically light methane by the consortia of archaea and bacteria.

The high abundance of such consortia in sediments overlying methane hydrate made them a perfect object to study the *physiology of AOM* under in vitro conditions. Nauhaus et al. (2002) demonstrated a methane-dependent sulfate reduction in sediment slurries of the hydrate location as well as a 1:1 ratio of AOM and sulfate reduction rates as predicted by the stoichiometry of the two processes. A special laboratory device enabled the scientists the

measurement of methane-dependent sulfate reduction at high hydrostatic pressure and thereby at higher methane concentrations than reachable under atmospheric pressure. The AOM-consortium revealed an increase in sulfate reduction rates with increasing methane concentration depicting the dependency of AOM on the availability of dissolved methane.

Although scientific knowledge about AOM and the respective microbial consortia substantially increased within the last 4 years, there are still many challenging questions to be answered by using combinations of new and classical methods of microbiology, molecular biology and geochemistry. It is still not known if AOM is an *enzymatic reversal of methanogenesis*. Just recently, convincing hints were found confirming this hypothesis. It was possible to link methyl coenzyme M reductase A (mcrA), a coenzyme specific for the process of methanogenesis (see section 2.3), with archaea involved in AOM (Hallam et al., 2003; Krüger et al., accepted). Furthermore, a modified form of mcrA was found concurrent with the presence of the AOM organisms (Krüger et al., accepted). The modified mcrA indicates a specialization of this enzyme possibly in catalyzing the first step in AOM. Moreover, it is still unknown, which kind of *intermediate* is exchanged between the archaea and sulfate-reducing bacteria. All substrates from which methanogens produce methane are preliminary suspected to be the product of AOM, i.e. the intermediate of the syntrophic consortium. There have been lots of laboratory experiments and free energy calculations resulting in the inclusion or exclusion of possible intermediates like hydrogen/CO_2, acetate, methanol, formate, or methylamine (Hoehler et al., 1994; Valentine and Reeburgh, 2000; Sørensen et al., 2001; Nauhaus et al., 2002). Nevertheless, methods for the direct identification of the intermediate exchanged during AOM are lacking. According to Valentine and Reeburgh (2000) and Hinrichs and Boetius (2002) the hypothetical gross reactions with the respective intermediate are as follows:

AOM with hydrogen as intermediate:

$$CH_4 + 2\,H_2O \rightarrow CO_2 + 4\,H_2 \quad (archaeal\ cell) \tag{13}$$

$$SO_4^{2-} + 4\,H_2 + H^+ \rightarrow HS^- + 4\,H_2O \quad (bacterial\ cell) \tag{14}$$

AOM with acetate as intermediate:

$$CH_4 + HCO_3^- \rightarrow CH_3COO^- + H_2O \quad (archaeal\ cell) \tag{15}$$

$$SO_4^{2-} + CH_3COO^- \rightarrow HS^- + 2HCO_3^- \quad (bacterial\ cell) \tag{16}$$

AOM with methanol as intermediate:

$$CH_4 + 4\,H_2O \rightarrow 4\,CH_3COH + 4\,H_2 \quad (archaeal\ cell) \tag{17}$$

$$3\,SO_4^{2-} + 4\,CH_3COH \rightarrow 3HS^- + 4\,HCO_3^- + 4\,H_2O + H^+ \quad (bacterial\ cell) \tag{18}$$

AOM with formate as intermediate:

$$CH_4 + 3\,HCO_3^- \rightarrow 4\,HCOO^- + H^+ + H_2O \quad (archaeal\ cell) \tag{19}$$

$$SO_4^{2-} + 4\,HCOO^- + H^+ \rightarrow HS^- + 4\,HCO_3^- \quad (bacterial\ cell) \tag{20}$$

A syntrophic relationship is defined to be a process by which two or more microorganisms cooperate to degrade a substance that can not be degraded by one organisms alone (Madigan et al., 2000). For the syntrophic AOM consortium a very small cell distance (<70 nm) was calculated for a thermodynamic favorable exchange of the assumed intermediates (Sørensen et al., 2001). However, it is unclear if a syntrophic consortium is actually necessary to mediate AOM. Although inhibitor experiments confirmed the involvement of methanotrophs and sulfate reducers, the chemicals used inhibited only processes and not specific organisms. It is also thinkable, that AOM is mediated by one organisms that comprises the enzymatic apparatus to mediate both methane oxidation and sulfate reduction.

Since the discovery of the microbes involved in AOM, much effort has been put on the *identification and phylogenetic classification* of AOM organisms from different habitats. Their phylogenetic classification is investigated using the relationships of 16S rDNA archaeal clones. Today there are three major groups identified: ANME-1, ANME-2 , and ANME-3 (Hinrichs et al., 1999; Boetius et al., 2000; Orphan et al., 2001; Orphan et al., 2001, K. Knittel and T. Lösekann, unpubl.). ANME is the acronym for anaerobic methanotrophs. All of them belong to the *Euryarchaeota,* the group that also comprises all methanogens. ANME-2 and ANME-3 belong to the *Methanosarcinales*. ANME-1 is distinct from, but related to, methanogenic archaea of the orders *Methanomicrobiales* and *Methanosarcinales*. A strongly simplified phylogenetic tree of the ANME groups is given in Fig. 9. The most complete overview on the phylogeny of sulfate reducers involved in AOM and associated with methane seeps has been published recently by Knittel et al. (2003).

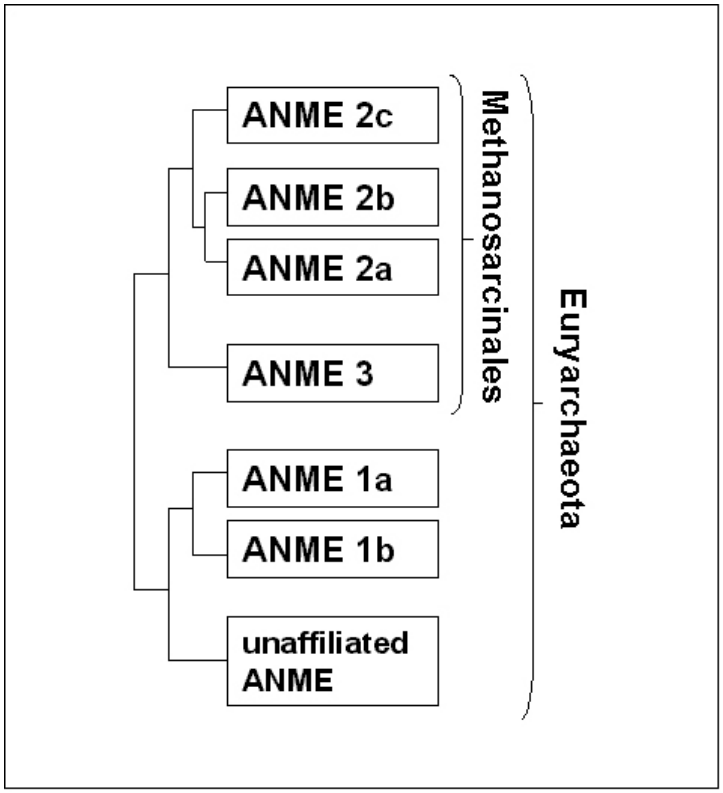

Figure 9. Simplified phylogenetic tree of archaeal groups involved in AOM (after K. Knittel and T. Lösekann, unpubl.)

2.7 Hot spots of AOM in marine habitats

In general, AOM can be expected wherever methane and sulfate coexist in anoxic environments. This includes all kinds of anoxic marine sediments but also anoxic marine waters. The methane source can be either recent or ancient, it can be microbial, thermogenic or abiotic, methane can occur dissolved, gaseous or enclosed in gas hydrates and can be transported by diffusive or advective flux. One main factor determining the magnitude of AOM is the methane supply because methane turnover rates increase with methane concentration (Nauhaus et al., 2002). There are several factors controlling the methane supply: (1) the rate of methane production (only important in recent methane habitats), (2) the methane flux, i.e. the flow of methane across a given surface, (3) pressure, temperature and salinity, the physical factors determining the solubility of methane (Yamamoto et al., 1976).

In Hinrichs and Boetius (2002) a review is given about AOM rates in marine sediments of different water depths as well as methane seeps. This first compilation of AOM field measurements and modelling suggests a direct coupling between methane supply and methane consumption in the habitat based on relatively few data available at time of publication.

Although the data reveal a large scatter, AOM rates of non-seeps are on average slightly higher in shelf sediments (290 ± 332 mmol m^{-2} a^{-1}, n = 10) compared to continental margins sediments (117 ± 157 mmol m^{-2} a^{-1}, n = 12). This could be correlated with the general decrease of organic matter supply with water depth (Gage and Tyler, 1996), resulting in weaker degradation processes including methanogenesis. At methane seeps of ancient methane reservoirs or gas hydrate locations, AOM rates are suggested to be 10 to 100 times higher compared to non-seep regions due an acceleration of AOM at habitats with high methane supply. However, the data of environmental AOM rates are still fragmentary. Especially at methane seeps, AOM was in most cases assumed from sulfate reduction rates. The present study contributes significantly to the global data base on AOM rates in marine habitats.

Hot spots of AOM are found in diverse habitats characterized by a wide range of environmental characteristics. In the following, different kinds of methane-bearing marine environments are briefly introduced, classified according to the nature of methane supply. The first three habitats were also investigated in this study. In Table 2 a compilation of examples for methane-bearing environments with local characteristics is given.

Diffusive systems- In these systems, molecular diffusion is the only transport mechanism for methane. This is different from methane seeps, were additional advective processes like rising fluid and bubbling gases accelerate the overall methane flux (Judd et al., 2002). The source of methane in diffusive systems is often in situ methanogenesis. The methane slowly diffuses upwards into the sulfate zone, were it is consumed by AOM (e.g. Iversen and Blackburn, 1981; Fossing et al., 2000). The sulfate-methane transition zone is sometimes located very deep - several meters to decameters - in the sediment, but the AOM community may still be limited to a narrow zone of a few centimetres depending on sufficient thermodynamic yields. Diffusive systems can be found in every kind of marine environments from coastal sediments (Iversen and Jørgensen, 1985; Thomson et al., 2001) to continental margins (Niewöhner et al., 1998; Fossing et al., 2000; Jørgensen et al., 2001). With water depth, i.e. hydrostatic pressure, methane solubility is increasing enabling more methane to be available in the pore water of the sediment.

Gassy coastal sediments- The origin of methane in these habitats is also in situ methanogenesis, however, the methane production is so intense that methane concentrations exceed methane saturation resulting in the formation of gas bubbles (e.g. Martens et al., 1986;

Hoehler et al., 1994; Martens et al., 1999). Rising gas bubbles represent a faster transport mechanisms for methane than molecular diffusion. The sulfate-methane transition is located in the top meter of the sediment.

Gas seeps- Gas seeps are associated with leakage from ancient gas reservoirs and, in some cases, with the formation and dissociation of gas hydrates (Judd et al., 2002). They provide a permanent high supply of methane to the surface sediment by rising gases, fluids and/or diffusion and ebullition from dissociating gas hydrates. Methane seeps were e.g. found in the Black Sea (Ivanov et al., 1991), or –in association with gas hydrates- at Hydrate Ridge (Oregon, Suess et al., 1999), in the Gulf of Mexico (Joye et al., accepted), and in the Eel River Basin (North California, Hinrichs et al., 1999).

Mud volcanoes and pockmarks- Mud volcanoes are formed by the expulsion of water, gas and mud from a deeper source (Judd et al., 2002). They occur in zones of tectonic compression or in areas of high sediment deposition rates. The principal driving force is an abnormally high pore fluid pressure caused by a combination of rapid sedimentation of fine-grained material, in situ gas generation and - in some cases - tectonic compression. Pockmarks are formed by the removal of sediment by escaping fluids (Hovland and Judd, 1988). The seeping fluid may be of hydrocarbon, hydrothermal or volcanic origin, or it may be groundwater. Many pockmarks are for example known from the North Sea (Hovland et al., 1984).

Hydrothermal vents- Hydrothermal vents are generated at spreading zones of oceanic plates. Methane can be formed by water-rock reactions (Westgate et al., 2001) or by pyrolysis of complex organic substances (Teske et al., 2002) (see also section 2.1). Microbes of this habitat must be adapted to very high temperatures.

Permanently anoxic waters- The Black Sea is the largest anoxic basin and the largest surface reservoir of dissolved methane (Reeburgh et al., 1991). Its methane content is similar to the annual methane emission to the atmosphere by wetlands and rice paddies (96 Tg). Reeburgh et al. (1991) detected AOM in the anoxic water column of the Black Sea. It is possible that AOM is also present in the water column other anoxic marine systems, e.g. anoxic basins of the Baltic Sea. AOM was also detected in the deeper anoxic waters of the hyper-saline Mono Lake, California (USA) (Joye et al., 1999).

Table 2. Examples of methane-bearing environments with some characteristics.

Location	Type	Area	Transport	Origin of methane	Water Depth (m)	Salinity	Temperature (°C)	Reference
Baltic Sea (Denmark)	diffusive system	coastal	diffusive	in situ production	16	brackish	5	Thomsen et al. (2001)
Kattegat/Skagerrak	diffusive system	coastal/shelf	diffusive	in situ production	43-200	brackish/ marine	8-9	Iversen & Joergensen (1985)
Atlantik (Namibia)	diffusive system	continental margin	diffusive	in situ production	1300-2000	marine	2-4	Fossing et al. (2000)
Cape Lookout Bight (Atlantik, North Carolina)	gassy coastal sediment	coastal	diffusive/ advective	in situ production	10	marine	6-28	Hoehler et al. (1994)
Eckernförde Bay (Baltic Sea, Germany)	gassy coastal sediment	coastal	diffusive/ advective	in situ production	28	brackish	4-11	Martens et al. (1999)
Black Sea (Ukraine)	gas seep	shelf	advective	fossil reservoir	250	brackish	9	Ivanov et al. (1991)
Hydrade Ridge (Pacific, Oregon)	gas seep/ gas hydrates	continental margin	advective	fossil reservoir	700	marine	4	Suess et al. (1999)
Gulf of Mexico	gas and oil seeps/	continental margin	advective	fossil reservoir	500	marine	5	Joye et al. (accepted)
Haakon Mosby mud volcano	mud volcano	continental margin	advective	fossil reservoir	1200	marine	-1.5	A. Boetius (unpubl.)
North Sea plateau	pockmarks	shelf	advective	fossil reservoir	ca. 100-200	marine	ca. 4	Hovland & Judd (1988)
Guaymas Basin (Gulf of CA, Mexico)	hydrothermal vent	ocean basin	advective	pyrolysis	ca. 1000	marine	2-130	Teske et al. (2002)
Central Black Sea	permanently anoxic water	water column below 120 m	advective/ currents	sediment	100-2200	brackish	9	Reeburgh et al. (1991)

3. Objectives

This study has two major objectives, whereof one represents the central part of this study and the other is considered as a supplement. The first, central objective is the detection, quantification and characterization of AOM hot spots in different methane-bearing marine habitats. This part concentrates on AOM in the environment. The second supplementary part deals with specific physiological investigations of AOM under defined laboratory conditions.

For environmental studies, three types of marine habitats with AOM hot spots were investigated: methane seeps with high advective methane fluxes, coastal sediments containing free gas, and continental margin sediments with diffusive methane fluxes. In these studies the main questions were:

- By which way and in which quantities is methane supplied and how is this reflected in the amount and distribution of AOM in the sediment?
- How much methane is retained in the sediment by AOM?
- What is the ratio between AOM and sulfate reduction in the habitat?
- What is the range of the small-scale variability of AOM in these sediments?
- How does AOM impact the environment?
- How does the environment impact AOM?
- Which organisms are involved in AOM of the respective habitat?
- How suitable were the applied methods for AOM determinations?

In general, rate measurements were performed ex situ, but under near in situ conditions except for hydrostatic pressure. This was important to gain data that are as close to the natural habitat as possible.

Investigations on the physiology of AOM, the second objective of this study, where performed in vitro, i.e. under laboratory conditions, and exclusively with mat pieces of the Black Sea reef and with homogenized sediment slurries of Hydrate Ridge. Both samples comprise a high abundance of methanotrophic cells, which make them a suitable object for physiological studies. Major questions of these investigations were:

- What is the ratio between AOM, sulfate reduction and methanogenesis under controlled conditions?
- What is the role of methanogenesis in AOM habitats?
- Are other electron acceptors used for AOM beside sulfate?
- Which pathways are used for carbon assimilation by methanotrophic communities?
- Can carbonate precipitation of methane-derived carbon be demonstrated in vitro?

4. Publications outline

This thesis includes six manuscripts. Four of them have been submitted to international journals, whereof two are already published. Two other articles will be submitted within the next three months. Manuscript 5 (Chapter 6, " Distribution of methane-oxidizers and methanotrophy in microbial mats from the anoxic Black Sea") contains my contributions to the collaborative work, but not all parts of the co-authors of the manuscript. All articles appear in the order described in the general introduction (this chapter). In the following I specify my contributions to each article.

1. Anaerobic oxidation of methane above gas hydrates at Hydrate Ridge, NE Pacific

Tina Treude, Antje Boetius, Katrin Knittel, Klaus Wallmann, Bo Barker Jørgensen

Marine Ecology Progress Series (2003), 264: 1-14

This study was initiated by Antje Boetius. Sampling and rate measurements were carried out by Tina Treude and Antje Boetius. Tina Treude established and improved the methods for determining AOM rates at the MPI. The aggregate counts were carried out by Katrin Knittel and Antje Boetius. The modeling was performed by Klaus Wallmann. Tina Treude wrote the manuscript with input from Antje Boetius, Bo Barker Jørgensen, and Klaus Wallmann.

2. Environmental control on anaerobic oxidation of methane in the gassy sediments of Eckernförde Bay (German Baltic)

Tina Treude, Martin Krüger, Antje Boetius, Bo Barker Jørgensen

Accepted by Limnology and Oceanography

This study was initiated by Tina Treude. The field work was organized and performed by Tina Treude. Except for potential rates, which were accomplished by Martin Krüger, Tina Treude carried out all samplings and measurements. The manuscript was written by Tina Treude with input from all co-authors.

3. Anaerobic oxidation of methane in the sulfate-methane transition along the Chilean continental margin

Tina Treude, Jutta Niggemann, Jens Kallmeyer, Paul Wintersteller, Carsten J. Schubert, Antje Boetius, Bo Barker Jørgensen

Accepted by Geochimica et Cosmochimica Acta.

This study on AOM was initiated by Tina Treude and Bo Barker Jørgensen. All sampling procedures and on-board measurements (porosity, density, pH, H_2S, temperature, methane) were performed in teamwork including Tina Treude, Jutta Niggemann, Jens Kallmeyer, and Paul Wintersteller. AOM rates were measured by Tina Treude. Sulfate reduction rates and sulfate concentrations were measured by Jens Kallmeyer. Organic parameters were determined by Jutta Niggemann. δ^{13}C-values were determined by Carsten Schubert. The manuscript was written by Tina Treude with input from Jutta Niggemann, Jens Kallmeyer, Carsten Schubert, Antje Boetius, and Bo Barker Jørgensen.

4. Microbial reef in the Black Sea fueled by anaerobic oxidation of methane

Walter Michaelis, Richard Seifert, Katja Nauhaus, Tina Treude, Volker Thiel, Martin Blumenberg, Katrin Knittel, Armin Gieseke, Katharina Peterknecht, Thomas Pape, Antje Boetius, Rudolf Amann, Bo Barker Jørgensen, Friedrich Widdel, Jörn Peckmann, Nikolai V. Pimenov, Maksim B. Gulin

Science (2002), 297, 1013-1015

This study was initiated by W. Michaelis, R. Seifert, F. Widdel and A. Boetius. The samples for all microbiological studies were taken by Tina Treude and Katja Nauhaus who were also responsible for all experimental designs. Tina Treude performed radiotracer rate measurements and radiotracer incubations for beta microimaging. All other data were contributed by the co-authors.

5. Distribution of methane-oxidizers and methanotrophy in microbial mats from the anoxic Black Sea

Tina Treude, Katrin Knittel, Armin Gieseke, Antje Boetius,

This study was initiated by Tina Treude and Antje Boetius. Katrin Knittel carried out the FISH and RNA analysis of the mat nodule in the sediment. Armin Gieseke carried out the sectioning of the mat pieces and the beta microimaging of the non-acidified mat sections. All other measurements were performed by Tina Treude. This manuscript contains data from lab experiments and field work carried out to study the Black Sea microbial mats in greater detail. The data will contribute to at least two manuscripts, one on the lab experiments on metabolism and growth by T. Treude et al., and one on the microbial diversity in the mat by K. Knittel et al.. The manuscript was written by Tina Treude with input from all co-authors. The manuscript(s) will be submitted within the next three months.

6. Environmental regulation of anaerobic oxidation of methane mediated by ANME-I and ANME-II- communities: a comparative analysis

Katja Nauhaus, Tina Treude, Antje Boetius, Martin Krüger

This study was initiated by Katja Nauhaus and Martin Krüger. Most of the physiological studies were performed by Katja Nauhaus and Martin Krüger. Martin Krüger and Tina Treude carried out AOM radiotracer measurements to test the use of alternative electron acceptors and the impact of electron captors. The manuscript was written by Katja Nauhaus with input by Antje Boetius and Martin Krüger and will be submitted to Environmental Microbiology within the next three months.

5. References

Amann, R.I., Binder, B.J., Olson, R.J., Chisholm, S.W., Devereux, R., Stahl, D.A. (1990). Combination of 16S rRNA-targeted oligonucleotide probes with flow cytometry for analyzing mixed microbial populations. Appl. Environ. Microbiol. 56, 1919-1925.

Amann, R.I., Krumholz, L., Stahl, D.A. (1990). Fluorescent-oligonucleotide probing of whole cells for determinative, phylogenetic, environmental studies in microbiology. J. Bacteriol. 172, 762-770.

ARM (2001). Global warming and methane. Atmospheric Radiation Measurement Programm (ARM) Facilities Newsletter ANL/ER/NL-01-07, www.arm.gov/docs/sites/sgp/news/sgpfacility/july01.pdf.

Augenstein, D. (1992). The greenhouse effect and US landfill methane. Global Environ.Change 2, 311-328.

Barnes, R.O., Goldberg, E.D. (1976). Methane production and consumption in anoxic marine sediments. Geology 4, 297-300.

Bertschi, I., Yokelson, R.J., Ward, D.E., Babbitt, R.E., Susott, R.A., Goode, J.G., Hao, W.M. (2003). Trace gas and particle emissions from fires in large diameter and below ground biomass fuels. J. Geophys. Res. 108(D13), 8472.

Beyer, H., Walter, W. (1991). Lehrbuch der organischen Chemie, S. Hirzel Verlag Stuttgart, pp. 1030.

Bice, L.K., Marotzke, J. (2002). Could changing ocean circulation have destabilized methane hydrate at the Paleocene/Eocene boundary. Paleoceanography 17(2), 1018.

Boetius, A., Ravenschlag, K., Schubert, C.J., Rickert, D., Widdel, F., Giesecke, A., Amann, R., Jørgensen, B.B., Witte, U., Pfannkuche, O. (2000). A marine microbial consortium apparently mediating anaerobic oxidation of methane. Nature 407, 623-626.

Borowski, W.S., Hoehler, T.M., Alperin, M.J., Rodriguez, N.M., Paull, C.K. (2000). Significance of anaerobic methane oxidation in methane-rich sediments overlying the Blake Ridge gas hydrates. In: C. K. Paull, R. Matsumoto, P. J. Wallace and W. P. Dillon (Eds.), Proceedings of the Ocean Drilling Program, Scientific Results. , pp. 87-99.

Potential Gas Commitee (1981). Potential supply of natural gas in the United States (as of December 31, 1980), Potential Gas Agency, School of Mines, Golden Colo, pp. 119.

D´Hondt, S., Rutherford, S., Spivack, A.J. (2002). Metabolic activity of subsurface life in deep-sea sediments. Science 295, 2067-2070.

Daniels, L., Sparling, R., Sprott, G.D. (1984). The bioenergetics of methanogenesis. Biochim. Biophys. Acta 768, 113-163.

Devol, A.H. (1983). Methane oxidation rates in the anaerobic sediments of Saanich Inlet. Limnol. Oceanogr. 28(4), 738-742.

Egorov, A.V., Crane, K., Vogt, P.R., Rozhkov, A.N. (1999). Gas hydrate that outcrop on the sea floor: stability models. Geo-Mar. Let. 19, 68-75.

Elvert, M., Suess, E. (1999). Anaerobic methane oxidation associated with marine gas hydrates: superlight C-isotops from saturated and unsaturated C_{20} and C_{25} irregular isoprenoids. Naturwissenschaften 86, 295-300.

Fossing, H., Ferdelman, T.G., Berg, P. (2000). Sulphate reduction and methane oxidation in continental sediments influenced by irrigation (South-East Antlantik off Namibia). Geochim. Cosmochim. Acta 64(5), 897-910.

Furukawa, Y., Inubushi, K. (2002). Feasible suppression technique of mehane emission from paddy soil by iron amendment. Nutr. Cycl. Agroecosyst. 64, 193-201.

Gage, J.D., Tyler, P.A. (1996). Deep-sea biology: A natural history of organisms at the deep-sea floor, Cambridge Univ. Press, pp. 504.

Ginting, D., Kessavalou, A., Eghball, B., Doran, J.W. (2003). Greenhouse gas emission and soil indicators four years after manure and compost applicazions. J. Environ. Quality 32, 23-32.

Gunsalus, R.P., Roemesser, J.A., Wolfe, R.S. (1978). Preparation of coenzyme M analogues and their activity in the methyl coenzyme M reductase system of *Methanobacterium thermoautotrophicum*. Biochemistry 17, 2374-2377.

Hallam, S.J., Girguis, P.R., Preston, C.M., Richardson, P.M., DeLong, E.F. (2003). Identification of methyl coenzym m reductase A (*mcr*A) genes associated with methane-oxidizing archaea. Appl. Environ. Microbiol. 69(9), 5483-5491.

Hammerschmidt, E.G. (1934). Formation of gas hydrates in natural gas transmission concepts. Ind. Eng. Chem. 26, 851-855.

Hansen, L.B., Finster, K., Fossing, H., Iversen, N. (1998). Anaerobic methane oxidation in sulphate depleted sediments: effects of sulphate and molybdate addition. Aquat. Microb. Ecol. 14, 195-204.

Henckel, T., Jäckel, U., Schnell, S., Conrad, R. (2000). Molecular analyses of novel methanotrophic communities in forest soil that oxidize atmospheric methane. Appl. Environ. Microbiol. 66(5), 1801-1808.

Heyer, J. (1990). Der Kreislauf des Methans, Akademie-Verlag Berlin, pp. 250.

Hinrichs, K.-U., Boetius, A. (2002). The anaerobic oxidation of methane: new insights in microbial ecology and biogeochemistry. In: G. Wefer, D. Billett, D. Hebbelnet al (Eds.), Ocean Margin Systems. Springer-Verlag, Berlin, pp. 457-477.

Hinrichs, K.-U., Hayes, J.M., Sylva, S.P., Brewer, P.G., De Long, E.F. (1999). Methane-consuming archaebacteria in marine sediments. Nature 398, 802-805.

Hinrichs, K.-U., Summons, R.E., Orphan, V., Sylva, S.P., Hayes, J.M. (2000). Molecular and isotopic analyses of anaerobic methane-oxidizing communities in marine sediments. Org. Geochem. 31, 1685-1701.

Hoehler, T.M., Alperin, M.J., Albert, D.B., Martens, C.S. (1994). Field and laboratory studies of methane oxidation in an anoxic marine sediments: evidence for methanogen-sulphate reducer consortium. Global Biochem. Cycles 8(4), 451-463.

Holmes, A.J., Roslev, P., McDonald, I.R., Iversen, N., Hendriksen, K., Murrell, J.C. (1999). Characterization of methanotrophic bacterial populations in soils showing atmospheric methane uptake. Appl. Environ. Microbiol. 65(8), 3312-3318.

Hovland, M., Judd, A.G. (1988). Seabed pockmarks and seepages, Graham & Trotman, London, pp. 293.

Hovland, M., Judd, A.G., King, L.H. (1984). Characteristic features of pockmarks on the North Sea floor and Scotian Shelf. Sedimentology 31, 471-480.

Ivanov, M.V., Polikarpov, G.G., Lein, A.Y., al., e. (1991). Biogeochemistry of the carbon cycle in the zone of Black Sea methane seeps. Dokl. Akad. Nauk SSSR 320(1235-1240).

Iversen, N., Blackburn, T.H. (1981). Seasonal rates of methane oxidation in anoxic marine sediments. Appl. Environ. Microbiol. 41(6), 1295-1300.

Iversen, N., Jørgensen, B.B. (1985). Anaerobic methane oxidation rates at the sulphate-methane transition in marine sediments from Kattegat and Skagerrak (Denmark). Limnol. Oceanogr. 30(5), 944-955.

Jørgensen, B.B. (1982). Mineralization of organic matter in the sea bed - the role of sulphate reduction. Nature 296, 643-645.

Jørgensen, B.B., Fenchel, T. (1974). The sulfur cycle of a marine sediment model system. Mar. Biol. 24, 189-210.

Jørgensen, B.B., Weber, A., Zopfi, J. (2001). Sulphate reduction and anaerobic methane oxidation in Black Sea sediments. Deep-Sea Res. I 48, 2097-2120.

Joye, S.B., Boetius, A., Orcutt, B.N., Montoya, J.P., Schulz, H.N., Erickson, M.J., Logo, S.K. (accepted). The anaerobic oxidation of methane and sulfate reduction in sediments from Gulf of Mexiko cold seeps. Chem. Geol.

Joye, S.B., Connell, T.L., Miller, L.G., Premland, R.S., Jellison, R.S. (1999). Oxidation of ammonia and methane in an alkaline, saline lake. Limnol. Oceanogr. 44(1), 178-188.

Judd, A.G., Hovland, M., Dimitrov, L.I., García Gil, S., Jukes, V. (2002). The geological methane budget at continental margins and its influence on climate change. Geofluids 2, 109-126.

King, G.M. (1992). Ecological aspects of methane oxidation, a key determinant of global methane dynamics. Adv. Microbiol. Ecol. 12, 431-468.

King, G.M. (1996). Regulation of methane oxidation: contrasts between anoxic sediments and oxic soils. In: M. E. Lidstrom and F. R. Tabita (Eds.), Microbial growth on C_1 compounds. Kluwer Academic Publishers, Intercept, Andover, UK, pp. .

Knittel, K., Boetius, A., Lemke, A., Eilers, H., Lochte, K., Pfannkuche, O., Linke, P. (2003). Activity, distribution, and diversity of sulfate reducers and other bacteria in sediments above gas hydrates (Cascadia Margin, Oregon). Geomicrobiol. J. 20, 269-294.

Krüger, M., Eller, G., Conrad, R., Frenzel, P. (2002). Seasonal variations in CH_4 oxidation and pathways of CH_4 production in rice fields determined by stable carbon isotopes and specific inhibitors. Glob. Change Biol. 8, 265-280.

Krüger, M., Frenzel, P., Conrad, R. (2001). Microbial processes influencing methane emission from rice fields. Glob. Change Biol. 7, 49-61.

Krüger, M., Meyerdierks, A., Glöckner, F.O., Amann, R., Widdel, F., Kube, M., Reinhard, R., Kahnt, J., Böcher, R., Thauer, R.K., Shima, S. (accepted). A conspicuous nickel protein in microbial mats that oxidise methane anaerobically. Nature.

Kvenvolden, K. (1993). A primer on gas hydrates. U.S. Geological Survey 1570, 279-291.

Kvenvolden, K.A. (1988). Methane hydrate - a major reservoir of carbon in the shallow geosphere? Chem. Geol. 71, 41-51.

Kvenvolden, K.A. (1988). Methane hydrates and global climate. Global Biochem. Cycles 2(3), 221-229.

Madigan, M.T., Martino, J.M., Parker, J. (2000). Brock Biology of Microorganisms 9/e, Prentice-Hall, New Jersey, pp. 1175.

Makogon, Y., F. (1981). Hydrates of natural gas, Pennwell Publishing Company, Tulsa, OK, pp. 237.

Mancinelli, R.L., McKay, C.P. (1985). Methane-oxidizing bacteria in sanitary landfills. In: A.A. Antonopoulos (Eds.), Biotechnical advances in processing municipal wastes for fuelsand chemicals. Argonne National Laboratory, Chicago, USA, pp. 437-450.

Martens, C.S., Albert, D.B., Alperin, M.J. (1999). Stable isotope tracing of anaerobic methane oxidation in the gassy sediments of Eckernförde Bay, German Baltic Sea. Am. J. Sci. 299, 589-610.

Martens, C.S., Berner, R.A. (1974). Methane production in the interstitial waters of sulphate-depleted marine sediments. Science 185, 1167-1169.

Martens, C.S., Blair, N.E., Green, C.D. (1986). Seasonal variations in the stable carbon isotopic signature of biogenic methane in a coastal sediment. Science 233, 1300-1303.

Nakaya, T., Kobayashi, K., Akagi, T., Kimura, K., Tai, H. (2000). Continous monitoring of the methane concentration in the atmosphere by IR spectromoetry with a 1.66-m diode laser. Analyt. Sci. 16, 1211-1214.

Nauhaus, K., Boetius, A., Krüger, M., Widdel, F. (2002). In vitro demonstration of anaerobic oxidation of methane coupled to sulphate reduction in sediment from marine gas hydrate area. Environ. Microbiol. 4(5), 298-305.

Niewöhner, C., Hensen, C., Kasten, S., Zabel, M., Schulz, H.D. (1998). Deep sulfate reduction completely mediated by anaerobic methane oxidation in sediments of the upwelling area off Namibia. Geochim. Cosmochim. Acta 62(3), 455-464.

Oremland, R.S., Marsh, L.M., Polcin, S. (1982). Methane production and simultaneous sulphate reduction in anoxic, salt marsh sediments. Nature 296, 143-145.

Orphan, V.J., Hinrichs, K.-U., Ussler III, W., Paull, C.K., Tayleor, L.T., Sylva, S.P., Hayes, J.M., DeLong, E.F. (2001). Comparative analysis of methane-oxidizing archaea and sulfate-reducing bacteria in anoxic marine sediments. Appl. Environ. Microbiol. 67(4), 1922-1934.

Orphan, V.J., House, C.H., Hinrichs, K.-U., McKeegan, K.D., De Long, E.F. (2001). Methane-consuming Archaea revealed by directly coupled isotopic and phylogenetic analysis. Science 293, 484-487.

Page, M., Ingpen, R. (1985). Encyclopaedia of things that never where, Dragon´s World Ltd, Limpsfield, pp. 240.

Pancost, R.D., Sinninghe Damsté, J.S., De Lint, S., Van der Maarel, M.J.E.C., Gottschal, J.C. (2000). Biomarker evidence for widespread anaerobic methane oxidation in

mediterranean sediments by a consortium of methanogenic archaea and bacteria. Appl. Environ. Microbiol. 66(3), 1126-1132.

Peters, K.E., Moldowan, J.M. (1993). The biomarker guide. Interpreting molecular fossils in petroleum and ancient sediments, Prentice Hall, New Jersey.

Ragajewski, S., Webster, G., Reay, D.S., Morris, S.A., Ineson, P., Nedwell, D.B., Prosser, J.I., Murrell, J.C. (2002). Identification of active methylotroph populations in an acidic forest soil by stable-isotope probing. Mircobiology 148, 2331-2342.

Rasmussen, R.A., Khalil, M.A.K. (1983). Global production of methane by termites. Nature 301, 704-705.

Reeburgh, W.S. (1976). Methane consumption in Cariaco Trench waters and sediments. Earth Planet. Sci. Lett. 28, 337-344.

Reeburgh, W.S. (1996). "Soft spots" in the global methane budget. In: L. M.E. and F. R. Tabita (Eds.), Microbial Growth on C_1 Compounds. Kluwer Academic Publishers, Intercept, Andover, UK, pp. 334-342.

Reeburgh, W.S., Ward, B.B., Whalen, S.C., Sandbeck, K.A., Kilpatrick, K.A., Kerkhof, L.J. (1991). Black Sea methane geochemistry. Deep-Sea Res. I 38(2), 1189-1210.

Roslev, P., Iversen, N., Henriksen, K. (1997). Oxidation and assimilation of atmospheric methane by soil methane oxidizers. Appl. Environ. Microbiol. 63(3), 874-880.

Sassen, R., MacDonald, I.R., Guinasso, N.L., Joye, S.B., Requejo, A.G., Sweet, S.T., Alcala-Herrera, J., DeFreitas, D.A., Schink, D.R. (1998). Bacterial methane oxidation in sea-floor gas hydrate: Significans to life in extreme environments. Geology 26, 851-854.

Seiler, W. (1984). Contribution of biological processes to the global budget of CH_4 in the atmosphere. In: M. J. Klug and C. A. Reddy (Eds.), Current perspectives in microbial ecology. American Society for Microbiology, Wasington, D.C.

Seiler, W., Conrad, R., Scharffe, D. (1984). Field studies of methane emission from termite nests into the atmosphere and measurements of methane uptake by tropical soils. J. Atmos. Chem. 1, 171-186.

Söhngen, N.L. (1906). Über Bakterien, welche Methan als Kohlenstoffnahrung und Energiequelle gebrauchen. Centralbl. Bakt. Parasitenk. II Abt. 15, 513-517.

Sørensen, K.B., Finster, K., Ramsing, N.B. (2001). Thermodynamic and kinetic requirements in anaerobic methane oxidizing consortia exclude hydrogen, acetate and methanol as possible electron shuttles. Microb. Ecol. 42, 1-10.

Stetter, K.O., Thomm, M., Winter, J., Wildgruber, G., Huber, H., Zillig, W., Janecovic, D., König, H., Palm, P., Wunderl, S. (1981). *Methanotermus fervidus*, sp. nov., a novel

extremelxy thermophilic methanogen isolated from an Icelandic hot spring. Zbl. Bakt. Hyg. I. Abt. Orig. C2, 166-178.

Suess, E., Torres, M.E., Bohrmann, G., Collier, R.W., Greinert, J., Linke, P., Rehder, G., Trehu, A., Wallmann, K., Winckler, G., Zuleger, E. (1999). Gas hydrate destabilization: enhanced dewatering, benthic material turnover and large methane plumes at the Cascadia convergent margin. Earth Planet. Sci. Lett. 170, 1-15.

Svensson, B.H. (1976). Methane production in a tundra peat. In: H. G. Schlegel, G. Gottschalk and N. Pfennig (Eds.), Microbial production and utilization of gases (H_2, CO_2, CH_4) Akademie der Wissenschaften, Göttingen, pp. 135-139.

Teske, A., Hinrichs, K.-U., Edgcomb, V., Gomez, A.d.V., Kysela, D., Sylva, S.P., Sogin, M.L., Jannash, H.W. (2002). Microbial diversity of hydrothermal sediments in the Guaymas Basin: evidence for anaerobic methanotrophic communities. Appl. Environ. Microbiol. 68(4), 1994-2002.

Thauer, R.K. (1998). Biochemistry of methanogenesis: a tribute to Marjory Stephenson. Microbiology 144, 2377-2406.

Thiel, V., Peckmann, J., Richnow, H.H., Luth, U., Reitner, J., Michaelis, W. (2001). Molecular signals for anaerobic methane oxidation in Black Sea seep carbonates and microbial mat. Mar. Chem. 73, 91-112.

Thomson, T.R., Finster, K., Ramsing, N.B. (2001). Biogeochemical and molecular signatures of anaerobic methane oxidation in a marine sediment. Appl. Environ. Microbiol. 67(4), 1646-1656.

Valentine, D.L., Reeburgh, W.S. (2000). New perspectives on anaerobic methane oxidation. Environ. Microbiol. 2(5), 477-484.

Wenzhöfer, F., Glud, R.N. (2002). Benthic carbon mineralization in the Atlantik: a synthesis based on in situ data from the last decade. Deep-Sea Res. I 49, 1255-1279.

Westgate, T.D., Ward, J., Slater, G.F., Lacrampe-Couloume, G., Sherwood Lollar, B. (2001). Abiotic formation of C_1-C_4 hydrocarbons on cristalline rocks of the Canadian Shield. 11th Annual V.M. Goldschmidt Conference, Hot Springs, Virginia, USA. , (CD-ROM; abstract 3140.pdf).

Whiticar, M.J. (1999). Carbon and hydrogen isotope systematics of bacterial formation and oxidation of methane. Chem. Geol. 161, 291-314.

Wolin, M.J. (1979). The rumen fermentation: a model for microbial interactions in anaerobic ecosystems. Adv. Microb. Ecol. 3, 49-77.

Wuebbles, D.J., Hayhoe, K. (2002). Atmospheric methane and global change. Earth Sci. Review 57(3-4), 177-210.

Yamamoto, S., Alcauskas, J.B., Crozier, T.E. (1976). Solubility of methane in distilled water and seawater. J. Chem. Eng. Data 21(1), 78-80.

Zehnder, A.J.B. (1988). Biology of anaerobic microorganisms, Wiley, New York, pp. .

Zehnder, A.J.B., Brock, T.D. (1979). Methane formation and methane oxidation by methanogenic bacteria. J. Bacteriol. 137(1), 420-432.

Zehnder, A.J.B., Brock, T.D. (1980). Anaerobic methane oxidation: occurrence and ecology. Appl. Environ. Microbiol. 39(1), 194-204.

Chapter 2

Anaerobic oxidation of methane above gas hydrates (Hydrate Ridge, NE Pacific)

Tina Treude[1]*, Antje Boetius[1,2,3], Katrin Knittel[1], Klaus Wallmann[4], Bo Barker Jørgensen[1]

[1]Max Planck Institute for Marine Microbiology, Department of Biogeochemistry, Celsiusstrasse 1, 28359 Bremen, Germany

[2]Alfred Wegener Institute for Polar and Marine Research, Department of Geochemistry, Am Handelshafen 12, 27515 Bremerhaven, Germany

[3]International University Bremen, Research II, Campusring 1, 28759 Bremen, Germany

[4]GEOMAR, Research Center for Marine Geosciences, Wischhofstrasse 1-3, 24148 Kiel, Germany

Marine Ecology Progress Series (2003) 264: 1-14

ABSTRACT: At Hydrate Ridge (HR), Cascadia convergent-margin, surface sediments contain massive gas hydrates formed from methane that ascends together with fluids along faults from deeper reservoirs. Anaerobic oxidation of methane (AOM), mediated by a microbial consortium of archaea and sulfate-reducing bacteria, generates high concentrations of hydrogen sulfide in the surface sediments. The production of sulfide supports chemosynthetic communities that gain energy from sulfide oxidation. Depending on fluid flow, the surface communities are dominated either by the filamentous sulfur bacteria *Beggiatoa* (high advective flow), the clam *Calyptogena* (low advective flow), or the bivalve *Acharax* (diffusive flow). We analyzed surface sediments (0 to 10 cm) populated by chemosynthetic communities for AOM, sulfate reduction (SR) and the distribution of the microbial consortium mediating AOM. Highest AOM rates were found at the *Beggiatoa* field with an average rate of 99 mmol $m^{-2}d^{-1}$ integrated over 0 to 10 cm. These rates are among the highest AOM rates ever observed in methane-bearing marine sediments. At the *Calyptogena* field, AOM rates were slightly lower (56 mmol $m^{-2}d^{-1}$). At the *Acharax* field, methane oxidation was extremely low (2.1 mmol $m^{-2}d^{-1}$) and was probably due to aerobic oxidation of methane. SR was fueled largely by methane at flow-impacted sites, but exceeded AOM in some cases, most likely due to sediment heterogeneity. At the *Acharax* field, SR was decoupled from methane oxidation and showed low activity. Aggregates of the AOM consortium were abundant at the fluid-impacted sites (between 5.1 x 10^{12} and 7.9 x 10^{12} aggregates m^{-2}) but showed low numbers at the *Acharax* field (0.4 x 10^{12} aggregates m^{-2}). A transport-reaction model was applied to estimate AOM at *Beggiatoa* fields. The model agreed with the measured depth-integrated AOM rates and the vertical distribution. AOM represents an important methane sink in the surface sediments of HR, consuming between 50 and 100% of the methane transported by advection.

INTRODUCTION

At Hydrate Ridge (HR) on the Cascadia convergent margin off the coast of Oregon (USA), fluids and methane ascend along faults from deep sediments to the surface because of tectonic activity along the Juan de Fuca and North American plate convergence (Whiticar et al. 1995, Suess et al. 1999). Under the prevailing conditions of low temperature and high hydrostatic pressure, gas hydrates form in the surface sediments at water depths between 600 and 800 m.

The hydrate composition is dominated by methane (vol% > 95; Suess et al. 1999). Due to the low molecular gases enclosed (methane, CO_2 and H_2S), hydrates occur as crystal structure 1 (Gutt et al. 1999). Hydrate-bearing surface sediments at HR are saturated with dissolved methane (around 70 mM; Torres et al. 2002). Samples of these methane-rich sediments provided the first microscopic evidence for a microbial consortium mediating anaerobic oxidation of methane (AOM) (Boetius et al. 2000b). During AOM, methane is oxidized using sulfate as an electron acceptor via the following net equation (Eq. 1):

$$CH_4 + SO_4^{2-} \rightarrow HCO_3^- + HS^- + H_2O \qquad (1)$$

The AOM consortium predominant at HR consists of sulfate-reducing bacteria of the branch *Desulfosarcina*/*Desulfococcus* and archaea of the ANME-2 group (Boetius et al. 2000b). The archaea are surrounded by the sulfate-reducing bacteria and both grow together in dense aggregates that comprise up to 90% of the microbial biomass in hydrate-bearing sediments. The current hypothesis on the functioning of AOM assumes that archaea oxidize methane in a process that is reverse to methanogenesis (Valentine & Reeburgh 2000, and references therein). The role of the sulfate-reducing bacteria in AOM-consortia is the oxidation of a so far unknown intermediate by simultaneous reduction of sulfate, thus creating the maintenance of thermodynamic conditions allowing methane oxidation to proceed exergonically.

Sulfate reduction (SR) rates of hydrate-bearing sediments at HR are extremely high compared to sediments of nearby hydrate-free sites where SR is below the detection limit, suggesting that SR is fuelled by methane rather than by organic detritus deposited from the overlying water column (Boetius et al. 2000b, Luff & Wallmann 2003). The present study presents AOM and SR rates and the distribution of aggregates within the uppermost 10 cm of surface sediments at HR. One aim of this study was to investigate methane-dependent sulfate reduction within different depth zones of the hydrate-bearing sediments. Highly ^{13}C-depleted archaeal-derived biomarkers suggest that methane is the primary carbon source of the AOM consortium (Elvert et al. 2001). In vitro experiments with HR sediment slurries (sediments amended with anoxic artificial seawater medium) demonstrated that SR increases with increasing methane concentration in a close 1:1 ratio with AOM (Nauhaus et al. 2002). Here, we are describing the interaction between AOM and SR processes in undisturbed natural sediments of HR.

Furthermore, we investigated differences in AOM resulting from variability in the flux regime, methane concentration, and vent biota. At HR, fluid flows create distinct provinces characterized by different advection rates and by different chemosynthetic communities, utilizing hydrogen sulfide, a product of AOM, as the energy source (Sahling et al. 2002, Torres et al. 2002, Tryon et al. 2002). Our hypothesis is that the availability of methane in the different provinces has a direct influence on AOM rates. We investigated AOM at sites dominated either by sulfide-oxidizing bacteria (*Beggiatoa)* or symbiotic clams (*Calyptogena* or *Acharax*) via radiotracer incubations with respect to their special characteristics. Finally, a transport-reaction model (Luff & Wallmann, 2003) was applied to estimate AOM rates in *Beggiatoa* fields. The model input includes measured porosity and sulfate concentrations as well as the average depth distribution and density of AOM consortia at *Beggiatoa* fields. The agreement between modeled and measured AOM rates is discussed.

MATERIALS AND METHODS

Study area. Sediment samples from different chemosynthetic provinces were collected along the top of the southern summit of Hydrate Ridge during RV SONNE cruise SO-148/1 in July 2000 (Fig. 1).

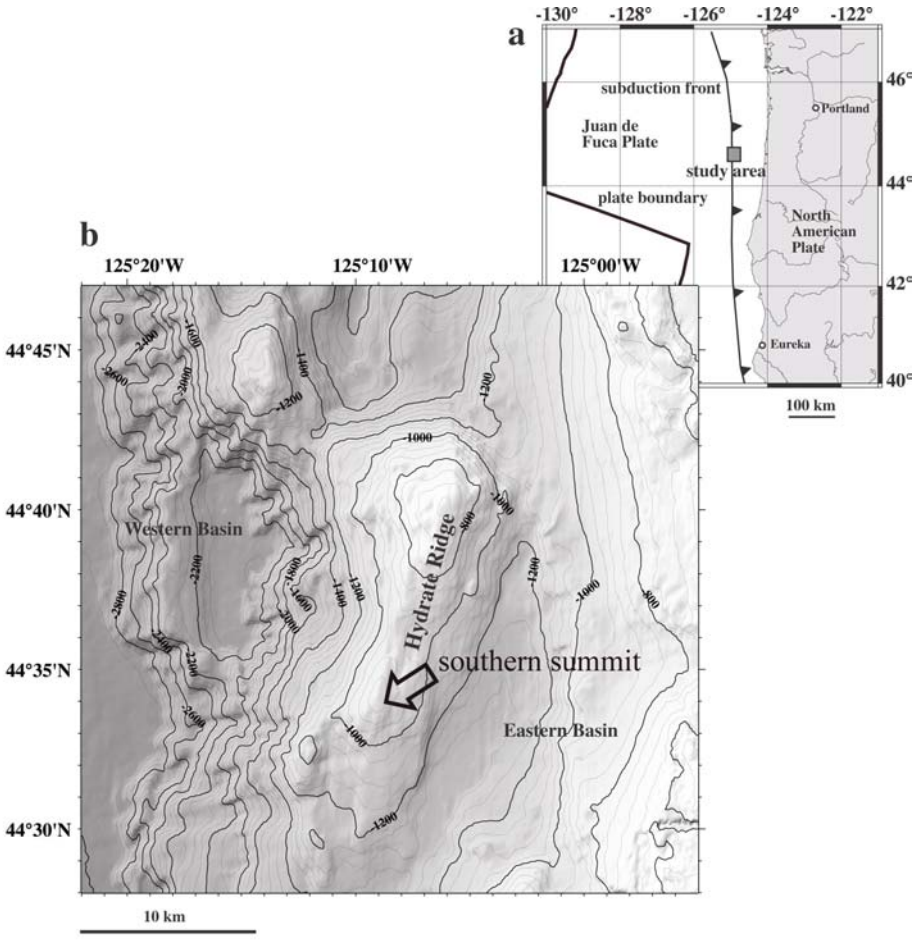

Figure 1. (a) Location of Hydrate Ridge on the Cascadia convergent margin off the Oregon coast. (b) Topographic map of Hydrate Ridge (modified from Sommer et al. 2002)

Referring to recent studies on fluid flow and macrofauna (Sahling et al. 2002, Torres et al. 2002, Tryon et al. 2002), the provinces at HR can be described as follows.

Gas vents. Active gas vents with rapid methane ebullition form gas plumes in the water column. The methane rises together with fluids through conduits from deeper reservoirs marked by the bottom simulating reflector (BSR) where free gas accumulates below the hydrate stability zone. The fluid-flow rate is about 10^6 to 10^7 cm yr^{-1} during maximum discharge. The methane content of the discharging gas is 99%.

Beggiatoa *fields.* Dense mats of filamentous chemosynthetic bacteria (*Beggiatoa* spp.) form white patches on surface sediments of decimeters to decameters in scale (Fig. 2). Methane hydrates, formed during transient gas injection, are located in the uppermost sediment layers. Fluid flows are directed upward at rates of 10 to 250 cm yr^{-1}. The dissolved methane is in equilibrium with methane hydrates. Hydrogen sulfide is present in high amounts (up to 26 mM) in the top 5 cm of the sediment.

Calyptogena *fields.* Vesicomyid clams (*Calyptogena* spp.), which harbor chemosynthetic bacteria in their gills, cover surface sediments in fields of meters to decameters in scale. These fields are either adjacent to *Beggiatoa* fields or occur separately. Whereas gas vents and *Beggiatoa* fields are presumably directly coupled to deeper flow systems, the processes at *Calyptogena* fields may only peripherally be linked to fluid-flow conduits. Here, an upward fluid-flow rate of 2 to 10 cm yr^{-1} occurs alternatively with periods of seawater down-flow caused by the pumping activity of the clams. High concentrations of hydrogen sulfide (>10 mM) occur below 5 cm sediment depth.

Acharax *fields.* The solemyid bivalve *Acharax* sp. harbors chemosynthetic bacteria in their gills. In contrast to *Calyptogena,* these bivalves live in the sediment in U-shaped burrows connected at both ends to the sediment surface. *Acharax* fields are located marginal to *Calyptogena* fields relative to the seeps, and the bivalves are hypothesized to "mine" the sediment to meet their hydrogen sulfide demand. Hydrogen sulfide is not present in the upper 15 cm and increases at low levels (0.1 to 0.3 mM) within 15 to 25 cm.

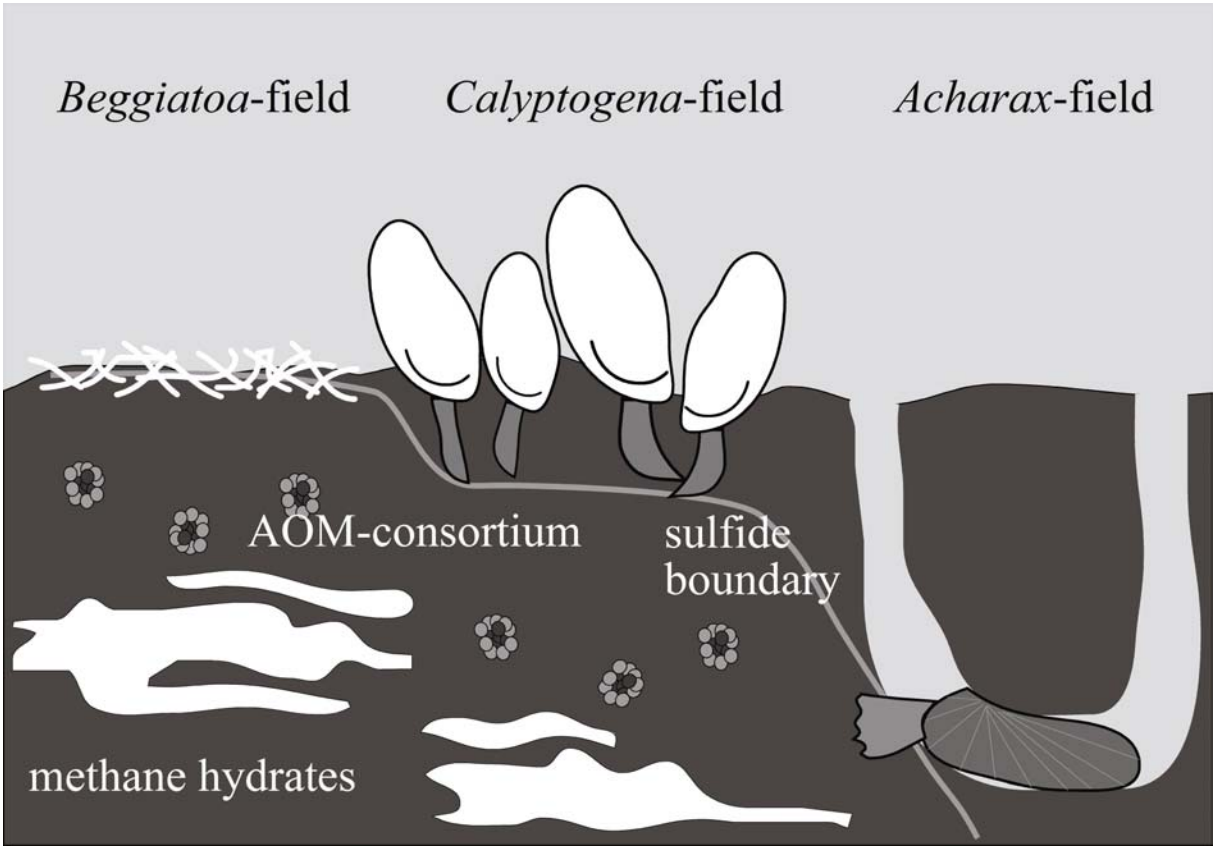

Figure 2. Scheme of the chemosynthetic communities at Hydrate Ridge (after Sahling et al. 2002)

Sampling. Surface sediments from chemosynthetic communities (*Beggiatoa*, *Calyptogena* and *Acharax* fields) were obtained using a video-guided multicorer equipped with 4 cores. After recovery, cores were immediately transferred to a cold (4°C) laboratory.

Field measurements: Samples were taken from 2 *Beggiatoa*, 1 *Caplytogena*, and 1 *Acharax* field (Table 1). Three cores per deployment were subsampled vertically with push-cores (acrylic core liners with an inner diameter of 26 mm) for measurements of AOM and SR (3 to 5 replicates each). Hence, average values from 1 station represent an area of almost 1 m^2. Using a whole core injection (WCI) method (Jørgensen 1978), radioactive tracers, i.e. $^{14}CH_4$ (dissolved in water, injection volume 10 µl, activity 1 kBq) and $^{35}SO_4$ (dissolved in water, injection volume 6 µl, activity 50 kBq), were each injected into separate replicate push-cores at 1 cm depth intervals to obtain rates of AOM and SR, respectively. The replicates were incubated on board at in situ temperature (4 to 5°C, Suess et al. 1999) for 24 hr in the dark. To stop bacterial activity, the upper 10 cm of the sediment cores were sectioned into 1 cm intervals and mixed with 25 ml sodium hydroxide (2.5% w/w) or 20 ml zinc acetate (20% w/w) for AOM and SR, respectively. The samples from control push-cores

were fixed before tracer addition. Fixed AOM samples were stored cooled in heat-welded, gas-tight bags (4 layers: 80 µm nylon, 6 µm ethylenevinyl alcohol, 80 µm nylon, 160 µm polyethylene) without headspace at 4°C. Fixed SR samples were stored in 50 ml Corning vials.

Potential rates. To insure that the applied short-term radiotracer incubation method is suitable to quantify the ratio between AOM and SR, we compared the method with a long-term in vitro incubation method (Nauhaus et al. 2002). By the latter method, AOM and SR rates are calculated, over long time periods (2 mo), from the simultaneous decrease of methane and the production of sulfide, respectively. Samples were taken from the 1 to 4 cm horizon in 2 *Beggiatoa* cores (Table 1). The sediment was stored anoxically in glass bottles without headspace at 4°C until the experiment started. Radioactive tracers, i.e. $^{14}CH_4$ (dissolved in water, injection volume 50 µl, activity 13 kBq) and $^{35}SO_4$ (dissolved in water, injection volume 10 µl, activity 100 kBq), were each injected into 5 gas-tight glass syringes filled with 4 cm^3 sediment slurry, and incubated for 27 hr at 12°C. A description of the preparation of the sediment slurry is given in Nauhaus et al. (2002). The incubation temperature corresponded to the temperature optimum of the AOM consortium at this site (Nauhaus et al. 2002). The glass syringes were filled under an anoxic atmosphere of N_2 and sealed without introducing gas bubbles. At the beginning of the incubation, the methane and sulfate concentration of the slurry pool was 0.82 mmol l^{-1} sediment and 14.5 mmol l^{-1} pore water, respectively. The slurry contained 0.2 g dry sediment cm^{-3}. After incubation the activity was stopped as described for whole-core injection and samples were transferred into 50 ml glass bottles and closed quickly with rubber stoppers (1.5 cm thickness). The glass bottles were shaken thoroughly to equilibrate the pore water methane between aqueous and gas phases. Controls were fixed before tracer addition.

Table 1. Station data of investigated provinces during RV "Sonne"cruise 148/1. WCI: Whole core injection; S: sulfate, P: porosity; A: aggregates; M: modeling

Station No.	Province	Date	Position	Depth (m)	Methods and Measurements
19-2	*Beggiatoa* -field (1)	27.07.2000	44°34.104N; 125°08.807W	777	WCI, S, P, A, M
14	*Beggiatoa* -field (2)	26.07.2000	44°34.218N; 125°08.804W	777	WCI, S, P, A, M
28	*Beggiatoa* -field (3)	28.07.2000	44°34.196N; 125°08.816W	777	in vitro stoichiometry
29	*Beggiatoa* -field (4)	28.07.2000	44°34.222N; 125°08.834W	777	in vitro stoichiometry
38	*Calyptogena* -field	30.07.2000	44°34.186N; 125°08.847W	787	WCI, S, P, A, M
51	*Acharax*- field	01.08.2000	44°34.198N; 125°08.858W	775	WCI, S, P, A, M

Analytical procedures. ***Methane analysis:*** AOM samples were transferred from gas-tight bags into 50 ml glass bottles. The glass bottles were closed quickly with rubber stoppers and shaken thoroughly as described above. To measure the total methane concentration of the sample, a 200 µl aliquot of the headspace was injected into a gas chromatograph (5890A, Hewlett Packard) equipped with a packed stainless steal Porapak-Q column (6 ft., 0.125 in, 80/100 mesh, Agilent Tecknologie) and a flame ionization detector. The carrier gas was helium at a flow rate of 30 ml min^{-1}. The column temperature was 40°C.

Measurement of $^{14}CH_4$: To measure $^{14}CH_4$, a slightly modified method of Iversen & Blackburn (1981) was used. The complete headspace of the sample was purged by a slow flow (25 ml min–1) of artificial air through a heated (850°C) quartz tube filled with Cu(II)-oxide. In the tube, the 14CH4 was oxidized to 14CO2, which was captured in 2 successive scintillation vials (20 ml) filled with a mixture of 1 ml phenylethylamine and 7 ml ethyleneglycolmonomethylether. After the addition of 10 ml scintillation cocktail (Ultima Gold XR, Packard), the sample activity was measured by scintillation counting (2500TR LSC, Packard).

Measurement of $^{14}CO_2$ (diffusion method): To determine the amount of microbially produced $^{14}CO_2$, a modified method of Boetius et al. (2000a) was used. The sample was quantitatively transferred into a 100 ml glass bottle. One drop of antifoam and 1 ml of bromothymol blue (transition range pH 5.8-pH 7.6, yellow-blue) were added to avoid foaming and to check the sample pH. As a trap for CO_2, a scintillation vial (20 ml) was prepared with a folded filter (#1001824, grade 1, Whatman) wetted with 4 ml phenylethylamine and placed on top of the sample inside the glass. The glass was closed with a rubber stopper (butyl, thickness 2 cm) and fixed with a screw cap. Six ml of hydrochloric acid (6M) was injected through the rubber stopper to degas the CO_2. The sample was left for 48 hr to capture the escaped $^{14}CO_2$ on the filter. After 24 hr, the pH was checked visually and additional hydrochloric acid was added if the pH of the sample had become alkaline. After 48 hr, the scintillation vial was removed and 6 ml ethanol were added to dissolve crusts formed by the reaction of CO_2 with phenyethylamine. After dissolution, 10 ml scintillation cocktail (Ultima Gold XR, Packard) was added and the activity of the sample was measured by scintillation counting (2500TR LSC, Packard). This method produced an average $^{14}CO_2$ recovery of 98% in prior tests.

Calculation of AOM: AOM rates were calculated by the following equation (Eq. 2):

$$AOM = \frac{^{14}CO_2 \times CH_4}{^{14}CH_4 \times v \times t} \quad (2)$$

where $^{14}CO_2$ is the activity of the produced radioactive carbon dioxide, CH_4 is the total amount of methane in the sample, $^{14}CH_4$ is the activity of the radioactive methane, v is the volume of the sediment, and t is the incubation time. This calculation is based on the ratio of methane to radioactive methane. It is assumed that any losses of CH_4 during incubation or storage occur at the same ratio for $^{14}CH_4$ as for $^{12}CH_4$.

Sulfate analysis: Samples were taken vertically with a push-core (inner diameter 26 mm; Table 1) from one core of each multicorer haul. Pore-water sulfate concentrations were measured using nonsuppressed ion chromatography with an autosampler (Spark Holland Basic and Marathon, injection volume 50 µl), an anion exchange column (LCA A14, Sycam) and a conductivity detector (S3110, Sykam). The eluant was a 7.5 mM Na_2CO_3 solution. The flow rate was set to 1.75 ml min^{-1}.

Sediment porosity: Samples were taken vertically with a push-core (inner diameter 26 mm; Table 1) from one core of the multicorer. Porosity was determined by drying a known volume of sediment. The wet sediment was weighed, lyophilized, and weighed again. From the difference of the 2 weights, the proportion of sediment dry mass and the porosity was calculated.

Sulfate reduction analysis: SR rates were determined using the single step acidic Cr-II method according to Fossing and Jørgensen (1989).

Bacterial counts: Samples were taken vertically with a push-core (inner diameter 26 mm) from one of the 3 cores which were also sampled for AOM and SR. The push-core was split into 1 cm intervals. One cm^3 of sediment from each depth interval was transferred into vials filled with 9 ml formaldehyde (2% in seawater, 0.22 µm filtered) and stored at 4°C. Aggregates of the AOM consortium were counted by applying acridine orange direct counts (AODC) according to Meyer-Reil (1983) as modified by Boetius & Lochte (1996). The consortia have a specific size and shape that can easily be recognized under the microscope when stained with AODC (Boetius et al. 2000b). In Hydrate Ridge sediments, nearly all cell aggregations have been identified as AOM consortia by a detailed study using fluorescence in situ hybridization (Knittel et al. 2003). Hence, at this location the simpler method of AODC counts can be used to obtain quantitative numbers of consortia in these sediments.

Numerical transport-reaction model. A transport-reaction model was applied for *Beggiatoa* fields 1 and 2 (Table 1) to estimate the change of methane concentrations over time in the surface sediments of these open and dynamic sedimentary environments. The model considers molecular diffusion and advection of dissolved sulfate and methane, and the specific rate of AOM. It is based on a system of 2 coupled differential equations (Eqs. 3 & 4) describing the concentration-depth profiles of dissolved sulfate and methane:

$$\Phi \cdot \frac{\partial [SO_4^{2-}]}{\partial t} = \frac{\partial \left(\Phi \cdot \frac{D_S}{\Theta^2} \cdot \frac{\partial [SO_4^{2-}]}{\partial x} \right)}{\partial x} - \Phi \cdot v \cdot \frac{\partial [SO_4^{2-}]}{\partial x} - \Phi \cdot R_{AOM} \qquad (3)$$

$$\Phi \cdot \frac{\partial [CH_4]}{\partial t} = \frac{\partial \left(\Phi \cdot \frac{D_M}{\Theta^2} \cdot \frac{\partial [CH_4]}{\partial x} \right)}{\partial x} - \Phi \cdot v \cdot \frac{\partial [CH_4]}{\partial x} - \Phi \cdot R_{AOM} \qquad (4)$$

where t is time, x is sediment depth, $[CH_4]$ and $[SO_4^{2-}]$ are concentrations of dissolved methane and sulfate in sediment pore-waters, D_S and D_M are molecular diffusion coefficients of sulfate and methane, Φ and Θ are sediment porosity and tortuosity, v is the velocity of vertical fluid flow, and R_{AOM} is the specific rate of AOM.

Sediment porosity changes with depth due to sediment compaction. The depth profile is approximated using the following exponential function (Berner 1980) (Eq. 5):

$$\Phi = \Phi_f + (\Phi_i - \Phi_f) \cdot e^{-p \cdot x} \qquad (5)$$

where the parameter values for Φ_f (porosity at infinite depth), Φ_i (porosity at zero depth), and p (attenuation coefficient for the exponential decrease of porosity with depth) are determined by fitting the porosity model to the corresponding porosity data.

Sediment tortuosity was calculated from porosity using the following empirical relation (Boudreau 1997) (Eq. 6):

$$\Theta^2 = 1 - \ln(\Phi^2) \qquad (6)$$

The rate of vertical fluid flow was calculated considering sediment burial, steady state compaction, and upward flow of deep-derived vent fluids (Luff & Wallmann 2003) (Eq. 7):

$$v = \frac{w_f \cdot \Phi_f - v_i \cdot \Phi_i}{\Phi} \qquad (7)$$

where w_f is sedimentation rate and v_i the rate of fluid flow at the sediment water interface. The fluid-flow velocity can be determined by fitting the model curves to measured sulfate pore-water profiles (Luff & Wallmann 2003).

The kinetic rate law for AOM was derived using recently published experimental data (Nauhaus et al. 2002) and unpublished results (K. Nauhaus, pers. comm.). Ongoing incubation studies show that specific AOM rates (R_{AOM}) are accelerated at high methane concentrations while the concentration of sulfate has no significant effect on the rate as long as sulfate concentration is greater than approximately 1 to 2 mM. A reasonable first order approximation of the rate law might thus be (Eq. 8):

$$R_{AOM} = k_{AOM} \cdot [CON] \cdot [CH_4] \cdot \frac{[SO_4^{2-}]}{K_S + [SO_4^{2-}]} \qquad (8)$$

where k_{AOM} is a kinetic constant, [*CON*] is the concentration of aggregates of the AOM consortium and K_S is a Monod constant (K_S = 1 mM) defining the inhibition of AOM at low sulfate concentrations (Nauhaus et al. 2002). Nauhaus et al. (2002) determined an AOM rate of 5 mol g^{-1}dry wt d^{-1} in an experimental incubation of sediments taken from an active vent site at the crest of the southern Hydrate Ridge during RV Sonne expedition 148. Prior to incubation, sediments were mixed with anoxic seawater to obtain a slurry with 0.2 - 0.3 g dry sediment cm^{-3}. The methane concentration in the slurry was approximately 15 mM and the slurry contained on average 9 x 10^7 aggregates per g sediment dry wt (Nauhaus et al. 2002). From these data, the value of the kinetic constant k_{AOM} can be derived as 3.7 x 10^{-9} cm^3 d^{-1}.

Boundary conditions were defined at the interface between surface sediment and overlying *Beggiatoa* mat and at the base of the model column at 20 cm sediment depth (Table 2). At the upper boundary, sulfate and methane concentrations were set to constant values corresponding to seawater concentrations ($[CH_4](x = 0) = M0 = 0$ mM, $[SO_4^{2-}](x = 0) = S0 =$ 29 mM). At the lower boundary the concentrations were set to constant values corresponding to the concentrations prevailing in the rising vent fluids ($[CH_4](x = 20) = ML = 68$ mM,

$[SO_4^{2-}](x = 20) = SL = 0$ mM**)**. The rising fluids were assumed to be in equilibrium with gas hydrates due to the widespread occurrence of hydrates in HR sediments. Therefore, the methane concentration applied at the lower boundary corresponds to the saturation value at the pressure and temperature conditions prevailing at HR (Luff & Wallmann 2003).

The model was run to steady state starting from arbitrary initial conditions. Due to the high reaction rates and flow velocities, steady state was usually attained within a few years. MATHEMATICA version 4.1 was used to implement the model and MATHEMATICA's NDSolve object was applied for the numerical integration of the differential equations. NDSolve uses the Method-of-Lines code for integration, a finite difference procedure which has been frequently applied in the modeling of early diagenetic processes (Boudreau 1996, Luff et al. 2000, Luff & Wallmann 2003).

Table 2. Parameter values used in the modelling (Luff and Wallmann, 2003)

Parameter	Symbol	Value
Length of the model column	L	20 cm
Sulfate concentration at zero depth	SO	28.9 mM
Sulfate concentration at 20 cm depth	SL	0 mM
Methane concentration at zero depth	MO	0 mM
Methane concentration at 20 cm depth	ML	68 mM
Molecular diffusion coefficient of sulfate at 4.2°C	D_S	185 $cm^2\ a^{-1}$
Molecular diffusion coefficient of methane at 4.2°C	D_M	334 $cm^2\ a^{-1}$
Sedimentation rate at infinitive depth	W_f	0.0275 cm a^{-1}
Kinetic constant for AOM	k_{AOM}	1.35 10^{-6} $cm^3\ a^{-1}$

RESULTS

Field measurements.

Beggiatoa field 1

AOM reached a maximum rate of 0.24 µmol $cm^{-3}\ d^{-1}$ (Fig. 3a) between 4 and 5 cm sediment depth. Peaks of AOM in replicate cores (>0.04 µmol $cm^{-3}\ d^{-1}$, n = 3) were distributed between 2 and 7 cm. In all replicates, AOM was low in the uppermost centimeter of the sediment (around 0.02 µmol $cm^{-3}\ d^{-1}$). Integrated over 0 to 10 cm sediment depth, the mean AOM was 5.1 (±4.4, n = 3) mmol $m^{-2}d^{-1}$ (Table 3). SR was an order of magnitude higher than AOM (with a maximum rate of 2.07 µmol $cm^{-3}\ d^{-1}$ between 4 and 5 cm, n = 5), but followed a similar depth pattern. Three replicates showed peaks (>0.4 µmol $cm^{-3}\ d^{-1}$) between 3 and 6

cm. All replicates had low rates at the sediment surface (around 0.12 µmol cm^{-3} d^{-1}), except for 1 replicate that showed high activity (1.55 µmol cm^{-3} d^{-1}) between 0 and 1 cm. One replicate had comparably low rates (around 0.04 µmol cm^{-3} d^{-1}) that changed little over depth. Although most of the SR replicates had similar depth patterns, the magnitude of SR peaks varied between 0.12 and 2.07 µmol cm^{-3} d^{-1}. Integrated over 0 to 10 cm sediment depth, the mean SR was 32 (±34, n = 5) mmol $m^{-2}d^{-1}$. Sulfate concentration decreased from 27.1 mM at the sediment surface to 2.0 mM at 6 cm, below which no further decrease was measured. At this depth SR reached a constant low level of around 0.14 µmol cm^{-3} d^{-1} in all replicates. Aggregate counts peaked at a mean of 1.27 x 10^8 cm^{-3} between 3 and 4 cm. Counts were lower at the sediment surface (0.51 x 10^8 cm^{-3}) and below 6 cm (around 0.30 x 10^8 cm^{-3}). Integrated over 0 to 10 cm sediment depth, 6.1 (±3.4) x 10^{12} aggregates m^{-2} inhabited the sediment.

Beggiatoa field 2

Here, AOM reached a maximum rate of 5.5 µmol cm^{-3} d^{-1} between 8 and 9 cm (Fig. 3b). These are the highest rates measured among all investigated provinces. The 4 replicates showed different profiles and magnitudes of activity. In some cases AOM increased beneath 2 cm sediment depth. One replicate had a peak between 2 and 3 cm as well as between 8 and 9 cm. In all replicates, AOM was low at the sediment surface. Integrated over 0 to 10 cm, the mean AOM rate was 99 (±102, n = 4) mmol $m^{-2}d^{-1}$. Sulfate was depleted from 27.9 mM at the sediment surface to 2.6 mM between 4 and 5 cm and stayed constant around 1.8 mM below this depth. Unfortunately, SR was not measured at this station. Aggregate counts were the highest between 2 and 5 cm with around 0.84 x 10^8 cm^{-3}. Another peak (0.82 x 10^8 cm^{-3}) was located at the sediment surface. Integrated over 0 to 8 cm sediment depth, 5.1(±3.0) x 10^{12} aggregates m^{-2} inhabited the sediment.

Calyptogena field

Rates of AOM and SR were variable between replicates as observed in *Beggiatoa* field 1. AOM rates of the 5 replicates were within the range of those observed in the *Beggiatoa*-samples (Fig. 3c). Rates reached a maximum of 2.70 µmol cm^{-3} d^{-1} between 3 and 4 cm. Except for one replicate that showed a distinct maximum between 2 and 5 cm, peaks were difficult to define for the other replicates. In some cores, AOM increased sharply (>0.30 µmol

cm^{-3} d^{-1}) beneath the surface and decreased again towards the deepest layer. In all replicates, AOM was low (<0.15 µmol cm^{-3} d^{-1}) beneath 9 cm. The same was true for the topmost layer (<0.30 µmol cm^{-3} d^{-1}) except for one replicate that exhibited a rate of 1.26 µmol cm^{-3} d^{-1}. Integrated over a 0 to 10 cm sediment depth, mean AOM was 56 (±54, n = 5) mmol $m^{-2}d^{-1}$. SR reached a maximum of 3.56 µmol cm^{-3} d^{-1} between 4 and 5 cm (n = 5). In 3 replicates, distinct peaks (>1 µmol cm^{-3} d^{-1}) were observed between 3 and 8 cm. Two replicates remained low compared to the others (around 0.26 µmol cm^{-3} d^{-1}) over the whole depth profile. At the surface as well as beneath 8 cm, SR dropped below 0.30 and 0.50 µmol cm^{-3} d^{-1}, respectively. Integrated over a 0 to 10 cm sediment depth, the mean SR was 65 (±58, n = 5) mmol $m^{-2}d^{-1}$. Comparing integrated rates of AOM and SR, a ratio of about 1:1 was observed. Sulfate concentration decreased continuously between 3 and 8 cm from 25.1 to 2.0 mM. Below 8 cm, sulfate concentration appeared to stay constant around 2 mM. Aggregate counts peaked between 1 and 2 cm (1.39 x 10^8 cm^{-3}) as well as between 8 and 9 cm (1.27 x 10^8 cm^{-3}). Above, between and below these maxima, aggregate counts were around 0.65 x 10^8 cm^{-3}. Integrated over a 0 to 10 cm sediment depth, 7.9 (±5.3) x 10^{12} aggregates m^{-2} inhabited the sediment.

Tabel 3. AOM, SR and aggregate counts integrated over 0-10 cm sediment depth. Standard deviations are given.

Field	AOM [mmol $m^{-2}d^{-1}$]	SR [mmol $m^{-2}d^{-1}$]	Aggregates [10^{12} m^{-2}]
Beggiatoa (1)	5.1 ± 4.4	32 ± 34	6.1 (± 3.4)
Beggiatoa (2)	99 ± 102		5.1 (± 3.0)*
Calyptogena	56 ± 54	65 ± 58	7.9 (± 5.3)
Acharax	2.1 ± 1.4	0.4 ± 0.3	0.4 (± 0.6)

*integrated over 0-8 cm sediment depth

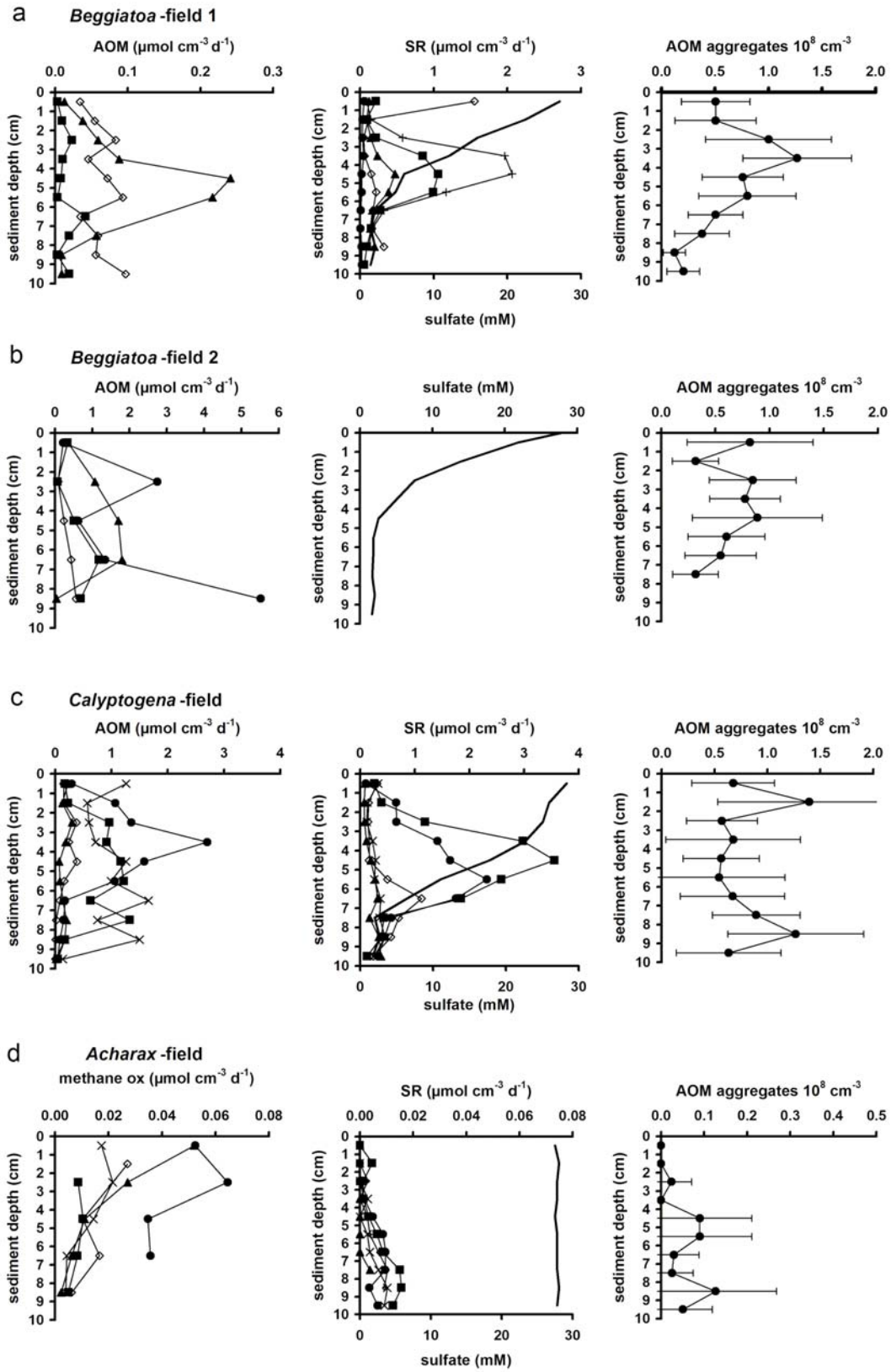

Figure 3. AOM and SR rate, sulfate concentration (—) and aggregate density (mean of counted grids, n = 25, 17, 30 and 20, respectively; standard deviation is given) of *Beggiatoa* field 1 (a) and 2 (b), *Calyptogena* field (c) and *Acharax* field (d). For *Beggiatoa* field 2 no SR was measured. Replicates are depicted with different symbols.

Acharax field

Methane oxidation, SR and aggregate profiles differed considerably from those at the *Beggiatoa* and *Calyptogena* fields. Methane oxidation reached a maximum of only 0.065 µmol cm^{-3} d^{-1} (Fig. 3d). The highest rates of all replicates were located at the top of the sediment and decreased with depth. Mean methane oxidation was 2.1 (±1.4, n = 5) mmol $m^{-2}d^{-1}$ integrated over 0 to 10 cm. SR reached a maximum of only 0.0016 µmol cm^{-3} d^{-1}. No SR was found at the sediment surface. Low rates ($\leq$ 0.005 µmol cm^{-3} d^{-1}) were detected between 1 and 5 cm. Below 5 cm, SR increased continuously with depth and reached a maximum between 7 and 9 cm. Integrated over 0 to 10 cm sediment depth, the mean SR was 0.4 (±0.3, n = 5) mmol $m^{-2}d^{-1}$. Sediment sulfate concentration was 27.8 mM and did not change over the whole sediment profile. Except for the depth section between 2 and 3 cm, no aggregates were found in the uppermost 4 cm. Below 4 cm, mean aggregate counts increased up to 0.13 x 10^8 cm^{-3} between 8 and 9 cm. Integrated over 0 to 10 cm sediment depth, only 0.4 (±0.6) x 10^{12} aggregates m^{-2} inhabited the sediment.

Potential rates

Potential rates of AOM and SR measurements in vitro were 0.58 and 0.89 µmol g^{-1}dry wt d^{-1}, respectively, averaged for all 5 replicates. The replicates had a good reproducibility with relatively low standard deviations (AOM ± 0.10 µmol g dry wt^{-1} d^{-1}, SR ± 0.08 µmol g^{-1} dry wt d^{-1}). SR rates were similar in comparison to those measured in long-term incubations at the respective methane concentration (about 0.5 µmol g^{-1} dry wt d^{-1}, Nauhaus et al. 2002). The ratio of AOM to SR was 0.7:1 in the present short-term radiotracer incubations compared to a ratio of 0.9:1 in long-term incubations. The ratio between AOM and SR indicates a close coupling between the 2 processes when compared with non-seep locations, where SR is fueled by degradation of organic matter and SR rates exceed AOM rates by a factor of 10 (Hinrichs & Boetius 2002).

DISCUSSION

The coupling of AOM and SR

Beggiatoa- and *Calyptogena* fields

A comparison of AOM and SR rates indicates that SR is fueled mainly by methane at fluid impacted sites of HR, as also suggested by Boetius et al. (2000b). However, the ratio between the 2 processes differed between the investigated fields: SR appeared to be 80 to 90% methane-dependent at the *Calyptogena* field. At the *Beggiatoa* field 1, average SR was 6-fold higher than average AOM. However, the peak of SR fell close to the peak of AOM biomass. A first conclusion would be that the sulfate-reducing bacteria of the AOM consortium at *Beggiatoa* field 1 may have used carbon sources other than methane to some extent. However, in vitro experiments with slurries from HR sediments demonstrated that methane-independent SR is low compared to slurries amended with methane (Nauhaus et al. 2002). Additional carbon sources such as the decaying parts of the *Beggiatoa*-mat or higher hydrocarbons can be ruled out as an explanation for discrepancies between AOM and SR. The growth rate of the *Beggiatoa* community (5.0 mmol C $m^{-2}d^{-1}$, Sommer et al. 2002), which should approximately balance decay, is only half of the maximum carbon input of deposited organic matter in this region (9.2 mmol C $m^{-2}d^{-1}$, Sommer et al. 2002). The presence of ethane, propane and butane was confirmed within the uppermost 10 m of the southern summit during cruise 204 of the Ocean Drilling Program (Trehu et al. in press), but concentrations did not even reach 1% of methane (C_1:$C_{2\ to\ 4} \geq 1000$). Therefore we hypothesize that the discrepancies between AOM an SR were attributed to both methodical problems, caused by methane losses during decompression and incubation, and the heterogeneity of the sediment. It has to be kept in mind that AOM and SR were measured in different cores. The system at the high fluid-impacted fields might be so variable that samples taken only centimeters apart from each other show such high variations. This heterogeneity could be caused by transient gas injections from the lower reservoir or by changes in pathways of fluids and gases. Authigenic carbonates that precipitate in surface sediments at HR as a product of AOM could redirect or inhibit rising gasses and fluids (Bohrmann et al. 1998). The close coupling between potential AOM and SR rates that was observed in the homogenized sediment confirms this assumption. A scheme illustrating the causes of heterogeneity at HR is shown in Fig. 4.

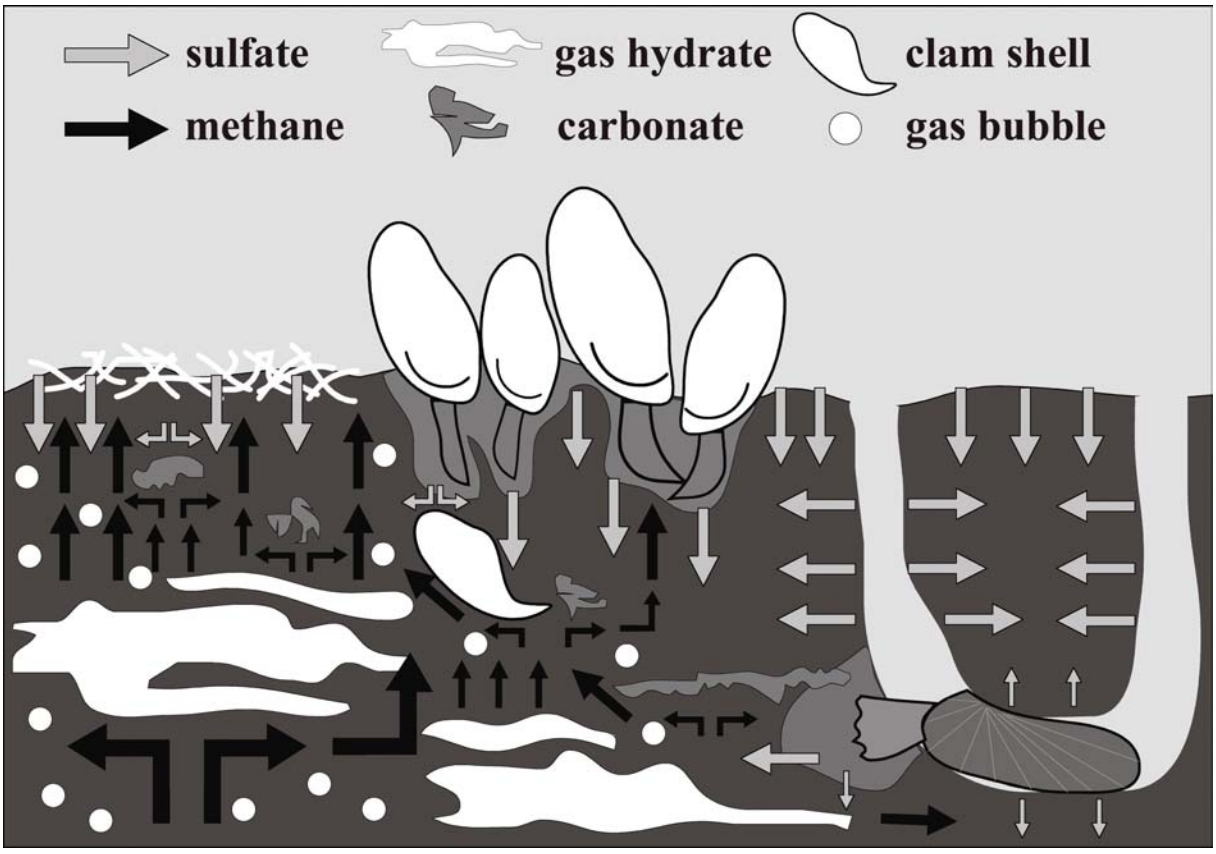

Figure 4. Scheme illustrating heterogeneity of surface sediments at HR causing high deviations in AOM and SR replicates

Acharax field

There is not enough methane supply to fuel a dense AOM community in the surface sediments of *Acharax* fields, which are located adjacent to the *Calyptogena* fields at HR seeps. Here, methane fluxes are significantly lower compared to other HR provinces and sulfide does not appear until 15 cm sediment depth (Sahling et al. 2002). Upward diffusing methane is most likely oxidized aerobically within the oxygenated surface sediment. Aerobic methane oxidation is also measured by the $^{14}CH_4$ injection method and can not be distinguished from AOM. Methane oxidation was not coupled to SR, but took place close to the sediment surface where oxygen was available. In contrast, SR was highest towards the bottom of the sediment cores. The SR rates are in the same order of magnitude compared to slope sediments (620 m water depth) off Washington coast (0.66 mmol m^{-2} d^{-1}, integrated over 0 to 30 cm sediment depth, Kristensen et al. 1999) and are therefore presumably not influenced by methane venting. Thus, SR seems to be solely fueled by organic matter deposited from the water column.

The role of sulfate

At the *Beggiatoa* field 1 and the *Calyptogena* field, SR decreased to low rates when sulfate dropped to concentrations around 2 mM. Below this zone, no further sulfate depletion was observed down to 10 cm sediment depth. At *Beggiatoa* field 2, sulfate concentration also did not decrease below 2 mM. It is unclear why sulfate is not depleted to zero as long as methane is available. A similar threshold value was observed in subsurface sediments of another gas hydrate location in the Gulf of Mexico (S. Joye, pers. comm.). Low sulfate concentrations accompanied by high sulfide concentrations, reaching values up to 26 mM below the sediment surface (Sahling et al. 2002), might make AOM thermodynamically unfavorable. It is possible that sulfide was toxic at these levels. For both *Beggiatoa* fields the drop in sulfate concentration was also accompanied with a decrease in aggregate numbers, again showing the coupling of AOM, SR and the biomass of the methanotrophic community.

Spatial and temporal variability of AOM

AOM rates at HR are among the highest ever measured in marine sediments (compare with Hinrichs & Boetius 2002 and references therein). Typically, marine sites with high rates of AOM are permanently supplied with large amounts of methane seeping from deep reservoirs. A special situation appears when methane seepage occurs within the gas hydrate stability zone, causing the formation of methane hydrates. Methane hydrates represent a temporary storage of methane (Kvenvolden 1993). At the stability limit, dissociating hydrates provide a steady flow of methane into the AOM zone replenishing the methane that has been consumed by the AOM consortium. When methane concentration surpasses saturation, free gas escapes as rising gas bubbles which bypass the AOM zone (Luff & Wallmann 2003). At HR, where methane hydrates form within the upper meter of the seafloor, AOM can be expected to reach high rates due to a steady supply of methane from below and input of sulfate from above.

Beggiatoa fields

Except for gas vents, *Beggiatoa* fields at HR are the provinces with the highest methane fluxes as well as the largest variation in fluxes (Torres et al. 2002, Tryon et al. 2002). Thus, maximum rates and a high patchiness of AOM were expected and observed. *Beggiatoa* field 2

revealed the highest AOM rates of all investigated sites. The peak rate agreed with estimates of Boetius et al. (2000b), who predicted a maximum AOM rate of about 5 μmol cm^{-3} d^{-1} at HR from SR measurements. But the comparably low rates found in *Beggiatoa* field 1 indicate that AOM may vary over an order of magnitude in this province. Variation in methane concentration were most likely responsible for differences in AOM, as both fields contained about the same amount of AOM consortia and showed similar sulfate profiles. High variation of AOM between replicates of the same deployment again signify that heterogeneity occurs even within small dimensions (i.e. <1 m^2; see also Fig. 4).

Based on methane effluxes between 10 and 100 mmol m^{-2} d^{-1} from the *Beggiatoa* fields into the overlying water column (Torres et al. 2002) and an AOM rate of about 100 mmol $m^{-2}d^{-1}$ (this study), we assume that the microbial filter is able to consume between 50 and 90% of the methane that is advectively transported through the surface sediments of *Beggiatoa* fields. Unpredictable variations of methane fluxes due to transient gas injection might account for releases of methane into the overlying water.

Peak rates of AOM located immediately below the *Beggiatoa*-mat (1 to 2 cm) as predicted from former investigations on SR rates (Boetius et al. 2000b), flux modeling (Luff & Wallmann 2003) and FDA (determination of exoenzymatic hydrolytic activity using fluorescein-di-acetate as substrate; Sommer et al. 2002), were not found in this study. In contrast, AOM rates in both *Beggiatoa* fields were low close to the sediment surface, with maxima always located below 2 cm depth.

Calyptogena field

Maximum SR and a rapid decline in sulfate concentration occurred below 3 cm sediment depth. We expected that the digging and pumping activity of the clams would affect the upper 3 to 4 cm of the sediment by irrigating the sediment with oxygenated seawater (Sahling et al. 2002). The energy supply of *Calyptogena* is based on sulfide-oxidizing bacteria, which are harbored in the gills of the clams (Fisher 1990). The clams dig their feet into the reduced sediments to take up sulfide. Sulfide is transported to the gills via sulfide-binding compounds in the clam blood where it is oxidized by the symbionts. We hypothesize that the digging and pumping activity of the clams enriches the upper sediment with oxidizing agents (e.g. O_2, NO_3^-) that may be toxic for the AOM consortium and therefore shift SR below the penetration depth of the clams' feet. The pumping activity of the clams is expected to enrich the sediment also with sulfate and thus to stimulate SR after the depletion of prior oxidizing

agents. The maximum AOM was also located below the depth of foot penetration but reached appreciable rates above that depth as well. It has to be taken into account that the uppermost rates represented aerobic oxidation of methane as they exceeded SR. The presence of aerobic methanotrophs in surface sediments of the *Calyptogena* fields has been confirmed in laboratory studies (A. Eppelin & M. Krueger unpubl.).

Methane effluxes into the overlying water column from *Calyptogena* fields are reported to be of a 1 to 2 order of magnitude lower than *Beggiatoa* fields (between 0 and 1 mmol m^{-2} d^{-1}, Torres et al. 2002). Considering that AOM rates were about 56 mmol $m^{-2}d^{-1}$ at the *Calyptogena* field, this would result in a consumption of 99.8 to 100% of the upward diffusing methane. Within this province, constant methane fluxes and a steady sulfate supply due to the pumping activity of the clam provide stable conditions for the AOM consortium. Methane is therefore removed efficiently before it reaches the overlying water. Deviations of AOM in replicates of the same deployment could be due to clam activity, uneven distribution of gas hydrates or the presence of carbonates (see also Fig. 4).

It has to be mentioned at this point that although highest methane turnover was found at *Beggiatoa* field 2, the integrated AOM rates within the *Calyptogena* field are nearly as high as the average depth-integrated AOM rates of the 2 *Beggiatoa* fields. We assume that AOM at the *Beggiatoa* fields is highest, but most variable due to fluctuating gas discharges. Gas discharge from greater depths thus represents a temporally variable methane supply in addition to methane supply from dissociating gas hydrates. In contrast, AOM at the *Calyptogena* fields should be relatively stable due to a permanent methane supply from dissociating gas hydrates. Further investigations of the different provinces are needed to confirm this assumption.

Acharax field

The methane oxidation in the uppermost layers of the *Acharax* field most likely represents aerobic processes. A correlation between AOM and SR in deeper parts of the sediment is tenuously based on molecular evidence. Whereas almost no aggregates are present in the assumed aerobic zone, small amounts were found within the zone of increasing SR (below 4 cm). However, signals of AOM specific lipid fatty acids, related to *Desulfosarcina/Desulfococus* (M. Elvert et al. unpubl.), are very weak at this province compared to active vent sites and the $\delta^{13}C$ values are not characteristic for AOM (M. Elvert pers. comm.). Considerable AOM derived biomass is either shifted to deeper parts of the

sediment or the aggregates in the SR zone represent relicts of former venting. *Acharax* fields sometimes include *Calyptogena* shells in deeper sediment layers, and *Acharax* shells were found in both *Calyptogena*- and *Beggiatoa* fields (T. Treude, pers. obs.). This may suggest that the horizontal distribution of methane-seepage at HR surfaces is most likely changing over time.

Numerical transport-reaction model

The transport-reaction model was applied to calculate AOM rates in surface vent sediments covered with *Beggiatoa*-mats. The model input includes measured porosity data and the average depth distribution and density of aggregates of the AOM consortium observed in surface sediments from *Beggiatoa* fields (Fig. 3a,b). The extent and location of the modeled AOM is principally affected by upward fluid flow. It was, however, not possible to measure fluid flow into the surface sediments in situ. Instead, the rate of upward fluid flow was estimated by fitting the dissolved sulfate profile to the measured concentration data. The resulting flow velocities (0 to 10 cm a^{-1}; Table 4) fall into the range of flow rates previously determined by modeling of sulfate profiles (Luff & Wallmann 2003) and are the low end of fluid flow measured in situ at *Beggiatoa* fields (Tryon et al. 2002). In the model, SR occurs only via AOM so that SR and AOM rates always have the same values. This approximation is appropriate for reasons mentioned above.

Table 4. Model results. Porosity at zero depth (P_0), porosity at infinite depth (P_f), attenuation coefficient defining the decrease of porosity with depth (p), upward fluid flow rate (v_i), depth integrated AOM rate, and flux of methane into the overlying bacterial mat and overlying water.

Field	P_0	P_f	p (cm^{-1})	v_i (cm a^{-1})	AOM (mmol m^{-2} d^{-1})	Benthic CH_4 efflux (mmol m^{-2} d^{-1})
Beggiatoa -field (1)	0.75	0.60	0.1	0	13.3	0.6
Beggiatoa -field (2)	0.65	0.65	0	10	15.4	4.0

The AOM rates derived from the model fall into the lower range of values determined by radiotracer measurements (rates between 13.3 and 15.4 mmol m^{-2} d^{-1} in the model (Table 4) compared to rates between 5.1 and 99 mmol m^{-2} d^{-1} in radiotracer measurements (Table 3)). For *Beggiatoa* field 1, the depth distribution of AOM and SR derived from radiotracer measurements and modeling both revealed subsurface maxima at 4 to 6 cm sediment depth (Fig. 5). Here, rising methane and sulfate diffusing into the sediment from the overlying

bottom water meet, allowing AOM and SR to proceed at maximum velocity. Measured AOM rates in *Beggiatoa* field 1 show the same magnitude as modeled rates, whereas measured SR rates revealed maxima up to 1 order of magnitude higher than predicted from the modeled AOM rates. Modeled AOM rates of *Beggiatoa* field 2 are 1 order of magnitude lower compared to measured rates.

The model shows that the major portion (between 79 and 96%) of methane transported to the surface as dissolved gas in rising vent fluids is oxidized anaerobically within the surface sediment (Table 4). The efficiency of methane oxidation depends on the rate of upward fluid flow so that a significant methane fraction can only be expelled into the bottom water at flow velocities >100 cm yr^{-1} (Luff & Wallmann 2003).

Comparison of rate measurement and rate modeling

In the 1-dimensional model approach used in this paper, it was assumed that concentration gradients and changes in reaction rates occur only with sediment depth. The radiotracer measurements revealed a strong lateral heterogeneity which was not anticipated and considered in the model. Thus, it is necessary to develop multi-dimensional models which allow for strong variability in all spatial dimensions to better simulate the complex processes in hydrate-bearing surface sediments. Radiotracer measurements, on the other hand, are not able to mirror exact in situ processes due to degassing methane upon retrieval leading to lowered methane concentrations and disturbances in the cores. However, at *Beggiatoa* fields, both tools came up with similar amounts of depth integrated AOM and its vertical distribution, although concerning different input parameters. It is therefore desirable to combine both tools in future studies in order to understand other highly dynamic systems above gas hydrates.

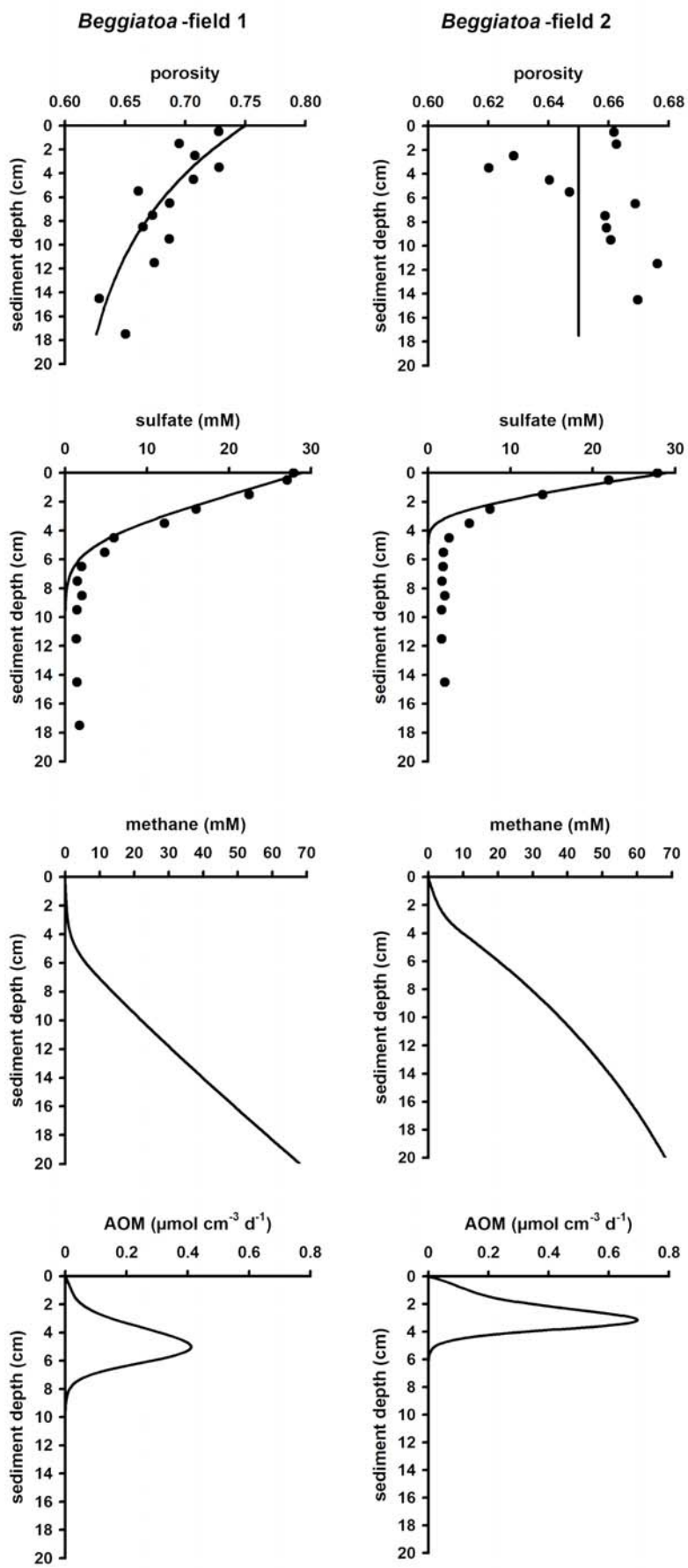

Figure 5. Sediment data and model results. (●) Indicates measured data while (▬) Gives the results of the transport-reaction model.

CONCLUSION

At HR, microbial AOM is an efficient filter for methane preventing its emission from the surface sediments to the hydrosphere as confirmed by modeling and measuring methane turnover. In the surface sediments (<10 cm) of *Beggiatoa* fields, between 50 and 90% of the rising methane is oxidized despite high flow rates , while in *Calyptogena* fields, nearly 100% is oxidized. Measured AOM rates of about 100 mmol $m^{-2}d^{-1}$ are among the highest ever found in methane-bearing sediments of the marine environment. SR is mostly fueled by methane at fluid impacted sites but exceeds AOM in some cases, most likely due to sediment heterogeneity. AOM is highest at *Beggiatoa* fields, where highest fluid flow and methane fluxes occur, followed by *Calyptogena* fields. At *Acharax* fields, methane fluxes are low and limit AOM. Measured AOM and SR rates reveal a high degree of patchiness at both the *Beggiatoa* and *Calyptogena* fields. Fluctuating gas discharges, differences in fluid flow, uneven distribution of gas hydrates and differences in macrofaunal activity may all contribute to this patchiness.

ACKNOWLEDGEMENTS

We thank the officers, crew and shipboard scientific party of RV SONNE for the excellent support during expedition SO-148/1. We particularly thank D. Rickert for providing sulfate and porosity data as well as T. Lösekann, H. Löbner and M. Hartmann for their technical assistance. The manuscript benefited from very helpful comments of K. Nauhaus, B. Orcutt, T. Ferdelman, and 3 anonymous reviewers. This study was made possible by the programs TECFLUX II (Tectonically induced Fluxes, grant 03G0148A), MUMM (Mikrobielle Umsatzraten von Methan in gashydrathaltigen Sedimenten, grant 03G0554A), LOTUS (Long-term observatory for the study of control mechanisms for the formation and destabilization of gas hydrate, grant 03G0565A) and OMEGA (Oberflächennahe Marine gas hydrate, grant 03G0566A) supported by the Bundesministerium für Bildung und Forschung (BMBF, Germany). Further support was from the Max-Planck-Gesellschaft (MPG, Germany). This is publication GEOTECH-20 of the GEOTECHNOLOGIEN program of the BMBF and the Deutsche Forschungsgesellschaft (DFG, Germany).

LITERATURE CITED

Berner RA (1980) Early diagenesis: a theoretical approach. Princeton University Press, Princeton, New Jersey

Boetius A, Lochte K (1996) Effect of organic enrichments on hydrolytic potentials and growth of bacteria in deep-sea sediments. Mar Ecol Prog Ser 140:239-250

Boetius A, Ferdelman T, Lochte K (2000a) Bacterial activity in sediments of the deep Arabian Sea in relation to vertical flux. Deep-Sea Res II 47:2835-2875

Boetius A, Ravenschlag K, Schubert CJ, Rickert D and 6 others (2000b) A marine microbial consortium apparently mediating anaerobic oxidation of methane. Nature 407:623-626

Bohrmann G, Greinert J, Suess E, Torres M (1998) Authigenic carbonates from the Cascadia subduction zone and their relation to gas hydrate stability. Geology 26(7):647-650

Boudreau BP (1996) A method-of-lines code for carbon and nutrient diagenesis in aquatic sediments. Comput Geosci 22(5):479-496

Boudreau BP (1997) Diagenetic models and their implementation. Springer, Berlin

Elvert M, Boetius A, Knittel K, Jørgensen BB (2003) Characterization of specific membrane fatty acids as chemotaxonomic markers for sulfate-reducing bacteria involved in anaerobic oxidation of methane. Geomicrobiology 20:403-419

Elvert M, Greinert J, Suess E, Whiticar MJ (2001) Carbon isotopes of biomarkers derived from methane-oxidizing microbes at Hydrate Ridge, Cascadia Convergent Margin. Geophysical Monograph 124, American Geophysical Union, Washington, DC p 115-129

Fisher CR (1990) Chemoautotophic and methanotrophic symbiosis in marine invertebrates. Rev Aquat Sci 2:399-436

Fossing H, Jørgensen BB (1989) Measurements of bacterial sulphate reduction in sediments: evaluation of a single-step chromium reduction method. Biogeochemistry 8:205-222

Gutt C, Asmussen B, Press W, Merkl C and 5 others (1999) Quantum rotations in natural methane-clathrates from the Pacific sea-floor. Europhys Lett 48(3):269-275

Hinrichs KU, Boetius A (2002) The anaerobic oxidation of methane: new insights in microbial ecology and biogeochemistry. In: G. Wefer, D. Billett, D. Hebbeln et al. (eds) Ocean Margin Systems. Springer, Berlin, p 457-477

Iversen N, Blackburn TH (1981) Seasonal rates of methane oxidation in anoxic marine sediments. Appl Environ Microbiol 41(6):1295-1300

Jørgensen BB (1978) A comparison of methods for the quantification of bacterial sulphate reduction in coastal marine sediments: I. Measurements with radiotracer techniques. Geomicrobiol J 1(1):11-27

Knittel K, Boetius A, Lemke A, Eilers H, Lochte K, Pfannkuche O, Linke P, Amann R (2003) Activity, distribution, and diversity of sulfate reducers and other bacteria above gas hydrate (Cascadia Margin, OR). Geomicrobiol J 20:269-294

Kristensen E, Devol AH, Hartnett HE (1999) Organic matter diagenesis in sediments on the continental shelf and slope of the Eastern Tropical and temperate North Pacific. Continental Shelf Res 19:1331-1351

Kvenvolden K (1993) A primer on gas hydrates. US Geol Surv No. 1570, p 279-291

Luff R, Wallmann K (2003) Fluid flow, methane fluxes, carbonate precipitation and biogeochemical turnover in gas hydrate-bearing sediments at Hydrate Ridge, Cascadia Margin: numerical modeling and mass balances. Geochim Cosmochim Acta 67 (18):3403-3421

Luff R, Wallmann K, Grandel S, Schlüter M (2000) Numerical modelling of benthic processes in the deep Arabian Sea. Deep-Sea Res II 47(14):3039-3072

Meyer-Reil LA (1983) Benthic response to sedimentation events during autumn to spring at shallow water station in the western Kiel Bight. Mar Biol 77:247-256

Nauhaus K, Boetius A, Krüger M, Widdel F (2002) In vitro demonstration of anaerobic oxidation of methane coupled to sulphate reduction in sediment from marine gas hydrate area. Environ Microbiol 4(5):298-305

Sahling H, Rickert D, Raymond WL, Linke P, Suess E (2002) Macrofaunal community structure and sulfide flux at gas hydrate deposits from the Cascadia convergent margin, NE Pacific. Mar Ecol Prog Ser 231:121-138

Sommer S, Pfannkuche O, Rickert D, Kähler A (2002) Ecological implications on surficial marine gas hydrates for the associated small-sized benthic biota at the Hydrate Ridge (Cascadia Convergent Margin, NE Pacific). Mar Ecol Prog Ser 243:25-38

Suess E, Torres ME, Bohrmann G, Collier RW and 7 others (1999) Gas hydrate destabilization: enhanced dewatering, benthic material turnover and large methane plumes at the Cascadia convergent margin. Earth Planet Sci Lett 170:1-15

Torres ME, McManus J, Hammond D, Angelis de MA and 5 others (2002) Fluid and chemical fluxes in and out of sediments hosting methane hydrate deposits on Hydrate Ridge, OR, I: Hydrological provinces. Earth Planet Sci Lett 201:525-540

Trehu A, Bohrmann G, Rack F, et.al. (in press). Drilling gas hydrate on Hydrate Ridge, Cascadia Continental Margin. Ocean Drilling Report, Leg 204 Preliminary Report.

Tryon MD, Brown KM, Torres ME (2002) Fluid and chemical flux in and out of sediments hosting methane hydrate deposits on Hydrate Ridge, OR, II: Hydrological processes. Earth Planet Sci Lett 201:541-557

Wallmann K, Linke P, Suess E, Bohrmann G and 6 others (1997) Quantifying fluid flow, solute mixing, and biogeochemical turnover at cold vents of the eastern Aleutian subduction zone. Geochim Cosmochim Acta 61 (24):5209-5219

Whiticar MJ, Hovland M, Kastner M, Sample JC (1995) 26. Organic geochemistry of gases, fluids, and hydrates at the Cascadia accretionary margin. Proc Ocean Drilling Program, Sci Res 146(1):385-397

Valentine DL, Reeburgh WS (2000) New perspectives on anaerobic methane oxidation. Environ Microbiol 2(5):477-484

Chapter 3

Environmental control on anaerobic oxidation of methane in the gassy sediments of Eckernförde Bay (German Baltic)

Tina Treude [1] *, Martin Krüger [1], Antje Boetius [1, 2], Bo Barker Jørgensen [1]

[1]Max Planck Institute for Marine Microbiology, Department of Biogeochemistry, Celsiusstrasse 1, D-28359 Bremen, Germany

[2]International University Bremen, Research II, Campusring 1, D-28759 Bremen, Germany

Accepted by Limnology and Oceanography

ABSTRACT: Organic mineralization in the muddy, organic-rich sediment of Eckernförde Bay is dominated by sulfate reduction (SR) and methanogenesis. Methane accumulates only below the depth of sulfate penetration, due to anaerobic oxidation of methane (AOM). It was the aim of the present study to investigate the effect of seasonal environmental changes on the rate and distribution of AOM and to identify the organisms involved in the process. Surface sediments were sampled in the Eckernförde Bay basin during September and March. Field rates of AOM and SR were measured by radiotracer methods. Additional parameters were determined that potentially influence AOM, i.e. temperature, salinity, methane, sulfate, and chlorophyll a. Potential rates of AOM, aerobic methane oxidation, and methanogenesis were measured in vitro. AOM revealed seasonal changes within the upper 20 cm of the sediment with rates between 1 and 14 nmol cm^{-3} d^{-1}. Its distribution was controlled by oxygen and sulfate penetration, temperature, and methane supply leading to a shallow AOM zone during the warm productive season and to a deeper AOM zone during the cold winter season. Rising methane bubbles were suggested to feed AOM above the sulfate-methane transition. *Methanosarcinales*-related ANME-2, identified with fluorescence in situ hybridization, appeared to mediate AOM in Eckernförde Bay. These are known also from other methane-rich locations, however, they were not associated with sulfate-reducing bacteria. AOM is most likely mediated solely by archaea that show a mesophilic physiology according to the seasonal temperature changes in Eckernförde Bay.

INTRODUCTION

The muddy, organic-rich sediments of Eckernförde Bay, German Baltic have very high methane concentrations that result in gas bubble development (Whiticar 1978; Abegg and Anderson 1997; Anderson et al. 1998; Wever et al. 1998). The widespread occurrence of gas bubbles within the central basin leads to the so-called "basin effect", an acoustic turbidity in sub-bottom profiler records, masking the sediment reflector deeper than 1-3 m. The methane is of biogenic origin produced by organic matter degradation in the Holocene deposits (Martens et al. 1999; Whiticar 2002). Methane accumulates only below the sulfate penetration due to anaerobic oxidation of methane (AOM) (Albert and Martens 1995; Bussmann et al. 1999; Martens et al. 1999).

During AOM, methane is oxidized with sulfate as electron acceptor via the following net reaction (Eq. 1):

$$CH_4 + SO_4^{2-} \rightarrow HCO_3^- + HS^- + H_2O \quad (1)$$

The process has in earlier studies of methane seeps been found to be mediated by methanotrophic archaea frequently associated with sulfate-reducing bacteria in a syntrophic consortium (Boetius et al. 2000; Orphan et al. 2001a; Michaelis et al. 2002).

AOM has been demonstrated and quantified by modeling, radiotracer turnover measurements, and stable isotope analysis in the sulfate-methane transition zone of Eckernförde Bay (Whiticar 1978; Albert et al. 1998; Martens et al. 1998; Bussmann et al. 1999; Martens et al. 1999; Whiticar 2002). AOM profiles, determined by radiotracer methods, revealed maximum rates between 10 and 44 nmol cm^{-3} d^{-1} in 23 to 60 cm sediment depth (Albert et al. 1998; Bussmann et al. 1999; Martens et al. 1999). However, understanding of the process at this location remains incomplete. Neither the organisms involved in AOM have been identified nor have temporal changes been investigated. Eckernförde Bay exhibits a strong seasonality, e.g. of temperature, salinity, primary production and organic matter degradation in the sediment (Bodungen 1975; Meyer-Reil and Graf 1984; Hansen 1993). Temperature changes are reported to control the depth of the sulfate-methane transition zone coastal sediments (Martens et al. 1986). Moreover, the location of the acoustic turbidity in Eckernförde Bay sediments, i.e. the zone of gas bubble formation, changes seasonally presumably caused by temperature dependent variations in methane solubility (Wever et al. 1998). It is therefore likely that seasonal variations also influence the distribution and rate of AOM in Eckernförde Bay over the year.

Rising gas bubbles have frequently been detected in the water column of Eckernförde Bay (Jackson et al. 1998) and may also supply methane to the surface sediment. The methane ebullition is reported to be controlled by hydrostatic pressure (Jackson et al. 1998), i.e. changes in sea level, and thus short-term temporal changes in methane supply and methane consumption may be found.

The present study aims for a better understanding of AOM in Eckernförde Bay sediments. Molecular, microbiological and biogeochemical investigations were carried out to answer following major questions:

1. Which organisms mediate AOM in Eckernförde Bay?

2. Is the rate and distribution of AOM in Eckernförde Bay controlled by seasonal changes in the environment?
3. Do gas bubble releases temporarily influence AOM in the surface sediment?

Finally, we drew global comparisons between AOM at Eckernförde Bay and other marine sites bearing methane to discuss correlations between methane supply and methane consumption rates.

MATERIALS AND METHODS

Study site. Eckernförde Bay is a semi-enclosed bay, located on the German Baltic Sea coast (Fig. 1) (Abegg and Anderson 1997; Wever et al. 1998). The bay opens into the Kiel Bight and is divided by the Mittelgrund shoal into a northern (Boknis) and a southern channel. The maximum depth is 28 m. The bay was formed by glaciers at the end of the Weichselian glaciation 25,000 years ago (Gripp 1964). The Holocene deposit is a fine-grained mud reaching 7 m thickness (Werner 1978). Sediment accumulation rates range between 0.3 and 1.1 cm yr^{-1} (Nittrouer et al. 1998). The upper 2 m of the sediment is characterized by a high organic carbon content (4-5 wt%) (Whiticar 2002). Bioturbation has been observed only in 0-1 cm of the sediment (Nittrouer et al. 1998).

The water column of Eckernförde Bay is influenced by fresh (rivers, rainfall and ground water) and salt (North Sea) water sources (Milkert et al. 1995; Bussmann et al. 1999) creating salinities between 14 and 24 psu. During warm periods, solar heating causes a warming of the surface layer and the formation of a thermocline. As a consequence, mixing in the water column is reduced and the thermocline strengthened the formation of a deep halocline (Hansen et al. 1999).

Primary production shows (Lenz 1996): (1) a pronounced peak in March/April (spring bloom) dominated by diatoms; (2) a moderate productivity over the summer months June, July and August (summer stagnation) dominated by dinoflagellates and cyanobacteria; and (3) a moderate peak in October/November (autumn bloom) dominated by dinoflagellates and diatoms. At the sea floor, three periods of organic matter input can be distinguished in spring, autumn and winter as a consequence of bloom sedimentation or erosion of terrestrial organic matter and macrophyte debris (Meyer-Reil and Graf 1984). These supplies of organic matter to the sea floor, especially in spring and autumn, are followed by an increase in benthic microbial degradation activity and a subsequent microbial biomass production (Meyer-Reil and Graf 1984).

During late summer when the water column is strongly stratified, oxygen saturation drops to <10% and, occasionally, to anoxia in the bottom water (below 20-25 m) (Hansen et al. 1999). Autumn storms and a decrease in surface water temperature cause a mixing of the water column and the introduction of oxygen into deeper water layers (Meyer-Reil and Graf 1984).

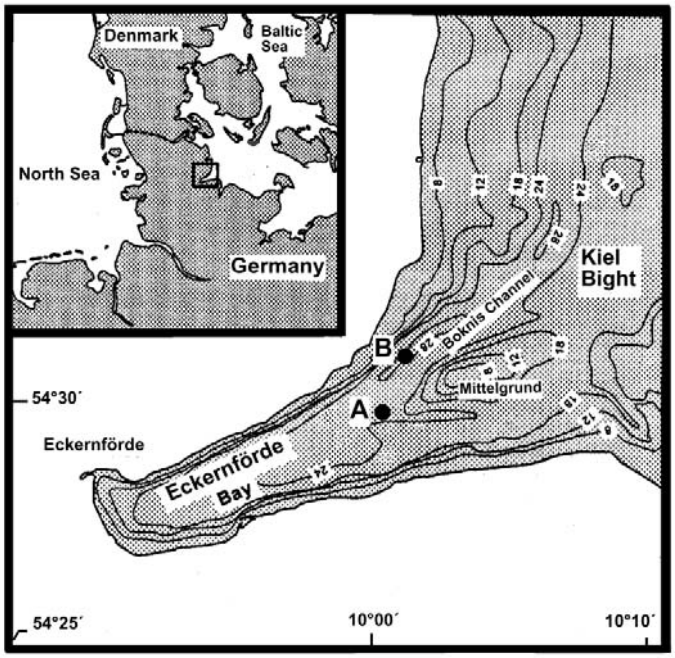

Figure 1. Eckernförde Bay and the location of the sampling stations. Map modified from (Abegg and Anderson, 1997).

Sampling sites. Samples were taken from two stations (Fig. 1). Station A (water depth 25 m, position 54°30´09N, 10°06´01E) was located westerly of Mittelgrund at a site former studied by the Naval Research Laboratory (NRL) and the Federal Armed Forces Underwater Acoustics and Marine Geophysics Research Institute (FWG) (see also Abegg and Anderson 1997; Wever et al. 1998; Martens et al. 1999). Station B (water depth 28 m, position 54°31´15N, 10°01´29E) was located in the northern Boknis channel. The stations were sampled during one-day cruises of the German research vessel "Littorina" in early (5th and 6th) and late (20th and 21th) September 2001 as well as in early (5th and 6th) March 2002. Between the early and late September sampling, a storm with wind forces up to 9 Beaufort from north/north-west (M. Lehwald, pers. commun.) occurred. It was the first autumn storm after a long period of calm and warm summer weather. In March, the weather was rough with wind from south/south-west reaching 6 Beaufort (M. Lehwald, pers. commun.).

Parameters of the water column. Pressure, temperature and salinity of the water column were determined by a multifunction probe (ECO-Sonde, Meerestechnik Elektronik) with an accuracy of ± 0.01 bar for pressure, ±0.01°C for temperature, and ± 0.02 mS cm^{-1} for conductivity. Salinity was determined from the relation between pressure, temperature and conductivity.

Sediment sampling. Sediment samples were taken with a small multiple corer based on the construction described by (Barnett et al. 1984). This "MiniMuc" takes four sediment cores of up to 50 cm length with an inner diameter of 10 cm within an area of ¼ m^2. The cores taken reached a length of 30-40 cm. Unless otherwise mentioned, core sub-samples were stored in a regulated refrigerator aboard at in situ temperature (10°C in September, 4°C in March), before further investigations proceeded in the home laboratory.

Chemistry and process rates. Samples for sediment chemistry and process rate measurements were taken at Station A and B in early and late September as well as March. Three replicate MiniMuc cores from one deployment were sub-sampled with small push-cores (length 30 cm, inner diameter 26 mm) and cut-off syringes.

Methane concentration. On board, 2 cm^3 sediment was taken at 1 cm intervals with cut-off syringes and transferred into 10 ml glass vials filled with 5 ml sodium hydroxide (2.5 % w/w). The vials were closed quickly with butyl rubber stoppers, sealed with aluminum crimps, and shaken thoroughly to equilibrate the pore water methane into the headspace. In the laboratory, the methane concentrations were determined by injection of 200 µl headspace into a gas chromatograph (5890A, Hewlett Packard) equipped with a packed stainless steal Porapak-Q column (6 ft., 0.125 in., 80/100 mesh, Agilent Tecknologie) and a flame ionization detector. The carrier gas was helium at a flow rate of 30 ml min^{-1}. The column temperature was 40°C.

Sulfate concentration. On board, 5 cm^3 sediment was taken at 1 cm intervals with cut-off syringes and transferred into 10 ml plastic tubes filled with 3 cm^3 zinc chloride (1 % w/w). The vials were closed with plastic stoppers, shaken thoroughly and frozen at –25°C. In the laboratory, the samples were thawn and centrifuged (2200 g, 10 min). Pore water sulfate concentrations were measured in the supernatant using nonsuppressed ion chromatography with a Waters 510 HPLC pump, Waters WISP 712 autosampler (100 µL injection volume), Waters IC-Pak anion exchange column (50 x 4.6 mm), and a Waters 430 Conductivity

detector. The eluent was 1 mmol L^{-1} isophthalic acid with 10% methanol, adjusted to pH 4.5. The flow was set to 1.0 ml min^{-1}.

Porosity, density and dry weight. On board, sediment samples (ca. 5 cm^3) were taken at 1 cm intervals with cut-off syringes and transferred into pre-weighed 15 ml plastic centrifuge vials with a volume scale bar and closed with a plastic screw cap. In the laboratory, the vials were centrifuged (2200 g, 10 min), weighed, filled with water to a defined volume, weighed again, dried and weighed a third time. From the weights, the sediment volume, density, dry weight, and porosity was calculated.

Anaerobic oxidation of methane (AOM). On board, three replicate and one control push-core were taken out of two MiniMuc cores. In the laboratory, radioactive methane ($^{14}CH_4$ dissolved in water, injection volume 15µl, activity 0.5 kBq) were injected into the replicate push-cores at 1 cm intervals according to the whole core injection method of (Jørgensen 1978). The push-cores were incubated at in situ temperature, i.e. 10°C in September and 4°C in March, for 48 hrs in the dark. To stop bacterial activity, the sediment cores were sectioned into 1 cm intervals and transferred into 50 ml glass vials filled with 25 ml sodium hydroxide (2.5% w/w) and closed quickly with rubber stoppers (1.5 cm thickness). The glass vials were shaken thoroughly to equilibrate the pore water methane between the aqueous and gaseous phase. Control push-cores were first fixed before addition of tracer. The rate of AOM was calculated by the ratio between the amount of CH_4 (determined by gas chromatography), $^{14}CH_4$ (determined by combustion) and $^{14}CO_2$ (determined by diffusion method) according to Treude (2003).

Sulfate reduction (SR). Sampling, injection and incubation was the same as for AOM samples. The injected radiotracer was carrier-free $^{35}SO_4^{2-}$ dissolved in water, injection volume 6 µL, activity 15 kBq. To stop bacterial activity after incubation, the sediment cores were sectioned into 1 cm intervals and transferred into 50 ml plastic centrifuge vials filled with 20 ml zinc acetate (20% w/w). Control push-cores were first fixed before addition of tracer. SR rates were determined using the single step acid Cr-II method according to Fossing and Jørgensen (1989).

Chlorophyll a (chl a) and pheophytin a (pheo a). On board, the samples were taken with a push-core. In the laboratory, the push-core was sectioned into 1 cm intervals. 2 cm^3 sediment of each slice was transferred into preweighed 15 ml plastic centrifuge vials, closed with a plastic screw cap and frozen at –25°C. Later, the samples were thawed and weighed. Chl a and pheo a were extracted in 4 ml 90% acetone. After sonication (320 Watt) for 10 min, the samples were centrifuged (2200g, 5 min) and the supernatant was transferred into 15 ml

plastic vials. The extraction was repeated twice and the supernatants of the extractions were combined. During all extractions, light was kept to a minimum to prevent a decay of the pigments. Chl a was determined by fluorometry (Hitachi F-2000 fluorometer; λ_{ex}=428 nm, λ_{em}=671 nm). Chl a (Fluka) was used as standard. The precision of the method was ±10%. As labile compounds are easily degraded by acid treatment, the pigment extracts were acidified with a few drops of hydrochloric acid and measured again. The ratio of the fluorescence intensities (FI) of the acid-treated and the untreated pigment extract provides a measure of the degradability of the pigments, because the resulting molecules have different fluorescence behavior than its precursor. This ratio is defined as the chlorin-index (Eq. 2, Schubert et al. 2002):.

$$chlorin-index\,(CI) = \frac{FI_{acidified\ sample}}{FI_{original\ sample}} \qquad (2)$$

Potential process rates. With potential process rate measurements the maximum capacity of a microbial community can be determined. Potential rates are measured under optimum conditions, i.e. no limitation in substrates. Sediment samples for potential rate measurements were taken at Station B in early September and March. On board, samples were taken by slicing MiniMuc cores into 5 cm sections. The sections were transferred into 250 ml glass bottles and sealed with butyl rubber stoppers and screw caps. Except for analysis of aerobic microbial activity, investigations in the laboratory proceeded in an N_2/CO_2 atmosphere using an anaerobic glove box (Mecaplex). Sediment samples were mixed with artificial seawater in a 1:1 ratio before further manipulations to obtain a homogenous sediment slurry. Sediment dry weights were determined after drying at 80°C for 2 days. Methane concentrations were determined from a GC 14B gas chromatograph (Shimadzu) equipped with a Supel-Q Plot column (30 m x 0.53 mm; Supelco) and a flame ionisation detector (Nauhaus et al. 2002). Sulfide was determined colorimetrically using the formation of colloidal copper sulfide (Cord-Ruwisch, 1985). All potential rates were first determined as nmol gdw^{-1} d^{-1} and recalculated into nmol cm^{-3} d^{-1} of the undiluted sediment using the volume to dry weight ratio of the undiluted sediment.

Potential anaerobic oxidation of methane (AOM). Potential AOM was determined in vitro as described previously (Nauhaus et al. 2002). Three cm^3 of sediment slurry were transferred into sterile glass tubes and mixed with 9 ml artificial seawater medium (Widdel and Bak 1992). The tubes were sealed with butyl rubber stoppers and incubated with a

headspace of pure methane at atmospheric pressure (0.1 MPa) or a N_2-CO_2-mixture (90/10 vol/vol) in controls. All incubations were done in triplicate at 12ºC. With slurry from 25-30 cm, early September, temperature dependent potential AOM was determined at 4, 8, 12, 16, 20, and 28°C in addition. Samples for chemical analyses were collected using microliter syringes (preflushed with N_2). AOM-activity was determined from the difference in sulfide production in incubations with and without methane.

Potential methanogenesis. The potential production of methane was measured in vitro as described in (Krüger et al. 2001). Three cm^3 of sediment slurry was transferred into sterile glass tubes as described above. Nine ml of artificial seawater medium was added and the tubes were sealed with butyl rubber stoppers. The headspace consisted of a N_2-CO_2-mixture (90/10 vol/vol). Incubation was the same as described for AOM. The incubation temperature was 12°C. Headspace samples (0.1 ml) were taken with pressure lock syringes twice per day, after shaking of the tubes by hand, and analyzed for methane.

Potential aerobic oxidation of methane (aerobic MO). Potential aerobic MO was determined in vitro according to Krüger et al. (2002). Sediment slurries were produced under oxic conditions. The slurries (20 cm^3) were transferred into sterile glass bottles (175 ml) and sealed with butyl rubber stoppers. The oxic headspace was supplemented with 10,000 ppm_v methane. The bottles were incubated at 12°C in the dark and shaken once per day. Methane depletion was followed by sampling the headspace from triplicate incubations, after thoroughly shaking the bottles, and subsequent gas chromatography. The first sample was taken 30 min after the amendment with methane, followed by sampling at 24 h intervals. Linear regressions were calculated from the mean methane depletion curves to obtain the aerobic MO rates.

Identification of microorganisms by fluorescence in situ hybridization (FISH). For sediment measurements, a push-core was sectioned at 1 cm intervals. For slurry measurements, an aliquot of the sediment slurries was taken. One cm^3 of each sediment slice or sediment slurry was transferred into 3 ml formaldehyde (final concentration 3%) and fixed for 2-3 h. After fixation, the sample was washed twice with 1xPBS (10 mmol L^{-1} sodium phosphate, 130 mmol L^{-1} NaCl) and finally stored in 1xPBS/EtOH (1:1) at –25°C. Fixed samples were diluted (1:10) with PBS and treated by mild sonication for 20 s with a MS73 probe (Sonoplus HD70, Bandelin, Germany) at an amplitude of 42 µm <10 W. An aliquot (40 µl) was filtered on 0.2 µm GTTP polycarbonate filters (Millipore, Eschborn, Germany). The filters were embedded in low gelling point agarose. Hybridization and microscopy counts

of hybridized and 4´,6´-diamidino-2-phenylindole (DAPI)-stained cells were performed as described previously (Snaidr et al. 1997). Mean values of aggregate numbers were calculated by using 200-400 randomly chosen fields of view for each filter section, corresponding to 700-1200 hybridized cells. Means of total free-living cells were calculated by using 16-17 randomly chosen fields of view for each filter section, corresponding to 700-1000 DAPI-stained cells. Cy3- and Cy5-monolabeled oligonucleotides were purchased from ThermoHybaid (Ulm, Germany). Probes and formamide (FA) concentrations used in this study were as follows: EeelMS932 targeting ANME-2 (Hinrichs et al. 1999; 40% FA), ANME-1 targeting ANME-1 (Hinrichs et al. 1999; 40% FA), EUB338 targeting Bacteria (Amann et al. 1990; 40% FA in double hybridization with EeelMS932), DSS658 targeting *Desulfosarcina* spp./*Desulfococcus* spp./*Desulfofrigus* spp. and *Desulfofaba* spp. (Manz et al. 1998; 40% FA in double hybridization with ANME-2, 60% FA in single hybridization). To avoid background signals 10% Blocking Reagent (Roche) was added to hybridization buffers (20% vol/vol).

RESULTS

Hydrographic conditions

In early September, the water column at Station A (Fig. 2, a-c) was clearly stratified into a cold, saline bottom layer and a warm, freshwater-influenced surface layer. Temperature decreased from 17°C at the surface to 10°C at the bottom. Salinity was lower at the surface (15 psu) compared to the bottom water (23 psu). A surface layer with a homogeneous temperature of 17°C was pronounced in the top 10 m of the water column. After the first autumn storm, a partial mixing of the water layers decreased surface temperatures to 15°C and caused an increase to 11°C at the bottom. Salinity was elevated to 17 psu at the surface and revealed a halocline at 5.6 m. At the bottom, salinity stayed constant. During winter, the water column was completely mixed and both temperature (4°C) and salinity (20 psu) were constant with depth in March.

At Station B (Fig. 3, a-c), the stratification of the water column during early September was similar to Station A, with a warm surface layer of 17°C and 15 psu and a colder bottom water of 10°C and 23 psu. The mixing of the water column after the storm was slightly more pronounced resulting in 14°C and 19 psu at the surface and 11°C and 23 psu at the bottom. In March, temperature (4°C) and salinity (20 psu) were homogeneous with depth.

Chemistry and process rates

Sediment description. At Station A, the surface of sediment cores was gray-greenish and very fluffy with a porosity of up to 0.92. This fluffy sediment reached a depth of 3 to 4 cm below which a black sediment was found. This black sediment had a porosity of about 0.86 and smelled strongly of hydrogen sulfide. During the late September and March sampling, the sediment surface had been strongly resuspended by wind-induced currents. In late September the resuspension was also monitored by a deployed camera system (Karpen 2002).

At Station B, the sediment revealed the same fluffy consistency and porosity as Station A. However, in early and late September the sediment was completely black with a strong smell of hydrogen sulfide. In March the sediment was also strongly resuspended by wind-induced currents and the upper 4 cm had turned into a brown color. Filaments of the sulfur-oxidizing bacteria *Beggiatoa* were visible at the sediment surface in early and late September. They occurred subsurface in March as demonstrated by microscopic investigation (A. Preisler, unpubl. data).

Sulfate and methane. At Station A, sulfate and methane concentrations (Fig. 2, d-f) in the sediment varied between the investigated seasons. The decrease in sulfate over depth was steepest in September with a penetration depth of approximately 23 cm, and lowest in March resulting in the deepest penetration of approximately 32 cm. In the topmost layer of the sediment (0-1 cm), sulfate concentration was highest in early September (21.4 mmol L^{-1}) and lowest in March (16.0 mmol L^{-1}). The lowered sulfate concentration in March is most likely correlated with the decrease in bottom water salinity (see above). Methane was nearly zero at the sediment surface (between 0.001 and 0.010 mmol L^{-1}) and increased to values between 0.2 and 0.8 mmol L^{-1} towards the bottom of the cores. The methane gradient was highest in March and lowest in early September.

At Station B (Fig. 3, d-f), the variations of sulfate and methane concentration were rather similar to Station A. The decrease in sulfate over depth was steepest in September with a penetration of approximately 25 cm, and lowest in March resulting in the deepest penetration depth of approximately 33 cm. In the topmost layer of the sediment (0-1 cm), sulfate concentration was highest in early September (21.9) and lowest in March (16.5 mmol L^{-1}). In all measurements, methane was near zero in the topmost layer (between 0.003 and

0.014 mmol L^{-1}) and increased to values between 0.3 and 1.6 mmol L^{-1} at the bottom of the cores. The methane gradient was highest in late September and lowest in early September.

Anaerobic oxidation of methane (AOM). In early September, AOM at Station A (Fig. 2, g-i) was detectable over the whole depth interval investigated (24 cm). In the upper 20 cm, rates varied between 0.5 and 7 nmol cm^{-3} d^{-1} without a clear peaking. In the deeper part (21-23 cm), rates were higher reaching a maximum of 14 nmol cm^{-3} d^{-1}. In late September, the zone of elevated rates moved upwards into depths between 17 and 22 cm. The activity close to the surface was reduced to 1 nmol cm^{-3} d^{-1} or less. In March, AOM was reduced to less than 1 nmol cm^{-3} d^{-1} between 0 and 15 cm. Elevated activity at the topmost layer (up to 4 nmol cm^{-3} d^{-1}) represented most likely aerobic MO, presumably due to a deeper penetration depth of oxygen caused by enhanced wind-induced currents in this season. Below 15 cm, AOM increased steadily and reached 10 nmol cm^{-3} d^{-1} between 23 and 24 cm. Integrated over 0-25 cm, AOM activity was highest in early September, 1.00 mmol m^{-2} d^{-1}, and decreased to 0.49 mmol m^{-2} d^{-1} in March (Table 1).

At Station B (Fig.3, g-i), AOM activity in early September was also detectable over the whole core. In the upper 20 cm, rates varied between 2 and 5 nmol cm^{-3} d^{-1}. In the deeper part (20-25 cm), rates were elevated reaching a maximum of 13 nmol cm^{-3} d^{-1}. In late September, AOM showed a distinct maximum in the middle of the core (mean value 11 nmol cm^{-3} d^{-1} at 14-15 cm) and decreased towards the upper and lower end of the core (mean values 0.65 nmol cm^{-3} d^{-1} at 0-1 cm, 1.22 nmol cm^{-3} d^{-1} at 24-25 cm). Single measurements reached maxima of 13 nmol cm^{-3} d^{-1} between 12 and 19 cm. In March, AOM was reduced to 2 nmol cm^{-3} d^{-1}or less between 5 and 15 cm. As for Station A, activity in the surface sediment represented most likely aerobic MO. In contrast to Station A, the aerobic rates were enhanced down to 4-5 cm and reached a maximum rate of 82 nmol cm^{-3} d^{-1}. Below 15 cm, AOM increased steadily up to 9 nmol cm^{-3} d^{-1} at 22-23 cm. Integrated over 0-25 cm, AOM activity was highest in late September (1.52 mmol m^{-2} d^{-1}, Table 1).

Test for differences in AOM between investigated seasons. For the analysis of differences in the rate and distribution of AOM between early September, late September and March at Station A and B, respectively, a paired-sample t-test was applied. AOM values of each season were divided into 5 cm depth intervals (0-5 cm, 5-10 cm, 10-15 cm etc.), corresponding to a total number of n=15 values per interval (3 replicates per cm multiplied by 5). Each depth interval of a season was tested against the respective depth interval of another season (early

Sept. vs. late Sept., late Sept. vs. March, March vs. early Sept.). *p*-values were determined and for $p<0.05$, AOM of the compared intervals differed significantly. AOM of the 20-25 cm interval revealed no significant changes between seasons at both stations. Most seasons revealed highly significant changes of AOM ($p<0.005$) between 5 and 20 cm. The only exception was early vs. late September at Station A. Here, AOM did not differ significantly in both seasons except for the upper most interval (0-5 cm). At Station A, methane oxidation of the 0-5 cm interval was significant different ($p<0.005$) in early September compared to late September and March. At Station B, methane oxidation in the 0-5 cm interval was significant different ($p=0.045$) in late September compared to early September and March.

Table 1. Rates of AOM and SR as well as chlorophyll a concentration per m^2 (integrated over 0-25 cm). Standard deviations of AOM and SR are given in parenthesis.

	AOM[1)] (mmol m^{-2} d^{-1})	SR (mmol m^{-2} d^{-1})	Chl a (mg m^2)
Station A			
early Sept.	1.00 (± 0.39)	7.3 (± 6.1)	187
late Sept.	0.84 (± 0.36)	4.1 (± 1.0)	143
early March	0.49 (± 0.21)	4.2 (± 2.4)	160
Station B			
early Sept.	0.99 (± 0.32)	10.5 (± 2.5)	203
late Sept.	1.52 (± 0.57)	7.8 (± 1.4)	198
early March	0.44 (± 0.25)	5.6 (± 2.0)	130

[1)] presumable aerobic rates are excluded

Sulfate reduction (SR). At Station A (Fig.2, j-l), SR was always highest close to the sediment surface with rates reaching up to 465 nmol cm^{-3} d^{-1} in early September. Most of the SR was restricted to the upper 10 cm of the sediment. Between early September and March, rates decreased to values between 20 and 90 nmol cm^{-3} d^{-1} in the upper sediment. Integrated over 0-25 cm, SR activity was highest in early September with 7.3 mmol m^{-2} d^{-1} and around 4 mmol m^{-2} d^{-1} during the later seasons (Table 1). Comparing integrated SR and AOM within the sulfate-methane transition zone, (15-25 cm, see small cutouts in SR profiles), the ratio between AOM and SR was 5:3, 2:1 and 1:2 in early and late September and March, respectively.

At Station B, SR (Fig.3, j-l) of the early and late September was highest in the top layer, reaching a maximum of 224 nmol cm^{-3} d^{-1} in late September. As for Station A, the majority of

SR activity was restricted to the upper 10 cm of the sediment at all times. Between early September and March, rates decreased to values between 10 and 50 nmol cm^{-3} d^{-1} in this most active zone. Integrated over 0-25 cm, SR activity was highest in early September with 10.5 mmol m^{-2} d^{-1} and decreased to 5.6 mmol m^{-2} d^{-1} in March (Table 1). Comparing SR and AOM within sulfate-methane transition zone, the ratio between AOM and SR was 1:1 in early September (integrated over 15-25 cm), 1:2 in late September (integrated over 5-25 cm) and 1:4 in March (integrated over 15-25 cm).

Chlorophyll a and chlorin-index. At Station A (Fig.2, m-o), the deposition of fresh algal material on the sediment surface, as measured by chl a concentrations, was highest in early September (1790 ng cm^{-3}) as a result of the summer phytoplankton sedimentation (Bodungen 1975). This increase in fresh organic matter, which is also confirmed by a low chlorin-index of 0.53, was restricted to 0-1 cm layer of the sediment. Below that layer, chl a concentrations stayed around 700 ng cm^{-3}, while the chlorin-index increased to around 0.66 as a result of the advancing decomposition. In late September, the picture was similar but the elevated chl a concentration reached a depth of 2 cm. The downward mixing could have been caused by wind-induced currents during the storm or by bioturbation. Over the winter, fresh organic matter was buried deeper into the sediment leading to reduced chl a concentrations in the 0-1 cm layer (831 ng cm^{-3}) and irregular profiles with maxima up to 1250 ng cm^{-3} in the top 10 cm of the sediment. Consequently, the chlorin-index showed an opposite profile. Integrated over 25 cm (Table 1), chl a concentrations were similar for all seasons investigated.

At Station B, the deposition of fresh algal material (Fig.3, m-o) onto the sediment was also highest in early September (1895 ng cm^{-3} in the 0-1 cm layer) and revealed peaks between 0 and 2 cm as well as between 6 and 8 cm. The deeper peak represents most likely buried material. This is confirmed by the chlorin-index revealing higher values (0.62) in the deeper peak compared to the surface (0.59), i.e. the proportion of degraded organic matter was larger in the deeper fraction. Below the peaks, the sediment had chl a values around 700 ng cm^{-3} with a chlorin-index of about 0.65. In late September, the deeper peak was not found again. Chl a concentration were elevated only at the surface (around 1500 ng cm^{-3} between 0 and 2 cm). Below the surface, chl a decreased steadily from 1000 to 360 ng cm^{-3}. The chlorin-index showed a mirrored profile with lowest values at the surface (0.57) and highest at the bottom of the core (0.67). In March, there was still a peak of chl a at the topmost layer (1213 ng cm^{-3}) but the high chlorin-index (0.64) shows that a larger fraction of the algal

material was already degraded. The deeper part of the sediment revealed a chl a concentration around 500 ng cm^{-3} and a chlorin-index of about 0.65. Integrated over 25 cm (Table 1), chl a in March was 60% of the concentration in early September.

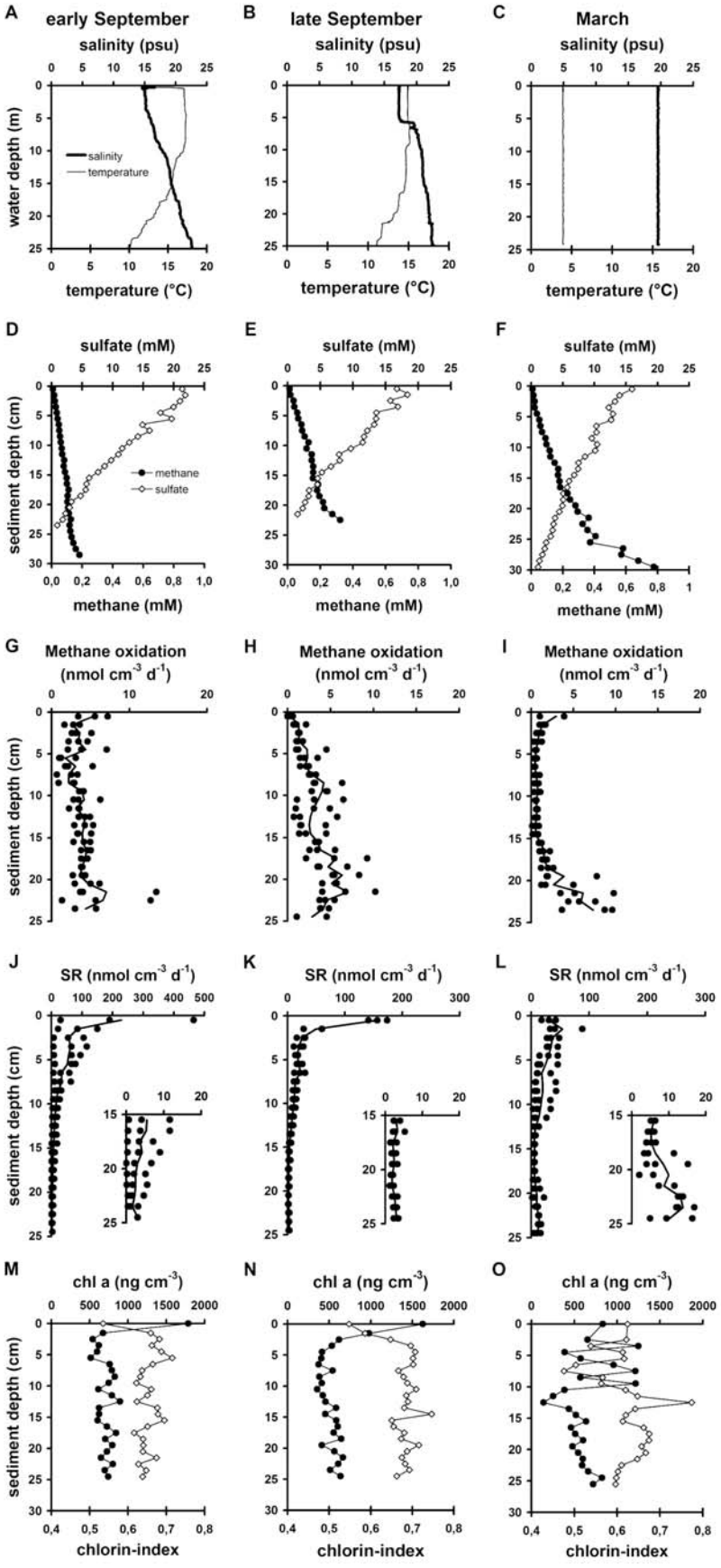

Figure 2 (A-O). Parameters measured at Station A. Chl a concentration = solid circles, chlorin-index = open rhomb. For SR deeper parts is given in higher resolutions (small insert).

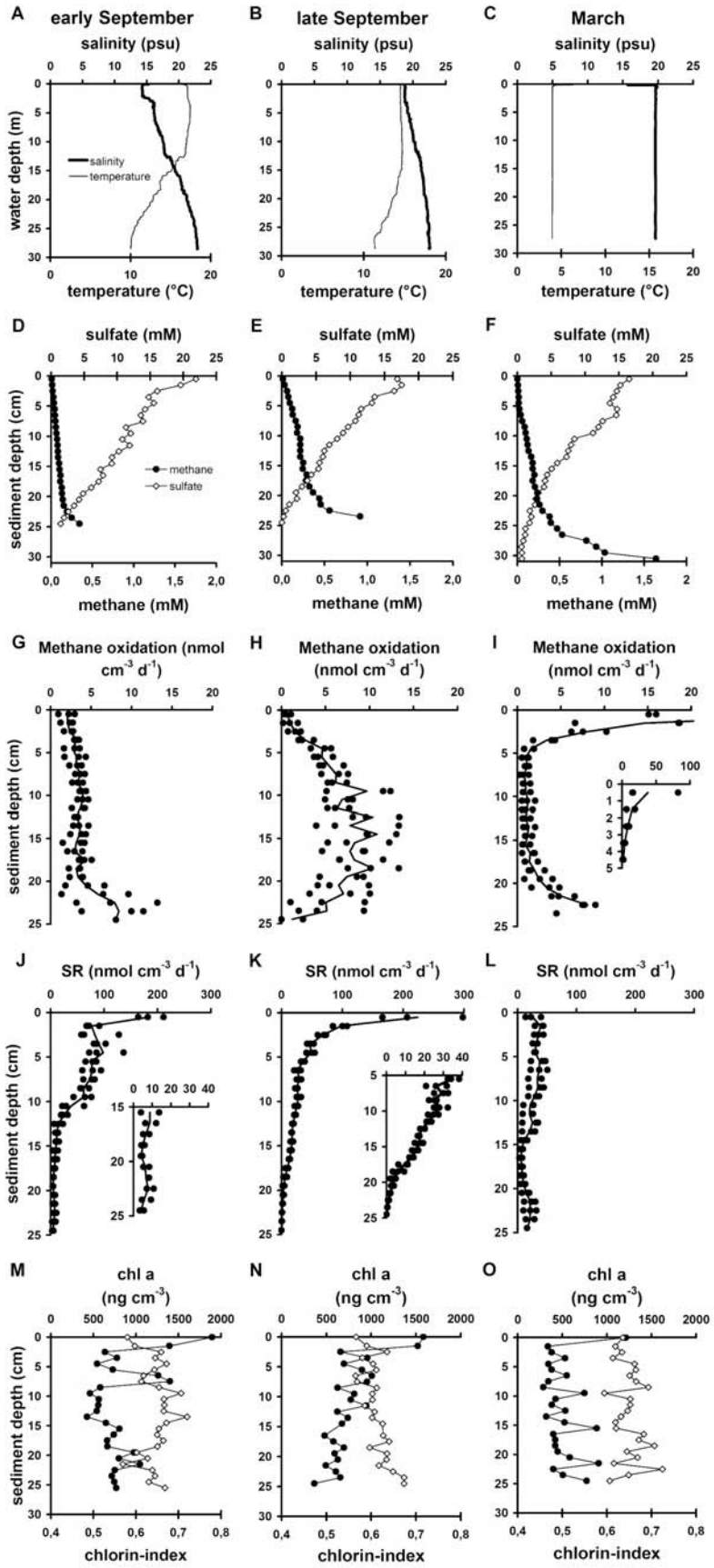

Figure 3 (A-O). Parameters measured at Station B. Chl a concentration = solid circles, chlorin-index = open rhomb. For SR deeper parts is given in higher resolutions (small insert).

Potential process rates

Potential methane production. The potential rates increased with depth in both seasons (Fig. 4, a and b). No considerable methane production was detected in the top section (0-5 cm). In early September, rates were lower compared to respective depth sections of March. In early September, methanogenesis reached a maximum of 9.8 nmol cm^{-3} d^{-1} between 25 and 30 cm (the maximum sampling depth). In March, a maximum of 37 nmol cm^{-3} d^{-1} was reached between 30 and 35 cm.

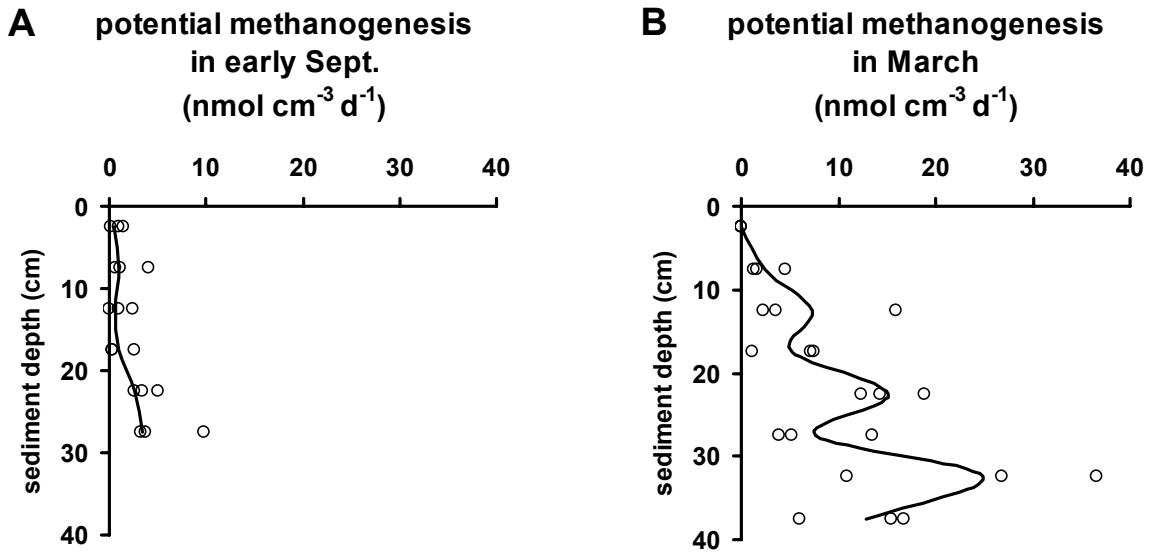

Figure 4. Potential methanogenesis in sediment slurries of Station B taken in early September and March (mean of three replicates shown as solid line).

Potential AOM. Averaged potential rates fluctuated between 20 and 90 nmol cm^{-3} d^{-1} in both periods (Fig. 5, a and b). Within the top 30 cm, no clear trend was visible and the periods revealed different profiles. In March, when the sampling depth was expanded to 40 cm, a decrease of AOM was measured below 30 cm.

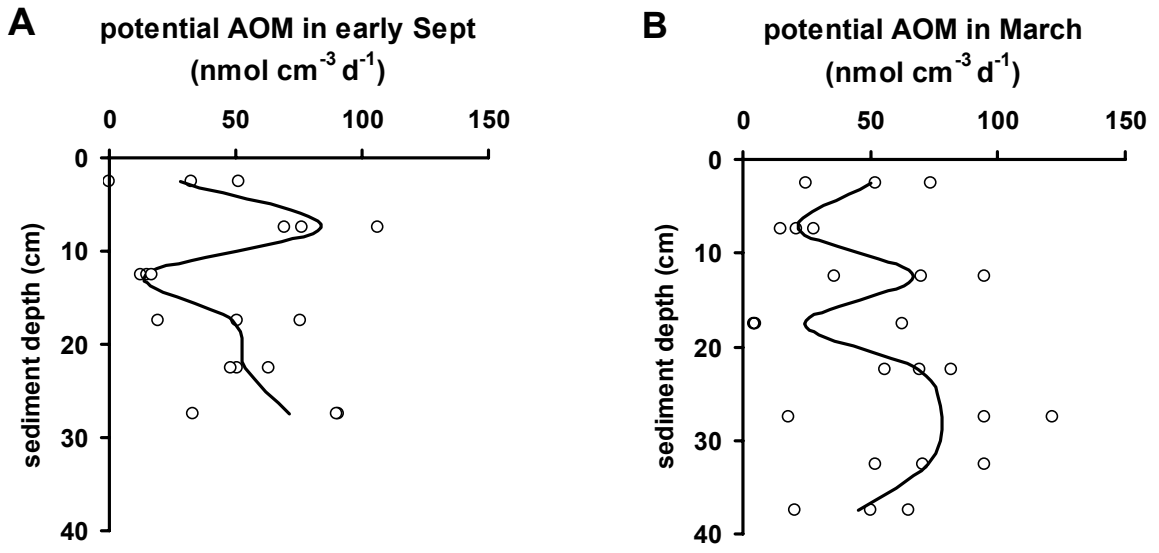

Figure 5. Potential AOM in sediment slurries of Station B taken in early September and March (mean of three replicates shown as solid line).

Temperature optimum of AOM. Temperature dependent potential AOM (25-30 cm, early September, Fig.6) revealed highest rates at 20°C (97 nmol cm^{-3} d^{-1}), characterizing the responsible organisms as mesophilic (Madigan et al. 2000). The rates increased steadily from 4°C (29 nmol cm^{-3} d^{-1}) to 20°C. At 28°C, AOM decreased to 87 nmol cm^{-3} d^{-1}.

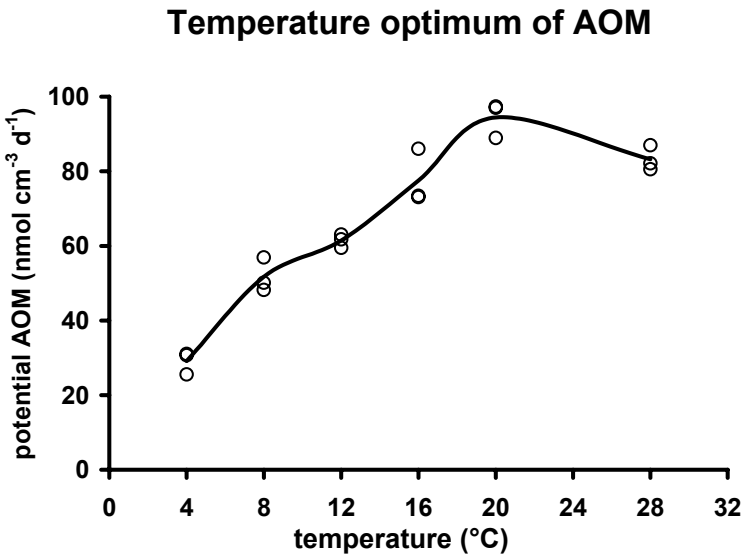

Figure 6. Temperature correlation of potential AOM in sediment slurries (25-30 cm) of Station B taken in early September (mean of three replicates shown as solid line).

Potential aerobic MO. Potential aerobic MO was 9.1 (± 2.5 *s.d.*) nmol cm^{-3} d^{-1} in early September and 4.6 (± 3.4 *s.d*) nmol cm^{-3} d^{-1} in March for the section 0-5 cm. In 5-10 cm no aerobic MO was detected.

Identification of microorganisms by fluorescence in situ hybridization (FISH)

Slurries (0-10 cm and 25-25 cm, early Sept.) as well as sediment of the most active AOM zones (Station A: 21-22 cm, early Sept.; 23-24 cm, late Sept.; 24-25 cm, March; Station B: 19-20 cm, early Sept.; 14-15 cm, late Sept.; 24-25 cm, March) were investigated with FISH. In all samples, abundant cell aggregates were detected by the EelMS932 probe targeting archaea of the ANME-2 cluster (Fig.7). These archaea are reported to mediate AOM in syntrophic consortia with sulfate-reducing bacteria of the branch *Desulfococcus*/*Desulfosarcina* (Boetius et al. 2000). The ANME-2 aggregates found in the Eckernförde Bay sediments had no apparent syntrophic partner. In EelMS932 (CY3)/DSS658 (CY5) or EelMS932 (CY3)/EUB338 (CY5) double-hybridizations (Fig. 7, a and c) the cells of the aggregates were targeted only by EelMS932. Control analysis of the DAPI signal also revealed no additional cells than those accounted for by EelMS932 (Fig. 7, b). Preliminary aggregate counts of the depth interval 24-26 cm of the March sampling revealed an ANME-2 aggregate density of 1.12 and 0.95 x 10^6 cm^{-3} for Station A and B, respectively. This corresponds to a cell density of 3.8 and 5.1 x 10^7 cm^{-3}, respectively (Table 2). The coccoid cells had a diameter of about 0.7 µm. The aggregates reached a maximum diameter of 6-8 µm with cell numbers between 300 and 500. However, the majority of the aggregates (93%) had lower cell numbers with an average of 22 ± 22 *m.d.* (n = 43; Fig. 7, d and e). In some cases the cells occurred in pairs (Fig. 7, f and g). No single cells were found. ANME-2 aggregates comprised 21 and 28% of the total microbial cell number in Station A and B, respectively. Other cells in the sediment were detected by the ANME-1 probe targeting cells of the ANME-1 cluster, archaea also known to be responsible for AOM (Michaelis et al. 2002). The cells revealed a rectangular shape, as it is typically for ANME-1, and occurred in short chains of 4-6 cells. But their abundance was too low for quantification (only 2 or 3 chains were found per filter analyzed).

Specimen of the assumed syntrophic ANME-2 partner, i.e. sulfate-reducing bacteria of the branch *Desulfococcus*/*Desulfosarcina* (targeted by probe DSS658), were also abundant in the sediment but occurred only as single cells or in aggregates without archaeal partners. The coccoid cells had a diameter of about 0.5 µm. Preliminary cell counts of the depth interval 24-

26 cm of the March samplings revealed a *Desulfococcus*/*Desulfosarcina* aggregate density of 5.1 and 6.7 x 10^5 cm^{-3} for Station A and B, respectively. This corresponds to a cell density of 3.4 and 5.1 x 10^6 cm^{-3}, respectively (Table 2). Therefore, the ratio between ANME-2 and *Desulfococcus*/*Desulfosarcina* cells in the sediment was about 10:1 at both stations. The aggregates of *Desulfococcus*/*Desulfosarcina* were smaller compared to ANME-2. The largest ones comprised between 30 and 44 cells. The majority of the aggregates (91%) had lower cell numbers with an average of 3 ± 1 *m.d.* (n = 31). Also single cells were found.

It has to be mentioned that the cell counts may represent underestimations, as the dilution of the sediment was chosen relatively low to obtain an appropriate number of aggregates per filter. Thus, the sediment formed more than one layer on the filter and could have hidden cells. However, the underestimation should be similar for ANME-2 and *Desulfococcus/Desulfosarcina* cells due to their similar cell size and aggregate properties.

Table 2. Preliminary cell numbers of EelMS932 (ANME-2) and DSS658 targeted cells. Single cell numbers were determined by counting DAPI stained, non-targeted cells.

	ANME-2 (cells cm^{-3})	DSS658 (cells cm^{-3})	Single cells (cells cm^{-3})
Station A 24-26 cm	3.8 x 10^7	3.4 x 10^6	1.4 x 10^8
Station B 24-26 cm	5.1 x 10^7	5.1 x 10^6	1.2 x 10^8

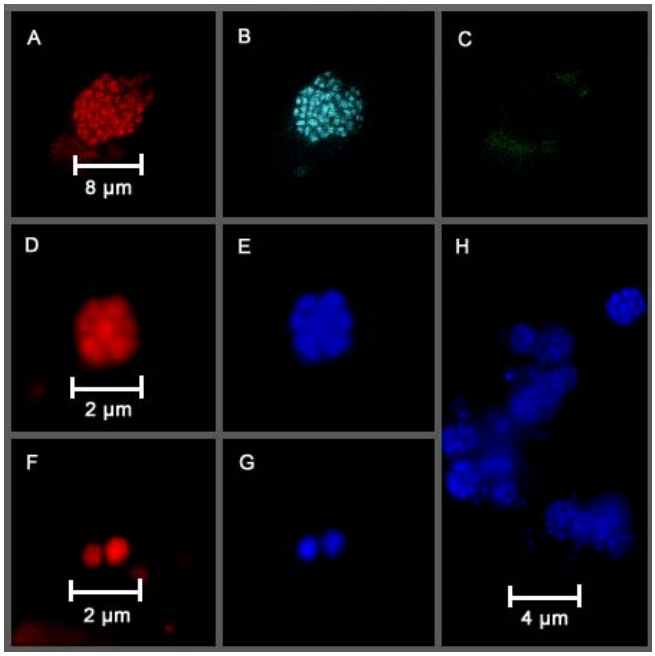

Figure 7 (A-H). In situ identification of ANME-2 aggregates with fluorescently labeled rRNA-targeted oligonucleotide probes. A-C: Confocal laser scanning micrograph of the hybridization with the CY3-labelled EelMS932 (A, shown in red), the CY5 labeled EUB338 (C, shown in green), and the DAPI staining (B, shown in blue). D/E, F/G: Epifluorescence micrographs of a small aggregate and a two-cell-stage hybridized with the CY3 labelled EelMS932 (left panel) and stained with DAPI (right panel). H: Accumulation of DAPI stained aggregates.

DISCUSSION

Organisms apparently mediating AOM in Eckernförde Bay

The sediments of Eckernförde Bay contained abundant aggregates belonging to the *Methanosarcinales*-related ANME-2 group. This archaeal group has been described to mediate AOM in consortia with sulfate-reducing bacteria of the *Desulfococcus*/*Desulfosarcina* branch in different methane-bearing sediments in the North Pacific (Boetius et al. 2000; Orphan et al. 2001a, 2001b). In contrast to those sites, the ANME-2 aggregates in Eckernförde Bay never had bacterial partners. Monospecific aggregates of ANME-2 were already described (Orphan et al. 2001a), but they were found only occasionally in sediments dominated by ANME-2/*Desulfococcus*/*Desulfosarcina* consortia. These findings raise the question whether methane-oxidizing archaea need to

interact with sulfate-reducing bacteria. Although monospecific aggregates of *Desulfococcus*/*Desulfosarcina* were also found in the sediments of Eckernförde Bay, their abundance was 10 times lower compared to ANME-2 aggregates. Moreover, AOM based on a loose co-occurence of archaeal and bacterial cells in the sediment is not likely to provide an efficient syntrophy since a close cell-to-cell contact is hypothesized to be needed for a transfer of metabolic intermediates (Sørensen et al. 2001).

Another difference of Eckernförde Bay ANME-2 compared to other AOM archaea is their temperature optimum. The optimal temperature of psychrophilic ANME-2 from Hydrate Ridge ranges between 4 and 16°C (Nauhaus et al. 2002). ANME-2 of Eckernförde shows a mesophilic temperature optimum between 16 an 28°C. This is most likely a consequence of the seasonal temperature changes in Eckernförde Bay in contrast to Hydrate Ridge, where ANME-2 experience a consistent temperature of 4°C (Suess et al. 1999). The occurrence of ANME-2 in temperate coastal habitats, observed here for the first time, has been proposed by (Orphan et al. 2001b) based on the occurrence of ANME-2-related phylotypes in highly reduced, methane-rich salt marsh sediments (Munson et al. 1997).

Sedimentary biomarkers related to ANME-2 were found only in trace ammounts (M. Elvert, pers. comm.). At Station B, within the section 25-30 and 30-35 cm, 20 and 80 ng gdw^{-1} *sn*-2-hydroxyarchaeol were detected, respectively. These concentrations are 10-50 times lower compared to gas hydrate-bearing sediments at Hydrate Ridge (M. Elvert, pers. comm.). This agrees with the abundance of aggregates: ANME-2/ *Desulfococcus*/*Desulfosarcina* aggregates at Hydrate Ridge are about 100 times more abundant and reveal on average more ANME-2 cells per aggregate as found for the monospecific ANME-2 aggregates at Eckernförde Bay (Boetius et al. 2000, Treude et al. 2003). More detailed investigations are needed of the ANME-2 distribution within the AOM zone of Eckernförde Bay sediments, as their abundance in the present study was determined only for a few sections of the sediment that revealed highest AOM. Nevertheless, the data indicate a correlation between aggregate abundance and methane availability, i.e. higher abundances are found at locations with higher methane fluxes into the sulfate-methane transition. This is also shown by the potential AOM revealing 10 times lower rates in Eckernförde Bay compared to Hydrate Ridge (Nauhaus et al. 2002; Treude et al. 2003).

Environmental control of AOM in Eckernförde Bay sediments

Two sites in Eckernförde Bay were investigated for seasonal changes in AOM. The sites were sampled in early September, late September and March. At both stations, significant changes in AOM rates occurred over time. In the following, we will discuss the parameters which are responsible for these temporal variations. In general, two major factors control AOM: the availability of sulfate and of methane (Hoehler et al. 1994; Nauhaus et al. 2002). AOM is restricted to sulfate containing sediments and its rate increases with methane concentration. Furthermore, AOM is limited to the anoxic sediment due to a high sensitivity to oxygen among the group of methanotrophic archaea (K. Nauhaus, pers. comm.). Hence, oxygen is an inhibitor for AOM in oxic sediments. Temperature, on the other hand, may regulate the rate of AOM depending on the temperature optimum of the organisms.

Oxygen

For early and late September we assume complete anoxic conditions in the sediments of Station B due to: (1) the pronounced water stratification, possibly limiting the penetration of oxygen into the deeper water column; (2) the sulfidic smell and black color of the sediment even at the sediment surface, caused by SR and the formation of FeS (Jørgensen 2000); (3) the occurrence of a white coating of sulfide-oxidizing bacteria, *Beggiatoa,* on the sediment surface, a genus preferentially located at the sulfide-oxygen transition (Nelson and Jannasch 1983). Therefore, AOM in the sediment was not inhibited by oxygen and occurred over the whole depth of sulfate and methane coexistence.

In March, the water column was homogeneously mixed, enabling the diffusion of oxygen into the bottom water. The strong resuspension of the surface sediment due to wind-induced currents and the presumably lowered sediment oxygen demand at low temperatures, led to a oxygen penetration into the surface sediment. This is confirmed by the color change in the top 4 cm from black to brown, caused by the oxidation of FeS, as well as the downward movement of *Beggiatoa* (Preisler, pers. commun.). The supply of oxygen to the sediment surface shifted AOM into aerobic MO. Activity and presence of aerobic methanotrophs within the top 0-5 cm was confirmed by potential rate measurements (this study), and by molecular identification of aerobic methanotrophs (Eppelin 2002).

At Station A, the color of the surface sediment gave no hint for changes in oxygen penetration over time as it was gray-greenish, i.e. oxidized in the top 4 cm during all investigations. However, the decrease in AOM in the top 4 cm in late September, when the sediment was strongly resuspended by wind-induced currents, indicates an increase in oxygen penetration compared to early September which inhibited AOM archaea (Zehnder and Brock, 1980). The aerobic methanotrophic community, on the other hand, probably reacted very slowly to the change from anoxic to oxic conditions. During potential rate measurements we observed a lag-phase between 50 and 1000 hrs in aerobic MO (this study and Eppelin 2002). This was the time, surface slurries of Eckernförde Bay sediments needed to show elevated activity of aerobic MO after the addition of oxygen and methane. The induction of aerobic MO is associated with the general ability of aerobic methanotrophs to form resting stages (exospores and cysts) during unfavorable periods (Heyer 1990).Therefore, an oxygen penetration into the sediment in late September could have inhibited AOM archaea whereas aerobic methanotrophs have yet been in a resting stage. This would explain the decrease of methane oxidation in late September compared to early September and March. In March, when aerobic methanotrophs had presumably already germinated and exhibited growth, aerobic MO rates clearly exceeded AOM in the surface sediment.

Sulfate

The penetration depth of sulfate in Eckernförde Bay sediments is mainly controlled by SR (Whiticar 1978; Bussmann et al. 1999; Whiticar 2002). In early and late September, SR at Station A and B was enhanced at the sediment surface due to freshly sedimentated organic matter. The fresh input of organic matter is confirmed by the high chl a content at the sediment surface. Sulfate penetration, and therefore AOM, was restricted to the upper 25 cm.

In March, sulfate penetrated deeper to >30 cm, although bottom water salinity, and therefore also sulfate concentration, was lower compared to September. The deeper penetration of sulfate is explained by a drop of SR to about one third of the September activity in the top 10 cm. This was mainly for two reasons: (1) the organic matter was in an advanced degradation stage, as reflected by reduced chl a concentrations and higher chlorin-indices compared to September; (2) the ambient temperature had dropped from 11 to 4°C. SR is reported to decrease threefold to fourfold during cold seasons (temperature change 10-15°C) even when high amounts of organic matter are available in the sediment (Westrich and Berner 1988; Klump and Martens 1989). The higher sulfate penetration should have enabled

AOM to proceed down to >25 cm depth. Unfortunately, AOM rates for depth >25 cm are not available but the steady increase in AOM below 20 cm at both stations confirms this hypothesis.

The deeper penetration of sulfate and thus the deeper presence of SR during cold ambient temperatures should have shifted considerable methanogenesis >30 cm. Sulfate-reducing bacteria generally outcompete methanogens for hydrogen and acetate, which are substrates for the two major pathways of methanogenesis (Zehnder 1988). Such a correlation between temperature and the depth distribution of SR and methanogenesis has been reported for seasonal variations at Cape Lookout Bight, North Carolina (Martens et al. 1986). However, in the Eckernförde Bay sediments we proved potential methanogenesis in slurries from March for depths between 5 and 40 cm. Thus, the metabolism of the methanotrophic archaea might be based on methylotrophic pathways utilizing non-competitive substrates. The clear decrease in potential rates towards the sediment surface indicates a decrease in the methanogenic population.

The higher potential methane production in March compared to September appears strange given the difference of in situ temperatures during sampling. We rather expected a larger methanogenic population during the warm season. However, the treatment of the slurries was the same and methodical impacts can therefore be excluded.

Temperature

Despite the indirect impact of temperature on the vertical distribution of AOM by the way of SR and sulfate penetration, temporal variations in AOM rate were also found to be directly correlated with temperature changes: in March, AOM at Station A and B was lower between 5 and 25 cm compared to early September, although methane concentrations at Station B were higher. This is most likely a consequence of low temperature, as potential AOM revealed half of the activity at 4°C compared to 12°C. The lower rates enabled more methane to diffuse upward until it reached the depth of aerobic MO were it was completely consumed.

Methane

We hypothesize that two transport mechanisms of methane impacted the vertical distribution of AOM in Eckernförde Bay sediments: (1) molecular diffusion of methane from the methanogenic into the sulfate-reducing zone; (2) advective transport of methane, in the form

of gas bubbles, from the depth of gas bubble formation to the sediment surface. We build this hypothesis on two observations: (1) AOM was frequently highest within the deepest interval (20-25 cm), i.e. the transition between methanogenic and sulfate-reducing sediment, without significant temporal changes; (2) considerable AOM was also detected in depths between 0 and 20 cm with, in some cases, distinct changes in distribution and velocity.

At the border between the methanogenic and sulfate-reducing zone, a consistent supply of upward diffusing methane can be expected and thus no fast temporal changes in AOM occur. However, when methane exceeds saturation, methane bubbles form in the sediment and migrate upward due to buoyancy until they encounter interstitial fluids under-saturated with respect to methane (Whiticar 2002). Here, parts of the gaseous methane can dissolve on their way to the sediment surface. A fast, but possibly erratic transport of methane beyond the diffusive border may explain fluctuating AOM activity in the upper 20 cm of the sediment. This situation is comparable with AOM in the surface sediments of Hydrate Ridge (OR, USA), where fast transient gas injections or slowly dissociating gas hydrates are hypothesized to create either fluctuating or stable methane consumption rates (Treude et al., 2003).

A possible short-term delivery of methane by rising gas bubbles was observed at Station B in late September causing increased AOM rates between 5 and 20 cm. This increase was not found at Station A. We can exclude variations in temperature or sulfate penetration as they were similar at the two stations. We rather assume that a change in hydrostatic pressure between the sampling at Station A and B caused a temporal increase in bubble rise. This is confirmed by a drop in sea level of about 40 cm between the sampling at Station A and B (Fig. 8). This correlation is not unlikely as releases of gas bubble into the water column of Eckernförde Bay from a water depth of 26 m have been reported to occur more often during sea level decreases of 20-40 cm (Jackson et al. 1998). Mattson and Likens (1990) reported methane ebullition in a shallow lake (11 m) to be correlated even with changes in local air pressure (18% increase per mbar drop in air pressure). The decrease in hydrostatic pressure could have resulted in an expansion of gas bubbles in the sediment. The expansion than leads to instability and rise of the bubbles due to the gained buoyancy.

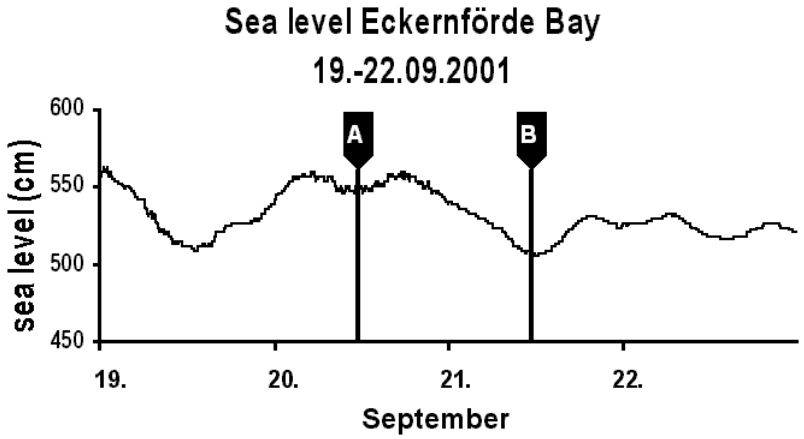

Figure 8. Sea level in Eckernförde Bay between 19. and 22. September 2001. The sampling time at Station A and B, respectively, is marked. Sea level is given in cm above absolute altitude. Data were provided by the Wasser- und Schiffahrtsamt Lübeck, Germany.

Our experiments with sediment slurries demonstrated that the organisms mediating AOM in Eckernförde Bay sediments have a large capacity to retain methane from below. Potential rates of AOM at methane saturation were always 4-10 times higher compared to field measurements at under-saturated conditions (Table 3). Even at low temperature (4°C, corresponding to the in situ temperature in March), potential rates still exhibit rates two to three times higher compared to field measurements (compare Fig. 2, 3 and 6). Thus, the organisms should be able to react to fast changes in methane supply. However, this fast response is not dependent on growth of the microbial population, because doubling times of methanotrophic ANME-2 cells are very long (4.5 months at 16 mmol L^{-1} methane, (K. Nauhaus, pers. commun.). Instead, ANME-2 cells readily change their consumption rate according to the methane partial pressure (Nauhaus et al. 2002).

Table 3. Comparison of potential and field AOM at station B. Rates determined in field measurements were averaged for the respective depth interval. For potential determination of AOM, methane was saturated at atmosperic pressure (ca. 1.3 mM).

	AOM (nmol cm^{-3} d^{-1})				
sediment depth (cm)	potential rate early Sept.	potential rate early March	field rate early Sept.	field rate late Sept.	field rate early March
0-5	28	50	3	2	- [1)]
5-10	84	21	3	6	1
10-15	15	67	4	8	1
15-20	49	24	3	8	2
20-25	54	69	7	6	5
sum	229	231	20	31	9

[1)] methane oxidation in this zone represent aerobic rates

Global comparison of AOM in Eckernförde Bay sediments

The magnitude of AOM (nmol cm^{-3} d^{-1}) in Eckernförde Bay can be determined as "medium" compared to other methane-bearing sediments or methane-seep locations (compare Hinrichs and Boetius (2002) and references therein). At sites bearing gas hydrates close to the sediment surface, methane turnover is up to 100 times higher (Joye et al., accepted; Treude et al. 2003), whereas the turnover in sediments from an anoxic basin in British Columbia (Saanich Inlet) was about 10 times lower (Devol 1983). The crucial factor determining the magnitude of AOM seems to be the methane flux: highest methane turnover rates were found at locations with highest methane fluxes (Hinrichs and Boetius 2002).

A system comparable with Eckernförde Bay was found in Cape Lookout Bight. Although sediment accumulation is about 10 times higher, there the system reveals similar characteristics (Martens and Klump 1980; Martens et al. 1986; Crill and Martens 1987; Hoehler et al. 1994; Martens et al. 1998): (1) methane is originating from recent methanogenesis, i.e. no seeping from old deposits; (2) methane saturation is reached within the top 50 cm; (3) seasonality is strong in temperature, sulfate penetration and methane ebullition; (4) AOM adjusts to the depth distribution of sulfate; (5) AOM rates range between 10 and 20 nmol cm^{-3} d^{-1}. Unfortunately, it is not known which Organisms could mediate AOM at Cape Lookout Bight and how large the size of their population is. For future work, it would be important to compare the size of AOM populations, the potential capacity of AOM, and the methane supply in different sediment systems.

CONCLUSIONS

The organisms mediating AOM in Eckernförde Bay apparently belong to the *Methanosarcinales*-related ANME-2 group that is known also from other methane-bearing locations. However, at Eckernförde Bay the organisms revealed a different strategy by forming bacterial-free aggregates. AOM in this habitat is therefore most likely mediated solely by archaea, harboring the enzymatic apparatus of both, AOM and SR.

AOM distribution and velocity in the gassy sediments of Eckernförde Bay is controlled by several environmental factors: (1) oxygen penetration, determining the upper boundary; (2) sulfate penetration determining the lower boundary; (3) temperature controlling the velocity of AOM; (4) methane supply by molecular diffusion or advection of gas bubbles creating either stable or fluctuating methane consumption rates, respectively.

Most of theses factors depend on seasonal changes like temperature, water stratification, primary production and microbial degradation processes, leading to a shallow AOM zone during the warm, productive summer season and to a deeper AOM zone during the cold winter season. The mesophilic physiology of the organisms involved in AOM is a consequence of the strong seasonal changes in temperature.

Beside seasonal factors, the drop in sea level can cause short-term variations in AOM due to the concurrent release of gas bubbles. Rising gas bubbles represent an additional methane supply beyond the diffusive border, enabling AOM in the upper 20 cm of the sediment.

Despite rising gas bubbles passing the microbial barrier, AOM in Eckernförde Bay effectively retains methane and prevents it from reaching the sediment-water interface. The methane turnover rates are intermediate compared with other methane-bearing marine locations.

ACKNOWLEDGEMENTS

We thank Captain V. Ohl, the crew of "Littorina" and the shipboard scientific party for excellent support during the cruises. We particularly thank W. Queisser, A. Krack and V. Karpen for logistic help during cruise preparations as well as I. Müller, A. Rohwedder, S. Knipp, R. Appel and A. Eppelin for technical help in the laboratory. We thank the Institut für Meereskunde, Kiel (in particular U. Rabsch) for offering laboratory facilities and the GEOMAR Research Center, Kiel for technical support. This study was made possible by the

program MUMM (Mikrobielle Umsatzraten von Methan in gashydrathaltigen Sedimenten, grant 03G0554A) supported by the Bundesministerium für Bildung und Forschung (BMBF, Germany). Further support was from the Max-Planck-Gesellschaft (MPG, Germany). This is publication GEOTECH-# of the GEOTECHNOLOGIEN program of the BMBF and the Deutsche Forschungsgesellschaft (DFG, Germany).

REFERENCES

Abegg, F., A.L. Anderson. 1997. The acoustic turbid layer in muddy sediments of Eckernfoerde Bay, Western Baltic: methane concentration, saturation and bubble characteristics. Mar. Geol. **137:** 137-147.

Albert, D., C.S Martens, M.J Alperin. 1998. Biogeochemical processes controlling methane in gassy coastal sediments- Part 2: groundwater flow control of acoustic turbidity in Eckernförde Bay Sediments. Cont. Shelf Res. **18:** 1771-1793.

Albert, D.B., C.S. Martens. 1995. Stable isotope tracing of methane production and consumption in the gassy sediments of Eckernförde Bay, Germany. Forschungsanstalt der Bundeswehr für Wasserschall und Geophysik (FWG), Kiel **22:** 114-120.

Amann, R.I., B.J. Binder, R.J. Olson, S.W. Chisholm , R. Devereux, D.A. Stahl. 1990. Combination of 16S rRNA-targeted oligonucleotide probes with flow cytometry for analyzing mixed microbial populations. Appl. Environ. Microbiol.. **56:** 1919-1925.

Anderson, A.L., F. Abegg, J.A Hawkins, M.E. Duncan, A.P. Lyons. 1998. Bubble populations and acoustic interaction with the gassy floor of Eckernförde Bay. Cont. Shelf Res. **18:** 1807-1838.

Barnett, P.R.O., J. Watson, D. Connelly. 1984. A multiple corer for taking virtually undisturbed samples from shelf, bathyal and abyssal sediments. Oceanol. Acta **7:** 399-408.

Bodungen, B.v. 1975. Der Jahresgang der Nährsalze und Primärproduktion des Planktons in der Kieler Bucht unter Berücksichtigung der Hydrographie. Ph.D. thesis. Universität Kiel.

Boetius, A., T. Ferdelman, K. Lochte. 2000. Bacterial activity in sediments of the deep Arabian Sea in relation to vertical flux. Deep-Sea Res. II **47:** 2835-2875.

Boetius, A., K. Ravenschlag, C.J. Schubert, D. Rickert, F. Widdel, A. Giesecke, R. Amann, B.B. Jørgensen, U. Witte, O. Pfannkuche. 2000. A marine microbial consortium apparently mediating anaerobic oxidation of methane. Nature **407:** 623-626.

Bussmann, I., P.R. Dando, S.J. Niven, E. Suess. 1999. Groundwater seepage in the marine environment: role for mass flux and bacterial activity. Mar. Ecol. Prog. Ser. **178:** 169-177.

Cord-Ruwisch, R. 1985. A quick method for the determination of dissolved and precipitated sulfides in cultures of sulfate-reducing bacteria. J. Microbiol. Methods **4:** 33-36.

Crill, P.M., C.M. Martens. 1987. Biogeochemical cycling in an organic-rich coastal marine basin. 6. Temporal and spatial variations in sulfate reduction rates. Geochim. Cosmochim. Acta **51:** 1175-1186.

Devol, A.H. 1983. Methane oxidation rates in the anaerobic sediments of Saanich Inlet. Limnol. Oceanogr. **28 (4):** 738-742.

Eppelin, A. 2002. Charakterisierung aerob methanoxidierender Mikroorganismen an marinen Standorten. Thesis. Universiät Bremen.

Fossing, H, B.B. Jørgensen. 1989. Measurements of bacterial sulphate reduction in sediments: evaluation of a single-step chromium reduction method. Biogeochemistry **8:** 205-222.

Gripp, K. 1964. Erdgeschichte von Schleswig-Holstein, Karl Wachholz Verlag, Neumünster, pp. 411.

Hansen, H.-P. 1993. Saisonale und langzeitliche Veränderungen chemisch-hydrographischer Parameter in der Kieler Bucht. Berichte aus dem Institut für Meereskunde **240:** 2-31.

Hansen, H.P., H.C. Giesenhagen, G. Behrends. 1999. Seasonal and long-term control of bottom-water oxygen deficiency in a stratified shallow-water costal system. ICES J. Mar. Sci. **56:** 65-71.

Heyer, J. 1990. Der Kreislauf des Methans, Akademie-Verlag Berlin, pp. 250.

Hinrichs, K.-U., A. Boetius. 2002. The anaerobic oxidation of methane: new insights in microbial ecology and biogeochemistry. In: G. Wefer, D. Billett, D. Hebbelnet al [eds.], Ocean Margin Systems. Springer-Verlag, Berlin, pp. 457-477.

Hinrichs, K.-U., J.M. Hayes, S.P. Sylva, P.G. Brewer, E.F. De Long. 1999. Methane-consuming archaebacteria in marine sediments. Nature **398:** 802-805.

Hoehler, T.M., M.J. Alperin, D.B. Albert, C.S. Martens. 1994. Field and laboratory studies of methane oxidation in an anoxic marine sediments: evidence for methanogen-sulphate reducer consortium. Global Biochem. Cycles **8 (4):** 451-463.

Jackson, D.R., K.L. Williams, T.F. Wever, C.T. Friedrichs, L.D. Wright. 1998. Sonar evidence for methane ebullition in Eckernförde Bay. Cont. Shelf Res. **18:** 1893-1915.

Jørgensen, B.B. 1978. A comparison of methods for the quantification of bacterial sulphate reduction in coastal marine sediments: I. Measurements with radiotracer techniques. Geomicrobiol. J. **1 (1):** 11-27.

Jørgensen, B.B. 2000. Bacteria and marine biogeochemistry. In: H. D. Schulz and M. Zabel [eds.], Marine Geochemistry. Springer Verlag, Berlin, pp. 173-207.

Joye, S.B., A. Boetius, B.N. Orcutt, J.P. Montoya, H.N. Schulz, M.J. Erickson, S.K. Logo. (accepted). The anaerobic oxidation of methane and sulfate reduction in sediments from Gulf of Mexiko cold seeps. Chem. Geol.

Karpen, V. 2002. Fluid discharge at different seep environments: distribution, flow rate, and influence on particle resuspension. Ph.D. thesis. Christian-Albrechts-Universität zu Kiel.

Klump, J.V., C.M. Martens 1989. The seasonality of nutrient regeneration in an organic-rich coastal sediment: Kinetic modeling of changing pore-water nutrient and sulfate distributions. Limnol. Oceanogr. **34 (3):** 559-577.

Krüger, M., G. Eller, R. Conrad, P. Frenzel. 2002. Seasonal variations in CH_4 oxidation and pathways of CH_4 production in rice fields determined by stable carbon isotopes and specific inhibitors. Glob. Change Biol. **8:** 265-280.

Krüger, M., P. Frenzel, R. Conrad. 2001. Microbial processes influencing methane emission from reice fields. Glob. Change Biol. **7:** 49-61.

Lenz, J. (1996). Plankton. In: G. Rheinheimer [eds.], Meereskunde der Ostsee. Springer Verlag, Berlin, pp. 136-150.

Madigan, M.T., J.M. Martino, J. Parker. 2000. Brock Biology of Microorganisms 9/e, Prentice-Hall, New Jersey, pp. 1175.

Manz, W., M. Eisenbrecher, T.R. Neu, U. Szewzyk. 1998. Abundance and spatial organization of Gram-negative sulfate-reducing bacteria in activated sludge investigated by in situ probing with specific 16S rRNA targeted oligonucleotides. FEMS Microb. Ecol. **25:** 43-61.

Martens, C.S., D.B. Albert, M.J. Alperin. 1998. Biogeochemical processes controlling methane in gassy coastal sediments-Part 1. A model coupling organic matter flux to gas production, oxidation and transport. Cont. Shelf Res. **18:** 1741-1770.

Martens, C.S., D.B. Albert, M.J. Alperin. 1999. Stable isotope tracing of anaerobic methane oxidation in the gassy sediments of Eckernförde Bay, German Baltic Sea. Am. J. Sci. **299:** 589-610.

Martens, C.S., N.E. Blair, C.D. Green. 1986. Seasonal variations in the stable carbon isotopic signature of biogenic methane in a coastal sediment. Science **233:** 1300-1303.

Martens, C.S., V.K. Klump. 1980. Biogeochemical cycling in an organic-rich coastal marine basin - I. Methane sediment-water exchange processes. Geochim. Cosmochim. Acta **44:** 471-490.

Mattson, M.D., G.E. Likens. 1990. Air pressure and methane fluxes. Nature **347:** 718-719.

Meyer-Reil, L.-A., G. Graf. 1984. Seasonal development of bacterial communities in a coastal marine sediment as related to the input of organic material. Actes de Colloques, Brest, France. IFREMER, **3:** 55-59.

Michaelis, W., R. Seifert, K. Nauhaus, T. Treude, V. Thiel, M. Blumenberg, K. Knittel, A. Gieseke, K. Peterknecht, T. Pape, A. Boetius, A. Aman, B.B. Jørgensen, F. Widdel, J. Peckmann, N.V. Pimenov, M. Gulin. 2002. Microbial reefs in the Black Sea fueled by anaerobic oxidation of methane. Science **297:** 1013-1015.

Milkert, D., U. Hentschke, F. Werner. 1995. Influence of storms on sediments in Eckernförde Bay. Forschungsanstalt der Bundeswehr für Wasserschall und Geophysik (FWG), Kiel **22:** 149-158.

Munson, M.A., D.B. Nedwell, T.M. Embley. 1997. Phylogenetic diversity of archaea in sediments samples from a coastal salt marsh. Appl. Environ. Microbiol. **63:** 4729-4733.

Nauhaus, K., A. Boetius, M. Krüger, F. Widdel. 2002. In vitro demonstration of anaerobic oxidation of methane coupled to sulphate reduction in sediment from marine gas hydrate area. Environ. Microbiol. **4 (5):** 298-305.

Nelson, D.C., H.W. Jannasch. 1983. Chemoautotrophic growth of marine *Beggiatoa* in sulfide-gradient cultures. Arch. Mikrobiol. **136:** 262-269.

Nittrouer, C.A., G.R. Lopez, L.D. Wright, S.J. Bentley, A.F. D´Andrea, C.T. Friedrichs, N.I. Craig, C.K. Sommerfeld. 1998. Oceanographic processes and the preservation of sedimentary structure in Eckernföde Bay, Baltic Sea. Cont. Shelf Res. **18:** 1689-1714.

Orphan, V.J., K.-U. Hinrichs, W. Ussler III, C.K. Paull, L.T. Tayleor, S.P. Sylva, J.M. Hayes, E.F. De Long. 2001b. Comparative analysis of methane-oxidizing archaea and sulfate-reducing bacteria in anoxic marine sediments. Appl. Environ. Microbiol. **67 (4):** 1922-1934.

Orphan, V.J., C.H. House, K.-U. Hinrichs, K.D. McKeegan, E.F. De Long. 2001a. Methane-consuming Archaea revealed by directly coupled isotopic and phylogenetic analysis. Science **293:** 484-487.

Schubert, C.J., G. Klockgether, J. Niggemann, T.G. Ferdelman, B.B. Jorgensen. 2002. The Chlorin-Index: A new parameter for organic matter freshness in sediments. Geochim. Cosmochim. Acta **66 (15A):** A689-A689.

Snaidr, J., R. Amann, I. Huber, W. Ludwig, K.H. Schleifer. 1997. Phylogenetic analysis and in situ identification of bacteria in activated sludge. Appl. Environ. Microbiol. **65:** 3976-3981.

Sørensen, K.B., K. Finster, N.B. Ramsing. 2001. Thermodynamic and kinetic requirements in anaerobic methane oxidizing consortia exclude hydrogen, acetate and methanol as possible electron shuttles. Microb. Ecol. **42:** 1-10.

Suess, E., M.E. Torres, G. Bohrmann, R.W. Collier, J. Greinert, P. Linke, G. Rehder, A. Trehu, K. Wallmann, G. Winckler, E. Zuleger. 1999. Gas hydrate destabilization: enhanced dewatering, benthic material turnover and large methane plumes at the Cascadia convergent margin. Earth Planet. Sci. Lett. **170:** 1-15.

Treude, T., A. Boetius A., K. Knittel, K. Wallmann, B.B.Jørgensen. (2003). Anaerobic oxidation of methane above gas hydrates (Hydrate Ridge, OR). Mar. Ecol. Prog. Ser **264**: 1-14.

Werner, R. 1978. Depression in mud sediments (Eckernförde Bay, Baltic Sea), related to sub-bottom and currents. Meyniana **30:** 99-104.

Westrich, J.T., R.A. Berner. 1988. The effect of temperature on rates of sulfate reduction in marine sediments. Geomicrobiol. J. **6:** 99-117.

Wever, T.F., F. Abegg, H.M. Fiedler, G. Fechner, I.H. Stender. 1998. Shallow gas in the muddy sediments of Eckernförde Bay, Germany. Continental Shelf Research **18:** 1715-1739.

Whiticar, M.J. 1978. Relationsships of interstitial gases and fluids during early diagenesis in some marine sediments. Sonderforschungsbereich 95: Wechselwirkung Meer-Meeresboden. Ph.D. thesis. Universität Kiel.

Whiticar, M.J. 2002. Diagenetic relationships of methanogenesis, nutrients, acoustic turbidity, pockmarks and freshwater seepages in Eckernförde Bay. Marine Geology **182:** 29-53.

Widdel, F., F. Bak. 1992. Gram-negative mesophilic sulfate-reducing bacteria. In: A. Balows, H. G. Trüper, M. Dworking, W. Harder and K.-H. Schleifer [eds.], The Prokaryotes. Springer-Verlag, New York, pp. 3352-3378.

Zehnder, A.J.B. 1988. Biology of anaerobic microorganisms, Wiley, New York.

Zehnder, A.J.B., T.D. Brock.1980. Anaerobic methane oxidation: occurrence and ecology. Appl. Environ. Microbiol. **39** (1): 194-204.

Chapter 4

Anaerobic oxidation of methane in the sulfate-methane transition along the Chilean continental margin

Tina Treude[1], Jutta Niggemann[1], Jens Kallmeyer[1,2], Paul Wintersteller[3], Carsten Johnny Schubert[4], Antje Boetius[1,5], Bo Barker Jørgensen[1]

[1]Max Planck Institute for Marine Microbiology, Department of Biogeochemistry, Celsiusstrasse 1, 28359 Bremen, Germany

[2]Geoforschungszentrum Potsdam, Telegrafenberg, 14473 Potsdam, Germany

[3]RF Forschungsschiffahrt GmbH, Blumenthalstrasse 15, 28023 Bremen, Germany

[4]Swiss Federal Institute for Environmental Science and Technology, Limnological Research Center, 6047 Kastanienbaum, Switzerland

[5]International University Bremen, Research II, Campusring 1, 28759 Bremen, Germany

Accepted by Geochimica et Cosmochimica Acta

ABSTRACT: Anaerobic oxidation of methane (AOM) and sulfate reduction (SR) were investigated in sediments of the Chilean upwelling region at three stations between 800 and 3000 m water depth. Major goals of the study were to quantify AOM in a coastal marine upwelling system, to analyze the impact of AOM on methane cycling, and to determine the contribution of AOM to SR within the sulfate-methane transition zone (SMT). Furthermore, we investigated the formation of authigenic carbonates within the SMT and the correlation between organic matter sedimentation and SR in the surface sediment. We determined the vertical distribution of AOM, SR, methane, sulfate, sulfide, pH, total chlorins, and various geochemical parameters. Depth-integrated rates of AOM within the SMT were between 75 and 2800 mmol m^{-2} a^{-1}, effectively removing methane below the sediment-water interface. Single measurements revealed AOM peaks of 2 to 51 nmol cm^{-3} d^{-1}, with highest rates at the shallowest station (800 m). The rates were higher than in other diffusive systems of similar ocean depth, indicating a higher methane turnover in the organic-rich sediments of this upwelling region. SR within the SMT was mostly fuelled by methane. AOM led to the formation of isotopically light dissolved inorganic matter (DIC) ($\delta^{13}C$ -24.6 ‰ VPDB) and of distinct layers of authigenic carbonates ($\delta^{13}C$ -14.6 ‰ VPDB). SR at the sediment surface showed correlations with water depth and latitude, i.e. increasing rates with decreasing water depth and higher southern latitude. Both can ce explained by the supply of fresh organic material.

INTRODUCTION

The microbial process of anaerobic oxidation of methane (AOM) effectively removes methane from marine sediments before it reaches the sediment-water interface (Hinrichs and Boetius (2002) and references therein). AOM thereby plays a significant role in the regulation of the global methane cycle and the atmospheric emission of methane, which is a potentially strong greenhouse gas.

During AOM, methane is oxidized with concurrent sulfate reduction (SR) according to the following net equation (Eq. 1):

$$CH_4 + SO_4^{2-} \rightarrow HCO_3^- + HS^- + H_2O \qquad (1)$$

Since sulfate is the electron acceptor, AOM is limited to the sulfate penetrated zone of the sediment. In diffusive systems, the activity of AOM leads to a typical concave-up profile of

methane concentration (Iversen and Jørgensen, 1985). The peak in AOM coincides with the sulfate-methane transition (SMT).

Experimental measurements of AOM in shelf sediments (<200 m water depth) were conducted in, e.g. the Baltic Sea, Cape Lookout Bight, and Scan Bay (Reeburgh, 1980; Iversen and Blackburn, 1981; Alperin and Reeburgh, 1985; Iversen and Jørgensen, 1985; Hoehler et al., 1994; Hansen et al., 1998; Bussmann et al., 1999). Most determinations of AOM rates in sediments from more than 200 m water depth are based on modeling (e.g. Reeburgh, 1976; Borowski et al., 2000; Jørgensen et al., 2001). Modeling, however, may potentially underestimate the true methane turnover as direct measurements with radiotracers often reveal higher rates (Hinrichs and Boetius, 2002). Several recent investigations of AOM have focused on extreme environments such as methane seeps and gas hydrate sites revealing high advective methane fluxes and AOM rates (Boetius et al., 2000; Orphan et al., 2001; Michaelis et al., 2002; Joye et al., accepted; Treude et al., 2003). Yet methane is a general product of organic matter degradation in marine sediments where considerable amounts of organic matter reach the ocean floor (Claypool and Kaplan, 1974; Reeburgh, 1996). Thus, AOM needs to be investigated throughout the productive marine regions worldwide, from littoral to bathyal depths.

Few data on AOM exist from coastal upwelling systems that provide some of the most productive regions of the ocean. Estimates of AOM were made in sediments off the Namibian coast by modeling the methane and sulfate profiles (Niewöhner et al., 1998; Fossing et al., 2000). Methane in these organic-rich sediments is completely consumed within the anoxic sediment. In the present study we investigated AOM in sediments from another important upwelling system – the shelf region off Chile. The euphotic zone along the Peruvian and Chilean shelf is the world's largest high-productivity area among the eastern boundary current systems (Berger et al., 1987) and has a biological productivity of about 0.83 mol C m^{-2} d^{-1} (Fossing et al., 1995). The ocean floor of shallow water depths (above 700 m) receive a permanent deposition of organic material produced by phytoplankton (Arntz and Fahrbach, 1991). As a result of organic matter degradation within the water column, high oxygen consumption leads to an oxygen minimum zone at water depths between 50 and 300 m along central and northern Chile. Below 700 m water depth, the sinking organic material has been extensively degraded in the overlying water column, leading to an increase of oxygen concentration in the bottom water (Ahumada et al., 1983; Arntz and Fahrbach, 1991). In the present study we sampled three stations along the Chilean continental margin at water depths between 800 and 3000 m. The aim was:

1. to quantify AOM in an upwelling system and analyze the control on methane retention in the sediment;
2. to determine the coupling between AOM and SR within the SMT;
3. to investigate correlations of water depth and latitude with differences in organic matter input and degradation processes;
4. to investigate, whether organoclastic SR at the sediment surface affects the distribution of sulfate and methane in the sediment;
5. to investigate the formation of authigenic carbonates related to AOM.

MATERIALS AND METHODS

Sampling sites. Sediments were sampled with gravity and multiple corers at three stations along the Chilean continental margin (Fig. 1, Table 1) during RV SONNE cruise SO-156/3 in April/May 2001. Station 7155 and 7165 were located off Central Chile between 34° and 38°S, Station 7186 was located further to the south at 44°S. A detailed core description for each station is given by Hebbeln and participants (2001). The main sediment characteristics can be summarized as follows:

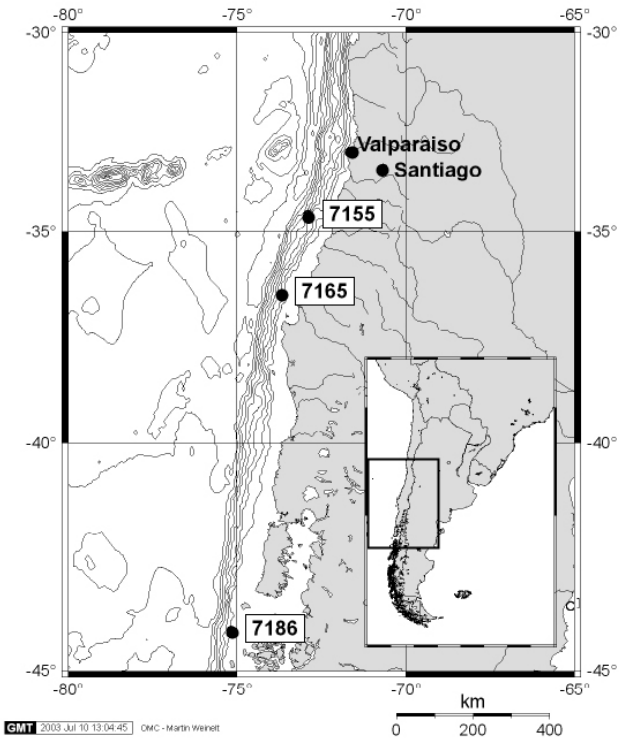

Figure 1. Location of the investigated stations along the Chilean continental margin.

At Station 7165 (800 m) the lithology changed between dark olive-green hemipelagic mud in the upper 320 cm to reddish-grey muddy clay from 320 cm downcore. Dark-colored burrows were found throughout the core. H_2S smell was detected below 200 cm.

At Station 7186 (1160 m) the sediment was dominated by hemipelagic mud. The upper 170 cm was olive-green with black-colored burrows. Below 170 cm the sediment color was olive-green with black patches and horizons, gradually turning into black with olive-green patches. H_2S smell was detected between 140 and 170 cm.

At Station 7155 (2750 m) the sediment was dominated by hemipelagic mud. The color was olive-green in the upper 200 cm, gradually changing to olive-green with black patches forming around faunal burrows. In the lower part (300 to 600 cm) the sediment was black.

Table 1. Data of GeoB stations (Geowisenschaften Bremen). Stations are sorted by water depth. Note that GeoB 7162 and 7165 represent the same location.

Station GeoB No.	Core type[1)]	Position	Sampling date 2001	Recovery (cm)	Water depth (m)
7162-5	MUC	36°32´32S 73°39´59W	24.04.	20	797
7165-2	GC	36°32´32S 73°40´02W	25.04	760	799
7186-2	GC	44°08´59S 75°09´31W	05.05.	490	1168
7186-4	MUC	44°09´00S 75°09´30W	05.05.	30	1151
7155-1	MUC	34°34´59S 72°53´13W	21.04.	40	2746
7155-4	GC	34°35´00S 72°53´11W	21.04.	670	2744

[1)] MUC = multiple corer, GC = gravity corer

Gravity core sampling. We pre-sampled the intact gravity core for methane concentration and other parameters to determine (1) the length of the subsections into which the core was later divided and (2) the sizes of the appropriate sampling intervals. Thereby, a disturbance of the AOM zone by unfavorable cuts was prevented and sampling intervals could be adapted appropriately based on known parameters.

Pre-sampling. After retrieval, the intact core (12 m in two 6 m long PVC-liners, ends sealed with plastic caps and gas-tight tape, inner diameter 120 mm) was placed horizontally

on a table at room temperature. For pre-sampling, windows of ca. 4 x 7 cm were cut in the core liner at 20 cm depth intervals from bottom to top using a vibro saw. Only one window was open at a time to avoid degassing of methane and oxidation of the sediment. After sampling, the window was sealed with gas-tight tape before the next window was opened. The duration of the whole procedure was kept to a minimum (approx. 2 hrs. per core) to reduce warming of the sediment.

First, a sediment sample of 2 cm^3 was taken with a cut-off plastic syringe to determine the methane concentration. The sample was transferred into a 10 ml glass vial filled with 5 ml sodium hydroxide (2.5 % w/w). The vial was closed immediately with a butyl rubber stopper, sealed with an aluminum crimp, and shaken thoroughly to equilibrate the pore water methane between the aqueous and the gaseous phases. After equilibration, the methane concentration of the sample was determined by gas chromatography (see analytical methods below).

After pre-sampling for methane, various probes were plugged into the sediment to measure the inner and peripheral temperature of the core, pH, sulfide, porosity and density (see analytical methods below).

According to the methane and sulfide profiles, the core was divided into sub-cores. The zone of the steep methane gradient and presence of sulfide, i.e. the presumable zone of AOM activity, was cut in a 1 m sub-core. Above and below that zone the core was divided into 1 m sub-cores. The sub-cores were sealed with plastic caps and gas-tight tape and stored at 4°C until further treatment.

Main sampling. The main sampling was done in a cold room (4°C). Sub-cores were positioned vertically and the sediment was pushed out of the liner using a plastic plunger and a car-jack. From the center of the core, samples were taken for AOM, SR, sulfate, total chlorins, and other geochemical parameters.

For AOM and SR, the sampling intervals were 10 cm (2 cm for core 7155) within the SMT and 20 cm above and below the SMT. Samples were taken vertically with glass tubes (5 ml) that were closed with butyl rubber stoppers at the ends. Two replicates per sampling depth as well as 10 controls from different depths were taken for AOM and SR, respectively. For core 7155, the SMT was sampled with push-cores (length 40 cm, inner diameter 26 mm) instead of glass tubes.

Sulfate samples were taken vertically with 20 ml cut-off plastic syringes at 10 cm intervals. The samples were transferred into 50 ml plastic centrifuge tubes filled with 20 ml zinc acetate (20 % w/w), capped, and frozen at -25°C.

Samples for total organic carbon (TOC), total inorganic carbon (TIC), C/N-ratio, $\delta^{13}C$ of TIC, and total chlorins were taken with 60 ml cut-off syringes in 20 cm intervals and transferred into polypropylene bags. The bags were immediately frozen at -25°C.

Pore water for the determination of $\delta^{13}C$ of DIC was extracted from sediment slices taken at 10 cm intervals within the SMT and 20 cm above and below the SMT. The pore water was extracted at 4°C using a Macrolon pore water press (Reeburgh squeezer) with cellulose acetate filters (0.45 type 11306-100-N, Sartorius, Germany) and an argon gas presssure of 3-4 bar. In order to minimize oxidation during loading of the pore water press, a continuous laminar flow of argon was directed over the sample holder. The pore water was collected in a 10 ml glass syringe and 1 ml was transferred into exetainers (glass vials, Labco Limited, England) filled with 10µl HgCl (in vacuum) and was frozen at -25°C .

Multi-core sampling. Multi-cores were sampled at the same sites as the gravity cores to investigate the surface sediment, which is usually disturbed upon retrieval of gravity cores. Undisturbed sediment cores with a maximum length of about 30 cm (inner diameter 100 mm) were sampled for SR, total chlorins, and other geochemical parameters. For total chlorins, TIC, TOC and C/N-ratio one core was sampled at 1 cm intervals from 0-6 cm, and at 2 cm intervals below 6 cm. The sediment was transferred into precombusted glass vials and frozen at -25°C. For SR, one core was sampled vertically with a push-core and/or cut-off glass tubes (5 ml, 2-3 replicates per interval) as described above. Push-cores were sliced into 1 cm intervals, whereas glass syringes covered a depth interval of 5 cm each.

Analytical procedures. ***Methane concentration.*** Methane concentrations were determined by the injection of 200 µl of the headspace of the glass vials into a gas chromatograph (5890A, Hewlett Packard). The gas chromatograph was equipped with a packed stainless steel Porapak-Q column (6 ft., 0.125 in., 80/100 mesh, Agilent Tecknologie) and a flame ionization detector. The carrier gas was helium at a flow rate of 30 ml min^{-1}. The column temperature was 40°C.

Temperature. Warming-up of the core during handling was recorded using two thermometers with steel probes (Amarell, digital thermometer, precision ± 0.1°C) that were positioned in the periphery or center of the core.

pH. Pore water pH was determined with an ion-selective Ross combination electrode (Orion). The precision of pH measurements was ±0.05 pH units.

Sulfide concentration. Pore water sulfide was determined with a WT-573-H_2S combination electrode (Water Test, Thailand). Total sulfide concentrations were calculated from the sulfide, pH and temperature measurements.

Porosity and density. Porosity and wet density of the sediment were determined from the specific electric resistance of the sediment using a resistivity probe constructed by (Bergmann, 1995). The probe consists of four equidistant (4 mm) platinum electrodes of 0.6 mm diameter embedded in a PVC rod (200 x 16 x 2.1 mm). The precision of sediment porosity determinations was ±0.02. The precision of sediment wet density was ±0.03 g cm^{-3}.

Anaerobic oxidation of methane (AOM). Radioactive methane ($^{14}CH_4$ dissolved in seawater, injection volume 15µl, activity 1 kBq) was injected into each sample. For the SMT of core 7155, radioactive methane was injected into push-cores at 1 cm-intervals according to the whole core injection method of (Jørgensen, 1978). The samples were incubated at in situ temperature (4°C, Hebbeln et al., 2000) for 24 hrs in the dark. To stop bacterial activity, the samples (push-cores were split into 2 cm-intervals) were transferred into 50 ml glass vials filled with 25 ml sodium hydroxide (2.5% w/w) and closed immediately with rubber stoppers (1.5 cm thickness). The glass vials were shaken thoroughly to equilibrate the pore water methane between the aqueous and the gaseous phase. Controls were fixed before addition of tracer. In the home laboratory, AOM was determined according to Treude et al.(2003). In short, a 200 µL aliquot of the headspace was injected into a gas chromatograph to measure the total methane concentration of the sample. The amount of residual $^{14}CH_4$ was determined by scintillation counting after the combustion of $^{14}CH_4$ at 850°C in a quartz tube filled with Cu(II)-oxide, and subsequent trapping of the formed $^{14}CO_2$ with phenylethylamine. The amount of microbially formed $^{14}CO_2$ was determined by scintillation counting after acidification of the aqueous sample and trapping of $^{14}CO_2$ on a filter saturated with phenylethylamine. AOM rates were calculated by the following equation (Eq. 2):

$$AOM = \frac{^{14}CO_2 \times CH_4}{^{14}CH_4 \times v \times t} \qquad (2)$$

were $^{14}CO_2$ is the radioactivity of the microbially produced carbon dioxide, CH_4 is the total amount of methane in the sample, $^{14}CH_4$ is the radioactivity of the residual methane, v is the volume of the sediment, and t is the incubation time.

Sulfate reduction (SR). Sampling, injection and incubation was the same as for AOM. The injected radiotracer was sulfate ($^{35}SO_4$ dissolved in NaCl solution (3% w/v), injection volume

5 µL, activity 250 kBq). To stop bacterial activity after incubation, the samples (push-cores were split into 2 cm-intervals) were transferred into plastic centrifuge tubes filled with 20 ml zinc acetate (20% w/w). Control samples were fixed before addition of tracer. SR rates were determined using a cold-chromium-distillation method according to (Kallmeyer et al., submitted). The samples were centrifuged (3500 g for 10 min) and the supernatant removed. An aliquot of the supernatant was taken for radioactivity measurement. The sediment samples were mixed with 20 ml of 1,2 N, N Dimethyl-Formamide (DMF) technical grade and immediately transferred into 3-neck glass flasks and flushed with N_2 to drive off oxygen. After 15 minutes, 8 ml 6 N HCl and 16 ml 1 N $CrCl_2$ solution were added. The total reduced inorganic sulfur species (TRIS, comprising metal mono- and disulfides and elemental sulfur) were liberated as H_2S and driven out of solution by flushing with N_2 for two hours. The outflowing gas was passed through an aerosol trap with 7 ml 1 N Na-citrate solution buffered at pH 4 and a final trap with 7 ml of zinc acetate (5 % w/w) and a drop of Antifoam. In this trap all the H_2S precipitated as zinc sulfide. Quantification of radioactivity was done by liquid scintillation counting. By comparing the activity of the radiolabeled TRIS to the activity of the injected sulfate radiotracer the sulfate reduction rate was calculated (Eq. 3):

$$SRR = \frac{[SO_4] \cdot \Phi \cdot aTRIS \cdot 1.06}{t \cdot aTOT} \qquad (3)$$

where *SRR* is the sulfate reduction rate, [*SO4*] is the pore water sulfate concentration, *Φ* is the porosity (as a fraction of 1), *aTRIS* is the radioactivity of TRIS, 1.06 is a correction factor for the expected isotopic fractionation (Jørgensen and Fenchel, 1974), *t* is the incubation time and *aTOT* is the total radioactivity injected.

Sulfate concentration. Samples were thawed and centrifuged (2200 g, 10 min). Pore water sulfate concentrations were measured in the supernatant using nonsuppressed ion chromatography with a Waters 510 HPLC pump, Waters WISP 712 autosampler (100 µL injection volume), Waters IC-Pak anion exchange column (50 x 4.6 mm), and a Waters 430 conductivity detector. The eluent was 1 mM isophthalatic acid with 10% methanol, adjusted to pH 4.5. The flow was 1.0 ml min^{-1}.

TOC, TIC, C/N. Prior to elemental analysis, the samples were freeze-dried and homogenized by gentle grinding in an agate mortar. Total carbon (TC) and total nitrogen (TN) concentrations were determined by combustion/gas chromatography (Carlo Erba NA-1500 CNS analyser) with a precision of ±0.7% for N and ±0.6% for C, respectively. Total

inorganic carbon (TIC) was measured on a CM 5012 CO_2 Coulometer (UIC) after acidification with H_3PO_4. The precision for TIC was ±0.4%. Total organic carbon (TOC) was calculated as the difference between TC and TIC. The C/N-ratio is given as the molar ratio of TOC and TN.

$\delta^{13}C$ of DIC and TIC. The carbon isotopic compositions of carbonate and DIC was measured using a MultiFlow system connected to an Isoprime (Micromass, UK) mass spectrometer. Sediment or water samples were introduced into exetainers (glass vials, Medical Instruments Corporation) to reach approximately 100 µg of carbonate content. After exchanging air with helium, samples were acidified with phosphoric acid (85%) and equilibrated at 90°C for 5-6 hours. The CO_2 that degassed from the samples was transported via a helium flow into the mass spectrometer. Results are reported in the δ notation (Eq. 4):

$$\delta^{13}C(‰) = \left\{ \frac{{}^{13}C/{}^{12}C_{sample}}{{}^{13}C/{}^{12}C_{standard}} - 1 \right\} \times 1000 \qquad (4)$$

and are related to the VPDB (Vienna Peedee belemnite) standard. Average standard deviation for four replicates was ±0.15 ‰ for DIC and ±0.12 ‰ for carbonate measurements.

Total chlorins and chlorin-index. For the determination of chlorins, which include a whole suite of degradation products of chlorophyll, 200 mg of freeze dried sediment was extracted with acetone by three-fold sonication and centrifugation. During extraction, the samples were cooled in an ice bath under low light conditions to prevent decomposition of the chlorins. The sediment extracts were measured fluorimetrically (Hitachi F-2000 fluorometer; λ_{ex}=428 nm, λ_{em}=671 nm) immediately after extraction. Chlorophyll a (Fluka) was transformed to pheophytin a by acidification with a few drops of hydrochlorid acid and used as standard. The pigment concentration is calibrated against pheophytin a. The relative precision of the method was ±10%. As labile compounds are easily degraded by acid treatment, the pigment extracts were acidified and measured again. The ratio of the fluorescence intensities (FI) of the acid-treated and the untreated pigment extract provides a measure of the degradability of the pigments, because the resulting molecules have different fluorescence behavior than its precursor. This ratio is defined as the chlorin-index (Eq. 5; Schubert et al., 2002):

$$chlorin-index\,(CI) = \frac{FI_{acidified\ sample}}{FI_{original\ sample}} \qquad (5)$$

Diffusive flux calculation. Diffussive fluxes of methane and sulfate were calculated from linear pore water concentration gradients according to Fick´s first law assuming steady state conditions (Eq. 6; e.g. Berner, 1980):

$$J = -\Phi \cdot D_s \cdot \frac{dc}{dx} \qquad (6)$$

where J is the diffusive flux [mmol m^{-2} a^{-1}], Φ is the porosity, D_s is the sediment diffusion coefficient [m^2 a^{-1}], C is the concentration of either sulfate or methane [mmol m^{-3}], and X is the depth [m]. The steepest concentration gradient into the SMT was used for calculations of the fluxes to get the best estimation. The gradients are marked by solid lines in the concentration profiles of methane and sulfate (Fig. 3a/b, 4a/b and 5a/b).
Sediment diffusion coefficients, D_s, of methane and sulfate were calculated according to Iversen and Jørgensen (1993) from the measured porosities (Eq. 7):

$$D_s = \frac{D}{(1 + 3(1 - \Phi))} \qquad (7)$$

At the in situ temperature of 4°C (Hebbeln et al., 2000) the molecular diffusion coefficients (D) in seawater are: $D_{methane}$ = 8.7 x 10^{-5} cm^2 s^{-1} and $D_{sulfate}$ = 5.5 x 10^{-5} cm^2 s^{-1} (Iversen and Jørgensen, 1993).

RESULTS

Temperature increase during pre-sampling and influence on methane solubility

Temperature records of the gravity core periphery and center during sampling from bottom to top are shown in Fig. 2. Highest temperatures of the periphery were 20.7°C, 13.7°C, and 15.9°C for core 7165, 7186, and 7155 , respectively. Highest temperatures of the center were 15.0, 9.2, and 10.0, respectively. Highest core temperatures were recorded towards the end of the pre-sampling procedure due to a gradual warming from in situ (4°C, Hebbeln et al., 2000) towards the ambient temperature (around 20°C).

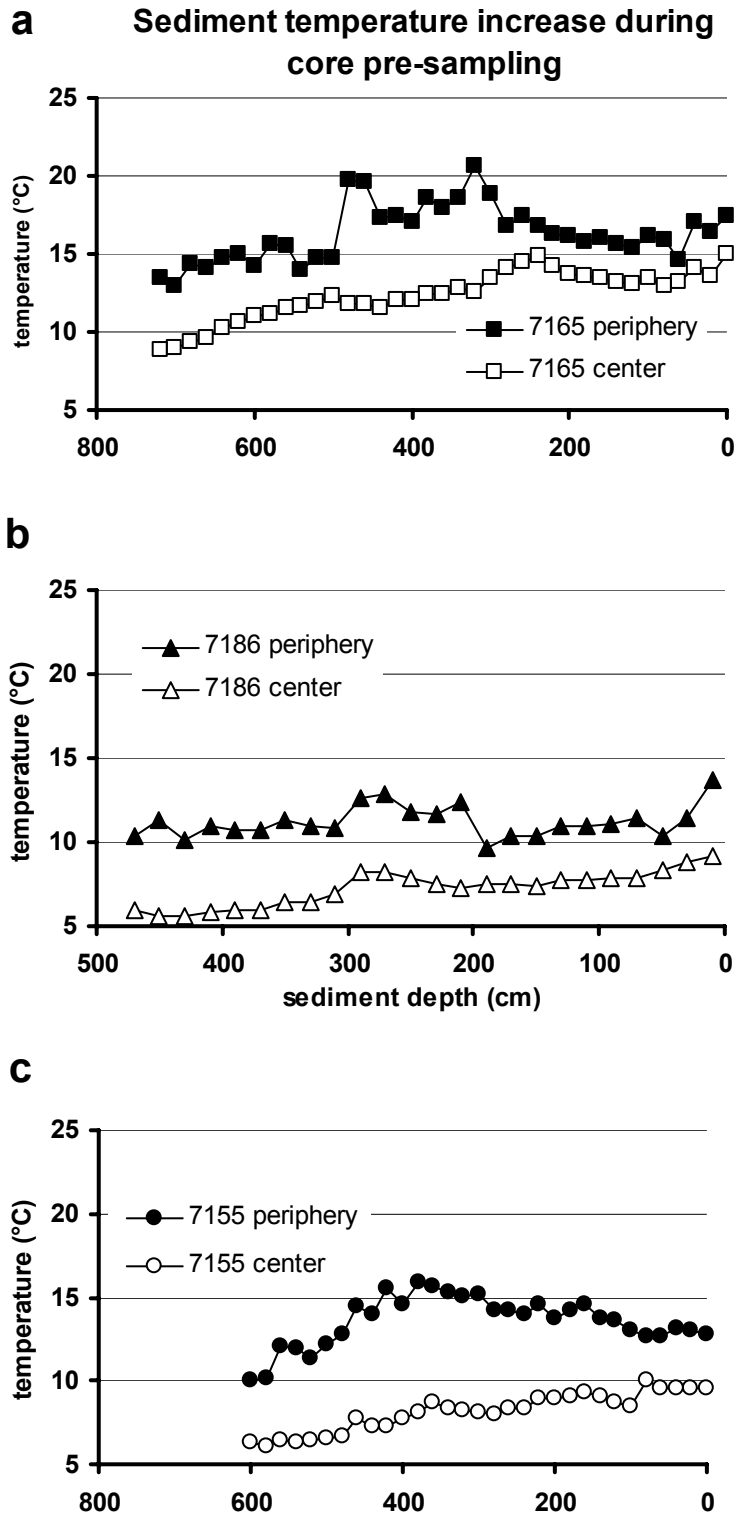

Figure 2 (a-c). Temperature increase of core periphery and core center during pre-sampling. Cores were successively sampled from bottom to top.

Porosity, density, C/N, total chlorins and chlorin-index

In core 7165 and 7155, porosity and density revealed a steady decrease and increase, respectively, with depth (data not shown). The porosity was 0.80 at the top (40 cm) of core 7165 and decreased to 0.72 at the bottom (750 cm). Density was 1.39 (40 cm) and 1.59 g cm^{-3} (750 cm), respectively. In core 7155, porosity was 0.80 at the top (0 cm) and decreased to 0.65 at the bottom (580 cm). Density was 1.36 (0 cm) and 1.60 g cm^{-3} (580 cm), respectively. For Station 7186 porosity and density data do not exist due to probe failure. For further calculations (pore water solvents) we assumed a depth-porosity correlation described by the following equation (Eq. 8):

$$\Phi\,[\%] = -3.506 \cdot \ln z + 90.22 \qquad (8)$$

were z is the sediment depth in cm. This equation was obtained by combining porosity data of several gravity cores taken along the Peruvian and Chilean coast (J. Kallmeyer, unpubl. data). A mean wet density of 1.5 g cm^{-3} was assumed for the determination of sediment volume from sediment wet weight at Station 7186.

The C/N ratio (Fig. 3j, 4h and 5g) at the shallowest Station 7165 was 8.5 at the sediment surface and increased to 10.0 at 150 cm most probably due to the loss of protein-rich material during early degradation of organic matter. Below 150 cm the C/N ratio steadily decreased to 8.2 at 355 cm and stayed constant below. The decrease of C/N ratio with depth is curious and might be caused by ammonium adsorption on clay minerals (Schubert et al., 2000 and references therein). At Station 7186 the C/N ratio was 6.7 at the sediment surface and increased to 8.7 at 115 cm and stayed constant below. For the deepest Station 7155 only data from the multicorer exist. The C/N ratio was about 9.8 in the top 30 cm.

Total chlorins (Fig. 3k, 4i and 5h) were highest at the sediment surface of all three stations. Surface concentrations decreased from the shallowest Station 7165 (22 µg g^{-1} d.w.) to the deepest Station 7155 (15 µg g^{-1} d.w.). At Station 7165, total chlorins dropped to <10 µg g^{-1} d.w. at 10 cm and further decreased to values around 3 µg g^{-1} d.w. below 230 cm. At Station 7186, total chlorins dropped below 10 µg g^{-1} d.w. at 10 cm and further decreased to values around 4 µg g^{-1} d.w. below 75 cm. For the deepest Station 7155, only data of multiple corers exits. Total chlorins dropped below 10 µg g^{-1} d.w. at 2.5 cm. Between 15 and 31 cm the values reached a constant level around 5 µg g^{-1} d.w..

The chlorin-index (Fig. 3l, 4j and 5i) was always lowest at the surface where relatively fresh chlorophyll was deposited. At the shallowest Station 7165, hardly any change occurred within the upper 230 cm (around 0.7). In the deeper parts of the sediment (270 cm to bottom of core), values fluctuated between 0.75 and 0.80. At Station 7186, the chlorin-index was low (0.67) only at the very surface. At 2.5 cm the index had increased to 0.74 and stayed relatively constant within the upper 30 cm. Below 30 cm, values increased to 0.85 at 175 cm and scattered between 0.78 and 0.83 in the deeper parts of the sediment. At the deepest Station 7155, the chlorin-index increased from 0.69 at the surface to 0.81 at 15 cm and stayed relatively constant to the bottom of the core (31 cm).

Sulfate, methane, sulfide concentrations and pH

At all stations, sulfate concentration revealed a steady decrease with depth (Fig. 3a, 4a and 5a). At the southern station 7186 this decrease started right from the sediment surface. At the central stations 7155 and 7165 the onset of the decrease was at 30 and 50 cm sediment depth, respectively. Total sulfate depletion was reached at 365, 290 and 215 cm at Station 7165, 7186 and 7155 respectively. At Station 7155, sulfate remained at low but non-zero concentration (max 0.5 mM) between 305 and 590 cm. We interpret this as an artifact. The zone was located in the lower sub-cores (> 305 cm) that were sampled several hours after the upper ones (< 305 cm). We assume that of the traces of sulfate originated from seawater that had entered between core and liner and had diffused from the periphery into the inner core. At Station 7186, the same might be valid for low concentrations of sulfate (max. 0.5 mM) detected below 180 cm.

At all stations, methane was present only at sub-micromolar concentrations at the top of the cores (Fig. 3b, 4b and 5b). A steep increase in methane concentration was found at all stations from the depth of sulfate depletion, thus sharply delimiting the SMT. At Station 7165 and 7155, methane concentrations exceeded atmospheric saturation levels below 460 and 220 cm, respectively. Thus, methane losses due to decompression and bubble formation most likely took place below those depths in spite of the smooth profiles. Perhaps the sampling technique from bottom to top was fast enough to obtain samples before a significant methane loss.

Sulfide was detected within the SMT at Station 7165 (0.2-1.6 mM between 340 and 420 cm, Fig. 3e) and 7186 (27 µM, Fig. 4e). At Station 7155, sulfide concentrations were below the detection limit throughout the core.

pH values (Fig. 3f, 4f and 5e) were elevated within the SMT. At Station 7165, a major pH peak (7.7) was located 60 cm above the SMT. However, the pH was still elevated (7.5 - 7.6) within the SMT compared to values at the top and the bottom of the core (between 7.3 - 7.4). At Station 7186 and 7155, the pH increased to a maximum of 7.6 and 7.4, respectively, within the SMT. In all cores, pH revealed an increase towards the bottom, most pronounced at Station 7155.

SR and AOM

SR had two maxima at all stations: at the sediment surface and within the SMT (Fig. 3c, 4c and 5c).

At Station 7165, the SR of the surface sediment reached a maximum of 9.3 nmol cm^{-3} d^{-1} at 18 cm (Fig. 3c insert). Within the SMT only one replicate showed SR activity (1.1 nmol cm^{-3} d^{-1} at 355 cm). However, this activity fitted perfectly with the depth of the SMT and with the occurrence of sulfide. Table 2 gives an overview of areal SR and AOM rates of the surface and the deep interval integrated over depth. 79% of the integrated SR was located within the top 70 cm of the sediment. The remaining activity was located at depths between 255 and 520 cm.

At Station 7186, SR steadily decreased from the surface (2.7 nmol cm^{-3} d^{-1} at 7.5 cm) to 125 cm (0.06 nmol cm^{-3} d^{-1}, Fig. 4c). Below 125 cm, SR increased to 0.9 nmol cm^{-3} d^{-1} at the maximum sampling depth of 270 cm. However, rates detected below 180 cm have to be regarded as possible artifacts for reasons mentioned above (see sulfate concentrations). Replicate samples showed relatively consistent rates. Integrated over depth (Table 2), 82% of the measured SR occurred within the top 120 cm of the sediment.

At Station 7155, SR of the surface sediment reached a maximum of 11.7 nmol cm^{-3} d^{-1} at 17.5 cm (Fig. 5c insert). Within the SMT, SR was detectable between 207 and 303 cm, reaching a maximum of 4.2 nmol cm^{-3} d^{-1} at 290 cm. Rates within the SMT revealed large deviations between the replicates. Often one replicate showed high SR activity whereas the other revealed low activity or was inactive. 48% of the integrated SR at Station 7155 was located within the top 90 cm of the sediment.

At all stations, the majority of AOM activity was located within the SMT (Fig. 3d, 4d and 5d). At Station 7165 and 7186, a separate zone of methane oxidation was detected close to the sediment surface revealing decreasing activity with depth.

At Station 7165, considerable rates of methane oxidation were detected close to the sediment surface with a maximum of 10.7 nmol cm^{-3} d^{-1} at 10 cm (Fig. 3d). The rates decreased with depth to zero at 90 cm. Within the SMT, AOM was recorded between 255 and 375 cm. A maximum of 51.2 nmol cm^{-3} d^{-1} was located at 365 cm. This peak fitted with the depth of methane and sulfate depletion. It was located 10 cm below the peak of SR. AOM rates revealed the same strong deviation within the replicates as observed for SR in this core (see above). Integrated over depth, 74% of the measured AOM was located between 255 and 520 cm (Table 2). In both the surface and the deep zone, AOM was much higher (4 to 50 times, respectively) than SR.

At Station 7186, methane oxidation was detected close to the sediment surface, revealing a maximum peak of 0.76 nmol cm^{-3} d^{-1} at 15 cm (Fig. 4d). Below 15 cm, methane oxidation decreased to 0.05 nmol cm^{-3} d^{-1} at 105 cm. Below 105 cm, i.e. the onset of the SMT, AOM increased steadily reaching a maximum of 1.81 nmol cm^{-3} d^{-1} at 270 cm, the maximum sampling depth. The increase of AOM within the SMT was in accordance with the increase of SR. As for SR, AOM rates measured below 180 m have to be considered as artificial due to sulfate contamination (see above). Integrated over depth, 54% of the measured AOM was located between 120 and 180 cm (Table 2). In this zone, AOM was twice the rate of SR.

At Station 7155, AOM was detectable between 205 and 305 cm revealing a peak of 5.0 nmol cm^{-3} d^{-1} at 222 cm (Fig. 5d). The peak was located 68 cm above the SR peak. Deviations of replicates were the same as described for AOM and SR in core 7155. Integrated over depth, 97% of the measured AOM was located between 90 and 305 cm (Table 2). In this zone, AOM was responsible for 74% of the SR rates.

Table 2. Depth integrated areal rates of measured AOM and SR. The sediment intervals were chosen according to zones of surface and deep activity. Rates that were expectedly artifacts due to contamination with seawater were excluded. For SR, data of multiple and gravity corer deployments were combined. For intergration, the means of replicates of the same depth interval were used.

Station GeoB No.	Methane oxidation (mmol m^{-2} a^{-1})	Methane oxidation % of total	Sulfate reduction (mmol m^{-2} a^{-1})	Sulfate reduction % of total	Methane oxidation % of sulfate reduction
7165 (880 m)					
0-70 cm	716	26	161	79	444
255-520 cm	2091	74	42	21	5021
Total	2807	100	203	100	1383
7186 (1160 m)					
0-120 cm	78	46	203	83	38
120-180 cm	93	54	44	18	211
Total	171	100	247	100	69
7155 (1750 m)					
0-90 cm	2	3	92	48	3
90-305 cm	73	97	99	52	74
Total	75	100	191	100	39

Calculated fluxes of methane and sulfate

Table 3 shows calculated fluxes of methane and sulfate for all three stations. The gradients used for calculations are plotted as solid line in Fig. 3a/b, 4a/b and 5a/b. Methane fluxes were between 25 and 47 mmol m^{-2} a^{-1}. Sulfate fluxes were on average higher, i.e. between 46 and 100 mmol m^{-2} a^{-1}. We calculated the ratio between AOM and SR by division of the fluxes according to Niewöhner et al. (1998). The result showed that 72, 27, and 47% of the SR was coupled to AOM at Station 7165, 7186, and 7155, respectively. Compared to depth-integrated measured rates of SR there was a good agreement between calculated sulfate fluxes and measured SR at the SMT. At station 7165 und 7155, the sulfate flux equaled SR (Table 2 and 3). At Station 7186, the calculated sulfate flux was twice the measured SR. The calculated methane flux was always lower compared to integrated AOM of the SMT. At Station 7165, measured AOM appeared to be 60 times higher than the calculated methane flux. However, at Station 7155 and 7186 the measured AOM was only two and four times higher than the calculated flux.

Table 3. Calculated methane and sulfate fluxes, sediment diffusion coefficient Ds, depth integrated porosities, and the ratio between AOM and SR expressed in % AOM of SR.

Station GeoB No.	Ds of methane (m^2 a^{-1})	Porosity	Diffusive flux of methane (mmol m^{-2} a^{-1})	Ds of sulfate (m^2 a^{-1})	Porosity	Diffusive flux of sulfate (mmol m^{-2} a^{-1})	Methane oxidation % of sulfate reduction
7165	1.49×10^{-2}	0.72	33.3	9.60×10^{-3}	0.72	46.0	72
7186	1.52×10^{-2}	0.73	25.4	9.92×10^{-3}	0.74	95.8	27
7155	1.52×10^{-2}	0.73	46.7	9.92×10^{-3}	0.74	99.7	47

TC, TOC, TIC, δ^{13}C-TIC and δ^{13}C-DIC

The TOC in core 7165 decreased with sediment depth from the top (2.3% d.w.) to 230 cm (0.94% d.w.) due to organic matter degradation (Fig. 3i). Below 315 cm, TOC stayed relatively constant around 0.7% d.w.. The TIC profile revealed some interesting anomalies. Beside a steady increase of TIC from the top (0.09% d.w.) to the bottom (0.35% d.w.), two distinct peaks of 0.86 and 1.3% d.w. occurred at 375 and 455 cm, respectively. The shallower peak fitted perfectly to the peak of AOM. The δ^{13}C-TIC exhibited a minimum of -14.6 ‰ VPDB (Vianna Peedee belemnite) for both TIC peaks (Fig. 3g) which was very distinct from the background level of about -4 ‰ VPDB. δ^{13}C-DIC revealed a steady decrease in ^{13}C below 150 cm reaching a minimum of -24.6 ‰ VPDB between 335 and 375 cm (Fig. 3h). This minimum was in accordance with the peaks in AOM and SR. Below 375 cm δ^{13}C-DIC values increased steadily reaching -4.8 ‰ VPDB at 590 cm, the maximum sampling depth.

At Station 7186 (Fig. 4g), TIC and TOC are available only from the multicorer and for distinct points above, within and below the SMT. In the top 30 cm, TIC and TOC stayed constant around 0.7 and 1.7% d.w., respectively. The profile of TC did not reveal distinct peaks within the SMT as it was the case for core 7165. TIC and TOC were almost constant (around 0.8 for TIC and 1.9 for TOC) with depth. The TC at Station 7186 was about 1.6 times higher compared to Station 7165 at similar depths.

For Station 7155, only data from the multicorer exist (Fig. 5g). TIC stayed constant around 0.3% d.w. in the top 30 cm. TOC decreased from 2.8% d.w. to 2.3% d.w. at 27 cm sediment depth.

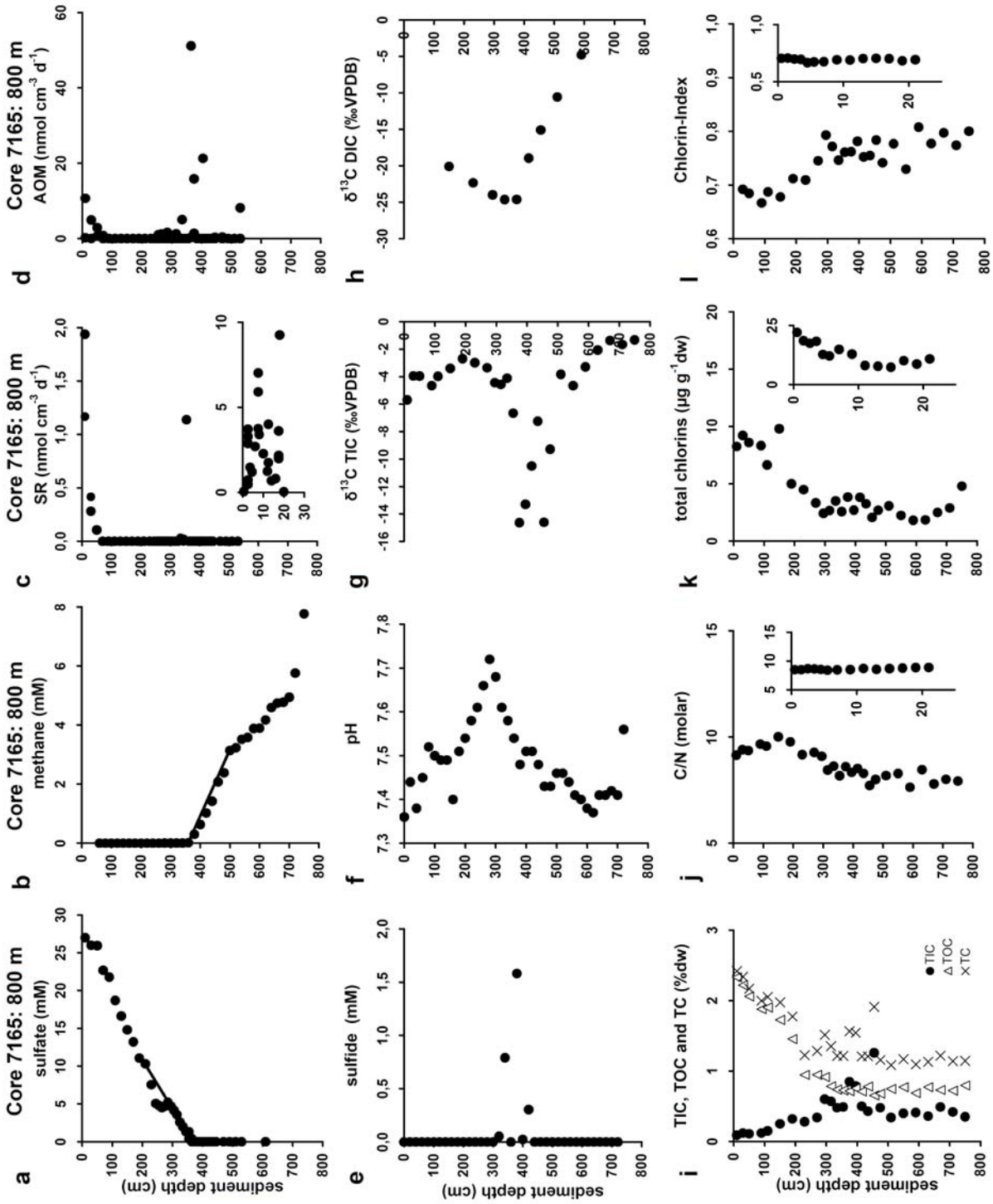

Figure 3 (a-l). Parameters measured at Station 7165. Gradients used for calculations of methane and sulfate fluxes are marked by solid lines. SR, C/N, total chlorins, and chlorin index of the surface are shown in inserts.

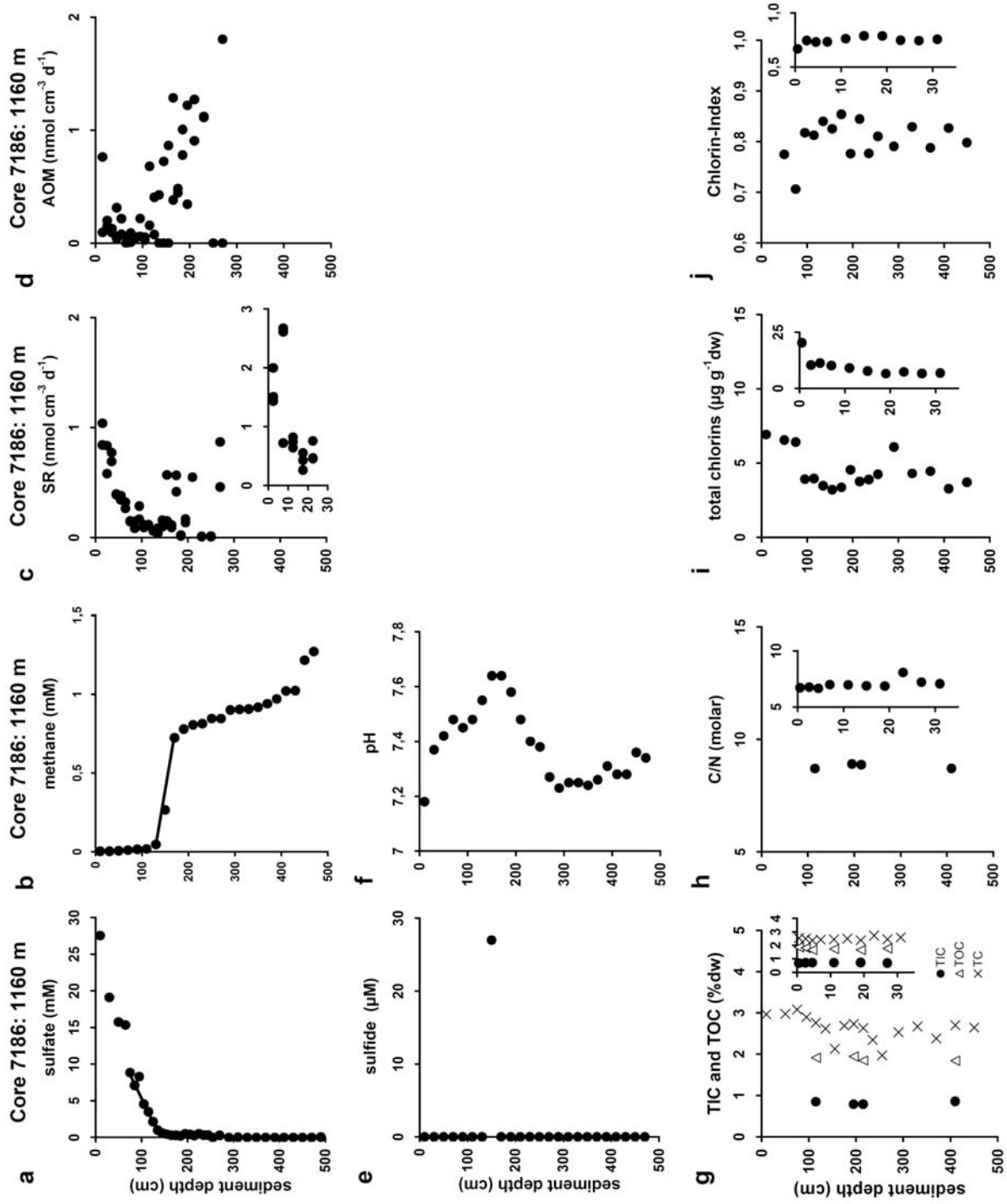

Figure 4 (a-j). Parameters measured at Station 7186. Gradients used for calculations of methane and sulfate are marked by solid lines. SR, TIC, TOC, C/N, total chlorins, and chlorin index of the surface are shown in inserts.

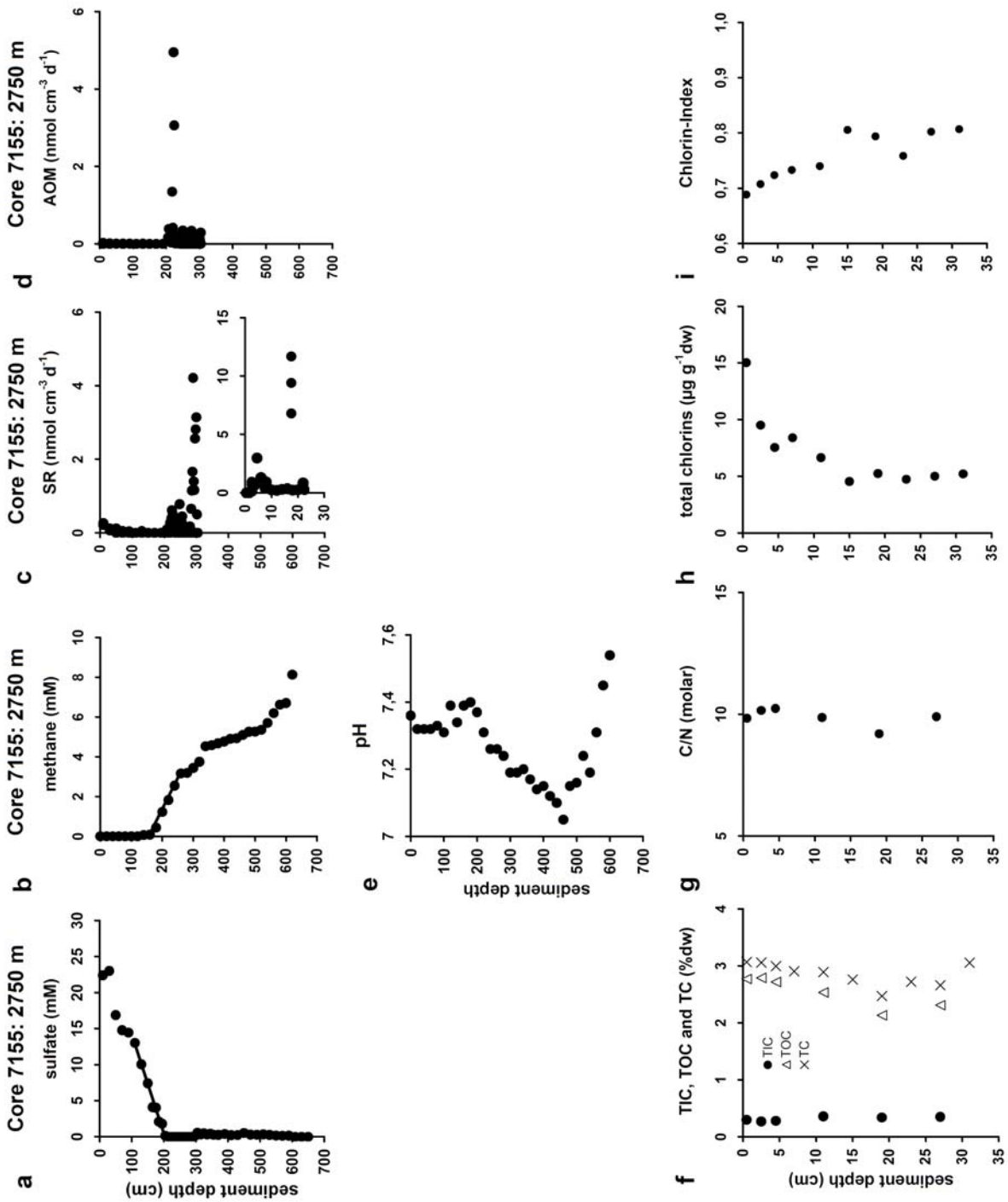

Figure 5 (a-i). Parameters measured at Station 7155. Gradients used for calculations of methane and sulfate are marked by solid lines. SR of the surface is shown in insert.
Note that total TIC, TOC, C/N, chlorins, and chlorin-index are given only for the surface.

DISCUSSION

Organic matter and its degradation at the sediment surface

Due to the degradation of organic matter as it sinks through the water column, the supply of fresh organic material to the ocean floor decreases with increasing water depth. This general correlation was also found for the three locations along the Chilean continental margin in this study. Highest amounts of total chlorins in the surface sediment were found at the shallowest station (7165, 800 m), whereas lowest concentrations were found at the deepest station (7155, 2750 m). Chlorins represent chlorophyll and its degradation products and are a measure of phytoplankton detritus (Schubert et al., 2000). The chlorin-index is an indicator of the degree of chlorophyll degradation (Schubert et al., 2002). Highest index values in the surface sediments were found at the deepest station thus showing the successive depletion of fresh organic matter with water depth. The availability of fresh phytodetritus should be reflected in the mineralization rates in the sediments. However, areal surface SR (Table 2) revealed highest rates at the southernmost station 7186 with intermediate water depth (1160 m). The depth profiles of SR for the upper 120 cm point to significant differences between 7186 and the two stations further north. While at 7165 and 7155 SR was primarily limited to the uppermost 30-50 cm, rates remained comparably high throughout the upper 120 cm of the sediment at 7186. This finding suggests that at 7186 highly degradable organic material is still available at greater sediment depth. The higher reactivity of the organic matter at 7186 can be expressed by the reaction rate coefficient k calculated from measured SR and the concentration of total organic carbon (Berner, 1980; Westrich and Berner, 1984; Schubert et al., 2000). In the depth interval 50-120 cm the mean k value of Station 7186 was 0.15×10^{-3} a^{-1}compared to only 0.01×10^{-3} a^{-1} at Station 7165 (no data of this zone are available for Station 7155). A better preservation of bioavailable organic compounds in the South is consistent with higher sediment and organic matter accumulation rates in the region South of 40°S as reported by Hebbeln et al. (2000), thus leading to a faster burial of newly deposited organic material. The comparably low TOC concentrations at 7186 are a consequence of the dilution with clastic material. Low C/N-ratios, representing high concentrations of highly reactive N-containing compound classes like proteins and nucleic acids, as well as the relatively high proportion of TOC, made up by chlorins, reflect the freshness of the organic material that can be ascribed to the depositional conditions. While the high productivity north of 40°S is sustained by coastal upwelling, advection of nutrients with the Antarctic Circumpolar Current

and a significant riverine input fuel the even higher productivity further to the south. This is again confirmed by investigations of Hebbeln et al. (2000), who found higher productivity along the Chilean margin south of 40°S based on organic carbon and $\delta^{15}N$ measurements in the sediment. Latitudinal changes in precipitation are the reason for increasing total sediment accumulation rates towards the South.

Coupling between sulfate reduction at the surface and the depth of the sulfate-methane transition?

We analyzed whether organoclastic SR at the sediment surface impacted the depth of sulfate penetration and therefore the location of the SMT. Former investigations at the Namibian continental margin (Niewöhner et al., 1998; Fossing et al., 2000) and the Black Sea (Jørgensen et al., 2001) demonstrated that the depth of sulfate penetration of diffusive systems is not very sensitive to high reduction rates at the sediment surface. This has been explained by biorrigation that maintains a high sulfate concentration in the inhabited surface sediment (Fossing et al., 2000) and by diffusion distance (Jørgensen et al., 2001). Due to the long diffusion distance from the surface sediment down to the depth of the SMT, the main drop in sulfate is located between the most active surface sediment (top few decimeters) and the SMT (Jørgensen et al., 2001). In comparison, the drop in sulfate within the most active surface sediment tends to be small.

In our study, the sulfate concentration profiles had a quasi-linear gradient from the surface to the depth of complete sulfate depletion. A consumption of sulfate above the SMT apparently did not cause a strong sulfate depletion or curvature of the sulfate profile. Therefore, organoclastic SR at the sediment surface, although clearly detected by radiotracer measurements, had little impact on the location of the SMT. The location was consequently determined primarily by the upward diffusive flux of methane from the methanogenic zone and the downward diffusive flux of sulfate from the sediment-water interface.

At the two northern Stations 7165 and 7155, an impact of bioirrigation on the sulfate concentration was detectable at the sediment surface. Here, the steepest sulfate decrease was located sub-surface. We found living polychaetes inside tubes within the upper 10 cm of multicores at both stations. Some 30 – 60% of the gravity cores were visibly bioturbated and black-colored burrows were found throughout (Hebbeln and participants, 2001) indicating recent and ancient activity of macrofauna in the sediment. Thus, an active transport of sulfate into the surface sediment by tube-dwelling fauna seems plausible.

Coupling of AOM and SR within the sulfate-methane transition

The methane profiles of the investigated cores demonstrated that methane was effectively consumed by AOM within the SMT and did not reach the sediment-water interface. AOM has been found at methane seeps to be mediated by a syntrophic consortium of methane oxidizing archaea and sulfate reducing bacteria (Hoehler et al., 1994; Hoehler and Alperin, 1996; Boetius et al., 2000). The archaea are phylogenetically related to the methanogens but are suspected to operate in reverse, i.e. to oxidize methane instead of producing it (Valentine and Reeburgh, 2000 and references therein). Sulfate reducers presumably create conditions that thermodynamically favor AOM by oxidizing a so far unknown intermediate with sulfate. During AOM, one mol of methane is oxidized by concurrent reduction of one mol of sulfate.

We wanted to know whether SR in the SMT was completely fueled by methane and therefore calculated the ratio between AOM and SR for depth-integrated rates and for fluxes of methane and sulfate. With respect to the depth-integrated rates, the ratio closest to a 1:1 stoichiometry of AOM was found at Station 7155 (Table 2). Here, measured AOM made up 74% of the SR. Disagreements were found at Station 7186 and 7165 where AOM was 2 and 50 times higher than the SR, respectively. This was in conflict with the stoichiometry of the process and it was not confirmed by the calculated methane and sulfate fluxes, where AOM was responsible for 27 and 47% of the SR, respectively (Table 3).

The depth-integrated rates of measured AOM and SR should be taken with caution. Especially core 7155 and 7165 revealed a high heterogeneity between replicates. In some cases, only one of the two replicates revealed activity. The heterogeneity may have different reasons as discussed in more detail below: (1) loss of methane; (2) penetration of oxygen; (3) microenvironments in the sediment.

The glass tubes used for rate measurements had to be sealed without headspace during incubation. This can be done easily when the sediment is soft and has a high water content. However, as the sediment becomes more consolidated at depth it also becomes more difficult to close the tubes without small air inclusions. A small headspace in the sample would lead to losses of methane from the pore water into the headspace and to the penetration of oxygen from the headspace into the sediment. The activity of AOM is very sensitive to changes in both parameters. Nauhaus and coworkers found methane turnover to increase with methane concentration and to be inhibited by oxygen (Zehnder and Brock, 1980; Nauhaus et al., 2002). Thus, air inclusions most probably affected some of the measured rates from greater depths.

We also found indications for the restriction of AOM to microenvironments by investigations of potential AOM, lipid biomarkers, and fluorescence in situ hybridization (FISH). During the main sampling, we took additional samples for the analysis of potential AOM and lipid biomarkers over the whole depth interval of the SMT and homogenized the samples in a glass bottle. The samples were kept anoxic and cold at 4°C. Samples for FISH were taken from the same depths as AOM and SR samples. Potential rate measurements of AOM according to Nauhaus et al. (2002) revealed no activity (M. Krüger, private communication). No lipid biomarkers, typical for organisms involved in AOM, were found (M. Elvert, private communication). No organisms could be detected in selected sediment samples from depths of known AOM activity using FISH probes targeting cells of the ANME-1 cluster (Hinrichs et al., 1999; ANME = anaerobic oxidation of methane), ANME-2 cluster (EeelMS932; Hinrichs et al., 1999), or archaea in general (ARCH915; Amann et al., 1990). We conclude from these results, that AOM organisms were too strongly diluted within the mixed samples to reveal detectable potential rates or to show signals in lipid biomarkers. Furthermore, we conclude that probe-targeted cells were either statistically too low in numbers to be found by microscopy, or FISH samples were taken outside of AOM spots. Thus, AOM might be limited to microenvironments within the sediment, and consequently the extrapolation of few AOM and SR data over broad depth intervals may not provide a representative picture of AOM distribution and activity. Of course, a higher number of replicates could have helped to gain a more realistic mean distribution of AOM. However, the gravity cores with an inner diameter of 12 cm strongly restricted the number of samples that could be taken from the same depth interval, especially since samples for other parameters needed to be taken in addition.

To answer the question whether SR is fueled by methane in the SMT we further analyzed the distribution of SR throughout the cores. In all cores there was a clear separation between SR in the surface sediment, i.e. involved in organic matter degradation, and SR within the SMT. Furthermore, the SMT was always very distinct showing the depletion of sulfate along with methane. Thus, we suggest that SR of the SMT was indeed fueled by methane and that discrepancies between stoichiometric and observed AOM to SR ratios were attributed to methodical problems and the heterogeneous distribution of the organisms involved.

Methane consumption above the sulfate-methane transition

At Station 7165 and 7186, considerable methane oxidation was measured above the SMT between 10-70 cm sediment depth, revealing increasing rates towards the sediment surface. Although methane concentrations were very low close to the surface (<1µM), concentrations of the experimentally added $^{14}CH_4$ were still <5% of the unlabelled methane. Thus, an artificial enrichment in methane concentration due to tracer is unlikely. Increasing methane consumption towards the sediment surface in spite of sub-micromolar concentration indicates that there is a production of methane but also a rapid re-oxidation. Methanogenesis is generally excluded from the sulfate zone due to substrate competition, yet it may take place at a low rate based on non-competitive substrates (Martens and Berner, 1974; Iversen and Jørgensen, 1985; Whiticar, 2002). The electron acceptor was unlikely to be oxygen throughout the 70 cm deep zone as oxygen is usually not penetrating several decimeters into upper slope sediments (Wenzhöfer and Glud, 2002). Therefore, aerobic oxidation of methane was most likely replaced by AOM below the depletion of oxygen.

Authigenic carbonates generated by anaerobic oxidation of methane

The formation of authigenic carbonates from AOM was implied in several studies of methane seeps (e.g. Bohrmann et al., 1998; Peckmann et al., 2001). AOM leads to an increase in alkalinity and consequently to an increase in pH due to pore water enrichment in CO_3^{2-} relative to HCO_3^-. These conditions favor the precipitation of carbonates. The net reaction of carbonate formation during AOM can be described by Eq. 9:

$$CH_4 + SO_4^{2-} + Ca^{2+} \rightarrow CaCO_3 + H_2S + H_2O \qquad (9)$$

A direct evidence for carbonate precipitation from AOM was given by (Michaelis et al., 2002), who demonstrated precipitation of radiolabeled carbonates in methanotrophic microbial mats of the anoxic Black Sea after incubation with $^{14}CH_4$. The formation of authigenic carbonates by AOM is also evident from the extremely light carbon isotopic signature. At methane seeps, AOM leads to an enrichment of the lighter isotope, ^{12}C, in the precipitated carbonate due to a discrimination against the heavier $^{13}CH_4$ during AOM (Hinrichs et al., 1999; Elvert et al., 2001; Thiel et al., 2001). Depending on whether the

methane is of biogenic or thermogenic origin, the enrichment is more or less pronounced since methanogens also discriminate against the heavier $^{13}CO_2$ during CO_2 reduction. In diffusive systems, the carbon isotopic signature of authigenic carbonates tends to reflect the methane isotopy due to a full consumption of upward diffusing methane.

In the present study we found strong indications for the formation of authigenic carbonates from AOM. At Station 7165, a distinct DIC peak with a $\delta^{13}C$ value of –24.6 ‰ VPDB was found along with AOM. We will perform a simple mass balance calculation to estimate the fraction, a, of AOM-derived DIC relative to "normal" pore water DIC contributing to the total DIC pool (Eq. 10):

$$-24.6 = a\,(\delta^{13}CH4) + (1\text{-}a)\,(\delta^{13}DIC) \qquad (10)$$

We assume a similar $\delta^{13}C$ value of the methane source as has been found earlier at Hydrate Ridge (-62 to -72 ‰ VPDB, Elvert et al., 2001) or in sediments of the Black Sea (-60 to -76 ‰ VPDB; Schubert et al., unpubl. data). Thus we use an average $\delta^{13}CH_4$ of -68 ‰ VPDB and the $\delta^{13}C$ value (-4 ‰ VPDB) of DIC that has been measured below the SMT zone. To produce DIC of –24.6 ‰ VPDB as has been measured in the SMT, a mixture of 35 % DIC related to AOM and 65 % of "normal" pore water DIC is calculated. This means that DIC related to AOM was not dominating the pore water DIC, however, its presence was still detectable in the SMT. TIC as well revealed a depletion in ^{13}C in this zone with a $\delta^{13}C$ value of -14.6 ‰ VPDB. The heavier carbon isotopic value of TIC could be explained by a dilution of the pure methane related signal with heavier carbonates occurring in the form of foraminifers. The sediments along the Chilean continental margin contain shells of pelagic foraminifera with a $\delta^{13}C$ signal ranging between –1.4 and 1.73 ‰ VPDB (Hebbeln et al., 2000). Since only the whole sediment has been measured without separating foraminifers from authigenic carbonates, the foraminifers with their relatively heavier carbon isotopic signal will certainly shift the whole $\delta^{13}C$ value of the sediments. The second, deeper peak of ^{13}C-depleted TIC might be interpreted as a former location of AOM. We assume that the SMT moves upwards over time due to a continuous accumulation of sediment.

The carbon isotopic signals of authigenic carbonates found in this study are less extreme than the super-light signals reported from authigenic carbonates at methane seeps (e.g. -41 ‰ VPDB in the Black Sea; Peckmann et al., 2001) or at gas hydrate locations (e.g. -54.2 ‰ VPDB at Hydrate Ridge, Oregon; Bohrmann et al., 1998). This may be explained by the lack of carbon fractionation during AOM in diffusive systems.

AOM in upwelling systems

Investigations of AOM in coastal upwelling systems are rare. To our knowledge only two other studies are published, namely from the upwelling area off Namibia (Niewöhner et al., 1998; Fossing et al., 2000), where cores were taken from water depths between 1300 and 2060 m. The SMT was located between 3 and 10 m sediment depth, i.e. generally deeper compared to our study. No direct measurements were made of the AOM, but the SR within the SMT revealed peak rates between 0.4 and 2 nmol cm^{-3} d^{-1}, which is very similar to our measurements.

Sediments of both the Chilean and the Namibian upwelling regions are diffusive systems and methane is quantitatively consumed within the SMT. These few observations indicate that AOM might be the major sink for methane throughout the sediments of marine upwelling systems. Methane is exhausted far below the sediment surface and releases of methane into the water column can be assumed to be insignificant small.

For future work, also AOM in continental shelf sediments of upwelling systems should be studied since even higher organic input and microbial turnover can be expected here. Unfortunately, coring at shallower depths was very ineffective during our investigation, due to very coarse grained sediments. Only very short cores were gained (<2 m) that did not reach down into the methane zone. Ferdelman et al. (1997) measured AOM in two cores from the Bay of Conceptión at 37 and 87 m water depth. The rates were low (between 0.04 and 0.12 nmol cm^{-3} d^{-1}) as they were measured above the SMT (maximum sampling depth 20 cm, sulfate concentration around 26 mM).

Compared to other methane-bearing sediments worldwide, AOM rates of the Chilean continental margin were higher than in other diffusive systems between 200-4000 m water depth (see Hinrichs and Boetius, 2002 and references therein). Especially Station 7165 (800 m water depth) revealed AOM maximum rates (20 - 51 nmol cm^{-3} d^{-1}) several times higher compared to maximum rates reported from 200-225 m water depth (0.75 – 12 nmol cm^{-3} d^{-1}; Devol, 1983; Iversen and Jørgensen, 1985). Higher methane turnover rates in the upwelling region off Chile is most likely caused by higher input of organic matter to the ocean floor, even at greater water depth, as compared to non-upwelling regions. Enhanced degradation of the organic matter is then leading to an enhanced formation and consumption of methane. Hence, the microbial methane barrier operates according to the methane supply from below confirming the important role of AOM in global methane cycling.

CONCLUSIONS

Following the aims of the present study, we conclude that:

1. AOM in the upwelling region off the Chilean coast is effectively controlling methane concentrations in the sediment. Methane is quantitatively removed within the SMT and a significant release into the water column is excluded.
2. SR within the SMT is to a major part fueled by methane.
3. the intensity of organoclastic SR is higher off South Chile due to a higher sediment and organic matter accumulation and a consequent fast burial of fresh material. At the two stations off Central Chile, SR reflected the general decrease in organic matter supply with depth.
4. sulfate penetration depths were insensitive to organoclastic SR near the sediment surface. High diffusion distances strengthened the effect of methanotrophic SR at depth, and thus only methane and sulfate fluxes determined the depth of the SMT.
5. AOM off the Chilean coast can lead to the formation of distinct layers of authigenic carbonates. The carbonates revealed a depleted $\delta^{13}C$ value due to the consumption of isotopic light methane.

ACKNOWLEDGEMENTS

We thank the officers, crew, and shipboard scientific party of RV SONNE for excellent support during expedition SO-156. We particularly thank D. Hebbeln for logistic support, F. Schewe and S. Stregel for excellent coring, J. Wulf, P. Boening and L. Toffin for technical help on board as well as M. Hartmann, A. Rohwedder and S. Knipp for technical help in the home laboratory. We would also like to thank M. Böttcher for helpful discussions about biogeochemical parameters in the sediment. This study was made possible by the programs PUCK (Wechselwirkungen zwischen Produktivität und Umweltbedingungen am chilenischen Kontinentalhang, FN 03G0156A) and MUMM (Mikrobielle Umsatzraten von Methan in gashydrathaltigen Sedimenten, FN 03G0554A) supported by the Bundesministerium für Bildung und Forschung (BMBF, Germany). Further support was given from the Max-Planck-Gesellschaft (MPG, Germany). This is publication GEOTECH-# of the GEOTECHNOLOGIEN program of the BMBF and the Deutsche Forschungsgesellschaft (DFG, Germany).

REFERENCES

Ahumada, R., Rudolf, G.A., Martinez, M.M. (1983). Circulation and fertility of waters in conception Bay. *Est. Coast. Shelf Sci.* **16**, 95-105.

Alperin, M.C., Reeburgh, W.S. (1985). Inhibition experiments on anaerobic methane oxidation. *Appl. Environ. Microbiol.* **50(4)**, 940-945.

Amann, R.I., Krumholz, L., Stahl, D.A. (1990). Fluorescent-oligonucleotide probing of whole cells for determinative, phylogenetic, environmental studies in microbiology. *J. Bacteriol.* **172**, 762-770.

Arntz, W.E., Fahrbach, E. (1991). El Niño. Klimaexperiment der Natur. Birkhäuser Verlag, Basel, pp. 264.

Berger, W.H., Fischer, K., Lai, C., Wu, G. (1987). Ocean productivity and organic carbon flux. Part I. Overview and maps of primary production and export production. San Diego, University of California.

Bergmann, U. (1995). Interpretation of digital Parasound echosounder records of the eastern Arctic Ocean on the basis of sediment physical properties. Alfred Wegener Institute for Polar and Marine Research, Bremerhaven. Berichte zur Polarforschung: 183.

Berner, R.A. (1980). Early diagenesis - A theoretical approach, Princeton Univ. Press.

Boetius, A., Ravenschlag, K., Schubert, C.J., Rickert, D., Widdel, F., Giesecke, A., Amann, R., Jørgensen, B.B., Witte, U., Pfannkuche, O. (2000). A marine microbial consortium apparently mediating anaerobic oxidation of methane. *Nature* **407**, 623-626.

Bohrmann, G., Greinert, J., Suess, E., Torres, M. (1998). Authigenic carbonates from the Cascadia subduction zone and their relation to gas hydrate stability. *Geology* **26(7)**, 647-650.

Borowski, W.S., Hoehler, T.M., Alperin, M.J., Rodriguez, N.M., Paull, C.K. (2000). Significance of anaerobic methane oxidation in methane-rich sediments overlying the Blake Ridge gas hydrates. In: C. K. Paull, R. Matsumoto, P. J. Wallace and W. P. Dillon (Eds.), Proceedings of the Ocean Drilling Program, Scientific Results. pp. 87-99.

Bussmann, I., Dando, P.R., Niven, S.J., Suess, E. (1999). Groundwater seepage in the marine environment: role for mass flux and bacterial activity. *Mar. Ecol. Prog. Ser.* **178**, 169-177.

Claypool, G.E., Kaplan, I.R. (1974). The origin and distribution of methane in marine sediments. In: I. Kaplan and R. Isaacs (Eds.), 1. Marine sediments - Gas content - Congresses. Plenum Press, New York, pp. 99-139.

Devol, A.H. (1983). Methane oxidation rates in the anaerobic sediments of Saanich Inlet. *Limnol. Oceanogr.* **28(4)**, 738-742.

Elvert, M., Greinert, J., Suess, E., Whiticar, M.J. (2001). Carbon isotopes of biomarkers derived from methane-oxidizing microbes at Hydrate Ridge, Cascadia Convergent Margin. *Geophys. Monogr*. **124**, 115-129.

Ferdelman, T.G., Lee, C., Pantoja, S., Harder, J., Bebout, B.M., Fossing, H. (1997). Sulfate reduction and methanogenesis in a Thioploca-dominated sediment off the coast of Chile. *Geochim. Cosmochim. Acta* **61(15)**, 3065-3079.

Fossing, H., Ferdelman, T.G., Berg, P. (2000). Sulphate reduction and methane oxidation in continental sediments influenced by irrigation (South-East Antlantik off Namibia). *Geochim. Cosmochim. Acta* **64(5)**, 897-910.

Fossing, H., Gallardo, V.A., Jørgensen, B.B., Hüttel, M., Nielsen, L.P., Schulz, H., Canfield, D.E., Forster, S., Glud, R.N., Gundersen, J.K., Küver, J., Ramsing, N.B., Teske, A., Thamdrup, B., Ulloa, O. (1995). Concentration and transport of nitrate by the mat-forming sulphur bacterium *Thioploca*. *Nature* **374**, 713-715.

Hansen, L.B., Finster, K., Fossing, H., Iversen, N. (1998). Anaerobic methane oxidation in sulphate depleted sediments: effects of sulphate and molybdate addition. *Aquat. Microb. Ecol.* **14**, 195-204.

Hebbeln, D., Marchant, M., Freudenthal, T., Wefer, G. (2000). Surface sediment distribution along the Chilean continental slope related to upwelling and productivity. *Mar. Geol.* **164**, 119-137.

Hebbeln, D. and participants (2001). PUCK: Report and preliminary results of R/V Sonne Cruise SO 156, Valparaiso (Chile) - Talcahuano (Chile), March 29 - May 14, 2001. Berichte aus dem Fachbereich Geowissenschaften der Universität Bremen: 182.

Hinrichs, K.-U., Boetius, A. (2002). The anaerobic oxidation of methane: new insights in microbial ecology and biogeochemistry. In: G. Wefer, D. Billett, D. Hebbelnet al (Eds.), Ocean Margin Systems. Springer-Verlag, Berlin, pp. 457-477.

Hinrichs, K.-U., Hayes, J.M., Sylva, S.P., Brewer, P.G., De Long, E.F. (1999). Methane-consuming archaebacteria in marine sediments. *Nature* **398**, 802-805.

Hoehler, T.M., Alperin, M.J. (1996). Anaerobic methane oxidation by a methanogen-sulphate reducer consortium: geochemical evidence and biochemical considerations. In: M. E.

Lidstrom and F. R. Tabita (Eds.), Microbial Growth on C_1 Compounds. Kluwer Academic Publishers, Intercept, Andover, UK, pp. 326-333.

Hoehler, T.M., Alperin, M.J., Albert, D.B., Martens, C.S. (1994). Field and laboratory studies of methane oxidation in an anoxic marine sediments: evidence for methanogen-sulphate reducer consortium. *Global Biochem. Cycles* **8(4)**, 451-463.

Iversen, N., Blackburn, T.H. (1981). Seasonal rates of methane oxidation in anoxic marine sediments. *Appl. Environ. Microbiol*. **41(6)**, 1295-1300.

Iversen, N., Jørgensen, B.B. (1985). Anaerobic methane oxidation rates at the sulphate-methane transition in marine sediments from Kattegat and Skagerrak (Denmark). *Limnol. Oceanogr.* **30(5)**, 944-955.

Iversen, N., Jørgensen, B.B. (1993). Diffusion coefficients of sulfate and methane in marine sediments: influence of porosity. *Geochim. Cosmochim. Acta* **57**, 571-578.

Jørgensen, B.B. (1978). A comparison of methods for the quantification of bacterial sulphate reduction in coastal marine sediments: I. Measurements with radiotracer techniques. *Geomicrobiol. J.* **1(1)**, 11-27.

Jørgensen, B.B., Fenchel, T. (1974). The sulfur cycle of a marine sediment model system. *Mar. Biol*. 24, 189-210.

Jørgensen, B.B., Weber, A., Zopfi, J. (2001). Sulphate reduction and anaerobic methane oxidation in Black Sea sediments. *Deep-Sea Res. I* **48**, 2097-2120.

Joye, S.B., Boetius, A., Orcutt, B.N., Montoya, J.P., Schulz, H.N., Erickson, M.J., Logo, S.K. (accepted). The anaerobic oxidation of methane and sulfate reduction in sediments from Gulf of Mexiko cold seeps. *Chem. Geol.*

Kallmeyer, J., Ferdelman, T.G., Weber, A., Fossing, H., Jørgensen, B.B. (submitted). Evaluation of a cold chromium distillation procedure for recovering very small amounts of radiolabelled sulfide related to sulfate reduction. *Limn. Oceaogr: Methods.*

Martens, C.S., Berner, R.A. (1974). Methane production in the interstitial waters of sulphate-depleted marine sediments. *Science* **185**, 1167-1169.

Michaelis, W., Seifert, R., Nauhaus, K., Treude, T., Thiel, V., Blumenberg, M., Knittel, K., Gieseke, A., Peterknecht, K., Pape, T., Boetius, A., Aman, A., Jørgensen, B.B., Widdel, F., Peckmann, J., Pimenov, N.V., Gulin, M. (2002). Microbial reefs in the Black Sea fueled by anaerobic oxidation of methane. *Science* **297**, 1013-1015.

Nauhaus, K., Boetius, A., Krüger, M., Widdel, F. (2002). In vitro demonstration of anaerobic oxidation of methane coupled to sulphate reduction in sediment from a marine gas hydrate area. *Environ. Microbiol.* **4(5)**, 298-305.

Niewöhner, C., Hensen, C., Kasten, S., Zabel, M., Schulz, H.D. (1998). Deep sulfate reduction completely mediated by anaerobic methane oxidation in sediments of the upwelling area off Namibia. *Geochim. Cosmochim. Acta* **62(3)**, 455-464.

Orphan, V.J., House, C.H., Hinrichs, K.-U., McKeegan, K.D., De Long, E.F. (2001). Methane-consuming Archaea revealed by directly coupled isotopic and phylogenetic analysis. *Science* **293**, 484-487.

Peckmann, J., Reimer, A., Luth, U., Luth, C., Hansen, B.T., Heincke, C., Hoefs, J., Reitner, J. (2001). Methane-derived carbonates and authigenic pyrite from the northwestern Black Sea. *Mar. Geol.* **177**, 129-150.

Reeburgh, W.S. (1976). Methane consumption in Cariaco Trench waters and sediments. *Earth Planet. Sci. Lett.* **28**, 337-344.

Reeburgh, W.S. (1980). Anaerobic methane oxidation: rate depth distribution in Skan Bay sediments. *Earth Planet. Sci. Lett.* **47**, 345-352.

Reeburgh, W.S. (1996). "Soft spots" in the global methane budget. In: L. M.E. and F. R. Tabita (Eds.), Microbial Growth on C_1 Compounds. Kluwer Academic Publishers, Intercept, Andover, UK, pp. 334-342.

Schubert, C.J., Ferdelman, T.G., Strotmann, B. (2000). Organic matter composition and sulphate reduction rates in the sediments off Chile. *Org. Geochem*. **31**, 351-361.

Schubert, C.J., Klockgether, G., Niggemann, J., Ferdelman, T.G., Jorgensen, B.B. (2002). The Chlorin-Index: A new parameter for organic matter freshness in sediments. *Geochim. Cosmochim. Acta* **66(15A)**, A689-A689.

Thiel, V., Peckmann, J., Richnow, H.H., Luth, U., Reitner, J., Michaelis, W. (2001). Molecular signals for anaerobic methane oxidation in Black Sea seep carbonates and microbial mat. *Mar. Chem.* **73**, 91-112.

Treude, T., Boetius, A., Knittel, K., Wallmann, K., Jørgensen, B.B. (2003). Anaerobic oxidation of methane above gas hydrates (Hydrate Ridge, OR). *Mar. Ecol. Prog. Ser.* **264**, 1-14.

Valentine, D.L., Reeburgh, W.S. (2000). New perspectives on anaerobic methane oxidation. *Environ. Microbiol.* **2(5)**, 477-484.

Wenzhöfer, F., Glud, R.N. (2002). Benthic carbon mineralization in the Atlantik: a synthesis based on in situ data from the last decade. *Deep-Sea Res. I* **49**, 1255-1279.

Westrich, J.T., Berner, R.A. (1984). The role of sedimentary organic matter in bacterial sulfate reduction: The G model tested. *Limnol. Oceanogr.* **29**, 236-249.

Whiticar, M.J. (2002). Diagenetic relationships of methanogenesis, nutrients, acoustic turbidity, pockmarks and freshwater seepages in Eckernförde Bay. *Marine Geology* **182**, 29-53.

Zehnder, A.J.B., Brock, T.D. (1980). Anaerobic methane oxidation: occurrence and ecology. *Appl. Environ. Microbiol*. **39 (1)**, 194-204.

Chapter 5

Microbial reefs in the Black Sea fuelled by anaerobic oxidation of methane

Walter Michaelis[1]*, Richard Seifert[1], Katja Nauhaus[2], Tina Treude[2], Volker Thiel[1], Martin Blumenberg[1], Katrin Knittel[2], Armin Gieseke[2], Katharina Peterknecht[1], Thomas Pape[1], Antje Boetius[3], Rudolf Amann[2], Bo Barker Jørgensen[2], Friedrich Widdel[2], Jörn Peckmann[4], Nikolai V. Pimenov[5], Maksim B. Gulin[6]

[1] Institute of Biogeochemistry and Marine Chemistry , University of Hamburg, Bundesstrasse 55, 20146 Hamburg, Germany.
[2] Max Planck Institute for Marine Microbiology, Celsiusstrasse 1, 28359 Bremen, Germany.
[3] Alfred Wegener Institute for Polar and Marine Research, 27515 Bremerhaven, and International University Bremen, 28725 Bremen, Germany.
[4] Geowissenschaftliches Zentrum, University of Göttingen, Goldschmidtstrasse 3, 37077 Göttingen, Germany.
[5] Institute of Microbiology, Russian Academy of Sciences, pr. 60-letiya Oktyabrya 7, k. 2, Moscow, 117811, Russia.
[6] Institute of Biology of Southern Seas, National Academy of Sciences of Ukraine, pr. Nakhimova 2, Sevastopol, Ukraine.

Science (2002) 297: 1013-1015.

ABSTRACT: Massive microbial mats covering up to 4-m-high carbonate buildups prosper at methane seeps in anoxic waters of the northwestern Black Sea shelf. Strong ^{13}C depletions indicate an incorporation of methane carbon into carbonates, bulk biomass, and specific lipids. The mats mainly consist of densely aggregated archaea (phylogenetic ANME-1 cluster) and sulfate-reducing bacteria (*Desulfosarcina/Desulfococcus* group). If incubated in vitro, these mats perform anaerobic oxidation of methane coupled to sulfate reduction. Obviously, anaerobic microbial consortia can generate both, carbonate precipitation and substantial biomass accumulation, which has implications for our understanding of carbon cycling during earlier periods of Earth's history.

MAIN TEXT

Until recently it was believed that only aerobic bacteria, depending on oxygen as electron acceptor, build up significant biomass from methane carbon in natural habitats (Hanson & Hanson, 1996). Because biogenic methane is strongly depleted in ^{13}C, a worldwide negative excursion in the isotopic signature of organic matter around 2.7 Ga (1 Ga = 10^9 years) ago was taken as an argument for methanotrophy and, consequently, an early oxygenation of the Earth's atmosphere (Hayes, 1994). However, recent investigations have shown the existence of methane-consuming associations of archaea and sulfate-reducing bacteria (SRB) in anoxic marine sediments (Boetius *et al.*, 2000; Orphan *et al.*, 2001a).

Microorganisms capable of anaerobic growth on methane have not been cultivated so far, and the biochemical pathway of the anaerobic oxidation of methane (AOM) remains speculative. Analyses of depth profiles and radiotracer studies in marine sediments (Hoehler *et al.*, 1994; Orphan *et al.*, 2002) as well as molecular (Elvert *et al.*, 1999; Hinrichs *et al.*, 1999; Thiel *et al.*, 1999; Pancost *et al.*, 2000) and petrographic studies (Peckmann *et al.*, 2001) argue for AOM (Valentine & Reeburgh, 2000) as a crucial process that channels ^{13}C-depleted methane carbon into carbonate and microbial biomass. Through AOM mediated by consortia of archaea and SRB, methane is oxidized with equimolar

amounts of sulfate, yielding bicarbonate and sulfide, respectively (Nauhaus *et al.*, 2002). Generation of alkalinity favors the precipitation of methane-derived bicarbonate according to the following net reaction:

$$CH_4 + SO_4^{2-} + Ca^{2+} \rightarrow CaCO_3 + H_2S + H_2O \qquad (1)$$

Here we provide evidence that vast amounts of microbial biomass may accumulate in an anoxic marine environment because of the use of methane as an electron donor for sulfate reduction (SR) and as an organic carbon source for cell synthesis.

In the northwestern Black Sea, hundreds of active gas seeps occur along the shelf edge west of the Crimea peninsula at water depths between 35 and 800 m (Ivanov *et al.*, 1991). At some of the shallow Crimean seeps, microbial mats were found associated with isotopically light carbonates. Aspects of the microbiology, sedimentology, mineralogy and selected biomarker properties of these deposits were recently described (Lein, *et al.*, 2002; Peckmann *et al.*, 2001; Thiel *et al.*, 2001a; Pimenov *et al.*, 1997). We explored the seeps on the lower Crimean shelf using the manned submersible *JAGO* from aboard the Russian R/V *Professor Logachev*. During dives to a seep area at 44°46'N, 31°60'E, we discovered a reef consisting of up to 4-m-high and 1-m-wide microbial structures projecting into permanently anoxic bottom water at around 230 m water depth (Fig. 1A). These buildups are formed by up to 10-cm-thick microbial mats that are internally stabilized by carbonate precipitates.

From holes in these structures, streams of gas bubbles emanate into the water column (Fig. 1A). The gas contains about 95% methane [see supporting online material (SOM)]. In cross sections, the outside of the soft mat has a dark gray to black color (Fig. 1B). Inside the structure, most of the mat is pink to brownish. The interior rigid parts are porous carbonates (aragonite and calcite with up to 14% $MgCO_3$). Much of the structures consist of interconnected, irregularly distributed cavities and channels filled with seawater and gases. Apparently, the cavernous structure of these precipitates enables methane and sulfate to be transported and distributed throughout the massive mats. Smaller microbial structures and nodules from nearby areas were of the same morphology, with compact mat enclosing

calcified parts and cavities. Obviously, the microorganisms do not grow on preformed carbonates but induce and shape their formation. Stable carbon isotope analyses of the carbonates yielded $\delta^{13}C$ values ranging from –25.5 to –32.2 per mil (‰) [for methods, see Peckmann *et al.*, 2001]. Compared with the $\delta^{13}C$ values of dissolved inorganic carbon in the Black Sea water column from +0.8‰ at surface to –6.3‰ at depth (Fry *et al.*, 1991), these values indicate that a major portion of the carbonate originates from the oxidation of methane. The methane seeping from the microbial structures, and from nearby sediment pockmarks is of biogenic origin, as indicated by $\delta^{13}C$ values of –62.4 to –68.3‰ (n = 6) (SOM) and most probably evolves from a deeper sedimentary source.

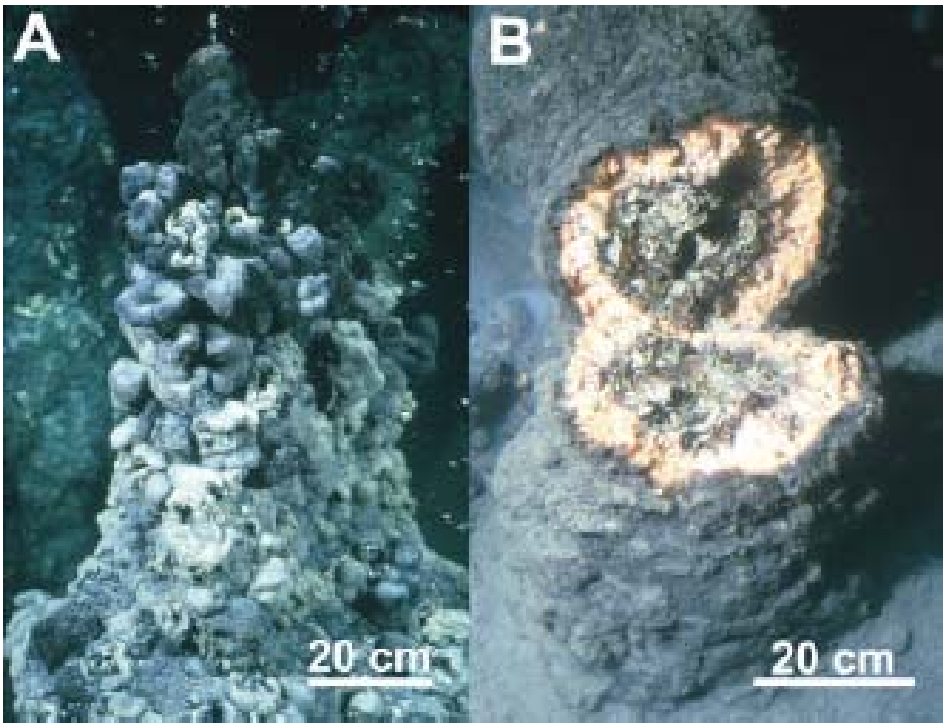

Figure 1. Image of microbial reef structures (as seen from the submersible). (A) Tip of a chimney-like structure. Free gas emanates in constant streams from the microbial structures into the anoxic sea water. (B) Broken structure of approx. 1 m height. The surface of the structure consists of grey-black coloured microbial mat, the interior of the massive mat is pink. The greenish-greyish inner part of the structure consists of porous carbonate which encloses microbial mats and forms irregular cavities.

Samples of living microbial mat were retrieved to investigate their microbiological and chemical composition as well as their catabolic activity. A short-term labeling experiment with added [^{14}C] methane and [^{35}S]sulfate (SOM) was performed directly after sampling. Pieces of mat incubated for 5 days in bottom water amended with methane (1.8 mM) exhibited AOM to carbon dioxide at a rate of 18 (±12) µmol (gram dry weight)$^{-1}$ d^{-1} and SR at a rate of 19 (±1) µmol (gram dry weight)$^{-1}$ d^{-1} (±SD; n = 3). In controls without mat samples, AOM and SR were below the detection limit. Results are in agreement with a stoichiometry of 1:1 between AOM and SR, as in experiments with sediment samples from a gas hydrate area (Nauhaus *et al.*, 2002). Methane-dependent SR to sulfide was also shown by chemical quantification with mat samples immediately incubated with and without methane, respectively (incubation time 60 days). SR rates under an atmosphere of methane were 34 (± 5.8) µmol (gram dry weight)$^{-1}$ d^{-1} (±SD, n = 6), whereas rates under nitrogen were 2.8 (± 0.55) µmol (gram dry weight)$^{-1}$ d^{-1} (±SD, n = 3), probably because of gradual decay of biomass. Chemical quantification in another, long-term incubation experiment (incubation time 166 days) again corroborated the 1:1 stoichiometry between AOM and SR (Nauhaus *et al.*, 2002). All these experiments indicate that methane is the main or only electron donor that accounts for SR and hence the buildup of the massive mat and carbonate structures in the investigated region of the Black Sea.

In extracts from homogenized mat samples, we observed isoprene-based constituents of archaeal lipids and hydrocarbons, such as archaeol, crocetane, and C_{40}-isoprenoids (acyclic, mono-, and dicyclic biphytanes) (Table 1) [see SOM (Fig. S1)]. A second compound cluster encompassed nonisoprenoid, linear and monomethyl-branched carbon skeletons of presumably bacterial origin. Most prominent among these structures are ω-3 monomethylated (*anteiso*-) C_{15} carbon chains bound in glycerol esters and glycerol diethers. No such lipids were found in a surface sediment of a nearby non-seep area, whereas similar biomarker patterns typically occur at modern and fossil methane seeps and were consistently related to contributions from methane-consuming archaea and associated SRB (Table 1). Indeed, strong ^{13}C depletions of the bulk biomass (–72.2‰) and of the bacterial and archaeal lipids there (Table 1) indicate that the mat microbiota must have incorporated methane-derived carbon into their biomass. Hence, archaeal AOM and

bacterial SR are relevant processes fuelling biomass production and reef formation in this permanently anaerobic seep environment.

Table 1. Selected biomarkers, their $d^{13}C$-values and most likely biological sources in the Black Sea microbial mat. The 'Literature' column quotes previous reports on these compounds in other methane-related environments. For additional information see (Fry *et al.* , 1991).

Compound	$\delta^{13}C$ [‰]	Source	Literature
Crocetane (2,6,11,15-tetramethylhexadecane)	-94.7 ± 0.7	Archaea (?)	*1
PMI (2,6,10,15,19-pentamethylicosane)	-95.6 ± 0.1	Archaea Methanosarcinales	*2
Archaeol (2,3-di-O-phytanyl-sn-glycerol)	-87.9 ± 0.6	Archaea	*3
***sn* -2-Hydroxyarchaeol** (2-O-3-hydroxyphytanyl-3-O-phytanyl-sn-glycerol)	-90.0 ± 1.0	Archaea Methanosarcinales	*4
Biphytane (from tetraether after HI/AlH4 cleavage)	-91.6 ± 0.6	Archaea	Thiel *et al* . (2001a)
***n* -Tricos-10-ene**	-90.9 ± 0.3	unknown (Bacteria?)	Thiel *et al* . (2001b)
***Anteiso* -pentadecanoic acid** (12-methyltetradecanoic acid)	-83.9 ± 0.1	SRB	*5
1,2-Di-O-12-methyltetradecyl-*sn* -glycerol	-89.5 ± 0.5	SRB	*6

*1 Boetius et al. (2000); Elvert et al. (2000, 2001); Hinrichs et al. (2000); Pancost et al. (2000); Orphan et al. (2001b); Thiel et al. (2001a,b)
*2 Boetius *et al* . (2000); Elvert *et al* . (2000, 2001); Hinrichs *et al* . (2000); Pancost *et al* . (2000); Orphan *et al* . (2001b); Thiel *et al* . (2001a,b)
*3 Hinrichs *et al* . (1999, 2000); Boetius *et al* . (2000); Elvert *et al* . (2000, 2001); Pancost *et al* . (2000); Orphan *et al* . (2001b); Thiel *et al* . (2001b)
*4 Hinrichs *et al* . (1999); Boetius *et al* . (2000); Pancost *et al* . (2000, 2001); Orphan *et al* . (2001b)
*5 Boetius *et al* . (2000); Hinrichs *et al* . (2000); Pancost *et al* . (2000, 2001); Orphan *et al* . (2001b)
*6 Orphan *et al* . (2001b); Pancost *et al* . (2001)

To directly trace the uptake and transformation of methane into organic and inorganic matter, we incubated 1-cm-thick pieces of microbial mat with radioactive methane ($^{14}CH_4$), and analysed thin sections using a β-microimager that provides two-dimensional images of radioactivity distribution (see SOM). Incorporation of radiotracer into the solid phase was recorded throughout the sections, which demonstrates that methane is readily assimilated into the microbial mat (Fig. 2E). Upon acidification of the thin sections about 25% of the ^{14}C radioactivity was lost. Obviously, a fraction of the methane carbon had been precipitated as carbonate. This approach provides direct laboratory evidence for methane-fuelled calcification and for the microbially mediated formation of carbonate structures.

Epifluorescence microscopy of sections of microbial mat revealed dense aggregations of archaea and bacteria (Fig. 2) (see SOM). The mats are penetrated by systems of microchannels that enable advective exchange with the surrounding seawater (Fig. 2A). The microchannels radiate out from the inner calcified part of the mat system and make up between 20 and 40% of the bulk mat volume. Fluorescence in situ hybridization (see SOM) shows that the mat biomass is dominated by one archaeal population comprising at least 70% of the mat biomass and belonging to the cluster ANME-1 (Fig. 2, B, C, D). ANME-1 is only distantly related to the Methanosarcinales and the ANME-2 cluster, which forms consortia with SRB and is known to be capable of AOM (Boetius *et al.*, 2000; Orphan *et al.*, 2001a, 2002). Nevertheless, the microbial mat dominated by ANME-1 comprises a similar pattern of the ^{13}C-depleted archaeal biomarkers crocetane, pentamethylicosane, pentamethylicosenes, archaeol, and *sn*-2-hydroxyarchaeol [see SOM (Fig. S1)], as Hydrate Ridge sediments (Boetius *et al.*, 2000; Elvert *et al.*, 1999), in which archaea of the ANME-2 cluster prevail (Boetius *et al.*, 2000). The most abundant bacterial population in the mats from the Black Sea belongs to the *Desulfosarcina/Desulfococcus* group, the same taxon of SRB as found in the ANME-2/SRB consortium (Boetius *et al.*, 2000).

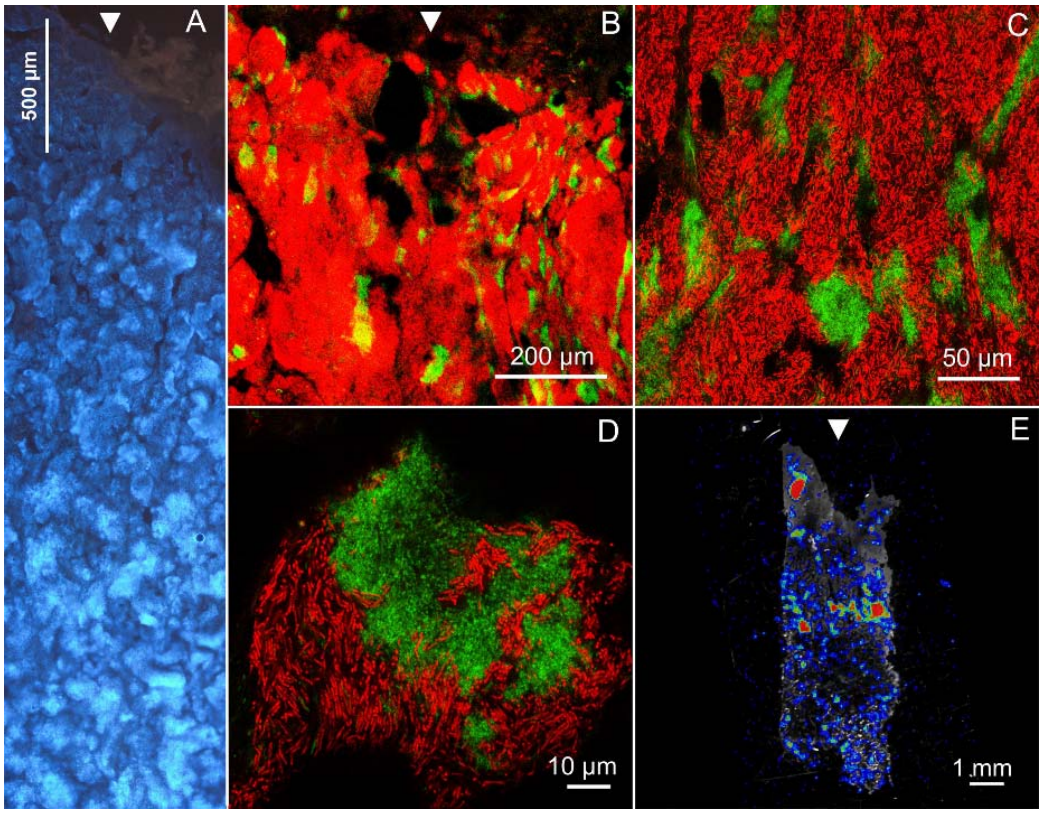

Figure 2. Fluorescence image showing a thin section of the pink mat. Scale bars indicate the different microscopic magnifications. The arrow marks the outside of the microbial mat. (A) A thin section of mat stained with DAPI (*18*). (B) Archaea of the cluster ANME-1 were targeted with a red-fluorescent group-specific oligonucleotide probe. The SRB were targeted with a probe specific for a cluster of δ-proteobacteria in the *Desulfosarcina*/*Desulfococcus* group and fluoresce green. These two populations comprise the bulk biomass in the microbial mat. (C) Microcolonies of SRB are surrounded by bulk ANME-I cell clusters. D) ANME-1 cells have a unique rectangular shape, SRB are small coccoid cells. Single SRB cells are dispersed throughout the ANME-I cell clusters. (E) beta-imager micrograph of a thin section of mat incubated with $^{14}CH_4$ (*18*). The micrograph shows the incorporated radioactivity of the mat after acidification. Green and red areas depict uptake of ^{14}C.

ANME-1 cells have a cylindrical shape and are autofluorescent under ultraviolet light, a feature typical for archaea containing coenzyme F_{420}. Their length is about 3.5 µm and their diameter about 0.6 µm (biovolume about 1 μm^3). The coccoid SRB (cell diameter, about

0.6 µm, biovolume, about 0.1 μm^3) occur in larger clusters of 10 to 50 µm diameter (Fig. 2, B and C). Smaller clusters and single cells of SRB are dispersed throughout the bulk ANME-1 biomass (Fig. 2D). One cm^3 mat contains about 10^{12} cells (see SOM), corresponding to approx. 25 mg carbon.

The growth yield of the mat community is currently unknown. Prokaryotes deriving their energy from dissimilatory SR generally have low growth yields. Pure cultures of SRB growing on conventional substrates (for example, organic acids) usually convert only one-tenth of the totally consumed organic compounds into cell mass, but the free energy gain obtained (for example on lactate, ΔG around −100 kJ per mol of sulfate) remains higher than that of AOM. Even with high methane partial pressure as at the active seeps studied (up to about 20 atm), the ΔG should not exceed −40 kJ per mol methane oxidized (see SOM). Hence, an even lower growth yield than for conventional cultures of SRB must be expected for the Black Sea mats. Consequently, the amount of methane oxidized for the buildup and maintenance of the existing mat structures should exceed their organic carbon content by more than an order of magnitude.

Microbial mats of the size presently observed are rarely found in oxic environments. This may reflect the absence of metazoan grazing and other mortality factors in the permanently anoxic and sulfidic environment of the Black Sea. There is increasing evidence that the capacity for AOM is present in several deep-branching clades of archaea (Orphan *et al.*, 2001b), which indicates an early evolutionary origin, just as for methanogenesis.

AOM may have influenced the carbon isotope record of the Archaean (Hinrichs & Boetius, 2002). Moreover, recent studies suggest that SR has already been prolific 3.5 Ga ago (Shen *et al.*, 2001), close to the first occurrence of microfossils (3.5 Ga ago) (Schopf, 1993) and the first isotopic traces of bioorganic carbon cycling (3.8 Ga ago) (Mojszis *et al.*, 1996). Hence, AOM may have represented an important link in the biological cycling of carbon in an anoxic biosphere. Even in the absence of free oxygen, methane formed by anaerobic degradation (fermentation and methanogenesis) of organic matter could have been recycled via AOM, leading to substrates (inorganic carbon and sulfide) for anoxygenic photosynthesis of new biomass. In this respect, the microbial reefs discovered at Black Sea methane seeps suggest how large parts of the ancient ocean might have looked

when oxygen was a trace element in the atmosphere, long before the onset of metazoan evolution.

ACKNOWLEDGEMENT

We thank the crew of the R/V Professor Logachev and the JAGO team for excellent collaboration during field work, and S. Beckmann, S. Ertl, O. Schmale, and M. Hartmann for analytical work. This study received financial support through programs GHOSTDABS (03G0559A) and MUMM (03G0554A) of the Bundesministerium für Bildung und Forschung (BMBF), the Deutsche Forschungsgemeinschaft (Th 713/2), the University of Hamburg, the ZEIT-Stiftung Ebelin und Gerd Bucerius, and the Max-Planck-Gesellschaft (Germany). This is publication GEOTECH-3 of the GEOTECHNOLOGIEN program of the BMBF and the DFG and publication No. 1 of the research program GHOSTDABS.

REFERENCES AND NOTES

Boetius, A.; Ravenschlag, K.; Schubert, C.; Rickert, D.; Widdel, F. *et al.* (2000) A marine microbial consortium apparently mediating anaerobic oxidation of methane. *Nature* **407**: 623-626.

Elvert, M.; Suess, E.; Whiticar, M.J. (1999) Anaerobic methane oxidation associated with marine gas hydrates: superlight C-isotopes from saturated and unsaturated C20 and C25 irregular isoprenoids. *Naturwissenschaften* **86**: 295-300.

Elvert, M.; Suess, E.; Greinert, J.; Whiticar, M.J. (2000) Archaea mediating anaerobic methane oxidation in deep-sea sediments at cold seeps of the eastern Aleutian subduction zone. *Organic Geochemistry* **31**: 1175-1187.

Elvert, M.; Greinert, J.; Suess, E.; Whiticar, M. (2001) Carbon isotopes of biomarkers derived from methane-oxidizing microbes at Hydrate Ridge, Cascadia Convergent Margin. In Dillon, W. und Paull, C. (eds.) *Natural Gas Hydrates: Occurrence, Distribution, and Detection*. American Geophysical Union, Monograph Series **124** pp: 115-129.

Fry, B.; Jannasch, H.W.; Molyneaux, S.J.; Wirsen, C.O.; Muramoto, J.A.; King, S. (1991) Stable isotope studies of the carbon, nitrogen and sulfur cycles in the Black Sea and the Cariaco Trench. *Deep Sea Research* **38**: S1003-S1019 (Suppl. 2).

Hanson, R.S. und Hanson, T.E. (1996) Methanotrophic bacteria. *Microbiological Reviews* **60**: 439-471.

Hayes, J.M. (1994) Global Methanotrophy at the Archaean-Proteozoic transition. Bengtson, S.; Bergstöm, J.; Gonzalo, V.; Knoll, A. (eds.) In *Nobel Symposium* (Columbia University Press, New York) pp: 220-236.

Hinrichs, K.-U.; Hayes, J.M.; Sylva, S.P.; Brewer, P.G.; DeLong, E.F. (1999) Methane-consuming archaebacteria in marine sediments. *Nature* **398**: 802-805.

Hinrichs, K.-U.; Summons, R.E.; Orphan, V.J.; Sylva, S.P.; Hayes, J.M (2000) Molecular and isotopic analysis of anaerobic methane-oxidizing communities in marine sediments. *Organic Geochemistry* **31**: 1685-1701.

Hinrichs, K.-U. und Boetius, A. (2002) The anaerobic oxidation of methane: new insights in microbial ecology and biogeochemistry. pp. 457-477. Wefer, G.; Billet, D.; Hebbeln, D.; Jørgensen, B.B.; Schlüter, M.; van Weering, T. (eds.) In: *Ocean margin Systems* Springer Verlag Berlin-Heidelberg.

Hoehler, T.M.; Alperin, M.J.; Albert, D.B.; Martens, C.S. (1994) Field and laboratory studies of methane oxidation in an anoxic marine sediment: evidence for a methanogen-sulfate reducer consortium. *Global Biogeochemical Cycles* **8**: 451-463.

Ivanov, M.V.; Polikarpov, G.G.; Lein, A.Y. *et al.* (1991) Biogeochemistry of the carbon cycle in the zone of Black Sea methane seeps. *Dokl. Akad. Nauk SSSR* **320**: 1235-1240.

Lein, A.Y.; Ivanov, M.V.; Pimenov, N.V.; Gulin, M.B. (2002) Geochemical characteristics of the carbonate constructions formed during microbial oxidation of methane under anaerobic conditions. *Microbiology* **70**: 78-90.

Mojszis, S.J.; Arrhenius, G.; McKeegan, K.D.; Harrison, T.M.; Nutman, A.P.; Friend, C.R.L. (1996) Evidence for life on earth before 3,800 million years ago. *Nature* **384**: 55-59.

Nauhaus, K.; Boetius, A.; Krüger, M.; Widdel, F. (2002) In vitro demonstration of anaerobic oxidation of methane coupled to sulphate reduction in sediment from a marine gas hydrate area. *Environmental Microbiology* **4**: 296-305.

Orphan, V.J.; House, C.H.; Hinrichs, K.-U.; McKeegan, K.D.; DeLong, E.F. (2001a) Methane-consuming archaea revealed by directly coupled isotopic and phylogenetic analysis. *Science* **293**: 484-487.

Orphan, V.J.; Hinrichs, K.-U.; Ussler III, W.; Paull, C.K.; Taylor, L.T. *et al.* (2001b) Comparative analysis of methane-oxidizing archaea and sulfate-reducing bacteria in anoxic marine sediments. *Applied and Environmental Microbiology* **67**: 1922-1934.

Orphan, V.J; House, C.H.; Hinrichs, K.-U.; McKeegan, K.D.; DeLond, E.F. (2002) Multiple archaeal groups mediate methane oxidation in anoxic cold seep sediments. *Proceedings of the National Academy of Science USA* **99**: 7663-7668.

Pancost, R.D.; Damsté, J.S.S.; DeLint, S.; van der Maarel, M.J.E.C.; Gottschal, J.C. (2000) Biomarker evidence for widespread anaerobic methane oxidation in Mediterranean sediments by a consortium of methanogenic archaea and bacteria. *Applied and Environmental Microbiology* **66**: 1126-1132.

Pancost, R.D.; Bouloubassi, I.; Aloisi, G.; Sinninghe Damsté, J.S., the Medinaut Shipboard Party (2001) Three series of non-isoprenoidal dialkyl glycerol diethers in cold-seep carbonate crusts. *Organic Geochemistry* **32**: 695-707.

Peckmann, J.; Reimer, A.; Luth, U.; Luth, C.; Hansen, B.T. *et al.* (2001) Methane-derived carbonates and authigenic pyrite from the northwestern Black Sea. *Marine Geology* **177**: 129-150.

Pimenov, N.V.; Rusanov, I.I.; Poglazova, M.N.; Mityushina, L.L.; Sorokin, D.Y. *et al.* (1997) Bacterial mats on coral-like structures at methane seeps in the Black Sea. *Microbiology* **66**: 354-360.

Schopf, J.W. (1993) Microfossils of the early Archaeen Apex Chert – New evidence of the antiquity of life. *Science* **260**: 640-646.

Shen, Y.; Buick, R.; Canfield, D. (2001) Isotopic evidence for microbial sulphate reduction in the early Archaeen era. *Nature* **410**: 77-81.

Thiel, V.; Peckmann, J.; Seifert, R.; Wehrung, P.; Reitner, J.; Michaelis, W. (1999) Highly isotopically depleted isoprenoids: molecular markers for ancient methane venting. *Geochimica et Cosmochimica Acta* **63**: 3959-3966.

Thiel, V.; Peckmann, J.; Richnow, H.H.; Luth, U.; Reitner, J.; Michaelis, W. (2001a) Molecular signals for anaerobic methane oxidation in Black Sea seep carbonates and a microbial mat. *Marine Chemistry* **73**: 97-112.

Thiel, V.; Peckmann, J.; Schmale, O.; Reitner, J.; Michaelis, W. (2001b) A new straight-chain hydrocarbon biomarker associated with anaerobic methane cycling. *Organic Geochemistry* **32**: 1019-1023.

Valentine, D.L.; Reeburgh. W.S. (2000) New perspectives on anaerobic methane oxidation. *Environmental Microbiology* **2**: 477-484.

Supporting Online Material

www.sciencemag.org/cgi/content/full/297/5583/1013/DC1

Materials and Methods

Fig. S1

Microbial reefs in the Black Sea fuelled by anaerobic oxidation of methane

W. Michaelis *et al.*, ms # 1072502

Supporting online material

MATERIALS AND METHODS

Gas sampling and analysis

Emanating gas was sampled by submersible at the sea floor. Methane concentrations were measured on board by direct injection into a gas chromatograph (GC). For GC set up see (Seifert *et al.*, 1999).

Stable carbon isotope analyses

Coupled gas chromatography-combustion-isotope ratio mass spectrometry (GC-C-IRMS) was conducted using a Finnigan DeltaPlusXL mass spectrometer equipped with a HP 6890 gas chromatograph and CuO/Ni/Pt combustion furnace operated at 940°C (biomarkers) or 1010°C (methane). For $\delta^{13}C$ of methane, gases were injected (2 or 10 ml) via an 8 Port Valco-valve into a carrier gas flow of about 6 ml min^{-1}. After passing a Nafion-dryer, the gasses were trapped on a Gerstel Cooled Injection System 4 (CIS4) packed with 10 mg PoraPak Q (80–100 mesh) and operated in splitless mode at -135 °C for 8 min. The gases were desorbed through heating the injector to 60 °C at 12 °C min^{-1} and held at this temperature for 1.6 min. The gas chromatograph was equipped with a CP Plot molsieve 5 Å capillary column (25 m, 0,32 mm i.d., 30 µm film thickness), which ensures separation of methane from N_2 at ambient temperatures (30 °C). Standard deviations for replicate

injections were less than 0.7‰. GC-C-IRMS precision was checked daily using a methane standard with known isotopic composition.

For lipids, samples were injected splitless (1 min) onto a 30 m fused silica column (DB5-MS, 0.32 mm i.d., 0.25 µm film thickness) using a Gerstel Cooled Injection System (CIS4) programmed from 48 °C (0 min) to 310 °C (10 min) at 12 °C sec^{-1}. Carrier gas: He. GC temperature program: 3 min at 80 °C; from 80 °C to 310 °C at 4 °C min^{-1}; 30 min at 310 °C. Standard deviations for replicate injections were less than 1.0‰. GC-C-IRMS precision was checked daily using a standard alkane mix (*n*-C_{15} to *n*-C_{29}) with known isotopic composition. The stable carbon isotope compositions are reported in the delta notation ($\delta^{13}C$) *vs.* the V-PDB Standard.

Short term incubations

Short term incubations were carried out at in situ salinity, temperature, and sulfate concentrations. AOM was measured with $^{14}CH_4$ as radiotracer according to Iversen & Blackburn (1981), with adaptations regarding the $^{14}CO_2$ trapping according to Boetius *et al.* (2001). SR was measured with $^{35}SO_4^{2-}$ as radiotracer according to Boetius *et al.* (2001).

Long term incubations

In long term incubation experiments, consumption of methane and simultaneous formation of sulfide were followed via chemical analysis (gas chromatography and colorimetric test, respectively). The incubations were carried out in strictly anoxic seawater medium with slight modifications of a method described elsewhere (Nauhaus *et al.*, 2002). The sulfate concentration was adjusted to the in situ concentration of 16 mM, and anoxic, stoppered culture tubes with a gas phase (methane, or nitrogen for control) were used instead of the completely filled devices (Nauhaus *et al.*, 2002). Both, gaseous and dissolved methane concentrations were determined.

Calculation of free energy change

The free energy change of AOM according to $CH_4 + SO_4^{2-} \rightarrow HCO_3^- + HS^- + H_2O$ under consideration of in situ concentrations and partial pressures was calculated as described in (Nauhaus *et al.*, 2002; Boetius *et al.*, 2000).

Imaging of ^{14}C uptake

Small pieces of samples (1-2 cm^3) stored in in situ water (13 cm^3) without gas headspace were incubated with ^{14}C-methane for 45 days at in situ temperature (9 °C). Samples were fixed with paraformaldehyde solution, and 20 µm thin sections were prepared as previously described (Schramm *et al.*, 1996). Sections were transferred to gelatine coated slides, and, after drying, used for high-resolution 2d beta imaging (Laniece *et al.*, 1998) on a beta microimager (Biospace Mésures, Paris, France). Scans were performed for 3 h. Individual section surface was between 15 and 80 mm^2, and total activity per section measured was between 0.18 and 2.89 cpm mm^{-2} (background: <0.04 cpm mm^{-2}). Sections washed with 0.1 M glycine buffer, pH 2.0, were used as a control for non-incorporated, precipitated radioactivity.

Microscopy and FISH

Microbial mat fixation and cutting was performed as previously described (Schramm *et al.*, 1996). Staining of cells with DAPI and fluorescence-in situ-hybridization was performed according to (8) by using the archaeal ANME-1 specific (ANME1-350-cy3-AGTTTTCGCGCCTGATGC) and the bacterial *Desulfococcus/Desulfosarcina* specific (DSS658-FLUOS- TCCACTTCCCTCTCCCAT) oligonucleotide probes (Boetius *et al.*, 2000). For other FISH probes see (Orphan *et al.*, 2002). Cy3- and carboxyfluorescein-(FLUOS-) labeled oligonucleotides were obtained from Interactiva (Germany). Digital images of mat sections after hybridization were taken by confocal laser scanning

microscopy on a Zeiss LSM510 microscope (Carl Zeiss, Jena, Germany). The size and number of cells and the biomass ratio between ANME-1 and SRB were determined by taking images via confocal laser scanning microscopy and subsequent half-automated image analysis (determination of pixel per area). The length and width of 120 cells from eight different slices of microbial mat were measured and the bacterial cell volume was calculated assuming a cylindrical (ANME-1) or spherical (SRB) shape.

Analyses of lipid biomarkers

Lipid biomarkers were analyzed from subsamples of the microbial mats used for the rate measurements and phylogenetic analyses. The wet mat sample (1.4 g) was saponified in 6% KOH in methanol (75 °C, 3 h) and extracted with *n*-hexane to yield the neutral lipids. Carboxylic acid methyl esters were obtained by acidification of the residual phase to pH 1, extraction with CH_2Cl_2, and treatment of the dry extract with trimethylchlorosilane (TMCS) in methanol (1:8, [v:v]; 2 h at 70 °C). The neutral lipids were separated by thin layer chromatography (silica gel 60, 0.25 mm, CH_2Cl_2) into (I) polar compounds including di- and polyols, such as mono- and tetraether lipids (Rf 0 to 0.1), (II) mono-alcohols including diether lipids (Rf 0.1 to 0.35), and (III) apolar compounds including hydrocarbons (Rf 0.35 to 1). Aliquots of the neutral lipid fractions (I) and (II) were combined and subjected to ether cleavage through HI treatment (2 h at 110 °C) and reduction of the resulting iodides using $LiAlH_4$ in dry ether under an Ar-atmosphere (King *et al.*, 1998). Biomarkers were analyzed by combined gas chromatography-mass spectrometry (GC-MS) using a Micromass Quattro II spectrometer (EI, 70 eV) interfaced to a HP6890 GC with a 30 m fused silica capillary column (DB5-MS, 0.32 mm i.d., 0.25 μm film thickness). Carrier gas: He. Temperature program: 5 min at 80 °C; from 80 °C to 310 °C at 4 °C min^{-1}; 20 min at 310 °C. Compounds were identified by comparison of mass spectra and retention characteristics with published data and/or reference compounds, in particular crocetane: synthetic standard (kindly provided by S. Rowland); archaeol: (Teixidor & Grimalt, 1992); *sn*-2-hydroxyarchaeol: (Hinrichs *et al.*, 2000); PMI: (Schouten *et al.*, 1997; Elvert *et al.*, 1999); biphytanes: authentic standards obtained from *Sulfolobus solfataricus* (kindly provided by G. Antranikian); 1,2-di-O-12-

methyltetradecyl (*anteiso*-C_{15})-*sn*-glycerol: (Pancost *et al.*, 2001) and $HI/LiAlH_4$ treatment of the combined neutral lipid fractions (II) and (III) yielding 3-methyltetradecane as a main compound (see Fig. S1, bottom).

REFERENCES

Boetius, A.; Ravenschlag, K.; Schubert, C.; Rickert, D.; Widdel, F. *et al*. (2000) A marine microbial consortium apparently mediating anaerobic oxidation of methane. *Nature* **407**: 623-626.

Boetius, A.; Ferdelmann, T.; Lochte, K. (2001) Bacterial activity in sediments of the deep Arabian Sea in relation to vertical flux. *Deep Sea Research* II **47**: 2835-2875.

Elvert, M.; Suess, E.; Whiticar, M.J. (1999) Anaerobic methane oxidation associated with marine gas hydrates: superlight C-isotopes from saturated and unsaturated C20 and C25 irregular isoprenoids. *Naturwissenschaften* **86**: 295-300.

Hinrichs, K.-U.; Hayes, J.M.; Sylva, S.P.; Brewer, P.G.; DeLong, E.F. (1999) Methane-consuming archaebacteria in marine sediments. *Nature* **398**: 802-805.

Hinrichs, K.-U.; Pancost R. D.; Summons R. E.; Sprott G. D.; Sylva S. P.; Sinninghe Damsté J. S.; Hayes J. M. (2000) Mass spectra of sn-2-hydroxyarchaeol, a polar lipid biomarker for anaerobic methanotrophy. *Geochemistry, Geophysics, Geosystems* **1**, Paper number 2000GC000042. Published May 30, 2000.

Iversen, N. und Blackburn, T.H. (1981) Seasonal rates of methane oxidation in anoxic marine sediments. *Applied and Environmental Microbiology* **41**: 1295-1300.

Jahnke, L.L.; Eder, W.; Huber, R.; Hope, J.M.; Hinrichs, K.-U.; Hayes, J.M.; Des Marais, D.J.; Cady, S.L.; Summons, R.E. (2001) Signature lipids and stable carbon isotope analyses of octopus spring hyperthermophilic communities compared with those of Aquificales representatives. *Applied and Environmental Microbiology* **67**: 5179-5189.

King, L.L.; Pease, T.K.; Wakeham, S.G. (1998) Archaea in Black Sea water column particulate matter and sediments - evidence from ether lipid derivatives. *Organic Geochemistry* **28**: 677-688.

Laniece, P.; Charon, Y.; Cardona, A.; Pinot, L.; Maitrejean, S.; Mastrippolito, R.; Sandkamp, B.; Valentin, L. (1998) A new high resolution radioimager for the quantitative analysis of radiolabelled molecules in tissue section. *Journal of Neuroscience Methods* **86**:1-5.

Nauhaus, K.; Boetius, A.; Krüger, M.; Widdel, F. (2002) In vitro demonstration of anaerobic oxidation of methane coupled to sulphate reduction in sediment from a marine gas hydrate area. *Environmental Microbiology*. **4**: 296-305.

Orphan, V.J.; Hinrichs, K.-U.; Ussler III, W.; Paull, C.K.; Taylor, L.T. *et al.* (2001) Comparative analysis of methane-oxidizing archaea and sulfate-reducing bacteria in anoxic marine sediments. *Applied and Environmental Microbiology* **67**: 1922-1934.

Orphan, V.J; House, C.H.; Hinrichs, K.-U.; MaKeegan, K.D.; DeLond, E.F. (2002) Multiple archaeal groups mediate methane oxidation in anoxic cold seep sediments. *Proceedings of the National Academy of Science USA* **99**: 7663-7668.

Pancost, R.D.; Bouloubassi, I.; Aloisi, G.; Sinninghe Damsté, J.S., the Medinaut Shipboard Party (2001) Three series of non-isoprenoidal dialkyl glycerol diethers in cold-seep carbonate crusts. *Organic Geochemistry* **32**: 695-707.

Rütters, H.; Sass, H.; Cypionka, H.; Rullkötter, J. (2001) Monoalkylether phospholipids in the sulfate-reducing bacteria *Desulfosarcina variabilis* and *Desilforhabdus amnigenus*. *Archives of Bacteriology* **176**: 435-442.

Schouten, S.; van der Maarel, M.J.E.C.; Huber, R.; Sinninghe Damsté, J.S. (1997) 2,6,10,15,19-Pentamethylicosenes in Methanolobus bombayensis, a marine methanogenic archaeon, and in Methanosarcina mazei. *Organic Geochemistry* **26**: 409-414.

Schramm, A.; Larsen, L.H.; Revsbech, N.P.; Ramsing, N.B.; Amann, R.; Schleifer, K.-H. (1996) Structure and function of a nitrifying biofilm as determined by in situ hybridization and the use of microelectrodes. *Applied and Environmental Microbiology* **62**: 4641-4647.

Seifert, R.; Delling, N.; Richnow, H.H.; Kempe, S.; Hefter, J ; Michaelis, W. (1999) Ethylene and methane in the upper water column of the subtropical Atlantic. *Biogeochemistry* **44**: 73-91.

Sinninghe Damsté, J.S.; Hopmans, E.C.; Pancost, R.D.; Schouten, S.; Geenevasen, J.A.J. (2000) Newly discovered non-isoprenoid glycerol dialkyl glycerol tetraether lipids in sediments. *Chemical Communications* **17**: 1683-1684.

Snaidr, J.; Amman, R.; Huber, I.; Ludwig, W.; Schleifer, K.-H. (1997) Phylogenetic analysis and in situ identification of bacteria in activated sludge. *Applied and Environmental Microbiology* **63**: 2884-2896.

Teixidor, P.; Grimalt, J.O. (1992) Gas-Chromatographic determination of isoprenoid alkylglycerol diethers in archaebacterial cultures and environmental samples. *Journal of Chromatography* **607**: 253-259.

Thiel, V.; Peckmann, J.; Seifert, R.; Wehrung, P.; Reitner, J.; Michaelis, W. (1999) Highly isotopically depleted isoprenoids: molecular markers for ancient methane venting. *Geochimica et Cosmochimica Acta* **63**: 3959-3966.

Thiel, V.; Peckmann, J.; Richnow, H.H.; Luth, U.; Reitner, J.; Michaelis, W. (2001) Molecular signals for anaerobic methane oxidation in Black Sea seep carbonates and a microbial mat. *Marine Chemistry* **73**: 97-112.

1. The isoprenoid crocetane is very characteristic for modern and ancient methane seep environments. It is considered to derive from particular, methane-consuming archaea, though no definite biological source has as yet been identified. The presence of crocetane in the Black Sea microbial mat might point to an origin from ANME-1 archaea. However, a previous study on deposits from another seep location in the Black Sea showed the absence of crocetane in a microbial mat but its prominent occurrence in an associated, massive carbonate (Thiel *et al.*, 2001). Other work reported the absence of crocetane in seep deposits populated by ANME-1 (Hinrichs *et al.*, 1999), but also, its presence in an 'ANME-2 environment', where ANME-1 archaea were found to be virtually lacking (Boetius *et al.*, 2000). At present, it is not clear whether this is due to sporadic biosynthesis of crocetane by these taxa under varying trophic conditions, or to the presence of other, yet unknown contributors of crocetane in these settings. In any case, occurrences of crocetane in fossil samples indicate the presence of the source organisms through

geological times and provide a specific fingerprint for AOM in ancient ecosystems (Thiel *et al.*, 1999, 2001).

2. Chemical degradation using HI/$LiAlH_4$ was performed to selectively release ether bonded alkyl moieties from membrane lipids. Whereas the C_{40} biphytanes derive from archaeal glycerol tetraethers, the C_{20}-isoprenoid hydrocarbon 3,7,11,15-tetramethylhexadecane (phytane) is probably released from archaeol and *sn*-2-hydroxyarchaeol. The presence of 3-methyltetradecane obviously derives from the abundant 1,2-di-O-12-methyltetradecyl-*sn*-glycerol (Fig. 1, top). Glycerol ether lipids with non-isoprenoidal substituents have recently been reported from a number of modern environments (Sinninghe Damsté *et al.*, 2000; Jahnke *et al.*, 2001), including methane-rich deposits (Hinrichs *et al.*, 1999; Pancost *et al.*, 2001). These lipids are not known from archaea, but occur in a small number of bacteria, such as thermophilic and mesophilic clostridia and especially the phylogenetically deeply-branching SRB *Aquifex pyrophilus* and *Thermodesulfobacterium commune* (references given in Pancost *et al.* (2001)). Notably, new results showed the presence of monoalkylether phospholipids in *Desulfosarcina variabilis* Rütters *et al.*, 2001), a member of the mesophilic SRB genus which is commonly observed in seep deposits (Orphan *et al.*, 2001) and is the predominant bacterial component in the microbial mat studied. This suggests that the non-isoprenoidal ether lipids characterize contributions from *Desulfosarcina/Desulfococcus* SRB living in syntrophic communities with archaea in methane-related environments.

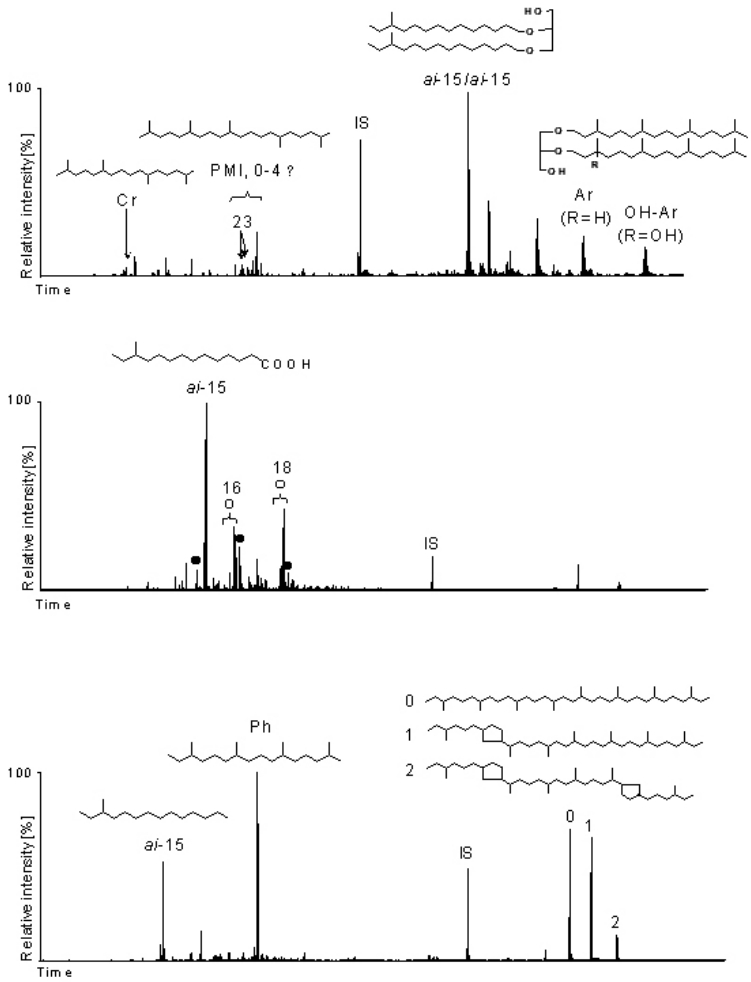

Figure S1. Total ion current chromatograms of lipid fractions from the Black Sea microbial mat. IS = internal standard. Top: total neutral lipids (TMS derivatives). Cr = 2,6,11,15-tetramethylhexadecane (crocetane) (1), PMI = 2,6,10,15,19-pentamethylicosane and unsaturated derivatives (0 to 4 double bonds), 23 = *n*-tricosenes, *ai*-15/*ai*-15 = 1,2-di-O-12-methyltetradecyl (*anteiso*-C_{15})-*sn*-glycerol, Ar = 2,3-di-O-phytanyl-*sn*-glycerol (archaeol), OH-Ar = 2-O-3-hydroxy-phytanyl-3-O-phytanyl-*sn*-glycerol (*sn*-2-hydroxyarchaeol). Middle: carboxylic acid fraction (methyl esters). Filled circles (numbers) = *n*-alkanoic acids (carbon chain length); *ai*-15 = 12-methyltetradecanoic acid (*anteiso*-C_{15}). Open circles = *n*-monoenoic C_{16}- and C_{18}-acids, respectively. Bottom: hydrocarbons after HI/$LiAlH_4$ treatment of the polar lipid fractions (2): *ai*-15 = 3-methyltetradecane; Ph = 3,7,11,15-tetramethylhexadecane (phytane); 0, 1, 2 = biphytane (= 0), and mono- (= 1) and dicyclic (= 2) derivatives thereof.

Chapter 6

Distribution of methane-oxidizers and methanotrophy in microbial mats from the anoxic Black Sea

Tina Treude [1] , Katrin Knittel [1], Armin Gieseke[1], Antje Boetius [1, 2]

[1]Max Planck Institute for Marine Microbiology, Department of Biogeochemistry, Celsiusstrasse 1, 28359 Bremen, Germany

[2]International University Bremen, Research II, Campusring 1, 28759 Bremen, Germany

This manuscript contains data from lab experiments and field work carried out to study the Black Sea microbial mats in greater detail. The data will contribute to at least two manuscripts, one on the lab experiments on metabolism and growth by T. Treude et al., and one on the microbial diversity in the mat by K. Knittel et al..

ABSTRACT. In the permanently anoxic zone of the northwestern Black Sea, large methanotrophic microbial reefs are located above methane seeps. The reefs consist of thick microbial mats covering porous carbonate chimneys formed by anaerobic oxidation of methane (AOM). This study focus on different aspects including the physiology, diversity and morphology of the microbial reef mats. With radiotracer techniques, high rates of AOM and sulfate reduction were measured in mats recovered from the reef chimneys as well as from the sediment. AOM and SR revealed a 1:1 ratio. Radiotracer measurements of potential methanogenesis rates of the CO_2 reduction pathway were of the same magnitude as AOM in the mats. Methanogenesis seemed to be coupled to AOM and both processes were most likely mediated by the same organisms, the archaeal ANME-1 cluster. Beta-imager micrographs of ^{14}C derived from $^{14}CH_4$ and $^{14}CO_2$ assimilation into mat biomass were used to track the hot spot zones of methanotrophy within the mat and to calculate carbon assimilation rates and growth of the mat. The micrographs revealed that methanotrophy takes place mainly in a narrow zone close to the mat periphery, which was shown to be dominated by ANME-1 in fluorescence in situ hybridizations (FISH). The zone above and below the layer of methanotrophic ANME-1 was dominated by different sulfate-reducing bacteria. It was further shown that ANME-1 seems to meet its carbon requirements not only by methanotrophy but to a major part by CO_2-fixation. Calculated growth rates from carbon assimilation rates demonstrated a very slow in vitro growth most likely due to low methane concentrations in laboratory experiments at atmospheric pressure. From photographic and videographic observations, a succession in the development of the microbial reef was hypothesized.

INTRODUCTION

In 1989, authigenic carbonate structures were discovered above methane seeps in the northwestern Black Sea south-west of the Crimean Peninsula at water depth between 60 and 600 m (Fig. 1) (Ivanov et al., 1991). This area was the study site of two Ukrainian-Russian-German-British joint expeditions in 1993 and 1994 (see Thiel et al., 2001 and references therein). The Black Sea is a unique setting for methane seeps because they occur along the depth and oxic/anoxic gradient, though the interface at 130 to 180 m (Luth et al., 1999). In the oxic zone, the carbonate structures associated with the seeps are flat and form around holes through which methane is emitted (Luth et al., 1999). Within the permanently anoxic zone below approx. 180 m, the structures protrude into the water column and form chimney-like reefs, covered by bacterial mats, through which streams of gas bubbles are emanating. The

first microbiological studies of the mats were carried out by Pimenov et al. (1997). They detected anaerobic oxidation of methane (AOM) and methanogenesis (MG) in incubated mat pieces using radiotracer techniques. MG from CO_2 was three times higher than the AOM activity. The authors concluded that the mat is methanogenic and that AOM occurs as an enzymatic re-reaction of MG. However, following studies on the carbon isotopic signature of the carbonates (δ^{13}C values down to –46 ‰) and lipid biomarkers (δ^{13}C value down to –112 ‰) in the mat suggested that the mats comprise methanotrophic communities (Peckmann et al., 2001; Thiel et al., 2001; Lein et al., 2002).

Identifications of the microorganisms and detailed studies on their metabolic processes in the microbial mats were possible when samples of large reefs were retrieved during submersible dives in 2001 (Michaelis et al., 2002). Single reefs reached 4 m height and 1 m in diameter consisting of an inner porous core of precipitated carbonates surrounded by a several centimeter thick microbial mat. The periphery of the mat was black changing into pink towards the mat center. On top of the reef chimneys, the mat formed "nodules", i.e. ball shaped structured of approx. 1 to 10 cm in diameter. Streams of gas (95% methane) percolated permanently though the reefs, and left through holes in the nodules growing on the chimneys.

Physiological investigations on the mat revealed high rates of AOM and methane-dependent sulfate reduction (SR) pointing to the methanotrophic character of the reef (Michaelis et al., 2002). The organisms apparently mediating AOM in the mat were identified with fluorescence in situ hybridization (FISH). The mat was dominated by the methanotrophic archeal cluster ANME-1, which comprised up to 70% of the mat biomass. The most abundant bacterial cells belonged to the sulfate-reducing *Desulfococcus/Desulfosarcina* group, which is known from other methane seeps, and which is supposedly mediating AOM in consortia with methanotrophic archaea (Boetius et al., 2000; Orphan et al., 2001a). The sulfate-reducing bacteria of the Black Sea mats occurred in colonies embedded in the bulk biomass of ANME-1 (Michaelis et al., 2002).

For a long time it was questioned whether the process of AOM can sustain a substantial biomass development due to its low energy yield (-22 to –35 kJ) (Hayes, 1994; Valentine and Reeburgh, 2000; Hinrichs and Boetius, 2002). The discovery of large microbial reefs in the permanently anoxic zone of the Black Sea fueled by AOM stimulated the discussion of such mats as model systems of carbon cycling under the anoxic conditions of early Earth.

In the present study we focused on several aspects including the physiology, diversity and morphology of the reef mats. Main objectives of this study were (1) to quantify turnover rates

of AOM and SR, (2) to test the presence of methanogenesis, (3) to investigate the diversity of microorganisms, (4) to test hypotheses on methanotrophic pathways, and (5) to estimate rates of carbon assimilation. Analyses of carbon assimilation rates and distribution of microorganisms in microbial mats requires the use of 2 or 3D imaging methods (Visscher et al., 1998). This was attempted by analyzing whole sections of mat by beta microimaging and confocal laser scanning microscopy. This study represents the first ecological investigation of a non-photosynthetic anaerobic microbial mat, which were proposed as a model for microbial ecosystems on early Earth (Nisbet and Sleep, 2001).

MATERIALS AND METHODS

Sampling. Samples were obtained by the German submersible "Jago" from water depths around 250 m during the cruise of the Russian RV "Professor Logachev" to the north-eastern Black Sea in June/July 2001 (Fig. 1, Table 1). The microbial reefs were sampled by breaking up large carbonated mat pieces from reef chimneys and by retrieving the soft mat nodules from the reef tops with the manipulator of the submersible. Different morphologies of reefs are presented in Fig. 2d/e. One mat nodule was found inside the sediment in the direct vicinity of the microbial reefs by sampling the sediment with a push-core (inner diameter of the push-core 8 cm). The push-core was sub-sampled with several sub-cores (inner diameter 26 mm, see also Fig. 2a) for different analyses. All samples were recovered under anoxic conditions.

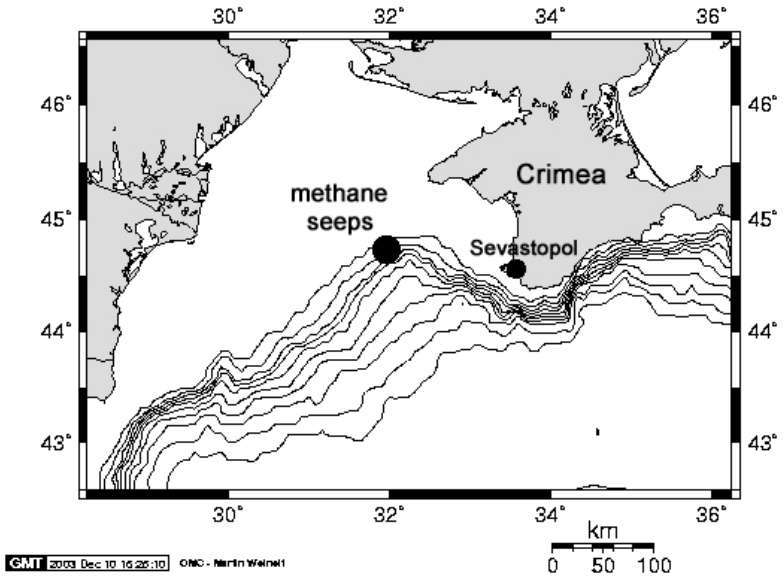

Figure 1. Location of investigated methane seeps in the Black Sea.

Table 1. Station data.

Station No.	Date	Latitude	Longitude	Water depth (m)	Sample
14	03.07.2001	44°46.616 N	31°58.877 E	182	pieces of microbial reef (nodules)
33	08.07.2001	44°44.280 N	31°47.315 E	320	pieces of microbial reef (trunk)
55	11.07.2001	44°46.479 N	31°59.530 E	226	pieces of microbial reef (trunk)
68	15.07.2001	44°44.112 N	31°47.309 E	350	sediment push-core

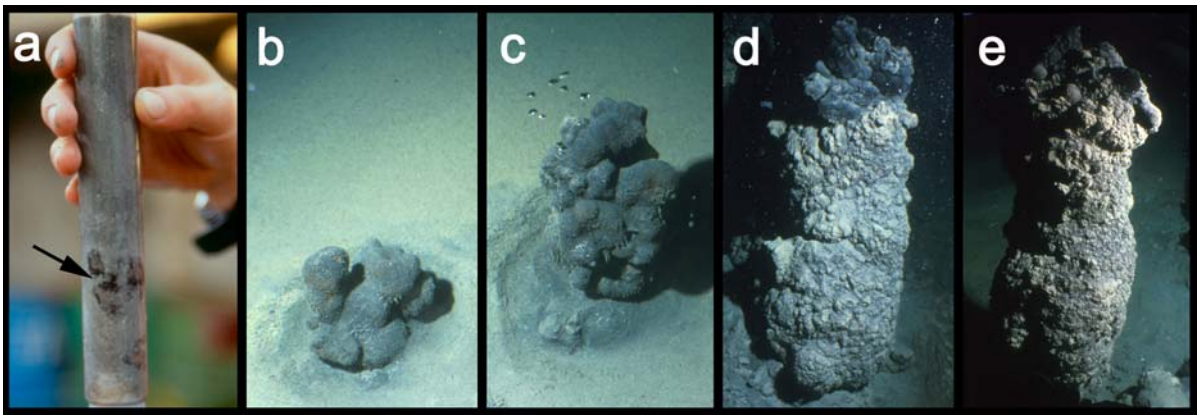

Figure 2. Pictures of different nodule (a-c) and reef stages (d and e). Figure a shows a sediment-nodule sub-core of this study; the location of the nodule in the sediment is marked by the arrow. Figures b-e are taken by the Jago-team and kindly provided by the GHOSTDABS project.

Incubations of mat pieces from the reef chimney with radiotracers. On board, small cylindrical sub-samples were cut out from one large mat piece (ca 2-3 kg) of the reef chimney using plastic tubes (inner diameter 1.5 cm, length 10 cm). The mat sub-samples were transferred to a 500 ml bottle, half-filled with anoxic bottom water. All mat sub-samples were covered with anoxic water. After sealing, the headspace was flushed with methane for several minutes to ensure anoxic conditions and a methane concentration of ca. 1.4 mM. The sample bottles were stored at 12°C. In the home laboratory, preparations of incubations were done under an anoxic atmosphere (N2/CO2, 4:1) using a glove box (Mecaplex).

AOM, MG and SR in the presence of methane and sulfate. Mat sub-samples were cut into pieces of about 1.5 x 1 x 0.3 cm with a wet weight between 0.2 and 0.5 g (3 replicates and 1 control per AOM, MG and SR incubations, respectively). The mat pieces revealed a clear color transition from black (periphery) to pink (central part). As controls served mat pieces fixed with 4% formaldehyde for 24 hrs before incubation. Each mat piece was

transferred into a 16 ml Hungate tube filled with 14 ml artificial seawater medium (17 mM sulfate, 30 mM HCO_3^-). Tubes with control pieces contained 13 ml medium and additionally 1 ml formaldehyde (37%). The tubes were sealed and the headspace (2 ml) was purged with methane for 1 min. After purging, the headspace concentration was set to 100% methane at 2 bar. Radiotracer was injected in replicate and control tubes as follows: (1) $^{14}CH_4$ (50 µl, 55 kBq, gaseous); (2) $H^{14}CO_3^-$ (100 µl, 185 kBq, dissolved in water) for MG incubations; (3) $^{35}SO_4^{2-}$ (50 ml, 1000 kBq, dissolved in water) for SR incubations. The Hungate tubes were stored horizontally in the dark for 62 days at 9°C (in situ temperature during sampling) and gently shaken twice per week.

After incubation, the headspace was removed using a gas-tight syringe and simultaneously replaced by the injection of distilled water. The AOM and MG incubation media were transferred into 50 ml glass vials filled with 25 ml sodium hydroxide (2.5% w/w). The SR incubation media were transferred into 50 ml plastic centrifuge vials filled with 20 ml zinc acetate (20% w/w). All vials were closed immediately and the respective headspace of the samples was subsequently injected to the appropriate vial and vials were shaken thoroughly. Water drops were gently removed from mat pieces by draining on cellulose filters and pieces were weighted and treated as described below.

MG in the presence or absence of methane and sulfate. Mat pieces (between 0.3 and 0.5 g) were incubated with $H^{14}CO_3^-$ as described in the former section. For each of the following conditions, three replicates were incubated: (1) methane headspace, 17 mM sulfate; (2) methane headspace, no sulfate; (3) no methane headspace, 17 mM sulfate; (4) no methane headspace, no sulfate. Medium without mat pieces was used as a control (one per condition). Nitrogen replaced methane in the headspace in incubations (3) and (4). The incubation time was 32 days.

MG in the presence of hydrogen and presence or absence of methane and sulfate. Several small pieces (volume per piece <10 mm^3, total weight 0.3 to 0.6 g per replicate) were incubated with $H^{14}CO_3^-$ as described in the former section. Water drops were gently removed from the samples by draining on cellulose filter before weighing and transferring into Hungate tubes. Methane or nitrogen were provided in the headspace at atmospheric pressure. One ml H_2/CO_2 mixture (4:1) was added to each headspace. The incubation time was 9 days. The tubes were gently shaken every day.

Incubation of the sediment-nodule core with radiotracers. $^{14}CH_4$ (dissolved in water, injection volume 15µl, activity 2 kBq) or $^{35}SO_4$ (dissolved in water, injection volume 6 µL,

activity 10 kBq) were injected into one sediment-nodule sub-core, respectively, at 1 cm intervals according to the whole core injection method of Jørgensen (1978). After an incubation time of 24 hrs at 9°C in the dark, the cores were split into 1 cm sections. AOM samples were transferred into 50 ml glass vials filled with 25 ml sodium hydroxide (2.5% w/w). The glass vials were closed quickly with rubber stoppers and shaken thoroughly. SR samples were transferred into plastic centrifuge vials filled with 20 ml zinc acetate (20% w/w). Control sediment was first fixed before addition of the respective tracer.

Analytical procedures. ***Mat dry weight.*** Mat dry weight per wet weight was determined by weighting 3 replicate mat pieces before (wet) and after (dry) freeze drying for 48 hrs.

Mat density. Mat density was determined by weighting 3 replicate mat pieces (1 cm^{-3}). Water drops were gently removed from the mat pieces by draining with cellulose filter before weighing.

Sediment porosity and density. Sediment samples were taken from 1 cm sections of one sediment-nodule sub-core and transferred into pre-weighed 15 ml plastic centrifuge vials with a volume scale bar. The vials were centrifuged (2200 g, 10 min), weighed, filled with water to a definite volume, weighed again, dried and weighed a third time. From the difference of the weights porosity and sediment density was calculated.

Sediment sulfate concentration. Pore water sulfate concentration was determined in 1 cm sections of one sediment-nodule sub-core. Sections were fixed with 20 ml zinc acetate (20 % w/w) in 50 ml plastic centrifuge tubes. After sealing, vials were shaken thoroughly and stored frozen at –25°C. In the laboratory, the samples were thawed and centrifuged (2200 g, 10 min). Pore water sulfate concentrations were measured in the supernatant using nonsuppressed ion chromatography with a Waters 510 HPLC pump, Waters WISP 712 autosampler (100 µl injection volume), Waters IC-Pak anion exchange column (50 x 4.6 mm), and a Waters 430 Conductivity detector. The eluent was 1 mM isophthalic acid with 10% methanol, adjusted to pH 4.5. The flow was set to 1.0 ml min^{-1}.

Anaerobic oxidation of methane. The rate of AOM was determined from the total amount of CH_4 (determined by gas chromatography), the activity of $^{14}CH_4$ (determined by combustion) and the activity of $^{14}CO_2$ (determined by diffusion method) according to Treude et al. (2003). AOM was calculated by

$$AOM = \frac{^{14}CO_2 \cdot CH_4}{^{14}CH_4 \cdot (dw\ or\ v) \cdot t} \qquad (1)$$

where AOM is the rate of methane oxidation (µmol g^{-1}dw d^{-1} or µmol cm^{-3} d^{-1}), $^{14}CO_2$ is the radioactivity of the microbial produced radioactive carbon dioxide (cpm), CH_4 is the total amount of methane in the Hungate tube or sediment sample (µmol), $^{14}CH_4$ is the radioactivity of the residual radioactive methane (cpm), *dw* or *v* is the dry weight (g) of the mat piece or the volume (cm^{-3}) of the sediment, and *t* is the incubation time (days).

Methanogenesis. The rate of methane production was determined from the total amount of CO_2 (known quantity), $^{14}CH_4$ (determined by combustion) and $^{14}CO_2$ (determined by diffusion method). $^{14}CH_4$ and $^{14}CO_2$ were determined according to Treude et al. (2003). MG was calculated by

$$MG = \frac{^{14}CH_4 \cdot CO_2}{^{14}CO_2 \cdot dw \cdot t} \qquad (2)$$

where MG is the methanogenesis rate (µmol g^{-1}dw d^{-1}), $^{14}CH_4$ is the activity of the microbial produced radioactive methane (cpm), CO_2 is the total amount of carbon dioxide in the Hungate tube (µmol), $^{14}CO_2$ is the activity of the residual radioactive carbon dioxide (cpm), *dw* is the dry weight of the mat piece (g) and *t* is the incubation time (days).

Sulfate reduction. SR rates were determined using the cold-chromium-distillation method according to Kallmeyer et al. (submitted). SR rates of mat pieces were calculated by

$$SRR = \frac{^{35}TRIS \cdot SO_4^{2-} \cdot 1.06}{^{35}SO_4^{2-} \cdot dw \cdot t} \qquad (3)$$

where *SRR* is the sulfate reduction rate (µmol g^{-1}dw d^{-1}), SO_4^{2-} is the total amount of sulfate in the Hungate tube (µmol), $^{35}TRIS$ is the radioactivity of the produced metal mono- and disulfides, and elemental sulfur (cpm), 1.06 is the correction factor for the expected isotopic fractionation (Jørgensen and Fenchel, 1974), $^{35}SO_4^{2-}$ is the radioactivity of the residual radioactive sulfate (cpm), *dw* is the dry weight of the mat, *t* is the incubation time (days). SR rates of sediment-nodule samples were calculated by:

$$SRR = \frac{[SO_4] \cdot \Phi \cdot ^{35}TRIS \cdot 1.06}{t \cdot ^{35}TOT} \qquad (4)$$

were *SRR* is the sulfate reduction rate (µmol cm^{-3} d^{-1}), [*SO4*] is the pore water sulfate concentration of the sediment sample (mM), Φ is the porosity of the sediment (as a fraction of 1) and ^{35}TOT is the total radioactivity used (cpm).

Beta microimaging with mat pieces from the reef chimney. Mat pieces of the $^{14}CH_4$ and $^{14}CO_2$ incubation from the 62 days incubation at the presence of methane and sulfate were fixed with 3% formaldehyde (in seawater) for 24 hrs. After fixation, the pieces were washed two times with 1xPBS and transferred into 1xPBS/EtOH (1:1). Thin sections of 20 µm thickness (replicates and controls, 24-30 sections per mat piece) were prepared from peripheral and central parts as described elsewhere (Schramm et al., 1996). Sections were transferred to gelatin coated glass slides, dried at room temperature, and subsequently used for high-resolution 2D beta microimaging (Lanièce et al., 1998) on a beta-imager (Biospace Mésures, Paris, France). Scans of each sample were performed for 12 hrs. Subsequently, the sections were washed with 0.1 M glycine buffer, pH 2.0 and scanned again for 12 hrs.

Calculation of ^{14}C assimilation and precipitation within the mat. Determinations of radioactivity in beta-imager micrographs were done using the Biospace (Paris) software ß-vision (version 4.2) provided by the manufacturer. The radioactivity of the total scan field (32 x 23 mm) was determined for comparisons between replicates, controls, and background.

To determine the radioactivity within restricted areas of the scans, the outline of the areas, i.e. individual sections or distinct zones within sections, were marked. The radioactivity of selected zones was calculated by the software and manually corrected for the background radioactivity. The total assimilated radioactivity per mat sample was calculated according to:

$$total\ \ radioactivity\ of\ \ mat\ \ piece = \frac{total\ \ volume\ mat\ \ piece \times \sum \text{section}\ \ radioactivity}{\sum \text{section}\ \ volume} \quad (5)$$

For the differentiation between precipitated ^{14}C-carbonate and ^{14}C- assimilated into biomass the total radioactivity of the mat pieces was determined from scans before and after acidification, respectively. For acidification, glycine buffer (pH 2) was used. Volumes of mat pieces were calculated from their weight and density.

From the total turnover of $^{14}CH_4$ by AOM (according to Eq. 1), the percentage of ^{14}C assimilated into mat biomass (cpm in mat after acidification) was calculated.

The rate of carbon assimilation was calculated from either radioactive methane or radioactive carbon dioxide by the following equation:

$$C_{assimilated} = \frac{^{14}C_{assimilated} \cdot CX_y}{^{14}CX_y \cdot t \cdot dw} \quad (6)$$

where $C_{assimilated}$ is the carbon assimilation rate (nmol C g^{-1}dw d^{-1}), $^{14}C_{assimilated}$ is the total radioactivity of the assimilated radioactive carbon from either methane or carbon dioxide (cpm), CX_y is the total amount of either methane or carbon dioxide in the Hungate tube (nmol), $^{14}CX_y$ is the activity of the radioactive methane or radioactive carbon dioxide in the Hungate tube (cpm), t is the incubation time (days), and dw is the dry weight of the mat piece (g).

In order to show the distribution of ^{14}C in the mat, assimilated radioactivity was determined from beta microimaging scans along a vertical grid of 1 x 50 cells (2.8 mm^2 per cell). The radioactivity of each cell was calculated and plotted against depth, i.e. ascending grid numbers. Data were corrected for background radioactivity

Identifications of microorganisms by FISH. FISH was used to identify specific phylogenetic groups of microorganisms in mat sections (see above), in mat homogenates and in the sediment-nodule core. Mat homogenates were produced from different reef samples by manually homogenizing peripheral (black), central (pink) or complete mat (black and pink) of the reef chimney as well as nodules from the top of the reef (for sampling locations see Table 1). Samples from the sediment nodule were taken from one sediment-nodule sub-core sectioned in 1 cm intervals. Mat homogenates and sediment-nodule samples were fixed in the same way as described above for mat sections. FISH and 4′,6′-diamidino-2-phenylindole (DAPI)-staining of all samples were performed as described previously (Snaidr et al., 1997). Probes and formamide (FA) concentrations used are given in Table 2. Oligonucleotides, mono-labeled with fluorescence dyes Cy3- and Cy5, were purchased from Thermo Electron Corporation, USA (support: Thermo Hybaid, Germany).

For mat sections, the vertical distribution (between mat periphery and center) of FISH-targeted cells was determined using a confocal laser scanning microscope (LSM510, Zeiss, Jena, Germany).

Aliquots of the mat homogenates (1.5 µl, mixed with 10 µl 0.1% low gelling point agarose) were transferred to glass slides and dried before hybridization. The presence of

different groups of microbes in homogenates was checked using an epifluorescence microscope.

Aliquots of the sediment-nodule samples (10 µl) were filtered on 0.2 µm GTTP polycarbonate filters (Millipore, Eschborn, Germany) before hybridization. The presence of different groups of microbes was checked and their relative abundance in the samples was estimated very roughly using an epifluorescence microscope.

RNA extraction and slot blot hybridization of the sediment-nodule core. RNA was extracted from 2.5-4 g wet sample (per section) of one sectioned sediment-nodule sub-core by bead-beating, phenol extraction and isopropanol precipitation as described previously (Sahm and Berninger, 1998). The quality of the RNA was checked by polyacrylamide gel electrophoresis. Approximately 20-50 ng RNA was blotted on nylon membranes (Magna Charge, Micron Separations, Westborough, MA) in triplicates and hybridized with ^{33}P-radioactively labelled oligonucleotide probes as described by (Stahl et al., 1988). Membranes were washed at different temperatures according to the probe dissociation temperature (Td). Probes used and dissociation temperatures are given in Table 3. The dissociation temperatures of the probes were determined as described by Raskin et al. (1994). For dissociation temperature determination and hybridizations of probe DSS658 washing buffer with a lower sodium dodecylsulfate (SDS) concentration was used (1xSSC: 150 mM NaCl, 15 mM sodium citrate, pH 7.0; 0.1% SDS).

Table 2. Oligonucleotide probes and formamide concentration (FA) used for FISH.

Probe	Target group	Reference	FA (%)
Mat sections			
DSS 658 [1)]	*Desulfosarcina* spp., *Desulfofaba* sp., *Desulfococcus* spp., *Desulfofrigus* spp.	Manz et al. (1998)	40
ANME-1 350 [1)]	ANME-1	Boetius et al. (2000)	40
EelMS 932 [1)]	ANME-2	Boetius et al. (2000)	40
EUB 338 [2)]	*Bacteria*	Amann et al. (1990a)	40
Arch 915 [2)]	*Archaea*	Amann et al. (1990b)	40
Mat homogenates			
DSR651	*Desulforhopalus* spp.	Manz et al. (1998)	35
DSS658	*Desulfosarcina* spp., *Desulfofaba* sp., *Desulfococcus* spp., *Desulfofrigus* spp.	Manz et al. (1998)	60
DSV 698	*Desulfovibrio* spp.	Manz et al. (1998)	35
DSV214	*Desulfomicrobium* spp.	Manz et al. (1998)	10
DSMA488	*Desulfarculus* sp., *Desulfomonile* sp.,	Manz et al. (1998)	60
DBUL660	*Desulfobulbus* spp.	Devereux et al. (1992)	60
DBAM221	*Desulfobacterium* spp.	Devereux et al. (1992)	35
DTM229	*Desulfotomaculum* spp.	Hristova et al. (2000)	15
DNMA657	*Desulfonema* spp.	Fukui et al. (1999)	35
DSB985	*Desulfobacter* spp., *Desulfobacula* spp.	Manz et al. (1998)	20
Sval428 (430)	*Desulfotalea* spp., *Desulfofustis* sp.	Sahm et al. (1999)	52
DSF672	*Desulfofrigus* spp., *Desulfofaba* sp.	Ravenschlag et al. (2000)	45
ALF968	alpha proteobacteria, wide variety of delta-proteobacteria	Neef (1997)	35
BET42a plus cGAM42a	beta proteobacteria (competitor gamma proteobacteria)	Manz et al. (1992) Neef (1998)	35
GAM42a plus cBET42a	gamma proteobacteria (competitor beta proteobacteria)	Manz et al. (1992) Neef (1998)	35
PLA886 plus cPLA886	*Planctomycetales*, some *Eucarya*	Neef (1998)	35
Sediment-nodule core			
EUB338 I-III	*Bacteria*	Amann et al. (1990a) Daims et al. (1999)	10
Arch915	*Archaea*	Amann et al. (1990b)	35
ANME-1-346	ANME-1	Knittel et al. (unpubl.)	40
ANME-1-365	ANME-1	Knittel et al. (unpubl.)	40
ANME-1-329	ANME-1	Knittel et al. (unpubl.)	40
ANME-2-538	ANME-2	Knittel et al. (unpubl.)	50

[1)] Dual hybridization DSS 658/ANME-1 350 respectively DSS 658/EelMS 932

[2)] Dual hybridization EUB 338/Arch 915

Table 3. Oligonucleotide probes used for slot blot hybridization in sediment-nodule samples.

Probe	Specificity	Sequence (from 5' to 3')	Position [1)]	slot blot Td (°C)	Reference
Uni1390	Universal- all organisms	GACGGGCGGTGTGTACAA	1390-1407	44	Zheng et al. (1996)
EUB338	*Bacteria*	GCTGCCTCCCGTAGGAGT	338-355	54	Amann et al. (1990a)
ARCH915	*Archaea*	GTGCTCCCCCGCCAATTCCT	915-935	56	Amann et al. (1990b)
ANME-1 350	ANME-1 cluster	AGTTTTCGCGCCTGATGC	350-367	60	Boetius et al. (2000)
DSS658	*Desulfosarcina* spp./*Desulfofaba* sp./ *Desulfococcus* spp./*Desulfofrigus* spp.	TCCACTTCCCTCTCCCAT	658-685	58 [2)]	Manz et al. (1998)

[1)] Position in the 16S rRNA of *E.coli*

[2)] Use of washing buffer containing 1xSSC, 0.1%SDS

RESULTS

Turnover rates

AOM, SR and MG in mat of the reef chimney. ***AOM, MG and SR in the presence of methane and sulfate.*** Mean AOM and SR revealed a 1:1 ratio in incubated mat pieces (Fig. 3). Rates of replicates ranged between 3.8 and 9.4 µmol g^{-1}dw d^{-1} for AOM and between 4.3 and 10.9 µmol g^{-1}dw d^{-1} for SR at methane and sulfate concentrations of 1.4 and 17 mM, respectively. Rates of MG from CO_2 and hydrogen were close to this range (between 1.6 and 8.2 µmol g^{-1}dw d^{-1}). No turnover of tracer was measured in controls of AOM, SR and MG with formaldehyde-fixed mat pieces.

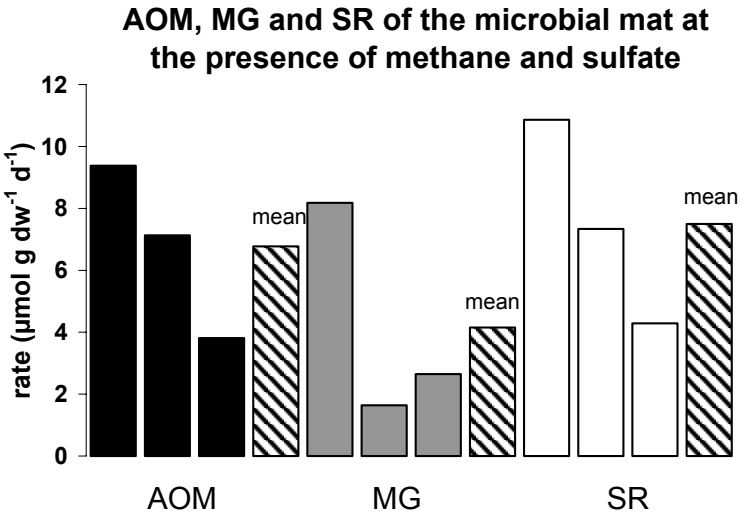

Figure 3. AOM, SR and MG in mat pieces of the reef chimney. Replicates (n = 3) and means are shown. The concentration of methane and sulfate was 1.4 and 17 mM, respectively during incubations.

MG in the presence or absence of methane and sulfate. Substantial rates of MG from CO_2 and hydrogen were detected only when methane (1.4 mM) was available (with or without sulfate (17 mM)). Rates were between 1.0 and 5.1 µmol g^{-1}dw d^{-1} (Fig. 4). In the absence of methane, MG was very low (0.02 µmol g^{-1}dw d^{-1}) or not detectable. No methane production from $H^{14}CO_3^-$ was detected in controls.

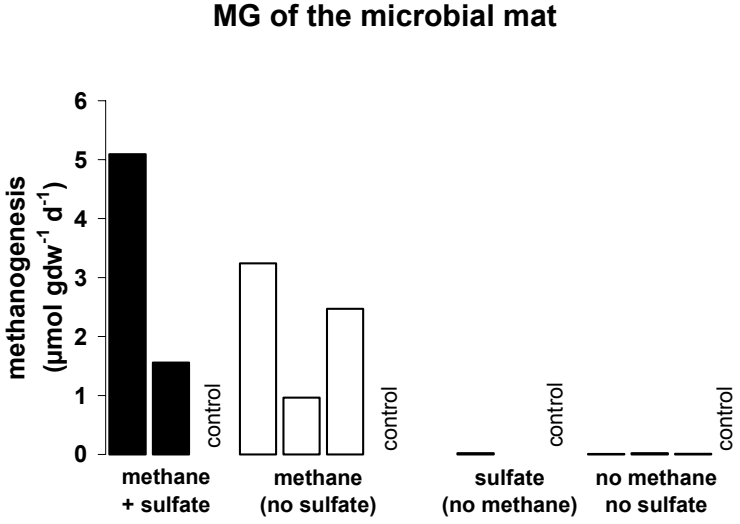

Figure 4. MG in mat pieces of the reef chimney at the presence or absence of methane (1.4 mM) or sulfate (17 mM). Replicates (n = 3) and controls are shown.

MG in the presence of hydrogen and presence or absence of methane and sulfate. Highest rates of MG from CO_2 and hydrogen were measured when methane (1.4 mM) and sulfate (17 mM) were present (between 1.2 and 2.3 µmol g^{-1}dw d^{-1}, Fig. 5). No MG was detected in incubations without methane and in controls. MG was very low (0.2 and 0.3 µmol g^{-1}dw d^{-1}) or not detectable when only methane and no sulfate was available.

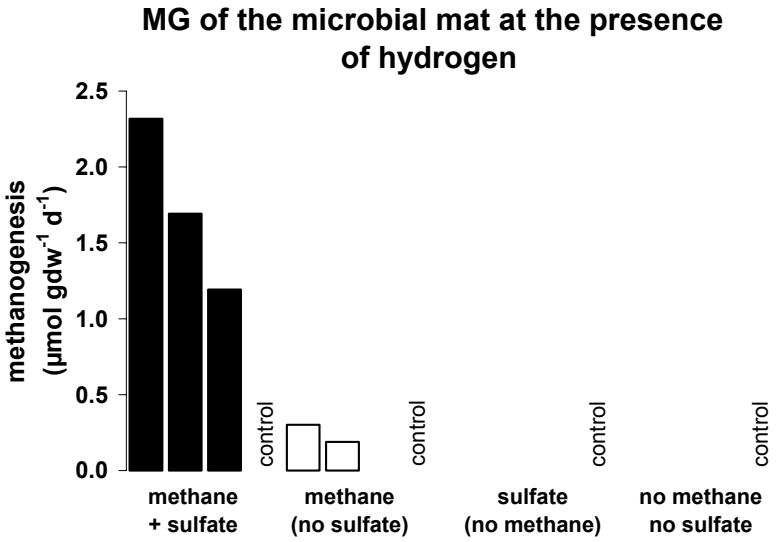

Figure 5. MG in mat pieces of the reef chimney at the presence or absence of methane (1.4 mM) or sulfate (17 mM) after the addition of hydrogen. Replicates (n = 3) and controls are shown.

AOM and SR in the sediment-nodule core. The sediment push-core taken close to the microbial reef contained a microbial nodule at about 6 cm sediment depth (Fig. 2a). The nodule was very soft, i.e. without detectable carbonate precipitates, with an inner pinkish and an outer black layer.

Activity in AOM and SR was detected between 6 and 16 cm (Fig. 6a) with a maximum in AOM at 12-13 cm (1.5 µmol cm^{-3} d^{-1}) and a maximum in SR at 11-12 cm (1.8 µmol cm^{-3} d^{-1}). The AOM profile seemed to be shifted 1 cm below the SR profile, presumably due to the shape of the nodule or due to small differences in its compression during sub-sampling. AOM and SR revealed a close 1:1 ratio.

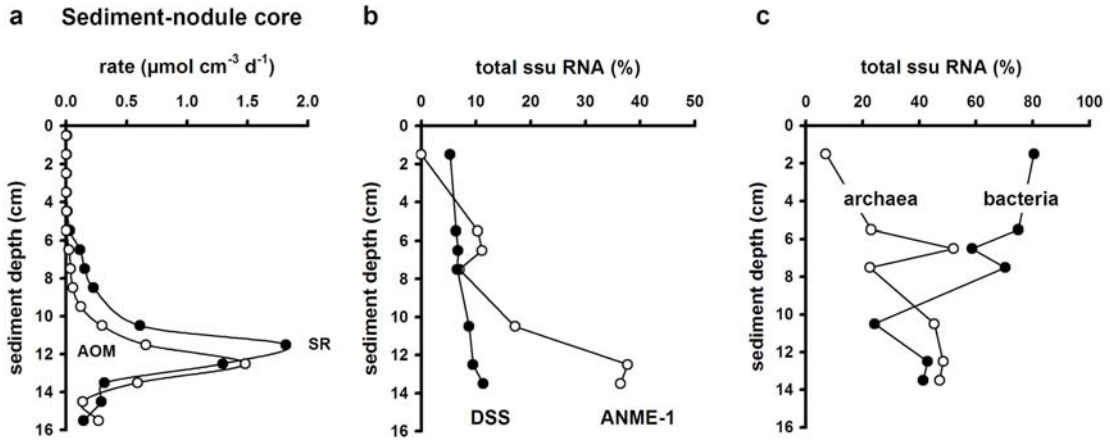

Figure 6. Measurements of the sediment-nodule core: a) AOM (○) and SR (●) rates; b) percentage 16S rRNA abundance of ANME-1 (○) and *Desulfococcus/Desulfosarcina* (●); c) percentage 16S rRNA abundance of archaea (○) and bacteria (●).

Identification of microorganisms in the anoxic microbial mats. ***FISH of mat sections of a reef chimney.*** Two mat pieces (one from the $^{14}CH_4$ and one from the $^{14}CO_2$ incubation) were analyzed by FISH for the distribution of microorganisms in the mat. The same sections of the pieces, which were used for beta microimaging, were analyzed in dual hybridizations targeting either bacteria (Cy5) and archaea (Cy3) , *Desulfococus/Desulfosacina* (Cy5) and ANME-1 (Cy3), or *Desulfococus/Desulfosacina* (Cy5) and ANME-2 (Cy3). The results were similar for both mat pieces. Examples of the distribution of microorganisms are presented in Fig. 7. ANME-1 was most abundant in the zone that was defined as the most active zone of ^{14}C assimilation by beta microimaging. Above and below that zone, ANME-1 and archaea were generally less abundant. Here, signals of bacterial cells were much stronger. In the lower parts of the mat pieces, small aggregates of ANME-2 were found. It was difficult to see whether they had cell-to-cell contact with sulfate-reducing bacteria. However, cells of the Desulfococcus/Desulfosarcina cluster were found nearby in the mat.

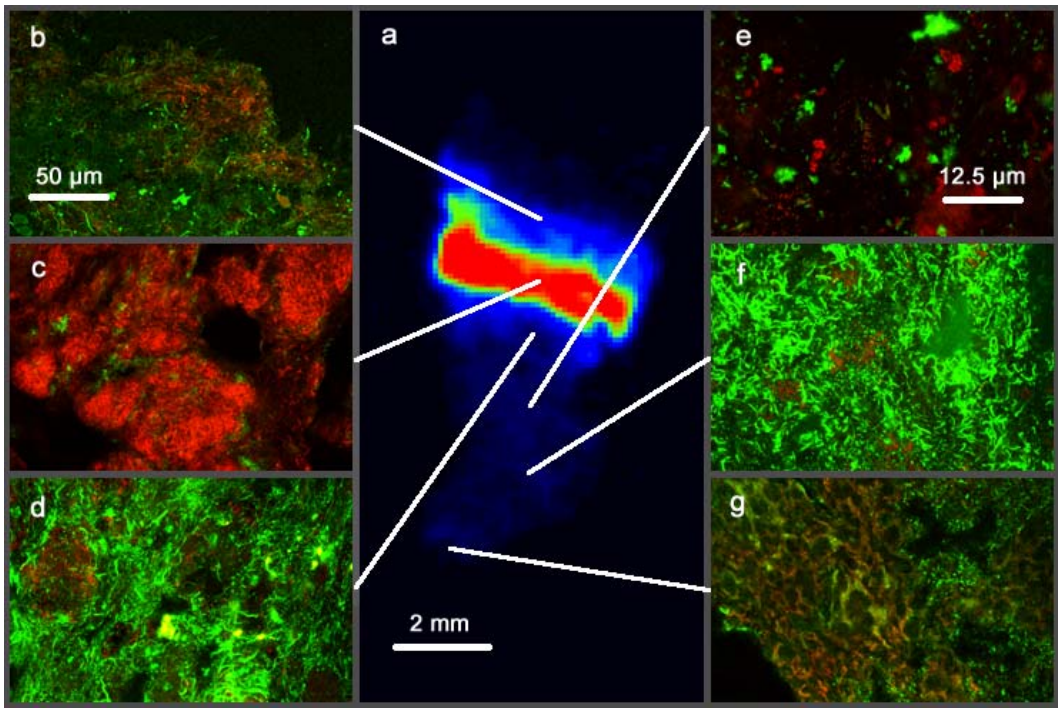

Figure 7. Distribution of microorganisms in mat sections of a reef chimney. Confocal laser scanning micrographs of hybridizations of different zones in mat sections (b-g) are compared with a beta-imager micrograph of a section from the same mat piece showing $^{14}CO_2$-derived carbon assimilation (a). Figure a shows high radioactivity of ^{14}C in red, low radioactivity in blue. Figure b, d, f and g show dual hybridizations of EUB 338 (stained green) and Arch 915 (stained red). Figure c and e show dual hybridizations of DSS 658 (stained green) and ANME-1 350 (stained red), respectively, DSS 658 (stained green) and EelMS 932 (stained red). The 50µm scale bar refers to b, c, d, f, and g.

FISH of homogenates from different mat zones. Homogenates of samples from different mat zones (periphery = black, center = pink, complete = black and pink) and nodules were investigated by FISH for the presence of different bacterial groups. The results are only qualitative, i.e. no quantification of cell abundance was carried out. Probe signals were regarded as positive if a cell was visualized by both FISH and DAPI staining. The detection and morphology of the labeled cells are given in Table 4. The results show that a variety of sulfate-reducing bacteria (SRB) were present in the mat homogenates. No alpha-, beta-, or gamma proteobacteria were found. Some groups of SRB were present only in the outer black mat layer (*Desulforhopalus* spp., *Desulfomicrobium* spp., *Desulfobacter* spp., *Desulfobacula* spp., *Desulfotalea* spp., *Desulfofustis* sp.) in the pinkish inner layer (*Desulfotomaculum* spp.) or in the nodule (*Desulfovibrio* spp.). Other groups were found in all samples (*Desulfosarcina* spp., *Desulfofaba* sp., *Desulfococcus* spp., *Desulfofrigus* spp., *Desulfonema* spp.). One distinct type of cells was always abundant and exclusively found in the outer black layer but

seemed to be labeled by different probes. The cells were short curved rods (Fig. 8).Our results suggest an unspecific binding of different probes to these cells which were easily identified by their shape.

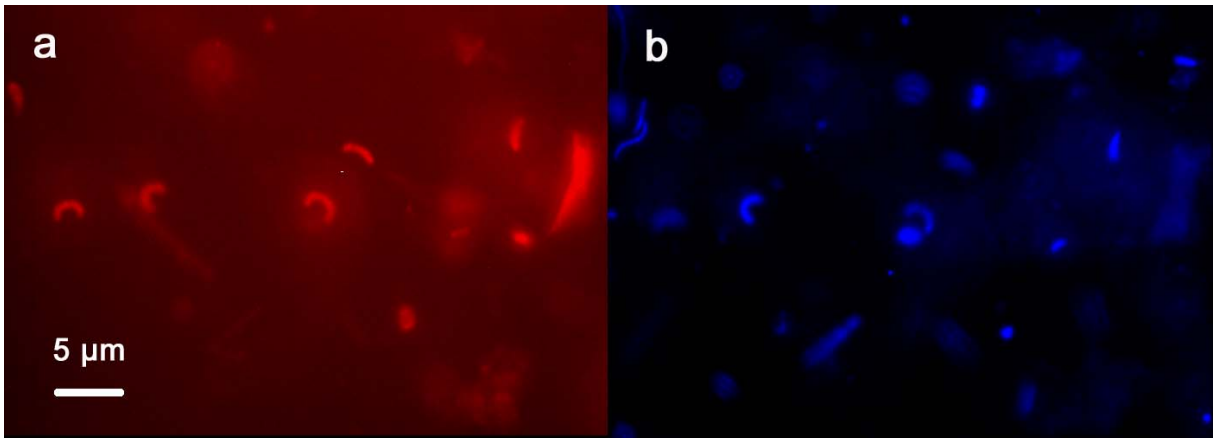

Figure 8. Curved rod-shaped cells in the periphery of the mat: a) cells targeted with DNMA 657 (CY3) by FISH, b) DAPI staining.

FISH and slot blot hybridization of the nodule in near-by sediments. Rough estimates of the abundance of AOM mediating communities in the sediment-nodule core using FISH revealed a high abundance (>10% of total cells) of ANME-1 cells between 8 and 14 cm sediment depth (Table 5). Archaeal abundance generally correlated with the distribution of ANME-1, however, in some depth horizons other archaea were present (1-2 cm, 4-6 cm and 12-14.5 cm). No ANME-2 cells were detected in the nodule. Bacteria also showed a higher abundance between 8 and 10 cm (5-10%) but reached only about half of the ANME-1 abundance (Table 5). Above and below that zone, bacterial abundance was low (<5%).

Using rRNA slot blot hybridization as another quantitative method, we studied vertical profiles of rRNA from ANME-1 and *Desulfosarcina*/*Desulfococcus*. No 16S rRNA of ANME-1 was found close to the sediment surface (1-2 cm, Fig. 6b). Within the 5-11 cm depth interval between 10 and 17% of total rRNA belonged to ANME-1. A distinct peak in ANME-1 rRNA (36-38%) was found at 12-14 cm. 16S rRNA of DSS was around 8% of total 16S rRNA with only a slight increase from top to bottom of the core. The 16S rRNA distribution of archaea and bacteria showed opposite values (Fig. 6c). At the sediment surface, the abundance of archaeal 16S rRNA was low (7%) where it was high for bacterial 16S rRNA (80%). At a sediment depth of 12 to 14 cm, abundances of archaea and bacteria were approximately equal.

Table 4. Identification of bacterial cells in the mat homogenates by fluorescence microscopy of hybridaized cells: dash = no labeled cells were found, for detected labelled cells the morphotype is given, the underlined bended cells seamed to represent the same type of cell that was labelled by different probes.

Probe	Target group	Station and origin of mat suspension			
		14 nodule	55 chimney (pink and black zone)	33 chimney (pink zone)	33 chimney (black zone)
DSR651	*Desulforhopalus* spp.	-	-	-	small coccoids
DSS658	*Desulfosarcina* spp., *Desulfofaba* sp., *Desulfococcus* spp., *Desulfofrigus* spp.	coccoids	coccoids	coccoids	coccoids curved rods
DSV698	*Desulfovibrio* spp.	long filaments	-	-	-
DSV214	*Desulfomicrobium* spp.	-	-	-	short thick filaments
DSMA488	*Desulfarculus* sp., *Desulfomonile* sp., *Syntrophus* spp.	small coccoids	small coccoids	-	curved rods
DBUL660	*Desulfobulbus* spp.	-	small coccoids	-	small coccoids
DBAM221	*Desulfobacterium* spp.	-	-	-	-
DTM229	*Desulfotomaculum* spp.		-	small coccoids	-
DNMA657	*Desulfonema* spp.	long filaments short rods	long filaments short rods	short rods	curved rods
DSB985	*Desulfobacter* spp., *Desulfobacula* spp.	-	-	-	short thick filaments
Sval428 (430)	*Desulfotalea* spp., *Desulfofustis* sp.	-	-	-	long filaments
DSF672	*Desulfofrigus* spp., *Desulfofaba* sp.	long filaments	-	rods	-
ALF968	alfa-proteobacteria, wide variety of delta-proteobacteria	-	-	-	-
BET42a	beta-proteobacteria	-	-	-	-
GAM42a	gamma-proteobacteria	-	-	-	-

Table 5. Estimated in situ-abundance of microorgansims in the sediment-nodule core as detected by FISH. The abundance ist given in percent of total cells (%); dash = no cells found, n.d. = not determined.

sediment depth (cm)	ANME-1	ANME-2	*Archaea*	*Bacteria*
1-2	<1	-	1-5	<1
2-3	<1	-	<1	<1
3-4	-	-	<1	<1
4-5	<1	-	1-5	<1
5-6	<1	-	1-5	<1
6-7	5-10	-	5-10	<1
7-8	5-10	-	5-10	<1
8-9	n.d.	-	>20	5-10
9-10	>20	-	>20	5-10
10-11	>20	-	>20	1-5
11-12	10-20	-	10-20	<1
12-13	10-20	-	>20	<1
13-14	10-20	-	>20	<1
14-14.5	5-10	-	10-20	1-5

Assimilation and precipitation of ^{14}C into mat of the reef chimney

Beta-imager micrographs (32 x 23 mm) of slides with replicate sections of mat pieces, incubated for 62 days either with $^{14}CH_4$ or $H^{14}CO_3^-$, revealed a substantially higher ^{14}C activity (measured as counts per hour and area) compared to slides with control sections or without sections (background slides) (Fig. 9 a and b). Formaldehyde-fixed controls and background slides revealed the same amount of radioactivity, i.e. no ^{14}C was assimilated or precipitated in fixed control mat pieces.

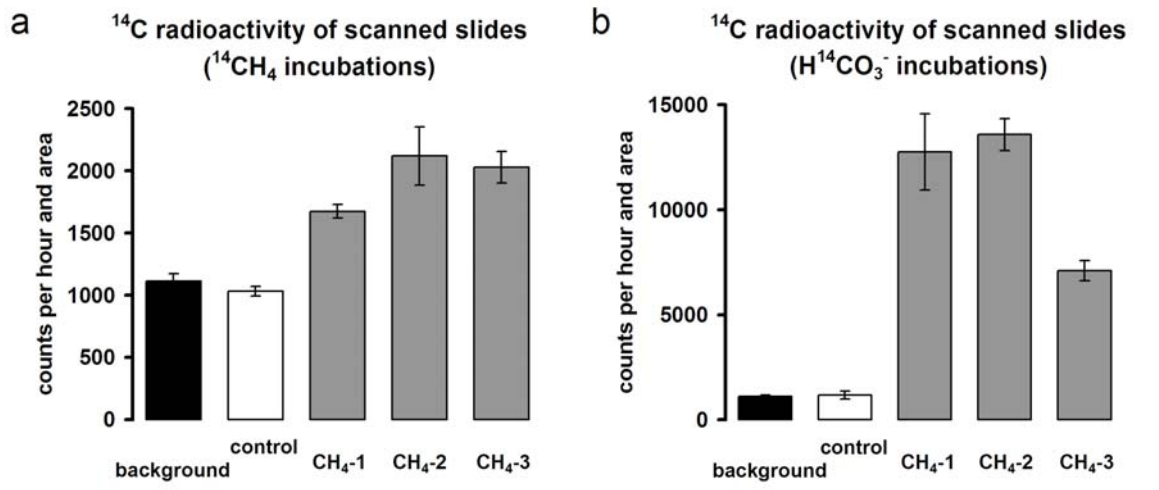

Figure 9. ^{14}C activity (counts per hour) measured in beta-imager micrographs of glass slides without (background) and with mat sections (samples and controls) incubated either with a) $^{14}CH_4$ or b) $H^{14}CO_3^-$. The micrographs had a size of 32 x 23 mm. The numbers of measured glass slides was 4 for background and 6-10 for glass slides with mat sections.

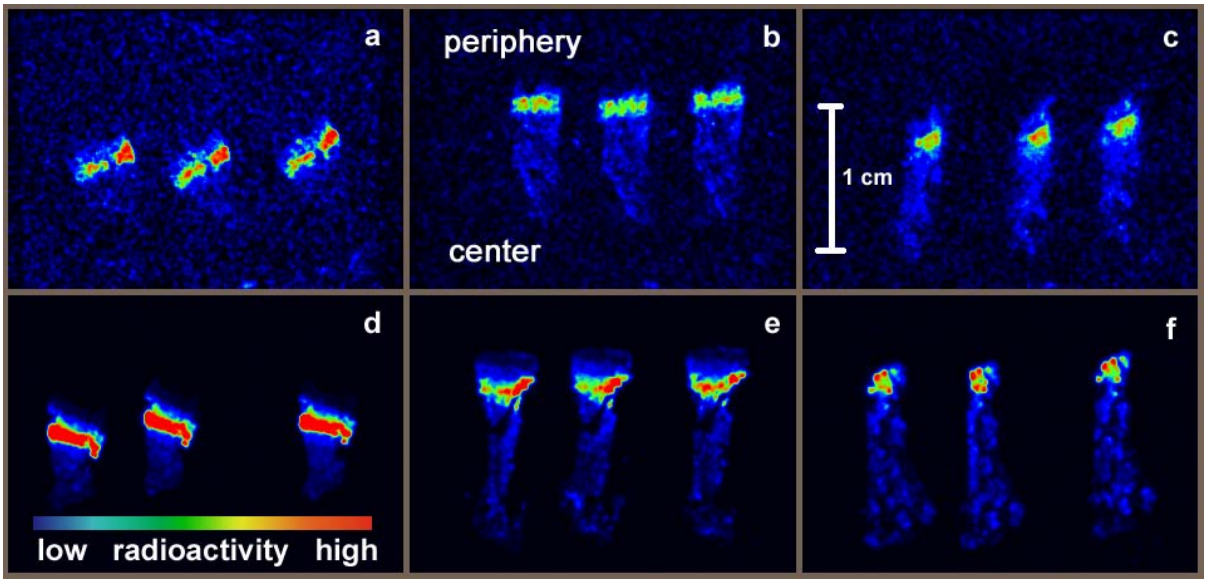

Figure 10. Overview of beta-imager micrographs of mat sections (3 consecutive sections per micrograph) incubated either with $^{14}CH_4$ (micrographs a-c) or $H^{14}CO_3^-$ (micrographs d-f). High ^{14}C radioactivity is depicted in red. The former periphery and center of the mat is marked.

Beta-imager micrographs revealed a distinct zone with higher activity in all mat pieces. This active zone comprised only 15% (± 3% s.d., n= 6) of the total volume of the mat pieces, but 52% (± 6% s.d., n= 6) of the ^{14}C activity. The active zone was located close to the

periphery of the mat (mat-water interface, Fig.10). Examples of radioactivity profiles from the periphery towards the center of the mat demonstrate the differences in methane and CO_2-derived ^{14}C distribution within the mat sections (Fig. 11 a and b).

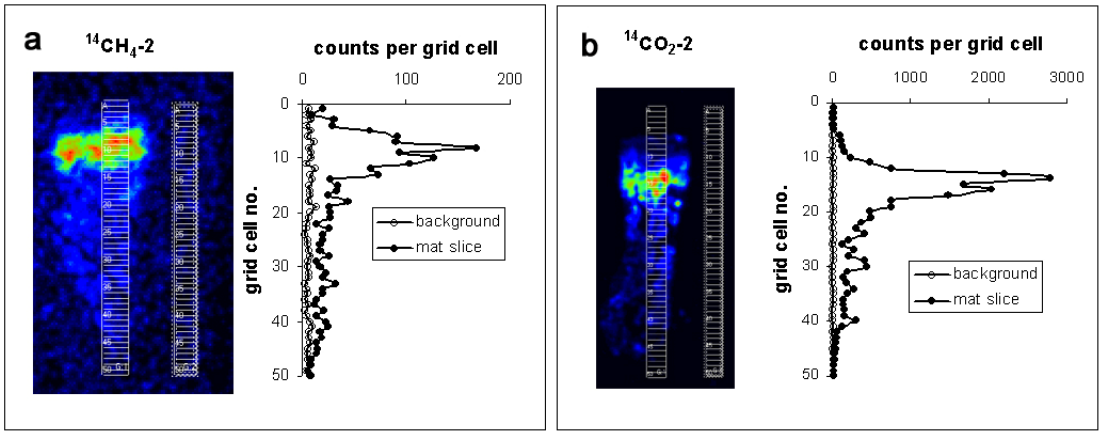

Figure 11. ^{14}C distribution in the mat sections incubated either with a) $^{14}CH_4$ or b) $H^{14}CO_3^-$ from the mat periphery (low grid cell no.) to the mat center (high grid cell no.). The radioactivity of background grids is also given. High radioactivity is depicted red.

In incubations with $^{14}CH_4$, the assimilation rate of carbon from methane was between 17.7 and 19.8 nmol C g^{-1}dw d^{-1} for whole mat pieces (n = 3). Comparing methane turnover and assimilation, 0.2 to 0.5% ^{14}C of the $^{14}CH_4$ was assimilated into mat biomass. In incubations with $H^{14}CO_3^-$, the assimilation rate of carbon from carbon dioxide was between 154 and 588 nmol C g^{-1}dw d^{-1} for whole mat pieces (n = 3). The assimilation rates were three to four times higher when calculated only for the most active zone (47.5 to 73.5 nmol C g^{-1}dw d^{-1} for methane, 713 to 2519 nmol C g^{-1}dw d^{-1} for carbon dioxide).

In most mat pieces, acidification with glycine buffer did not result in degassing of $^{14}CO_2$ precipitated as carbonate and hence revealed no significant loss of ^{14}C in the scanned sections (p>0.05, paired-sample t-test between non-acidified and acidified sections). Thus, ^{14}C was in most cases completely assimilated into biomass. Only one mat piece incubated with $H^{14}CO_3^-$ showed a significant loss (p = 0.02, n = 9) in ^{14}C of 15% of the total uptake into the mat. These 15% represent most likely precipitated carbonates.

DISCUSSION

Turnover rates in the mats

Anaerobic oxidation of methane and sulfate reduction

During AOM, one molecule methane is oxidized by the concurrent reduction of one molecule sulfate (Barnes and Goldberg, 1976):

$$CH_4 + SO_4^{2-} \rightarrow HCO_3^- + HS^- + H_2O \qquad (7)$$

In the present study, radiotracer measurements with mat pieces from the reef chimney as well as with the nodule recovered from below seafloor revealed very high AOM rates. The magnitude of the methane turnover in the Black Sea mats is in the same range as at other methane seeps such as Hydrate Ridge, Cascadia Margin, where AOM rates are among the highest worldwide (Hinrichs and Boetius, 2002 and references therein). At a methane concentration of about 1.4 mM, in vitro AOM of the mat pieces was twice the in vitro AOM of sediment slurries from Hydrate Ridge (Nauhaus et al., 2002; Nauhaus, 2003). The activity in the sediment nodule was similar to field measurements at Hydrate Ridge sites with very high methane fluxes (Treude et al., 2003). The Black Sea mat consists of a nearly pure microbial biomass with approx. 10^{12} cells cm^{-3} (Michaelis et al., 2002). Hydrate Ridge sediments contain very small methanotrophic aggregates with a cell density of approx. 9×10^9 cells cm^{-3} sediment (Boetius et al., 2000). Considering this difference in cell abundance, the biomass-specific rates of the Black Sea mats appear relative low. Beta-imager micrographs of the mat pieces incubated with $^{14}CH_4$ indicated by methane-derived carbon assimilation that major AOM is mediated only in a narrow zone close to the periphery of the mat. This might lead to underestimations when calculating AOM rates for pieces including also inactive parts of the mat.

The ratio of 1:1 between AOM and SR in mat pieces from the reef chimney and in the sediment nodule confirmed the finding of Michaelis et al. (2002) and Nauhaus (2003) that AOM of the methanotrophic reef is tightly coupled to SR. The current study presents, to our knowledge, for the first time AOM activity of a subsurface microbial mat recovered from

sediments. This finding appears interesting with regard to development of the reef growth which will be discussed below.

Are there evidences for methanogenesis in the mats?

Zehnder and Brock (1979) first hypothesized that AOM is a reversal of methanogenesis, i.e. methanotrophic archaea oxidize methane instead of producing it by using the identical enzymatic apparatus that is used for MG backwards. Recent molecular studies found a specific nickel containing enzyme in sediments containing AOM communities which was related to methyl coenzyme M reductase, the enzyme catalyzing the terminal step in methanogenesis (Hallam et al., 2003; Krüger et al., accepted). The most widespread pathways of microbial methanogenesis are the formation of methane from either acetate or CO_2 and hydrogen (e.g. Heyer, 1990):

$$4\ HCOOH \rightarrow CH_4 + 3\ CO_2 + 2\ H_2O \quad \Delta G^0 = -119.5\ kJ\ mol^{-1} \qquad (8)$$

$$4\ H_2 + CO_2 \rightarrow CH_4 + 2\ H_2O \quad \Delta G^0 = -138.8\ kJ\ mol^{-1} \qquad (9)$$

Experiments of Pimenov and coworkers (1997) showed with radiotracer experiments adding either $H^{14}CO_3^-$ or ^{14}C-actetate, that CO_2 reduction is the dominant pathway for methanogenesis in the mats of the Black Sea. In comparison, the acetoclastic pathway was of minor importance (0.1%). The results could indicate the presence of a methanogenic population in the mat. However, radiotracer experiments revealed also sulfate reduction in the mat (Pimenov et al., 1997; Michaelis et al., 2002). A co-occurrence of methanogenesis from H_2/CO_2 and sulfate reduction appears surprising. In marine sediments, CO_2-reducing methanogens are usually outcompeted by sulfate reducers which are more efficient in hydrogen uptake (Zehnder, 1988). As a consequence, zones of sulfate reduction and methanogenesis of the CO_2 reduction pathway do not overlap in sediments.

In the present study, we incubated mat pieces with $H^{14}CO_3^-$ to measure the rate of methanogenesis in the presence or absence of methane or sulfate. The mat pieces revealed MG rates similar to AOM and SR. Most strikingly, MG was highest when both sulfate and methane were present, but was absent when no methane was provided. Furthermore, the addition of hydrogen did not stimulate MG. In 16S rRNA gene libraries no clone sequences related to methanogenic archaea beside the ANME-1 and ANME-2 group were found (number of clones >300, K. Knittel unpubl. data).

We conclude from these observations that MG in the mat was not mediated by genuine methanogens but was coupled to the process of AOM and ANME-1. Many methanogenic archaea are known to exhibit AOM at a minor fraction (between 0.001 and 0.3%) of the methane production presumably due to the reversibility of the catalyzing enzymes (Zehnder and Brock, 1979). The biochemical process of AOM is not understood, however, it might be possible that methane production also occurs as a re-reaction during AOM. The magnitude of the re-reaction might depend on the concentrations of substrates and products on both sides of the reactions (Zehnder and Brock, 1979). If the first step of AOM is catalyzed by a modified methyl coenzyme M reductase, as hypothesized by Krüger et al. (accepted), differences in the magnitude of the re-reaction of either AOM or MG could be also due to a modification in the enzyme responsible in the first step in AOM.

It is also possible that methane production may occur in micro-environments inside the mat, in which methanogenesis becomes thermodynamically favorable.

Microbial diversity in the mat

The diversity of microorganisms in the mat was analyzed by FISH and rRNA slot blot hybridization identifying different archaea and bacteria (Fig. 6 , 7 and 8, Table 4 and 5). We used three types of samples: (1) mat sections from the reef chimney, (2) mat homogenates from a reef chimney (periphery and center of mat) and from nodules of the reef top, and (3) a sediment core containing a mat nodule.

Microbial diversity and distribution in the reef

The ANME-1 zone. In mat sections of the reef chimney, ANME-1 was most abundant in a distinct zone directly below the periphery of the mat. The zone coincides with the most active zone in beta-imager micrographs of the mat sections revealing highest methane-derived carbon assimilation. Therefore bulk ANME-1 biomass and coupled methanotrophy seemed to be restricted to a narrow layer of the mat. In a former study of mat sections such a zonation was not observed by FISH and beta microimaging investigations (Michaelis et al., 2002). Here, the dense mat matrix investigated was described to be to 70% dominated by ANME-1. Smaller clusters and single cells of sulfate-reducing bacteria were dispersed throughout the bulk ANME-1 biomass. Also beta-imager micrographs revealed no zonation in methane-derived ^{14}C assimilation. However, it is possible that the distribution of ANME-1 might vary

between reefs or even within the same reef. More investigations are needed to get a better picture about the microbial variability in the reef mats. Furthermore, it remains unknown if the rate of AOM is correlated with the variation in methane assimilation.

The periphery of the mat. It is curious that the most active zone of AOM was not located directly at the mat-water interface where a sufficient supply with sulfate from the surrounding water can be expected. Microchannels, which make up 20 to 40% of the bulk mat volume, have been suggested to enable an exchange of substrates and products of AOM with the surrounding water (Michaelis et al. 2002). Nevertheless, a direct contact with the water appears favorable. One reason for the formation of a surface layer around the methanotrophic mat could be a colonization by heterotrophs. The microbial reef may represent a substrate for heterotrophic bacteria as it offers a large accumulation of organic substances. During submersible dives we saw large flakes of marine snow in the water column and the deposition of organic matter was visible on the surface of the reefs. The presence of a variety of sulfate-reducing groups in the homogenate of the outer black layer (Table 4) indicates that the periphery of the mat might be independent from methane oxidation and could be involved in the degradation of deposited particles. This hypothesis should be further tested by high resolution studies of the isotope signature of specific microbial biomarkers or by investigations of the $^{12}C/^{13}C$ ratio of peripheral mat sections by secondary ion mass spectrometry.

The interior zones of the mat. In mat sections, abundances of ANME-1 and the assimilation of methane-derived ^{14}C decreased towards the interior parts of the mat. This may be due to a general depletion of sulfate supply from the surrounding water with increasing mat depth, which could limit the growth of the AOM consortium.

Below the ANME-1 zone, aggregates of ANME-2 were found sporadically. ANME-2/ *Desulfococcus/Desulfosarcina* aggregates mediate AOM at gas hydrate locations in the North-East Pacific (Boetius et al., 2000; Orphan et al., 2001a/b). Their importance in the methane cycling of the methanotrophic reef is unclear as they were found in a zone that revealed only minor activity of methane-derived ^{14}C-assimilation.

The bulk biomass of the deeper mat parts was dominated by bacteria. We found no cells belonging to the alpha-, beta-, and gamma proteobacteria in the homogenates of this zone. The numerous bacterial cells seem to belong mainly to sulfate-reducing groups of the delta proteobacteria. Some of the identified groups were found exclusively in this part and not in the periphery of the mat (Table 4). The role of the sulfate-reducing bacteria is not clear. If sulfate is depleted in this zone, the cells may meet their minimum energy requirements by

fermentation of degraded microbial biomass (Widdel, 1988). However, there should be other heterotrophic microorganisms present in the mat initiating the first steps in organic matter decomposition, providing the substrates for the sulfate reducers.

Microbial diversity and distribution in the sediment nodule

The nodule found within the sediment possibly represents a very early stage in the formation of the methanotrophic reef. Investigations with FISH and slot blot hybridizations revealed ANME-1 to be the dominant archaeal group in the sediment nodule. No ANME-2 cells were found by FISH, hence we can exclude a relevant contribution of this group to the formation of the nodule. Interestingly, the steep increase in 16S rRNA of ANME-1 in the nodule (10-14 cm below sediment surface) was not accompanied with a significant increase in the 16S rRNA of the *Desulfococcus/Desulfosarcina* cluster, the supposed syntrophic partner of AOM in the microbial reefs. Either their abundance of the sulfate reducers in the sediment and mat was high enough to sustain AOM, or the ANME-1 group is capable to mediate both AOM and SR. To date there are no habitats reported in which methanotrophic archaea occur and no sulfate reducers were found, however, the hypothesis of a true syntrophy between archaea and sulfate-reducers is debated since sulfate-reducing bacteria are not always physically associated with the methanotrophic archaea (Orphan et al., 2001; Lösekann, 2002; Treude et al., submitted).

Methanotrophy and growth of the mat

The existence of methanotrophic archaea was first confirmed by Hinrichs et al. (1999) by the identification of specific biomarkers with depleted $\delta^{13}C$ values, indicating an assimilation of methane-derived carbon into archaeal biomass. During AOM, methanotrophic archaea discriminate against the heavier $^{13}CH_4$ leading to a depletion of ^{13}C in their biomass (Whiticar, 1999). If the substrate methane is of microbial origin, the biomass depletion can reach values of <-110‰ (Hinrichs and Boetius, 2002). Further studies of biomarkers from different methane-rich marine environments followed, confirming the assimilation of methane-derived carbon into the biomass of AOM organisms (Elvert et al., 2000; Pancost et al., 2000; Elvert et al., 2001; Thiel et al., 2001). The methane emanating from the Black Sea seeps is of biogenic origin with $\delta^{13}C$ values around -65 ‰ (Michaelis et al., 2002). Biomarkers in the reef mats associated with methanotrophic archaea revealed $\delta^{13}C$ values

between -90 and -96 ‰, indicating a substantial methane-derived carbon assimilation into mat biomass (Michaelis et al., 2002). So far, the biochemical pathways of carbon assimilation of methanotrophic archaea are not known. The question remains if methane is directly assimilated into biomass or if methane is first oxidized and the carbon is subsequently assimilated by CO_2-fixation. For methanogenic archaea different substrates have been identified as carbon source: CO_2, acetate, methanol, formate and methylamine (Heyer, 1990). Some methanogenic archaea, e.g. *Methanosarcina barkeri*, are not specialized but assimilate carbon from all these different sources (Heyer, 1990). However, it is unknown if methanotrophic archaea can utilize the same carbon sources. In a previous study we were able to demonstrate a net assimilation of methane-derived carbon into the microbial mat of the Black Sea reef using $^{14}CH_4$ (Michaelis et al., 2002). With these long term experiments running for weeks, it cannot be distinguished between a direct uptake of $^{14}CH_4$ into the mat, or an uptake of the $^{14}CO_2$ product of AOM. In the present study, mat pieces were incubated with either $^{14}CH_4$ or $H^{14}CO_3^-$ to investigate if methane-derived carbon could theoretical be assimilated through CO_2-fixation and to estimate total carbon assimilation and growth of the microbial mat. Furthermore, the precipitation of ^{14}C-carbonates from $^{14}CH_4$ and $H^{14}CO_3^-$ in the mat was studied.

Which role does CO_2-fixation play in the carbon assimilating pathways of methanotrophic archaea?

In both radiolabeled substrates, most of the ^{14}C was assimilated in the zone dominated by ANME-1. The total assimilation rate of methane-derived carbon was on average 20 times lower compared to the assimilation rate of CO_2-derived carbon. Thus, ANME-1 seems to meet its carbon requirements not exclusively from methane but to a substantial fraction also by CO_2 fixation. However, it has to be considered that the percentage of methane-derived carbon assimilation could be much higher at in situ concentrations of methane. AOM shows a linear increase with methane concentration (Nauhaus et al., 2002) and thus rates of methane oxidation and possibly also methanotrophy may be underestimated in incubations at atmospheric pressure. At the investigated methane seep, free gas was bubbling though the mats, hence – assuming a dissolved methane concentration at equilibrium- methane concentrations may be around 45 mM taking into account the Bunsen solubility coefficient of methane (Yamamoto et al., 1976) and the hydrostatic pressure at 250 m water depth.

Can we calculate realistic growth rates of the reef from methane- and CO_2-derived carbon assimilation and precipitation?

An underestimation of in situ carbon assimilation is obvious when roughly estimating the doubling time of the ANME-1 cells from the measured carbon assimilation. The biovolume of an ANME-1 cell is about $1 \mu m^3$ (Michaelis et al., 2002). We assumed a carbon content of 2.5×10^{-5} nmol C per cell according to the conversion factor of Børsheim et al. (1990). The averaged calculated carbon assimilation rate (including methane- and CO_2-derived carbon) of the most active zone was 1.5×10^{-10} nmol C d^{-1} per cell. For a doubling of its carbon content, i.e. to form two cells, a cell would need about 450 years. Assuming a cell density of 10^{12} cells cm^{-3} in the mat (Michaelis et al., 2002) and an exponential growth of the cells it would take a colony about 25,000 years to grow to the size of a bowling ball. With this growth rate, the microbial reef had never reached its recent size because the deeper water column of the Black Sea is anoxic only since only 9000 years (Calvert et al., 1987) and the age of methane that is emanating from the seeps has been estimated to be <5100 years old (Ivanov et al., 1991). Despite the hypothesized sluggish carbon assimilation in vitro due to low methane concentrations, the grow rate could also be underestimated if other carbon sources like acetate, formate, methanol or methylamine are used. However, macroscopic pieces of microbial mat that were kept in our laboratory for over two years with sulfate (17 mM) and saturated methane concentration (1.4 mM) revealed no visible growth. This strengthens our assumption that we have not met the conditions needed to stimulate an in situ grow rate.

Carbonate is precipitated during AOM by the following reaction:

$$CH_4 + SO_4^{2-} + Ca^{2+} \rightarrow CaCO_3 + H_2S + H_2O \qquad (10)$$

In an earlier study we could demonstrate precipitation of methane-derived carbonates into the microbial mat by beta-imager micrographs (Michaelis et al., 2002). In the present study a significant precipitation of carbonates was measured in only one mat replicate of the $H^{14}CO_3^-$ incubations. The calcification seems to be irregular and our data do not allow an estimate of carbonate precipitation in the mat. Nevertheless, calcification seems to be an important process in the mat, as precipitated carbonate builds the internal structure and stabilization of the reef.

The development of the methanotrophic reef - a hypothetical model

The following section discusses a hypothesized development of the methanotrophic reefs from benthic colonies of ANME-1. This hypothetic pathway is illustrated in Fig.12 and is mainly based on photographic (Fig. 2) and videographic observations (this study and Michaelis et al., 2002). We assume that the formation of the methanotrophic microbial reefs begins with the growth of a population of ANME-1 cells within the sediments of the Black Sea. In sediments of Hydrate Ridge (K. Knittel, unpubl. data) and Eel River Basin (Orphan et al., 2001a/b) ANME-1 has been observed occurring as single cells or in the form of short chains. The initial step that leads from a loose cell accumulation to the first mat matrix is unknown. Since such methanotrophic mats have so far only been found in the permanently anoxic part of the Black Sea, we assume that factors supporting the formation of a mat could be the lack of any bioturbation and grazing by metazoans in the anoxic environment of the Black Sea as well as the permanent and high discharge of methane gas.

The methanotrophic nodule found in the sediment, a few meters away from the main reef, may represent a primitive stage of the reef. The nodule was very soft, i.e. without macroscopic carbonate crusts. If methane is permanently discharged in the vicinity of the nodule, this may cause a further growth, probably leading to carbonate precipitation in the mat. Different structures of mats and carbonates from subsurface cements to the development of small chimneys protruding from the seafloor was previously observed in a study of the wider area of the Crimean shelf (Luth et al., 1999). The precipitation of carbonate as a product of AOM seems to enable the mat to rise into the water column. Mat nodules which we have observed during the submersible dives seemed to have grown around streams of emanating gas. Some of the nodules growing on the carbonate were found to enclose gaseous methane. The nodules were hollow and had a ball-shape, a form that offers most stability for enclosing gas. Small openings in the nodules prevent the bursting of the mat by allowing gas bubbles to leave the nodule when overpressure is reached. After surfacing the sediment, the reef could continue to grow into the anoxic water of the Black Sea. The growth of microbial mats within the sediments should be limited by the low diffusion rates within the clay sediments. In contrast, the flow of bottom water around the reef structures could largely increase the availability of sulfate as electron acceptor. Deeper parts of the mat anchored in the sediment may get increasingly cemented, forming the basic support for the reef. New nodules could grow on top of the solid structures. The emanating methane can reach the nodules through cavities and channels in the porous carbonated center of the chimney. The constant flow of

gas through the chimneys may cause a re-flow of seawater into the mat and chimney enabling a sulfate supply to its inner parts. Beside the upwards-directed growth of the chimney, the mat could also continue to grow radial to the outside of the chimney. The distribution of methane and sulfate within the mats and the chimneys remains unknown. The mats are penetrated by a system of microchannels, possibly enabling substrate exchanges (Michaelis et al., 2002).The location of the AOM zone close to the mat periphery, as shown in this study, indicates that the AOM organisms might depend on the supply of sulfate from the surrounding water. More investigations are needed to measure methane and sulfate gradients from the mat surface to the inner core of the chimney.

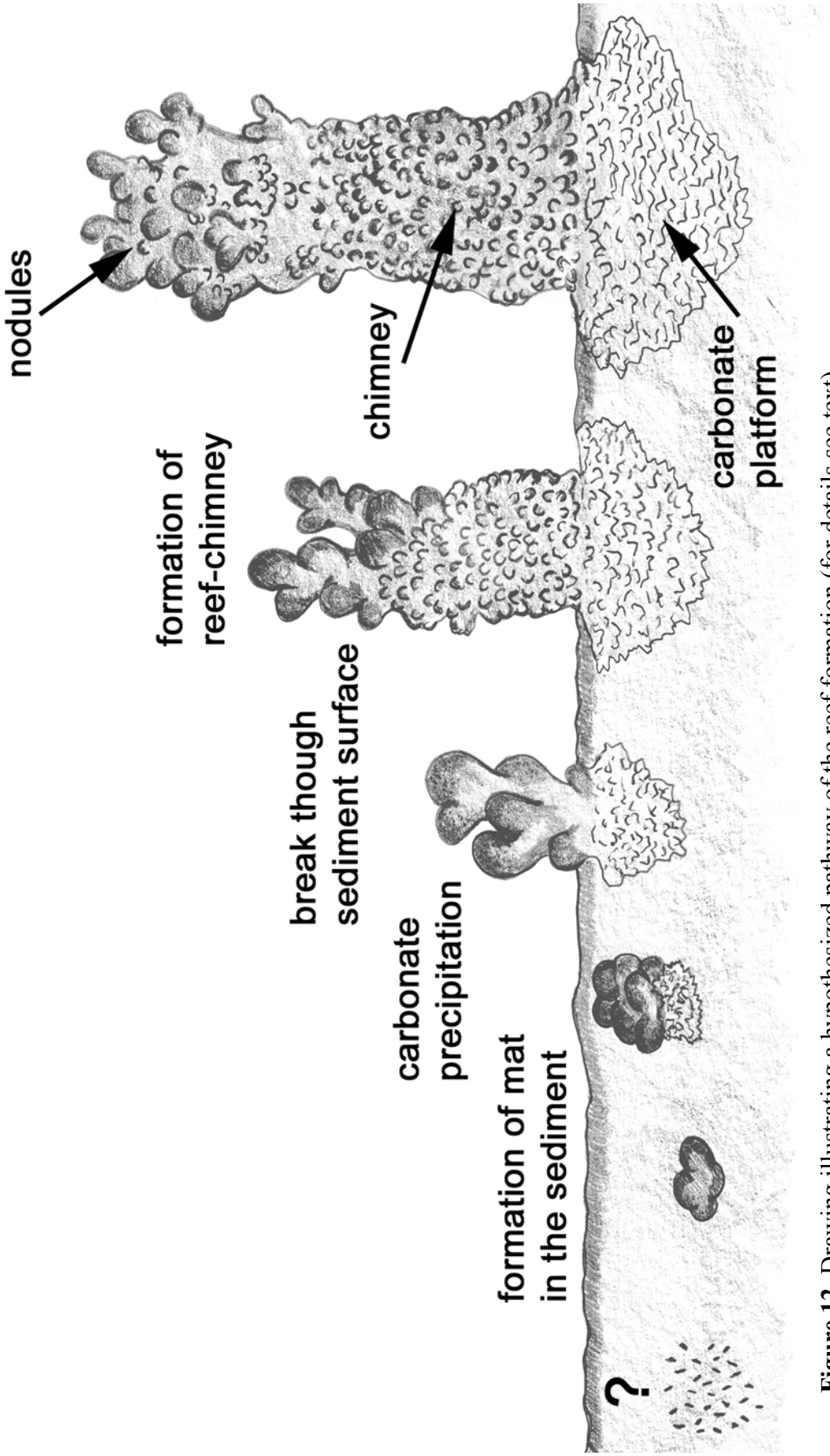

Figure 12. Drawing illustrating a hypothesized pathway of the reef formation (for details see text).

CONCLUSIONS

Several conclusions but also further questions arise from the results of the present study:

1. Anaerobic oxidation of methane (AOM) is the main metabolic process of the microbial reefs above Black Sea methane seeps and is primarily mediated by the archaeal ANME-1 group.
2. The ratio between AOM and sulfate reduction is 1:1 pointing to a close coupling of the two processes.
3. ANME-1 may be able to mediate methanogenesis in the mat. However, it could not be clarified if methanogenesis occurs as an enzymatic re-reaction of AOM or if ANME-1 cells can act as "true" methanogens under specific thermodynamic conditions.
4. Methanotrophy and the bulk biomass of ANME-1 is restricted to a narrow zone of the mat close to the mat-water interface, to facilitate a supply of sulfate as electron acceptor and possibly also other substrates from the surrounding water.
5. A high diversity of sulfate-reducing bacteria was found above and below the AOM zone. Their role in the mat is currently unknown.
6. It could not be determined if methane is directly used as carbon source, however, CO_2 fixation was found to play a major role in carbon assimilation of ANME-1.
7. In vitro conditions in the lab did not support substantial growth rates. Low methane concentrations at atmospheric pressure may be one reason for this.
8. The development of the reef possibly starts with the accumulation of ANME-1 cells in the sediments of methane seeps, forming first nodules, then chimney like structures which grow upward into the bottom water of the Black Sea.

In conclusion, important subjects of further studies on the methanotrophic microbial reefs of the Black Sea should be:

1. the pathway of methanogenesis in the mat,
2. the substrates of carbon assimilation in methanotrophic archaea,
3. the methane and sulfate gradients and fluxes in the mat,
4. the role of non-methanotrophic microbes in the mat, and
5. the understanding of the reef biology as whole, especially its development, dynamics and the time-scales of growth.

ACKNOWLEDGEMENTS

We thank the officers, crew and shipboard scientific party of RV Prof. LOGACHEV and the JAGO team during the Black Sea cruise in summer 2001 for excellent support. We greatly acknowledge Julia Polanski, Tina Lösekann and Tomas Wilkop for technical assistance. We thank Friedrich Widdel and Katja Nauhaus for fruitful discussions about methanogenesis in the mat. Many thanks are due to Walter Michaelis and Richard Seifert for providing the reef pictures. This study was made possible by the programs GHOSTDABS (Gas Hydrates: Occurrence, Stability, Transformation, Dynamic, and Biology in the Black Sea), and MUMM (Mikrobielle Umsatzraten von Methan in gashydrathaltigen Sedimenten, FN 03G0554A) supported by the Bundesministerium für Bildung und Forschung (Germany). Further support came from the Max-Planck-Gesellschaft (Germany).

REFERENCES

Amann, R.I., Binder, B.J., Olson, R.J., Chisholm, S.W., Devereux, R., Stahl, D.A. (1990). Combination of 16S rRNA-targeted oligonucleotide probes with flow cytometry for analyzing mixed microbial populations. Appl. Environ. Microbiol. 56, 1919-1925.

Amann, R.I., Krumholz, L., Stahl, D.A. (1990). Fluorescent-oligonucleotide probing of whole cells for determinative, phylogenetic, environmental studies in microbiology. J. Bacteriol. 172, 762-770.

Barnes, R.O., Goldberg, E.D. (1976). Methane production and consumption in anoxic marine sediments. Geology 4, 297-300.

Boetius, A., Ravenschlag, K., Schubert, C.J., Rickert, D., Widdel, F., Giesecke, A., Amann, R., Jørgensen, B.B., Witte, U., Pfannkuche, O. (2000). A marine microbial consortium apparently mediating anaerobic oxidation of methane. Nature 407, 623-626.

Børsheim, K.Y., Bratbak, G., Heldal, M. (1990). Enumeration and biomass estimation of planktonic bacteria and viruses by transmission electron microscopy. Appl. Environ. Microbiol. 56, 352-356.

Calvert, S.E., Vogel, J.S., Southon, J.R. (1987). Carbon accumulation rates and the origin of the Holocene sapropel in the Black Sea. Geology 151, 918-921.

Daims, H., Brühl, A., Amann, R., Schleifer, K.H. (1999). The domain-specific probe EUB338 is insufficient for the detection of all Bacteria: Development and evaluation of a more comprehensive probe set. Syst. Appl. Microbiol.. 22, 434-444.

Devereux, R., Kane, M.D., Winfrey, J., Stahl, D.A. (1992). Genus- and group specific hybridization probes for determinative and environmental studies of sulfate-reducing bacteria. Syst. Appl. Microbiol. 15, 601-609.

Elvert, M., Greinert, J., Suess, E., Whiticar, M.J. (2001). Carbon isotopes of biomarkers derived from methane-oxidizing microbes at Hydrate Ridge, Cascadia Convergent Margin. Geophysical Monograph 124, 115-129.

Elvert, M., Suess, E., Greinert, J., Whiticar, M.J. (2000). Archaea mediating anaerobic methane oxidation in deep-sea sediments at cold seeps of the eastern Aleutian subduction zone. Org. Geochem. 31, 1175-1187.

Fukui, M., Teske, A., Aßmus, B., Muyzer, G., Widdel, F. (1999). Physiology, phylogenetic relationships, and ecology of filamentous sulfate-reducing bacteria (genus *Desulfonema*). Arch. Microbiol. 172, 193-203.

Hallam, S.J., Girguis, P.R., Preston, C.M., Richardson, P.M., DeLong, E.F. (2003). Identification of methyl coenzym m reductase A (*mcr*A) genes associated with methane-oxidizing archaea. Appl. Environ. Microbiol. 69(9), 5483-5491.

Hayes, J.M. (1994). Global methanotrophy at the Archean-Proterozoic transition. In: S. Bengtson (Eds.), Early life on Earth. Columbia U.P., New York.

Heyer, J. (1990). Der Kreislauf des Methans, Akademie-Verlag Berlin, pp. 250.

Hinrichs, K.-U., Boetius, A. (2002). The anaerobic oxidation of methane: new insights in microbial ecology and biogeochemistry. In: G. Wefer, D. Billett, D. Hebbelnet al (Eds.), Ocean Margin Systems. Springer-Verlag, Berlin, pp. 457-477.

Hinrichs, K.-U., Hayes, J.M., Sylva, S.P., Brewer, P.G., De Long, E.F. (1999). Methane-consuming archaebacteria in marine sediments. Nature 398, 802-805.

Hristova, K.R., Mau, M., Zheng, D., Aminov, R.I., Mackie, R.I., Gaskins, H.R., Raskin, L. (2000). Desulfotomaculum genus- and subgenus-specific 16S rRNA hybridization probes for environmental studies. Environ. Microbiol. 2, 143-159.

Ivanov, M.V., Polikarpov, G.G., Lein, A.Y., al., e. (1991). Biogeochemistry of the carbon cycle in the zone of Black Sea methane seeps. Dokl. Akad. Nauk SSSR 320(1235-1240).

Jørgensen, B.B. (1978). A comparison of methods for the quantification of bacterial sulphate reduction in coastal marine sediments: I. Measurements with radiotracer techniques. Geomicrobiol. J. 1(1), 11-27.

Jørgensen, B.B., Fenchel, T. (1974). The sulfur cycle of a marine sediment model system. Mar. Biol. 24, 189-210.

Kallmeyer, J., Ferdelman, T.G., Weber, A., Fossing, H., Jørgensen, B.B. (submitted). Evaluation of a cold chromium distillation procedure for recovering very small amounts of radiolabelled sulfide related to sulfate reduction. Limnol. Oceanogr.: Methods.

Krüger, M., Meyerdierks, A., Glöckner, F.O., Amann, R., Widdel, F., Kube, M., Reinhard, R., Kahnt, J., Böcher, R., Thauer, R.K., Shima, S. (accepted). A conspicuous nickel protein in microbial mats that oxidise methane anaerobically. Nature.

Lanièce, P., Charon, Y., Cardona, A., Pinot, L., Maitrejean, S., Mastrippolito, R., Sandkamp, B., Valentin, L. (1998). A new high resolution radioimager for quantitative analysis of radiolabelled molecules in tissue section. J. Neurosci. Methods 86, 1-5.

Lein, A.Y., Ivanov, M.V., Pimenov, N.V., Gulin, M.B. (2002). Geochemical characteristics of the carbonate constructions formed during microbial oxidation of methane under anaerobic conditions. Mikrobiologiya 71(1), 89-103.

Lösekann, T. (2002). Molekularbiologische Untersuchungen der Diversität und Struktur mikrobieller Lebensgemeinschaften in methanreichen, marinen Sedimenten (Håkon-Mosby-Schlammvulkan. Diploma thesis, Fachbereich Biologie/Chemie, Universität Bremen, Germany.

Luth, C., Luth, U., Gebruck, V., Thiel, H. (1999). Methane seeps along the oxic/anoxic gradient in the Black Sea: manifestations, biogenic sediment compounds, and preliminary results on benthic ecology. P.S.Z.N. Mar. Ecol. 20, 221-249.

Manz, W., Amann, R., Ludwig, W., Wagner, M., Schleifer, K.-H. (1992). Phylogenetic oligodeoxynucleotide probes for the major subclasses of proteobacteria: problems and solutions. Syst. Appl. Microbiol. 15, 593-600.

Manz, W., Eisenbrecher, M., Neu, T.R., Szewzyk, U. (1998). Abundance and spatial organization of Gram-negative sulfate-reducing bacteria in activated sludge investigated by in situ probing with specific 16S rRNA targeted oligonucleotides. FEMS Microb. Ecol. 25, 43-61.

Michaelis, W., Seifert, R., Nauhaus, K., Treude, T., Thiel, V., Blumenberg, M., Knittel, K., Gieseke, A., Peterknecht, K., Pape, T., Boetius, A., Aman, A., Jørgensen, B.B.,

Widdel, F., Peckmann, J., Pimenov, N.V., Gulin, M. (2002). Microbial reefs in the Black Sea fueled by anaerobic oxidation of methane. Science 297, 1013-1015.

Nauhaus, K. (2003). Mikrobiologische Studien zur anaeroben Oxidation von Methan (AOM). PhD. Thesis, Fachbereich Biologie/Chemie. Univerität Bremen, Germany.

Nauhaus, K., Boetius, A., Krüger, M., Widdel, F. (2002). In vitro demonstration of anaerobic oxidation of methane coupled to sulphate reduction in sediment from marine gas hydrate area. Environ. Microbiol. 4(5), 298-305.

Neef, A. (1997). Anwendung der in situ-Einzelzell-Identifizierung von Bakterien zur Populations-Analyse in komplexen mikrobiellen Biozönosen. PhD. Thesis, Fakultät für Chemie, Biologie und Geowissenschaften. München, Technische Universität München, Germany.

Neef, A., Amann, R., Schlesner, H., Schleifer, K.H. (1998). Monitoring a widespread bacterial group: In situ detection of planctomycetes with 16S rRNA-targeted probes. Microbiology 144, 3257-3266.

Nisbet, E.G., Sleep, N.H. (2001). The habitat and nature of early life. Nature 409, 1083-1091.

Orphan, V.J., Hinrichs, K.-U., Ussler III, W., Paull, C.K., Tayleor, L.T., Sylva, S.P., Hayes, J.M., DeLong, E.F. (2001b). Comparative analysis of methane-oxidizing archaea and sulfate-reducing bacteria in anoxic marine sediments. Appl. Environ. Microbiol. 67(4), 1922-1934.

Orphan, V.J., House, C.H., Hinrichs, K.-U., McKeegan, K.D., De Long, E.F. (2001a). Methane-consuming Archaea revealed by directly coupled isotopic and phylogenetic analysis. Science 293, 484-487.

Pancost, R.D., Sinninghe Damsté, J.S., De Lint, S., Van der Maarel, M.J.E.C., Gottschal, J.C. (2000). Biomarker evidence for widespread anaerobic methane oxidation in mediterranean sediments by a consortium of methanogenic archaea and bacteria. Appl. Environ. Microbiol. 66(3), 1126-1132.

Peckmann, J., Reimer, A., Luth, U., Luth, C., Hansen, B.T., Heincke, C., Hoefs, J., Reitner, J. (2001). Methane-derived carbonates and authigenic pyrite from the northwestern Black Sea. Mar. Geol. 177, 129-150.

Pimenov, N.V., Rusanov, I.I., Poglazova, M.N., Mityushina, L.L., Sorokin, D., Yu., Khmelenina, V.N., Trotsenko, Y.A. (1997). Bacterial mats on coral-like structures at methane seeps in the black Sea. Microbiology 66(3), 354-360.

Raskin, L., Poulsen, L.K., Noguera, D.R., Rittmann, B.E., Stahl, D.A. (1994). Quantification of methanogenic groups in anaerobic biological reactors by oligonucleotide probe hybridization. Appl. Environ. Microbiol. 60(4), 1241-1248.

Ravenschlag, K., Sahm, K., Pernthaler, J., Amann, R. (1999). High bacterial diversity in permanently cold marine sediments. Appl. Environ. Microbiol. 65, 3982-3989.

Sahm, K., Berninger, U.G. (1998). Abundance, vertical distribution, and community structure of benthic prokaryotes from permanently cold marine sediments (Svalbard, Arctic Ocean). Mar. Ecol. Prog. Ser. 165, 71-80.

Sahm, K., Knoblauch, C., Amann, R. (1999). Phylogenetic affiliation and quantification of psychrophilic sulfate-reducing isolates in marine arctic sediments. Appl. Environ. Microbiol. 65, 3976-3981.

Schramm, A., Larsen, L.H., Revsbech, N.P., Ramsing, N.B., Amann, R., Schleifer, K.-H. (1996). Structure and function of a nitrifying biofilm as determined by in situ hybridization and the use of microelectrodes. Appl. Environ. Microbiol. 62, 4641-4647.

Snaidr, J., Amann, R., Huber, I., Ludwig, W., Schleifer, K.H. (1997). Phylogenetic analysis and in situ identification of bacteria in activated sludge. Appl. Environ. Microbiol. 65, 3976-3981.

Stahl, D.A., Flesher, B., Mansfield, H.R., Montgomery, L. (1988). Use of phylogenetically based hybridization probes for studies of ruminal microbial ecology. Appl. Environ. Microbiol. 54, 1079-1084.

Thiel, V., Peckmann, J., Richnow, H.H., Luth, U., Reitner, J., Michaelis, W. (2001). Molecular signals for anaerobic methane oxidation in Black Sea seep carbonates and microbial mat. Mar. Chem. 73, 91-112.

Treude, T., Boetius, A., Knittel, K., Wallmann, K., Jørgensen, B.B. (2003). Anaerobic oxidation of methane above gas hydrates at Hydrate Ridge, NE Pacific. Mar. Ecol. Prog. Ser. 264, 1-14.

Treude, T., Krüger, M., Boetius, A., Jørgensen, B.B. (submitted). Anaerobic oxidation of methane in the gassy sediments of Eckernförde bay (German Baltic). Limnol. Oceanogr.

Valentine, D.L., Reeburgh, W.S. (2000). New perspectives on anaerobic methane oxidation. Environ. Microbiol. 2(5), 477-484.

Visscher, P.T., Reid, R.P., Bebout, B.M., Hoeft, S.E., Macintyre, I.G., Thompson, J.A. (1998). Formation of lithified micritic laminae in modern marine stromatolites (Bahamas): the role of sulfur cycling. Am. Mineral. 83, 1482-1493.

Whiticar, M.J. (1999). Carbon and hydrogen isotope systematics of bacterial formation and oxidation of methane. Chem. Geol. 161, 291-314.

Widdel, F. (1988). Microbiology and ecology of sulfate- and sulfur-reducing bacteria. In: A. D. J. Zehnder (Eds.), Biology of anaerobic microoganisms. John Wiley & Sons, New York, N.Y., pp. 469-585.

Yamamoto, S., Alcauskas, J.B., Crozier, T.E. (1976). Solubility of methane in distilled water and seawater. J. Chem. Eng. Data 21(1), 78-80.

Zehnder, A.J.B. (1988). Biology of anaerobic microorganisms, Wiley, New York, pp. .

Zehnder, A.J.B., Brock, T.D. (1979). Methane formation and methane oxidation by methanogenic bacteria. J. Bacteriol. 137(1), 420-432.

Zheng, D., Alm, E.W., Stahl, D.A., Raskin, L. (1996). Characterization of universal small subunit rRNA hybridization probes for quantitative molecular microbial ecology studies. Appl. Environ. Microbiol. 62, 4314-4317.

Chapter 7

Environmental regulation of anaerobic oxidation of methane mediated by ANME-I- and ANME-II-communities: a comparative analysis

Katja Nauhaus[1], Tina Treude[1], Antje Boetius[1, 2], Martin Krüger[1]

[1] Max Planck Institute for Marine Microbiology, Celsiusstrasse 1, 28359 Bremen, Germany

[2] International University of Bremen, Campusring 1, 28759 Bremen, Germany

This manuscript is a preliminary version and will be prepared for submission to Environmental Microbiology

SUMMARY: Anaerobic oxidation of methane is one of the major sinks for methane on earth and it is known to be mediated by at least two phylogenetically different groups of archaea, ANME-I and ANME-II. We present the first comparative in vitro investigation of the environmental regulation and physiology of two different methane oxidizing communities dominated by ANME-I or ANME-II, both live in association with sulfate-reducing-bacteria (SRB) of the phylogenetic cluster *Desulfosarcina*/*Desulfococcus*. The ANME-II dominated sediments from Hydrate Ridge (HR, Cascadia Margin, off Oregon, USA) were compared to microbial mats from the Black Sea (BS) predominantly consisting of ANME-I. The stoichiometric relation of 1:1 between methane oxidation and sulfate reduction was shown for both samples. Methane dependent sulfate reduction (SR) showed higher cell specific rates for the ANME-II dominated community at similar experimental conditions. Besides the reduction of sulfate, no other electron acceptor was used for the anaerobic oxidation of methane. Only disproportionation of sulfite and thiosulfate was also performed with methane as electron donor by ANME-I and ANME-II communities. The processes of AOM and SR could not be uncoupled by selectively stimulating the SRB with potential intermediates like acetate, formate or molecular hydrogen. Also the effective removal of electrons by AQDS, humics or phenazines did not stimulate the activity of the archaeal partner. The process of AOM was completely inhibited if 2-bromoethanesulfonate (BES) a specific inhibitor for methanogens was added. Molybdate, an inhibitor for SRB lead to a complete inhibition in HR samples but only partially inhibited AOM in BS samples. Antibiotics selectively affecting bacteria had no effect on the overall process of methane dependent sulfate reduction.

A variation of environmental parameters like sulfate concentration, pH and salinity did not significantly influence the activity of the ANME-I and ANME-II communities within rather broad ranges. However, both communities responded to elevated methane partial pressures with increased substrate turnover, indicating the importance of the prevailing methane availability for the activity of the AOM community. Temperature also influences the intensity of methane fuelled SR. The psychrophilic ANME-II community of HR was most active at low temperatures and was negatively affected by temperatures above 16 °C. The ANME-I community in BS samples had a temperature optimum between 10 °C and 24 °C. The ecological niches of ANME-I and ANME-II seem to be mainly defined by the

availability of methane and sulfate, and thus presumably enable AOM performing micro-organisms to thrive in different habitats where those two prerequisites are met.

INTRODUCTION

The anaerobic oxidation of methane (AOM) occurs in marine habitats where fluxes of methane coincide with fluxes of sulfate (Hinrichs & Boetius, 2002). Up to 85% of the methane rising from deeper sediment horizons is oxidized within the upper, anoxic part of the sediment, effectively preventing the release of this important greenhouse gas into the atmosphere (Ehalt, 1974; Iversen, 1996). AOM is therefore an important process in the global methane cycle (Crutzen, 1994; Reeburgh, 1996). However, it remains unknown how the process functions in detail and how the high biomass of AOM communities found in some marine environments is maintained by a process yielding only very little free energy (Boetius *et al*., 2000; Michaelis *et al*., 2002). Molecular studies show that the anaerobically methane oxidizing archaea (ANME) so far identified are more or less closely affiliated with the *Methanosarcinales* (Hinrichs *et al*., 1999; Orphan *et al*., 2002). Both known ANME groups (I and II) are associated with sulfate-reducing-bacteria (SRB) of the *Desulfosarcina*/*Desulfococcus* group (Boetius *et al*., 2000; Michaelis *et al*., 2002; Knittel *et al*., 2003). The nature of the cooperation between the two organisms could so far not be elucidated (Sörensen *et al*., 2001; Nauhaus *et al*., 2002; Valentine, 2002). According to thermodynamic calculations the amount of free energy available from AOM is crucially dependent on the environmental settings, especially on the methane partial pressure (Zehnder & Brock, 1980; Iversen & Blackburn, 1981). So far only few experimental data are available to determine the effect of variable environmental factors, and their influence on the effectiveness of the process (Valentine & Reeburgh, 2000; Nauhaus *et al*., 2002). The availability of sulfate in subsurface sediments could also be a major factor regulating methane fluxes to the sea floor. Global climate changes might lead to increase in water temperature, a factor strongly influencing the stability of gas reservoirs such as methane hydrates and therefore also methane availability at continental margins (Paull *et al*., 1991; Kvenvolden, 1993).

Environmental factors do not only regulate the occurrence and intensity of AOM, they are probably also crucial factors influencing the development of specific AOM communities in different habitats. The phylogenetic diversity at least within the archaeal partner might be an indication for specialized communities in habitats with different environmental conditions.

In the present study we performed laboratory experiments with two samples from different marine environments with phylogenetically different AOM populations. A first set of experiments with sediments from the gas hydrate bearing sediments of Hydrate Ridge (HR; Cascadia margin, USA) dominated by an ANME-II community proved that AOM depends on sulfate as electron acceptor and is influenced by methane availability (Nauhaus *et al*., 2002). These and additional experiments with sediment slurries from HR were compared to experiments with the recently discovered microbial mats building carbonate reefs at gaseous methane seeps in the anoxic waters of the Black Sea (BS) (Michaelis *et al*., 2002). These mats are dominated by ANME-I archaea associated with SRB of the same phylogeny (*Desulfosarcina*/*Desulfococcus* group) as at HR.

With the in vitro experiments we are addressing the questions 1) if ANME-I and ANME-II communities have similar activities and stoichiometries of AOM in vitro, 2) if the phylogenetically different populations (ANME-I and ANME-II) exhibit physiological differences and 3) how environmental factors influence the activity of both anaerobically methane oxidizing communities.

RESULTS AND DISCUSSION

The process of anaerobic oxidation of methane can be mediated by at least two phylogenetic groups of archaea: the ANME-II cluster as well as the ANME-I cluster (Boetius *et al*., 2000; Michaelis *et al*., 2002; Orphan *et al*., 2002). ANME-I and ANME-II communities have now been found in a variety of marine environments, usually associated with the same type of SRB from a branch within the *Desulfosarcina/Desulfococcus* cluster of the Deltaproteobacteria (Orphan *et al*., 2002, Knittel *et al*., 2003; Boetius & Suess, 2003). The first in vitro investigations of the activity and stoichiometry of communities dominated by ANME-II were just recently presented (Nauhaus *et al*., 2002; Girguis *et al*.,

2003). Unexpectedly a whole microbial reef ecosystem formed by ANME-I dominated methanotrophic mats in permanently anoxic waters of the Black Sea was discovered (Michaelis *et al*., 2002). The possibility of a buildup of high biomasses of methanotrophic organisms under anoxic conditions has been debated for many years (Hartgers *et al*., 1994, Nisbet & Sleep, 2001; Hinrichs & Boetius, 2002). We were able to use this living model system for a presumably ancient form of life for the first physiological investigations of an ANME-I community.

Just by visual inspection of the two AOM communities studied, derived from the surface sediments above gas hydrate impacted by fluid flow at Hydrate Ridge (Cascadia Margin, OR) and the microbial reefs from the anoxic part of the Crimea margin (Black Sea), a variety of differences become obvious. In HR sediments, the ANME-II/DSS consortia occur in high abundance as small aggregates of a few hundred cells dispersed within the sediment. The highest abundance is found in a zone of one to four centimeters directly below the seafloor, characterized by high methane fluxes from below. In this zone above gas hydrates, some of the highest densities of sulfate reducers and highest rates of AOM and SR known from marine environments have been found (Boetius *et al*., 2000; Boetius & Suess, 2003; Treude *et al*., 2003). Due to the high fluxes methane is available in excess in both environments (Michaelis *et al*., 2002; Boetius & Suess, 2003) However, at high rates of AOM sulfate becomes rapidly depleted within sediments because of the comparatively slow diffusive flux (Luff & Wallmann, 2003). Wherever sulfate is mixed into the sediments e.g. through the dwelling activity of the chemosynthetic clams, numbers of consortia and rates of AOM increase over a broader area and are not restricted to sediments below mats of the giant sulfide oxidizing bacteria *Beggiatoa*. The permanently anoxic bottom waters of the Black Sea do not provide conditions appropriate for metazoan life requiring oxygen. But the anaerobic microbial mats are enabled to expand into the water column and profit from advective sulfate flux due to bottom water currents. Increase in HCO_3^- and HS^- concentrations due to AOM activity and the resulting increase in alkalinity supports carbonate precipitation. The anoxic conditions in the Black Sea allow carbonate precipitates associated with microbial mats to build structures of up to 4 m high into the water column with a diameter of up to 1 m (Michaelis *et al*., 2002). The in vitro experiments were carried out to test potential physiological differences between ANME-II and ANME-I

communities, as well as to further analyze which environmental parameters are significantly influencing AOM activity.

Does in vitro AOM differ between ANME-I and ANME-II communities?

Strictly anoxic incubations of homogenized microbial mat dominated by ANME-I cells showed continuous sulfide production in the presence of methane and sulfate. In controls incubated with nitrogen instead of methane, significantly less sulfide production occurred. An increase in sulfide concentration from <1 mM at the beginning of an experiment to about 12 mM took on average 60 days with 0.2 ml of fresh material of the ANME-I mat from the BS under methane saturation (ca. 1.3 mM at 1 atm). Previous experiments with ANME-II dominated samples from HR showed the same results regarding the time course of the experiment (Nauhaus *et al*., 2002).

Methane dependent sulfate reduction in the BS mats were on average 41 ± 16 (n = 38) µmol d^{-1} g_{dw}^{-1}, ranging from 15 to 81 µmol d^{-1} g_{dw}^{-1}. Sediment slurries from HR sediments revealed an SR of 2.5 ± 0.3 µmol d^{-1} g_{dw}^{-1}. To compare the environmental activity in both incubations, rates were calculated per gram dry weight of sediment (HR) or mat (BS). However, for a comparison on the basis of specific cell activity, this is misleading because the biomass density in the HR sediment slurries is much lower then in the mats which are mainly composed of cells. The investigated sediment horizon (1 – 4 cm) of the HR samples contained on average 9×10^7 consortia per gram dry weight of sediment. An average consortium consists of approx. 100 archaeal cells of the ANME-II group and 200 SRB cells, with a diameter of about 0.5 µm (Boetius *et al*., 2000). Comparing methane driven sulfate reduction per SRB cell revealed that HR samples (20 mmol d^{-1} g [cell dry mass]$^{-1}$) are almost ten times more active than SRB in BS mat samples (1 mmol d^{-1} g [cell dry mass]$^{-1}$). It is however so far not known if all the cells in the consortium and in the mat are equally active. Cells that have no direct contact with the other partner might not be active or to a lesser extend than cells with direct contact. Due to the low energy yield of the process and the presumably low concentration of the intermediate, the diffusive loss even over a small distance of a few µm is significant (Boone *et al*., 1989). Therefore, many cells

are probably not within the narrow optimal concentration range required for sufficient energy conservation (Sörensen *et al.*, 2001).

The in situ hydrostatic pressures at the investigated sites (70 bar at HR and 20 bar at BS) in general would not lead to physiological effects in microbes. However, these hydrostatic pressures considerably affect the in situ availability of methane. At atmospheric pressure only approx. 1.3 mM methane are dissolved, depending on temperature and salinity (Yamamoto *et al*., 1967). Dissolution of the gas increases linearly with pressure. Free gas ebullition was observed both at the microbial reefs of the Black Sea and at Hydrate Ridge. This indicates methane saturation at these sites with theoretical concentra-tions of 2.3 MPa (40 mM) and 7.9 MPa (138 mM) for BS and HR, respectively. Increasing the methane partial pressure in vitro from 0.1 MPa to 1.1 MPa (15 mM) increased the methane driven sulfate reduction rate five fold in HR (Nauhaus *et al*., 2002) and two fold in BS samples. Simultaneous measurements of methane oxidation and sulfide production from the reduction of sulfate revealed a molar ratio of 1:1 between the two processes (methane oxidation and sulfate reduction) for both communities (for HR samples published in Nauhaus *et al*., 2002).

Are there different electron donors for AOM and SR of ANME-I and ANME-II communities?

Whereas methane clearly fuels the activity of ANME-I and ANME-II communities, higher alkanes, ethane, propane and butane were not oxidized coupled to sulfate reduction. In contrast, the addition of these compounds in concentrations >10 mM resulted in an inhibition of AOM of both ANME-I and ANME-II communities (data not shown). In Nauhaus *et al*. (2002) we have shown that the addition of a number of different exogenous electron donors other than methane (acetate, formate, molecular hydrogen and methanol) did not stimulate sulfate reduction in the absence of methane in HR sediment slurries. These data were obtained within a one week incubation to minimize the enrichment of SRB on the added compounds. In additional experiments we could also show that neither carbon monoxide nor methylamines have stimulating effects on SR compared to methane alone (Fig. 1). The same experiments were performed with the ANME-I dominated BS mats

using acetate, formate and molecular hydrogen as electron donors. While the rates with acetate were as low as in the control experiment without any electron donor, sulfide production was in the same range as with methane with formate and molecular hydrogen (Fig. 1). In our simultaneously performed isolation attempts with the BS mats, we observed enrichments of different SRB with hydrogen and formate within weeks. None of these isolates however belonged to the *Desulfosarcina/Desulfococcus* group associated with ANME-I. If the SRB partner relies on the substrate supplied by the methanogen operating in reverse, it should immediately respond with higher sulfate reducing activity than with methane as an indirect electron donor, if this substance is supplied in high, but non-inhibitory concentrations. Even though sulfate reduction rates were not in all cases significantly lower then with methane as electron donor, they never exceeded methane fuelled sulfate reduction. Even though the experiments with the potential intermediates were only performed for one week, it is most likely that the observed high sulfate reduction rates are due to the enrichment of other SRB.

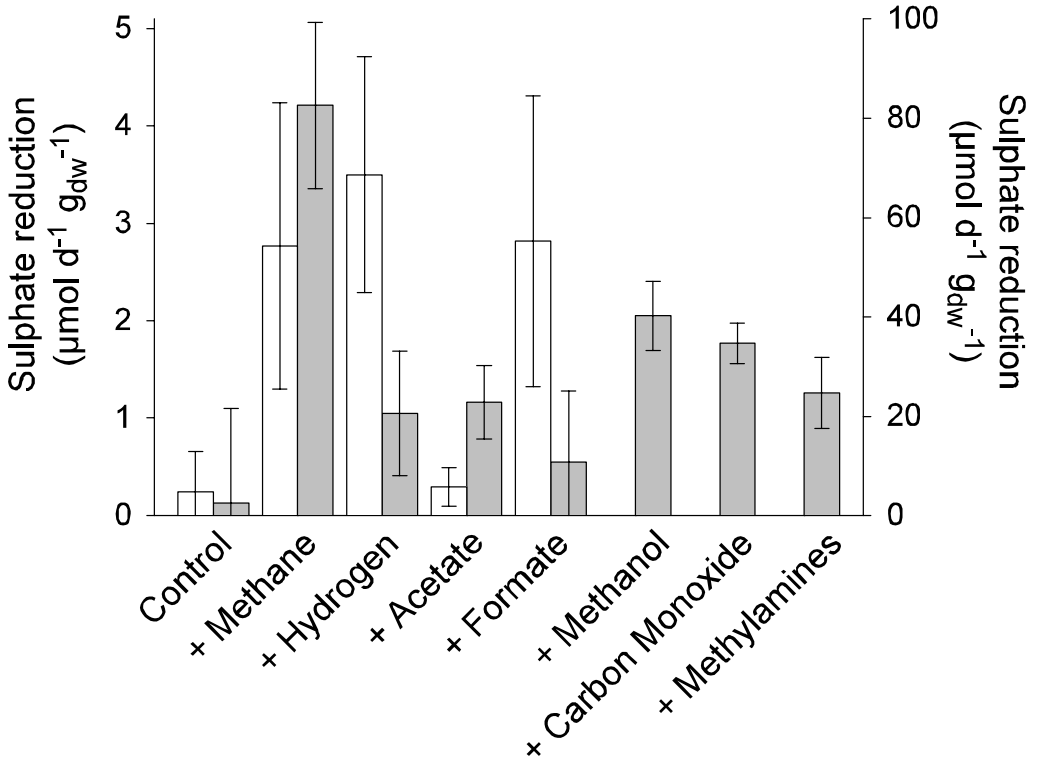

Figure 1. Effect of different possible intermediates of AOM (molecular hydrogen, acetate, formate, methanol[*1], carbon monoxide[*1], methylamines[*1]) on sulfate reduction rates in HR[*2] (■) and BS (□) samples, in comparison to sulfate reduction with methane and in controls without electron donor. Mean values ± s.d. (n = 3) are given. Note the different y-axes for HR (0-5 µmol d^{-1} g_{dw}^{-1}) and BS (0-100 µmol d^{-1} g_{dw}^{-1}).

[*1] not determined for BS samples

[*2] partially shown in Nauhaus et al. (2002)

Also the possibility of electrons being transferred directly between the archaeal and the SRB partner alternate to the exchange of a C-compound has been discussed for the AOM consortia (Sørensen *et al*., 2001; Nauhaus *et al*., 2002). Syntrophy based on electron transfer has previously been reported for other anaerobic reactions (Seeliger *et al.*, 1998; Spormann & Widdel, 2000; Schink & Stams, 2001). To test this possibility, compounds that are able to capture electrons (phenazines, AQDS and humic acids) were added to incubations with sediment slurries from Hydrate Ridge at atmospheric methane partial pressure. If the process of AOM would depend on a transfer of electrons to the SRB partner, the added compounds would replace the function of the SRB. In this case AOM should not be affected, however, methane driven sulfate reduction should decline. We used

radiolabeled methane in tracer quantities and determined the production of radiolabeled CO_2. However, with each of the added compounds the oxidation of methane to CO_2 as well as the reduction of sulfate was completely halted (Table 1). Phenazines play an important role in membrane bound electron transport, but they might also have toxic effects (Abken *et al*., 1998; Ingram & Blackwood, 1970). Even though Straub & Schink (2003) showed that AQDS may serve as electron shuttle for iron reducing bacteria, the redox conditions in the incubations might change upon the addition of AQDS or humics making AOM impossible to occur (Hernandez & Newman 2001; Shuy *et al*., 2002). In summary, our experiments did not provide evidence for a methanogenic substrate acting as an intermediate in the reverse process, or for electrons being transferred between the two partners. These results together with the observation that archaeal cells of the ANME-I cluster (rarely of the ANME-II cluster) occur as single cells or as aggregations in AOM environments (Orphan *et al*., 2002; Knittel, pers. comm.) suggests the possibility of both processes being carried out by one organism. Recently methyl-coenzyme M reductase, the terminal enzyme in methanogenesis and the methanogen specific cofactor F_{430} have been detected in the microbial mats from the Black Sea (Krüger *et al*., accepted). Furthermore Hallam *et al*. (2003) found gene sequences of the *mcrA* subunit of the same enzyme in sediments with AOM activity which they assign to the ANME-II group. Because of these evidences and the fact, that the sulfate-reducing archaeon *Archaeoglobus fulgidus* possesses genes and enzymes for methanogenesis (Klenk *et al*., 1997) it seems possible that the ANME groups comprise the genes for both pathways.

Table 1. Effect of different electron capture compounds on AOM activity in the presence or absence of sulphate (n = 3 – 5) (HR sediment).

Compound added	Reduction of the compound chemical analysis	Methane oxidation (without sulfate) Oxidation of ^{14}C-CH_4 to CO_2	Methane oxidation (with sulfate) Oxidation of ^{14}C-CH_4 to CO_2
AQDS[1]	Yes	No	No
AQDS[1] with Fe[2]	Yes	No	No
Humic acids	n. d.[4]	No	No
Phenazine-methosulphate	n. d.[4]	No	No
Phenazine-ethosulphate	n. d.[4]	No	No
only methane (control)	-	No	Yes

[1] AQDS: Anthroquinone-disulfonate; [2] Fe^0 added as possible electron sink to reoxidise AQDS, if the SRB are not able to take electrons from AQDS

[4] n. d.: not determined

Is sulphate the only electron acceptor for methane oxidation?

Nitrate, sulfur, ferric iron, iron citrate and manganese (IV) oxide were added to anoxic, sulfate free incubations of replicate HR sediment slurries containing an ANME-II community. The indigenous microbial populations reduced all of the added compounds. However, the reduction was in no case coupled to the oxidation of methane as was shown by measuring the formation of $^{14}CO_2$ from the oxidation of radio labeled methane (Table 2). HR samples as well as the microbial mats from the Black Sea were able to oxidize methane with sulfate concentrations form 10 to 100 mM (data not shown). Without sulfate, no AOM activity could be observed, showing once more the dependency on both the electron donor methane and the electron acceptor sulfate. Because methane dependent sulphate reduction rates were not significantly lower with 10 then with 28 mM, sulfate or more the minimum concentration required to drive AOM is somewhere between 10 mM

and 0 mM sulfate. Interestingly, both samples (HR and BS) revealed the ability to disproportionate thiosulfate or sulfite with methane as the only electron donor. Rates were calculated from the amount of sulfide produced within 100 days of incubation, during which sulfite and thiosulfate were added in small amounts several times to prevent toxicity. Sulfide production with sulfite was highest in both samples (HR = 1.96, BS = 81.63 μmol d^{-1} g_{dw}^{-1}, n = 3), even higher than with methane and sulfate (HR = 0.97, BS = 47.29 μmol d^{-1} g_{dw}^{-1}), this is probably due to the higher yield of free energy from this process. Sulfide production from thiosulfate was in a similar range as with sulfate (HR = 1.01, BS = 36.81 μmol d^{-1} g_{dw}^{-1}). However, dilutions to enrich the organisms under disproportionation conditions lead to a complete loss of activity. This is probably due to the presumed inability of marine bacteria to couple disproportionation to energy conservation, nevertheless disproportionation is usually not an unimportant process in marine environments (Jørgensen & Bak, 1991). In conclusion, no oxidation of methane could be observed in the presence of any other electron acceptor if sulfate was absent. However, the ability of both the ANME-I and the ANME-II communities to oxidize methane by a disproportionation of sulfite and thiosulfate is a very important result with regard to the origin of anaerobic methane oxidation. The geological time at which the oxidation of the oceans on early Earth began is strongly debated, especially with regard to the concentrations of sulfate in seawater (Habicht *et al*., 2002). Knowing the regulation of methane oxidation by sulfate availability is critical to understanding the early cycling of methane on Earth.

Table 2 Reduction of different electron acceptors in HR sediment and their coupling to AOM (n = 3).

Compound added	Reduction of the electron acceptor	Simultaneous oxidation of methane
	measurement of the concentration of reduced compound	measurement of the oxidation of $^{14}CH_4$ to $^{14}CO_2$
Nitrate	Yes	No
Mn^{4+} (MnO_2)	Yes	No
Fe^{3+} (ferrihydrite)	Yes	No
Fe^{3+} (ferric-citrate)	Yes	No
Sulphur	n. d.[1]	No
Fe^0	n. d.[1]	No
Fumarate	Yes	No
Sulphate (as control)	Yes	Yes

[1] n. d.: not determined

Which environmental parameters are controlling AOM?

The process of anaerobic oxidation of methane is effective in preventing emission of the green house gas methane to the atmosphere. There are indications that the intensity of the process is correlated with certain environmental parameters, mainly methane and sulfate fluxes and the availability of other hydrocarbons (Joye *et al*., accepted; Treude *et al*., 2003). Methane partial pressure is influenced by the methane flux from subsurface reservoirs which is influenced by temperature and hydrostatic pressure (Paull *et al*., 1991; Kvenvolden, 1993). To estimate the effect of climate changes and consequential temperature shifts on the activity of the "methane biofilter" provided by AOM, it is essential to know the responses of the organisms towards these and other environmental parameters.

Even though the respective in situ temperatures differ only by 4 °C (Tab. 3), the HR community has a psychrophilic temperature profile whereas the BS samples are mesophilic, with highest methane driven sulfate reduction activity between 16 and 24 °C (Fig. 2). Since the rates at 12 °C (the optimum for HR) were considerably high also in the ANME-I community, all incubations with both samples (HR and BS) were performed at 12 °C, to keep the experiments standardized. Small temperature differences in situ may have a selective effect on the type of AOM community that establishes in a certain habitat.

Samples from both study sites were incubated at different salinities ranging from 0 to 63‰. Similar SRR for both ANME communities were achieved with 22 and 33‰, showing the adaptation of the organisms to the marine environment, but no advantage of either population under their in situ conditions (Fig. 3A, B). With respect to the effect of pH changes, ANME-II from HR sediments had a distinct maximum of sulfate reduction rates at pH 7.4 (0.75 µmol d^{-1} g_{dw}^{-1}) but decreased below pH 6.9 and above pH 8 to 0.53 µmol d^{-1} g_{dw}^{-1} (Fig. 3C, D). The pH tolerance was broader for the samples from the BS ranging from pH 6.8 to 8.1 (higher values not tested).

Table 3 In situ values of environmental parameters at HR and at the methane seeps in the BS.

Parameter	Hydrate Ridge	Black Sea
Pressure [bar]	801	231
Temperature [°C]	42	82
Salinity [‰]	333	223
pH	8.25	8.52
Sulphate [mM]	284	173

[1] calculated; [2] shipboard measurements; [3] laboratory measurements; [4] Linke & Suess (2000)

A strong effect on methane driven sulfate reduction was obtained by varying the methane partial pressure. Significantly higher sulfate reduction rates were observed when the methane partial pressure was raised from 0.1 to 1.1 MPa. The HR samples responded

with a 4 to 5 fold increase (Nauhaus *et al*. 2002), whereas sulfate reduction in BS mats only doubled from 54 to 107 µmol d^{-1} g_{dw}^{-1}. Because of technical limitations we could not determine methane saturation values and conduct kinetic calculations of methane turnover for AOM (for a detailed discussion of this aspect see Nauhaus *et al*., 2002).

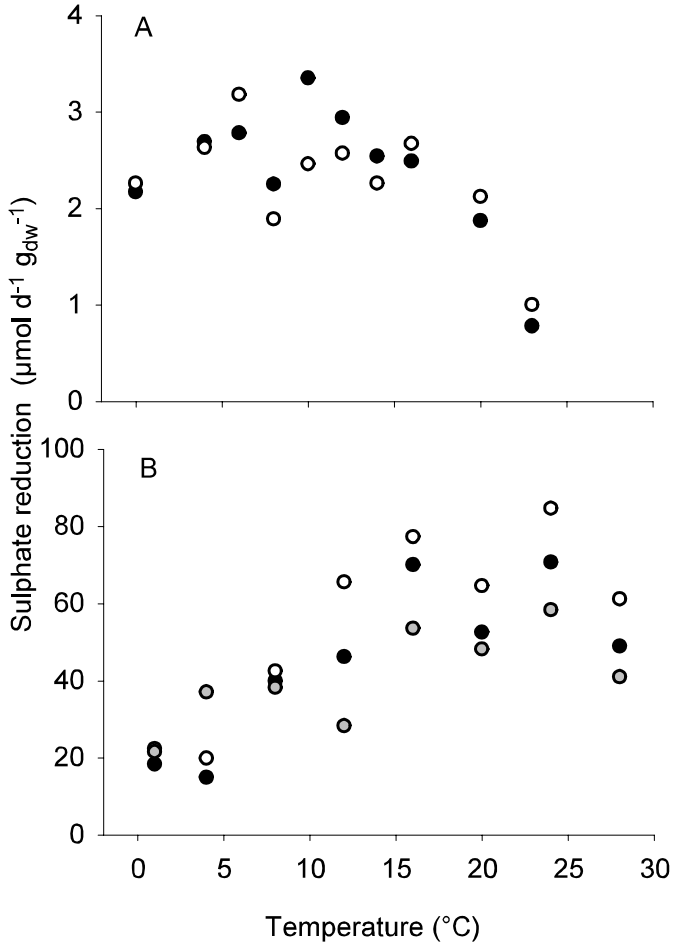

Figure 2. Methane dependent sulfate reduction (µmol d^{-1} g_{dw}^{-1}) at different temperatures in HR samples (A), 2 replicates, and BS mats (B), 3 replicates.

Are there physiological differences in response to specific inhibition of AOM/SR and the SRB partner by ANME-I, ANME-II populations?

If the oxidation of methane with sulfate is not carried out in one step but in subsequent reactions, it should theoretically be possible to uncouple methane oxidation from sulfate reduction by using specific inhibitors for the two processes. If these reactions are not

carried out by one cell, but are separated between the two partners, archaea and bacteria, it might also be possible to study AOM and SR after inhibition of either partner.

Na-molybdate a specific inhibitor for sulfate reduction and 2-bromoethane-sulphonate (BES) an inhibitor for methanogenesis were added to triplicate incubations with sulfate and methane. With BES, methane driven sulfate reduction of both ANME-I and ANME-II communities was completely inhibited. Molybdate also inhibited ANME-II in HR samples completely, whereas in BS samples the methane driven SR decreased to less than half the rate as in incubations without molybdate (Fig. 4A). Hydrogen concentrations increased in both samples with BES and without inhibitors to approx. 100 ppmv within the first 8 days of the incubation. Between day 9 and 11 it dropped below the detection limit (<5 ppmv) and stayed that low. The hydrogen is most probably consumed by developing hydrogen utilizing SRB. Only in incubations with molybdate, hydrogen was not consumed and reached concentrations of more than 800 ppmv. HPLC and IC analysis of supernatants of incubations with and without inhibitors did not reveal an accumulation of any other substances possibly involved as intermediate in the process of AOM.

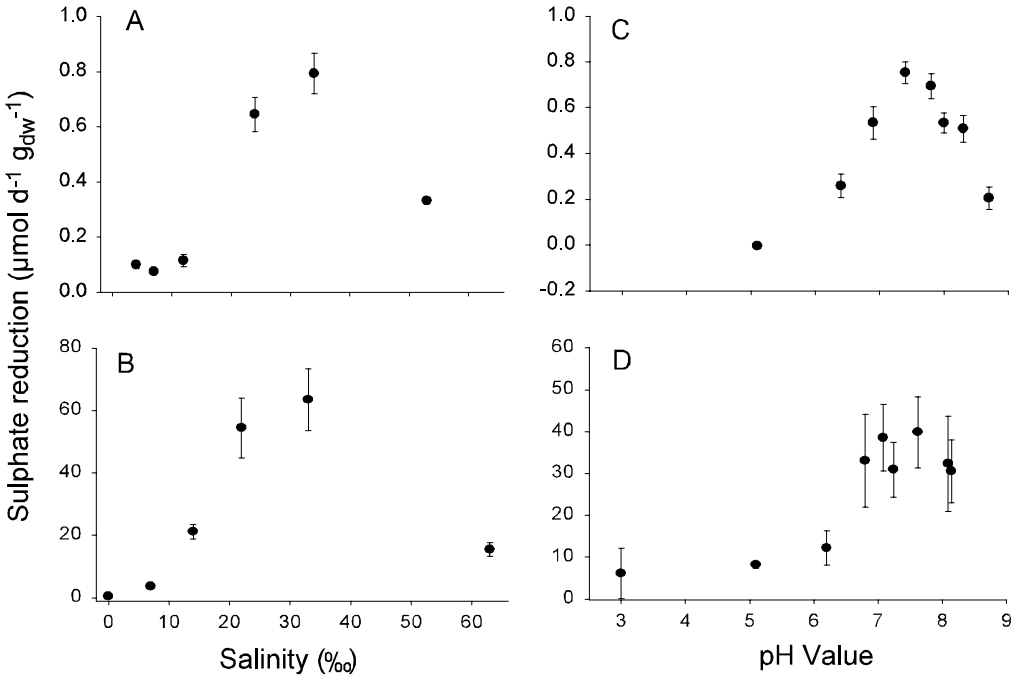

Figure 3. Methane dependent sulfate reduction (µmol d^{-1} g_{dw}^{-1}) at different salinities (A, B) and different pH values (C, D) for HR (A, C) and BS (B, D) samples, mean values ± s.d. (n = 3).

Inhibition studies have to be interpreted carefully, since there are often uncertainties regarding necessary concentrations and the resulting specificity. The inhibition of each process separately by a specific inhibitor (BES for methanogens and molybdate for SRB) completely stopped AOM. This is however, no proof for syntrophy or symbiotic association between the two partners. A complete inhibition would also be observed if both, methane oxidation and sulfate reduction, are occurring within one organism. BES is a structural analogue to coenzyme M, consequently a specific inhibitor of methanogens (Oremland & Capone, 1988). However, it is halogenated and thus chemically reactive, and the application of higher concentrations will probably lead to unspecific inhibitions of other processes. The complete inhibition of AOM by BES at concentrations of >1 mM indicates the biochemical relatedness of methanogenesis and anaerobic oxidation of methane, thus strengthening the reversal of methanogenesis as proposed earlier (Hoehler *et al.*, 1994). Indeed, in a recent study with the BS samples first biochemical evidence for this hypothesis was found (Krüger *et al.*, accepted).

Molybdate on the other hand inhibits the activation of sulfate to APS in sulfate reduction. Hydrogen utilizing SRB were effectively inhibited, this is evident from the accumulation of hydrogen only in those experiments with molybdate. However, molybdate might have side effects on a variety of organisms and processes especially when applied in marine environments (Oremland & Capone, 1988). The incomplete inhibition of the ANME-I community of the BS samples by molybdate might be explained by adsorption of molybdate onto the EPS-material, in which the mat-microorganisms are embedded, thus preventing the build-up of inhibitory concentrations. The SRB in the AOM mediating syntrophy seem to be different from conventional hydrogen utilizing SRB, because those were effectively inhibited by molybdate as shown by the lack of hydrogen consumption in molybdate amended incubations.

The antibiotics kanamycin and ampicillin act specifically against bacteria and consequently should not affect archaea (Dawson *et al*., 1986). The methane driven sulfate reduction by ANME-I and ANME-II communities, however, was not affected by these antibiotics (Fig. 4B). The proper function of these antibiotics against SRB was confirmed by incubating both samples (HR and BS) with molecular hydrogen and carbon dioxide but without sulfate. In the presence of antibiotics, methanogens were enriched, whereas without

antibiotics SRB growing as acetogens appeared. However, these antibiotics, as most of them, do only affect growing cells. The AOM mediating organisms are presumed to grow very slowly, therefore their catabolism is most probably not halted by antibiotics.

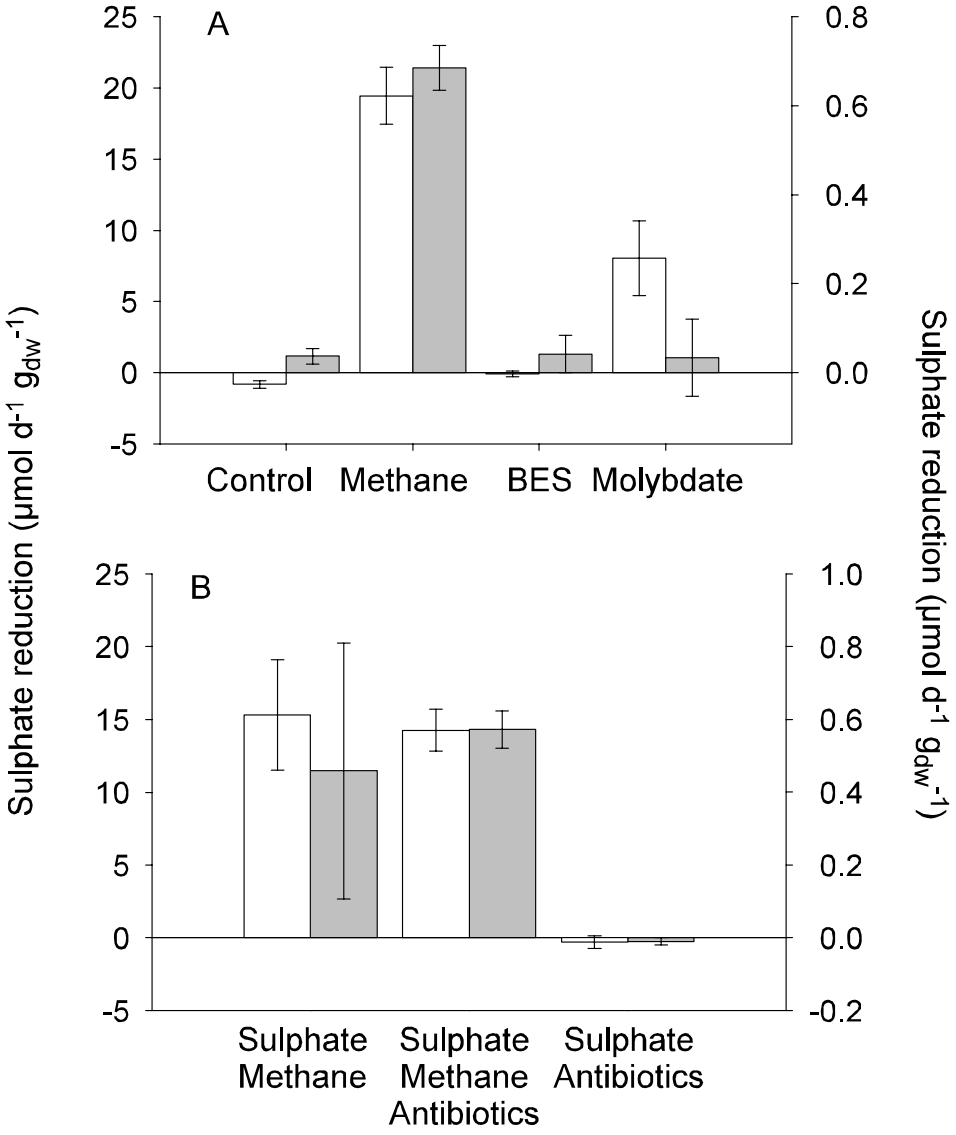

Figure 4. Effect of specific inhibitors, 2-bromoethanesulfonate (BES) and molybdate (A) and the antibiotics knamycin and ampicillin (B) on methane dependent sulfate reduction (µmol d^{-1} g_{dw}^{-1}) in HR (■) and BS (□) samples (mean values ± sd, n = 3).

Environmental regulation of AOM

Can we hypothesize that ANME-I communities occupy a different ecological niche than ANME-II communities? The range of data sets available today (Hinrichs & Boetius, 2002; Michaelis *et al*., 2002; Orphan *et al*., 2002; Teske *et al*., 2002, Boetius & Suess, 2003; Knittel *et al*., 2003, Treude *et al*., 2003) suggests that the co-occurrence of methane and sulfate is the major environmental factor defining the ecological niche occupied by anaerobic methane oxidizing communities. Within this niche we still do not know which factors select for which type of communities. We could not find a clear relation between phylogenetic affiliation and specific environmental parameters like temperature, pressure and methane concentration. Overmann & van Gemerden (2000) discussed the same aspect for phototrophic consortia. These organisms occupy a distinct niche with low light intensities and low sulfide concentrations (Overmann *et al*., 1998) but exhibit a variety of morphotypes in geographically different habitats also with different phylogenetic affiliations at least of the phototrophic partner. Also for other closely related organisms in one habitat distinct ecological niches were observed or postulated (Moore *et al*., 1990; Rowan & Knowlton, 1995). So far, we do not know of any environment where only one of the two known anaerobic methane oxidizers occurs. However, quantitative analyses of the community composition clearly show a dominance of either one or the other group, indicating yet unknown environmental selection pressures.

METHODOLOGY

Origin and storage of samples. Sediment samples were taken during RV SONNE cruise SO-148/1 in August 2000 at the crest of the southern Hydrate Ridge, NE Pacific (44°34' N, 125°09' W; 780 m water depth) in areas of active gas seeping using a video-guided multiple corer (Linke & Suess, 2000; Treude *et al*., 2003). For the experiments, the most active samples from 1-4 cm sediment depth were used. The sediment samples were stored anoxically in glass bottles at 5 °C until further processing in the laboratory.
Microbial mats were obtained during RV Prof. LOGACHEV cruise in July 2001 in anoxic waters of the NW Black Sea shelf (44°46´N, 31°60´E), in a water depth of 230 m

(Michaelis *et al*., 2002). Mat pieces were taken with the robot arm of the German submersible JAGO and placed into a barrel filled with anoxic in situ water, which was then closed and transported to the surface. On board the samples were transferred into glass bottles, sealed with butyl-rubber stoppers and stored at 8 °C under an atmosphere of methane or nitrogen until further processing.

Anoxic incubations. If not stated otherwise experiments were carried out in glass tubes (20 ml) sealed with butyl-rubber stoppers and screw caps. For HR 3 ml of sediment slurry with 9 ml artificial seawater medium (Widdel & Bak, 1992) were used as described in Nauhaus *et al*. (2002). To obtain homogeneous samples of microbial mat from the Black Sea, pieces of mat material were whisked in a bowl using a small fork, yielding a granular suspension. Aliquots of 0.2 ml mat suspension were taken in 2 ml cut-off syringes and incubated in 12 ml artificial seawater medium prepared after Widdel & Bak (1992). Salinity and sulfate concentrations were adjusted to the respective in situ conditions 33‰ and 28 mM for HR samples, and 22‰ and 16 mM for BS samples. All manipulations were performed under an atmosphere of N_2/CO_2 (90/10 [v/v]) in an anoxic glove chamber (Mecaplex). The headspace of the incubation tubes consisted either of methane (100%) or of nitrogen/carbon dioxide (90/10 [v/v]) in control experiments. Triplicate tubes were incubated horizontally at 12 °C and gently shaken once per day to facilitate mixing of methane and sulfate.

Samples for chemical analysis were withdrawn with hypodermic needles and plastic syringes pre-flushed with N_2 through the butyl rubber stoppers.

In experiments for the simultaneous measurements of sulfide and methane to determine the AOM stoichiometry only 70% of the gas phase contained methane, the remaining 30% were N_2/CO_2 (90/10 [v/v]) or He (100%).

Dry weight of sediment and mat was determined after drying at 70 °C for 48 h. Sulfate reduction rates were calculated per gram dry weight (g_{dw}) of sediment or mat material for HR and BS samples, respectively.

Manipulations for experiments. As potential intermediates we added the following final concentrations: acetate (10 mM), formate (15 mM), methanol (10 mM), methylamines (10 mM), molecular hydrogen, carbon monoxide and methane (each 0.1 MPa (1 atm) in the headspace). Phenazine – methosulfate and - ethosulfate, (0.2 mM each), AQDS

(1 – 5 mM), humic acids (commercially available mixture of soil humics, Sigma Aldrich; 10 mg/12 ml) were added as electron capture substances. As alternative electron acceptors sulfur (approx. 50 mg/12 ml), ferrihydrate (7.1 mM; preparation after Schwertmann & Cornell, 1991, modified after Jäckel, 1997), nitrate (5 mM), Fe-citrate (30 mM), fumarate (10 mM) and manganese oxide (5 mM) were used. Only ferrihydrate was added already during the medium preparation. For disproportionation experiments thiosulfate (5 mM) and sulfite (1 mM, subsequent additions during the incubation) were supplied. For all experiments on alternative electron acceptors sulfate-free medium was used. The effect of antibiotics was tested with ampicillin and kanamycin (300 mg/l each). Specific inhibitors for sulfate-reducing bacteria, Na-molybdate (100 mM) and for methanogens, 2-bromoethanesulphonate (1 mM) were added. All substances added were taken from anoxic sterile stock solutions and added after autoclaving the medium.

To obtain different pH values, increasing amounts of sterile HCl or $NaHCO_3$ were added to 50 ml aliquots of medium. The pH determination took place after flushing an additional tube with methane, to account for the pH change due to CO_2 loss. As controls, samples were incubated without methane in all experiments unless indicated otherwise.

Analytical procedures. Sulfide as the product of the methane dependent sulfate reduction was determined using the formation of copper sulfide (Cord-Ruwisch, 1985) or the methylene blue assay (Aeckersberg *et al*., 1991). Methane was determined using a GC 14B gas chromatograph (Shimadzu) as described in Nauhaus *et al*., (2002). Additionally, rates of AOM in some experiments (methane oxidation with alternative electron acceptors and addition of electron capture substances) were also determined via the conversion of $^{14}CH_4$ to $^{14}CO_2$ as described in Treude *et al.*, 2003; Iversen & Blackburn, 1981). The formation of Fe^{2+}, Mn^{2+}, and the disappearance of nitrate were followed using commercially available test stripes (Merck, Darmstadt, Germany). The pH was measured using a pH-electrode (Type 464, Knick, Berlin, Germany). Salinity was determined using a refractometer.Molecular hydrogen measurements were performed using a GC equipped with a reductive gas analyzer as described in Hoehler *et al*. (1998). HPLC analysis of supernatants for short chain fatty acids was carried as described in Rabus *et al*. (1996).

ACKNOWLEDGEMENTS

We thank the officers, crew and shipboard scientific party of RV SONNE during expedition SO-148/1 and of RV Prof. LOGACHEV and the JAGO team during the Black Sea cruise in summer 2001 for excellent support. We greatly acknowledge Ramona Appel, Imke Müller, Niko Finke and Melanie Albrecht for technical assistance. We thank Friedrich Widdel for support and fruitful discussions throughout the work and preparation of the manuscript. This study was made possible by the programs TECFLUX II (Tectonically induced Fluxes, FN 03G0148A), GHOSTDABS (Gas Hydrates: Occurrence, Stability, Transformation, Dynamic, and Biology in the Black Sea), and MUMM (Mikrobielle Umsatzraten von Methan in gashydrathaltigen Sedimenten, FN 03G0554A) supported by the Bundesministerium für Bildung und Forschung (Germany). Further support came from the Max-Planck-Gesellschaft (Germany). This is publication GEOTECH-# of the program GEOTECHNOLOGIEN of the BMBF and the DFG, and publication # of the GHOSTDABS project of the University of Hamburg, Germany.

REFERENCES

Abken, H.-J.; Tietze, M.; Brodersen, J.; Bäumer, S.; Beifuss, U.; Deppenmeier, U. (1998) Isolation and characterization of methanophenazine and function of phenazines in membrane-bound electron transport of *Methanosarcina mazei* Gö1. *Journal of Bacteriologl* **180:** 2027-2032.

Aeckersberg, F.; Bak, F.; Widdel, F. (1991) Anaerobic oxidation of saturated hydrocarbons to CO_2 by a new type of sulfate-reducing bacterium. *Archives of Microbiology* **156:** 5-14.

Boetius, A.; Ravenschlag, K.; Schubert, C. J.; Rickert, D.; Widdel, F.; Gieseke, A. *et al*. (2000) A marine microbial consortium apparently mediating anaerobic oxidation of methane. *Nature* **407:** 623-626.

Boetius, A. & Suess, E. (accepted) Hydrate Ridge: a natural laboratory for the study of microbial life fueled by methane from near-surface gas hydrates.

Boone, D.R.; Johnson, R.L.; Liu, Y. (1988) Diffusion of the interspecies electron carriers H_2 and formate in methanogenic ecosystems and its implications in the measurement of Km for H_2 or formate uptake. *Applied and Environmental Microbiology* **55**: 1735-1741.

Cord-Ruwisch, R. (1985) A quick method for the determination of dissolved and precipitated sulfides in cultures of sulfate-reducing bacteria. *Journal of Microbiological Methods* **4:** 33-36.

Crutzen, P.J. (1994) Global Budgets for non-CO_2 green house gases. *Environmental Monitoring and Assessment* **31**: 1-15.

Dawson, R. M. C.; Elliot, D. C.; Elliot, W. H.; Jones, K.M. (1986) Data for Biochemical Research. 3rd ed. Oxforf Science Publications.

Ehalt, D. H. (1974) The atmospheric cycle of methane. *Tellus* **26**: 58-70.

Girguis, P.R.; Orphan, V.J.; Hallam, S.J.; DeLong, E.F. (2003) Growth and methane oxidation rates of anaerobic methanotrophic archaea in a continuous-flow bioreactor. *Applied and Environmental Microbiology* **69**: 5472-5482.

Habicht, K.S.; Gade, M.; Thamdrup, B.; Berg, P.; Canfield, D.E. (2002) Calibration of sulfate levels in the Archaean Ocean. *Science* **298**: 2372-2374.

Hallam, S.J.; Girguis, P.R.; Preston, C.M.; Richardson, P.M.; DeLong, E.F. (2003) Identification of methyl coenzyme M reductase A (*mcr*A) genes associated with methane-oxidizing archaea. *Applied and Environmental Microbiology* **69**: 5483-5491.

Hartgers, W.S.; Sinninghe Damsté, J.S.; Allan, J.; Hayes, J.M.; Deleeuw, J.W. (1994) Evidence for only minor contributions from bacteria sedimentary organic-carbon. *Nature* **369**: 224-227.

Hernandez, M. E. & Newman, D. K. (2001) Extracellular electron transfer. *Cellular and Molecular Life Sciences* **58:** 1562-1571.

Hinrichs, K.-U.; Hayes, J.M.; Sylva, S.P.; Brewer, P.G.; DeLong, E.F. (1999) Methane-consuming archaebacteria in marine sediments. *Nature* **398**: 802-805.

Hinrichs, K. U. & Boetius, A. B. (2002) The anaerobic oxidation of methane: new insights in microbial ecology and biogeochemistry. In *Ocean Margin Systems*. Wefer, G.;

Billet, D.; Hebbeln, D.; Jørgensen, B. B.; Schlüter, M.; van Weering, T. (eds.) Heidelberg: Springer-Verlag, 457-477.

Hoehler, T. M.; Alperin, M. J.; Albert, D. B.; Martens, C. S. (1994) Field and laboratory studies of methane oxidation in an anoxic marine sediment: Evidence for a methanogen – sulfate reducer consortium. *Global Biogeochemical Cycles* **8**: 451-463.

Hoehler, T. M.; Alperin, M.J.; Albert, D.B.; Martens, C.S. (1998) Thermodynamic control on hydrogen concentrations in anoxic sediments. *Geochimica et Cosmochimica Acta* **52:** 1745-1756.

Ingram, J. M. & Blackwood, A. C. (1970) Microbial production of phenazines. *Advances in Applied Microbiology* **13:** 267-282.

Iversen, N. & Blackburn, T.H. (1981) Seasonal rates of methane oxidation in anoxic marine sediments. *Applied and Environmental Microbiology* **41:** 1295-1300.

Iversen, N (1996) Methane oxidation in coastal marine environments. In *Microbiology of atmospheric trace gases*. Murrel, J. C. and Kelly, D. P. (eds.) Heidelberg: Springer-Verlag, 51-68.

Jäckel, U. (1997) Die Bedeutung der mikrobiellen Eisenreduktion im Reisfeldboden. Diploma Thesis, University of Marburg.

Jørgensen, B.B. & Bak, F. (1991) Pathways and microbiology of thiosulfate transformations and sulfate reduction in a marine sediment (Kattegat, Denmark). *Applied and Environmental Microbiology* **57**: 847-856.

Joye, S. B.; Boetius, A.; Orcutt, B. N.; Montoya, J. P.; Schulz, H. N.; Erickson, M. J.; Lugo, S. K. (accepted) The anaerobic oxidation of methane and sulfate reduction in sediments from Golf of Mexico cold seeps. *Chemical Geology*

Klenk, H.-P.; Clayton, R. A.; Tomb, J.-F.; White, O.; Nelson, K. E., *et al*. (1997) The complete genome sequence of the hyperthermophilic, sulphate reducing Archaeon *Archaeoglobus fulgidus*. *Nature* **390**: 364-370.

Knittel, K.; Boetius, A.; Lemke, A.; Eilers, H.; Lochte, K. *et al*. (2003) Activity, distribution, and diversity of sulfate reducers and other bacteria in sediments above gas hydrate (Cascadia Margin, OR). *Geomicrobiology Journal* **20**: 369-294.

Krüger, M.; Meyerdierks, A.; Glöckner, F. O.; Amann, R.; Widdel, F. *et al*. (accepted) A conspicuous nickel protein in microbial mats that oxidize methane anaerobically. *Nature*

Kvenvolden, K. A. (1993) Gas hydrates – geological perspectives and global change. *Geophysical Reviews* **31**: 173-187

Linke, P. & Suess, E. (2000) RV Sonne cruise report SO148. *TECFLUX-II-GEOMAR Report* **98:**122.

Luff, R. Und Wallmann, K. (2003) Fluid flow, methane flux, carbonate precipitaion and biogeochemical turnover in gas hydrate-bearing sediments at Hydrate Ridge, Cascadia margin: Numerical modeling and mass balances. *Geochim. Cosmochim. Acta* **67**: 3403-3421.

Michaelis, W.; Seifert, R.; Nauhaus, K.; Treude, T.; Thiel, V. *et al*. (2002) Microbial reefs in the Black Sea fueled by anaerobic oxidation of methane. *Science* **297:** 1013-1015.

Moore, L.G.; Rocap, G.; Chisholm, S.W. (1998) Physiology and molecular phylogeny of coexisting *Prochlorococcus* ecotypes. *Nature* **393**: 464-467.

Nauhaus, K.; Boetius, A.; Krüger, M.; Widdel, F. (2002) In vitro demonstration of anaerobic oxidation of methane coupled to sulphate reduction in sediments from a marine gas hydrate area. *Environmental Microbiology* **4:** 296-305.

Nisbet, E.G. & Sleep, N.H. (2001) The habitat and nature of early life. *Nature* **409**:1083-1091.

Oremland, R. S. & Capone, D. G. (1988) Use of "specific" inhibitors in biogeochemistry and microbial ecology. *Advances in Microbial Ecology* **10:** 285-383.

Orphan, V. J.; House, C. H.; Hinrichs, K.-U.; McKeegan, K. D.; DeLong, E. F. (2002) Multiple archaeal groups mediate methane oxidation in anoxic cold seep sediments. *Proceedings of the National Academy of Science* **99:** 7663-7668.

Overmann, J.; Tuschak, C.; Fröstl, J.; Sass, H. (1998) The ecological niche of the consortium "*Pelochromatium roseum"*. *Archives of Microbiology* **169**: 120-128.

Overmann, J. & van der Gemerden, H. (2000) Microbial interactions involving sulfur bacteria: implications for the ecology and evolution of bacterial communities. *FEMS Microbiology Reviews* **24**: 591-599.

Paull, C. P.; Ussler, W.; Dillon, W. (1991) Is the extend of glaciation limited by methane gas-hydrates? *Geophysical Research Letters* **18**: 432-434

Rabus, R.; Fukui, M.; Wilkes, H.; Widdel, F. (1996) Degradative capacities and 16S rRNA-targeted whole-cell hybridization of sulfate-reducing bacteria in an anaerobic enrichment culture utilizing alkylbenzenes from crude oil. *Applied and Environmental Microbiology* **62:** 3605-3613.

Reeburgh, W. S. (1996) "Soft spots" in the global methane budget. In *Microbal growth on C1 compounds*. Lidstrom, M. E. & Tabita, F. R. (eds.) Kluwer Academic Publishers: 334-342.

Rowan, R. & Knowlton, N. (1995) Interspecific diversity and ecological zonation in coral-algal symbiosis. *Proceedings of the National Academy of Science USA*. **92**: 2850-2853.

Schink, B. & Stams, A. J. M. (2001) Syntrophism among prokaryotes. In *The Prokaryotes, an Evolving Electronic Resource for the Microbiological Community*. Dworkin, M., Falkow, S., Rosenberg, E., Schleifer, K.-H., and Stackebrandt, E. (eds). Heidelberg: Springer Science Online. (www.prokaryotes.com).

Schwertmann, U. & Cornell, R.M. (1991) Iron oxides in the laboratory, preparation and characterisation. VCH, Weinheim.

Seeliger, S. R.; Cord-Ruwisch, R.; Schink, B. (1998) A periplasmic and extracellular c-type cytochrome of *Geobacter sulfurreducens* acts as ferric iron reductase and as electron carrier to other acceptors or to partner bacteria. *Journal of Bacteriology* **180:** 3686-3691.

Shyu, J. B. H.; Lies, D. P.; Newman, D. K. (2002) Protective role of *tol*C in efflux of the electron shuttle anthraquinone-2,6-disulfonate. *Journal of Bacteriology* **184:** 1806-1810.

Sørensen, K. B.; Finster, K.; Ramsing, N. B. (2001) Thermodynamic and kinetic requirements in anaerobic methane oxidizing consortia exclude hydrogen, acetate and methanol as possible shuttles. *Microbial Ecology* **42:** 1-10.

Spormann, A. & Widdel, F. (2000) Metabolism of alkylbenzenes, alkanes, and other hydrocarbons in anaerobic bacteria. *Biodegradation* **11:** 85-105.

Straub, K. L. & Schink, B. (2003) Evaluation of electron-shuttling compounds in microbial ferric iron reduction. *FEMS Microbiology Letters* **220:** 229-233.

Teske, A.; Hinrichs, K.-U.; Edgcomb, V.; Gomez, A.D.V.; Kysela, D. *et al*. (2002) Microbial diversity of hydrothermal sediments in the Guyamas Basin: Evidence for anaerobic methanotrophic communities. *Applied and Environmental Microbiology* **68**: 1994-2007.

Treude, T.; Boetius, A.; Knittel, K.; Wallmann, K.; Jørgensen, B. B. (2003) Anaerobic oxidation of methane above gas hydrates (Hydrate Ridge, OR). *Marine Ecology Progress Series* **264**: 1-14.

Valentine, D.L. & Reeburgh. W.S. (2000) New perspectives on anaerobic methane oxidation. *Environmental Microbiology* **2**: 477-484.

Valentine, D. L. (2002) Biogeochemistry and microbial ecology of methane oxidation in anoxic environments: a review. *Antonie van Leeuwenhoek* **81**: 271-282.

Widdel, F. & Bak, F. (1992) Gram negativ mesophilic sulfate-reducing bacteria. In *The Prokaryotes*. Balows, A., Trüper, H. G., Dworkin, M., Harder, W., and Schleifer, K.-H. (eds). New York: Springer, 3352-3378.

Yamamoto, S.; Alcauskas, J. B.; Crozier, T. E. Solubility of methane in distilled water and seawater. *Journal of Chemical and Engineering Data* **21**: 78-80.

Zehnder, A. & Brock, T. (1980) Anaerobic methane oxidation: occurrence and ecology. *Applied and Environmental Microbiology* **38:** 194-204.

Chapter 8

Final Discussion and Conclusions

Preface

In this study, different types of methane-bearing habitats were investigated to detect, quantify, and characterize hot spots of AOM. Studies were carried out:

- at Hydrate Ridge, a gas hydrate-bearing methane seep in the North Pacific;
- in gassy sediments of Eckernförde Bay in the German Baltic;
- in a diffusive sediment system of the Chilean continental margin;
- with methanotrophic mats from microbial reefs above gas seeps in the anoxic part of the Black Sea.

In section 1, results from the different habitats will be summarized and discussed. Section 2 is comparing advantages and disadvantages of the applied methods. In section 3, an outlook for future research on AOM is given.

1. Comparison of AOM habitats and global implications

In Table 1, main characteristics of the investigated habitats are given. Fig. 1 compares the maximal AOM rates measured under standardized conditions in the different habitats.

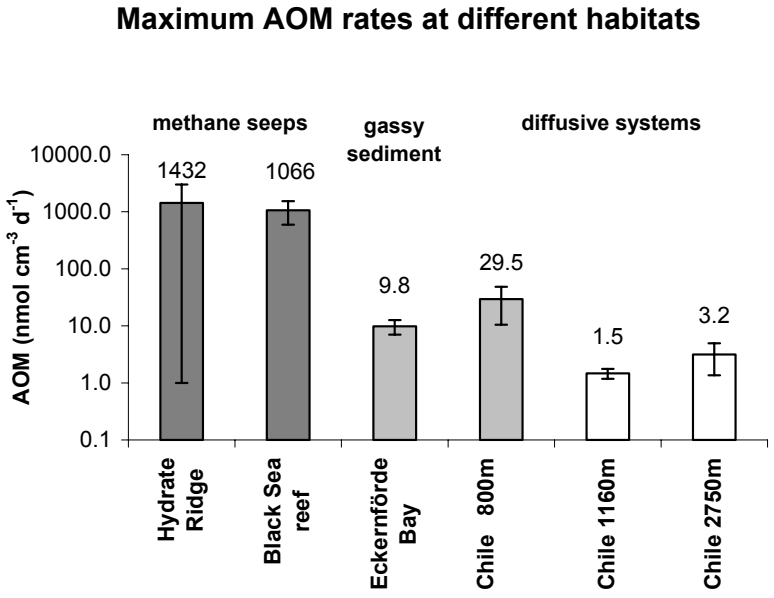

Figure 1. Mean rates and standard deviations of AOM hot spots in investigated habitats. For Hydrate Ridge, the maximum values of the replicates at *Beggiatoa*- and *Calyptogena* fields (n = 11), for the Black Sea reef, the highest values of incubated mat pieces (n = 13), for Eckernförde Bay, the maximum values of the replicates (n = 18) and for Chile, the highest rates at each station (n = 3 per station) were averaged.

Table 1. Characteristics of habitats investigated in this study (Black Sea reef excluded).

Location	Type	Methane transport	Methane origin	Cell density of archaeal methanotrophs (cm^{-3} sediment)	Sulfate penetration depth (cm)	Depth of methane disappearance (cm)	Depth (Thickness) of AOM hot spot (cm)	Measured areal AOM (mmol m^{-2} d^{-1})	Calculated methane flux (mmol m^{-2} d^{-1})	Retention of methane in the sediment (%)
Hydrate Ridge	gas seep/ gas hydrates	advective	fossil reservoir	1×10^{10}	10	methane reaches hydrosphere	0-10 (10)	56-100	56-200*	50-100
Eckernförde Bay	gassy coastal sediment	diffusive/ advective	in situ production	$3\text{-}5 \times 10^{7}$	30	0-5	20-25 (5)	0.4-1.5	0.6-1.3**	100 (except rising gas bubbles)
Chilean continental margin	diffusive system	diffusive	in situ production	not detected	150-350	110-360	365-405 (40) 115-180 (65) 218-222 (4)	0.2-5.7	0.07-0.13	100

* calculated from methae consumption (this study) and methane effluxes (Torres et al. 2002)

* *estimated from methane profiles of Abegg et al.1997

1.1 Is AOM adjusted to the methane flux of the habitat?

The investigated habitats differed by orders of magnitude in methane turnover rates and abundance of methanotrophic cells. The range of AOM was not related to water depth, however, it matched the difference in biomass of AOM communities. AOM rates as well as AOM biomass was correlated with calculated methane fluxes (Fig. 1 and Table 1). At seep sites with very high methane fluxes (up to 200 mmol m^{-2} d^{-1} at Hydrate Ridge), methane turnover rates were two to three orders of magnitude higher compared to non-seep sites with methane fluxes <2 mmol m^{-2} d^{-1}. The permanently high advective methane supply at cold seeps supports a dense biomass of AOM organisms. In the Black Sea, methanotrophic mats with appr. 10^{12} cells cm^{-3} mat developed above methane seeps (Chapter 5). Methanotrophic ANME-2 cells in Hydrate Ridge sediments were about three orders of magnitude more abundant (appr. 10^{10} cells cm^{-3} sediment) compared to ANME-2 cells in the gassy sediments of Eckernförde Bay (appr. 3-5 x 10^{7} cells cm^{-3} sediment) (Table 1). At the Chilean continental margin, in a diffusive system, AOM organisms were not found either because they represent an unknown group not detectable with recent oligonucleotide probes or because their abundance was so low that the signals of fluorescently labeled probes was not detected.

This study shows that the magnitude of AOM is controlled by the methane flux of a habitat and by the biomass of AOM community. The study further shows that AOM leads to a substantial (seeps and gassy sediments) or even complete (diffusive systems) oxidation of methane in the sediment before it reaches the hydrosphere (Table 1). Methane may escape to the hydrosphere if free gas is accumulating and if ebullition is caused by an overpressurization of the system. Our findings confirm the assumption of Reeburgh, (1996) that AOM controls methane emission from the ocean over a wide range of methane fluxes. Considering that the investigated sites included as different systems as coastal and deep-sea sediments, oceanic and brackish environments as well as surface and subsurface sediments, this study also confirms that AOM is a ubiquitous process in marine systems.

1.2 Small-scale variability and environmental control of AOM

Vertical distribution of AOM. The investigated habitats revealed differences in the vertical distribution of AOM that correlated with methane fluxes (Table 1). At HR, the AOM zone is defined by high advective methane fluxes from below and low diffusive sulfate fluxes

from the bottom waters into the sediments. Hence, the hotspot zone of AOM is shifted to the sediment surface. The high sulfate demand led to a nearly complete depletion of sulfate within the top 10 cm. At Eckernförde Bay, with intermediate methane fluxes, the hot spots of AOM were located between 20 and 25 cm and sulfate was depleted at about 30 cm. At the Chilean continental margin, where methane fluxes were diffusive and three orders of magnitude lower compared to Hydrate Ridge, AOM was located between 1 and 4 m with a respective deep sulfate penetration. Thus, we can expect a shift of AOM towards the sediment surface with increasing methane fluxes when sulfate fluxes remain diffusive. In the case of the microbial reefs in the permanently anoxic zone of the Black Sea, the AOM zone extended into the water column in the form of calcifying microbial mats.

Thickness of AOM zone. The thickness of the AOM zone, however, shows no obvious correlations with methane fluxes. It was narrow at Hydrate Ridge (10 cm) but also at one station at the Chilean continental margin (4 cm). At other stations on the Chilean margin, the zone was 40-65 cm thick. Apart from minor activities in the top 20 cm of the sediment, the peak AOM rates of Eckernförde Bay mainly occurred in a 5 cm thick zone (20-25 cm). It seems that the hot spots of AOM are sometimes concentrated in a very narrow zone of the sediment in that nearly all methane is consumed. This makes it sometimes difficult to hit the zone when sampling long sediment cores. The occurrence of both narrow and broad AOM zones bears problems in interpreting depth-integrated areal AOM rates. Areal rates give no information about the distribution of AOM. Methane could be consumed in a 1 cm or a 1 m thick layer. AOM is best described by volumetric rates and the zone of its occurrence. Calculation of areal rates are only helpful for the estimation of methane budgets of large areas.

Lateral heterogeneity. A strong lateral heterogeneity in AOM and sulfate reduction rate was found at Hydrate Ridge caused by transient gas injection, inhomogeneous distribution of gas hydrates, precipitated carbonates and bioturbation by chemoautotrophic clams (Chapter 2). The standard deviation between replicates was often 85-110% of mean rates at fluid impacted sites. This heterogeneity makes it very difficult to constrain methane turnover rates at methane seeps and to reveal environmental factors controlling AOM. Geochemical and biological parameters that are measured on different samples may vary strongly even when taken close-by. In Eckernförde Bay, the sediments were comparative homogenous revealing smaller standard deviations between replicates (15-65% of mean rates) of AOM and SR. Here, the lack of major advective processes causes a clear zonation dominated either by methane production, methane consumption, or organoclastic sulfate reduction. At the Chilean

continental margin, such a zonation was also expected due to the diffusive sediment system; however, AOM and SR activity was often found in only one of the two replicates. The reasons for this variation are not clear and methodological problems increase at the detection limit.

Methane-driven sulfide production. High activity of AOM at Hydrate Ridge was correlated with the occurrence of filamentous bacteria of *Beggiatoa* at the sediment-water interface. Sulfide fluxes above gas hydrate can be as high as 63 ± 36 mmol m^{-2} d^{-1} (Sahling et al., 2002). These organisms meet their energy demand by the oxidation of sulfide, a product of AOM. Whereas the benefit of *Beggiatoa* from an association with AOM communities is obvious there might also be a benefit of the AOM community from the sulfide oxidation of *Beggiatoa*. Possibly, *Beggiatoa* sustains thermodynamic favorable conditions for AOM due to the removal of sulfide and a supply of sulfate. The sediments of Eckernförde Bay were also covered by *Beggiatoa*, however, the main source of the sulfide was organoclastic sulfate reduction. The abundance of Beggiatoa at Hydrate Ridge was approx. twice the abundance at Eckernförde Bay (per cm^{-3} in the 0-0.5 cm layer, A. Preisler, pers. comm.) pointing to the higher sulfate reduction rates at the seep-site.

Methane-driven carbonate precipitation. CO_2 is produced during AOM and accumulates as dissolved carbonate in the pore water. Carbonate precipitation follows in zones where an oversaturation of carbonate is reached, at increased pH and availability of Ca^{2+} ions. It is possible that carbonate precipitation plays a role in maintaining AOM thermodynamic favorable. Methane-based carbonates are known from a variety of fossil and recent habitats (Von Rad et al., 1996; Bohrmann et al., 1998; Bouloubassi et al., 2000; Naehr et al., 2000; Peckmann et al., 2001; Thiel et al., 2001; Lein et al., 2002). Prominent carbonate structures and cements related to methane seepage have been found at and below the seafloor of Hydrate Ridge (Bohrmann et al., 1998) and the Black Sea (Peckmann et al., 2001). In this study, very light δ^{13}C-values of the carbonates in the Black Sea microbial reefs (Chapter 5) and the Chilean sediment (Chapter 4) indicated AOM-related calcification. A possible role of AOM communities in calcification was also indicated by the precipitation of ^{14}C-carbonate from $^{14}CH_4$ in the Black Sea mats (Chapter 5). Considering that carbonate precipitation was found in both advective and diffusive systems, we can assume that methane-driven carbonate precipitations occurs over a wide range of methane fluxes.

1.3 Methane seeps – a Cockaigne for AOM but also a loophole for methane?

We demonstrated that methane seeps reveal the by far highest methane turnover rates of marine habitats (see also Fig. 1 and Table 1). AOM rates of up to 100 mmol m^{-2} d^{-1} matched extremely high sulfate reduction rates at fluid impacted sites of Hydrate Ridge (Chapter 2, Boetius et al. 2000). The sulfate reduction rates (32 –65 mmol m^{-2} d^{-1}, Chapter 2) also corresponded with extremely high oxygen consumption rates recently determined by in situ chamber experiments (54 mmol m^{-2} d^{-1}, Sommer et al., 2003). The oxygen is consumed by chemoautotrophic communities during the oxidation of the produced sulfide (Sahling et al. 2002; W. Ziebis, unpubl. data). Oxygen consumption rates of near-by non-seep sites were comparatively low (1.5 mmol m^{-2} d^{-1}, Sommer et al., 2003). From the Black Sea reefs we have learned that constant methane seepage in an anoxic environment is able to sustain the buildup of large methanotrophic biomass with very high methane consumption rates.

Methane seeps therefore represent extreme marine habitats with respect to the exceptionally high availability of methane and the consequently high methane turnover rates. Methane seeps are hot spot systems comparable with upwelling areas supporting an extreme high primary production, due to an unusually high nutrient supply.

However, although methane seeps provide ideal growth conditions for AOM organisms, these habitats might represent a significant source of methane emission from the oceans to the hydrosphere. This study shows that only in diffusive systems AOM is able to completely inhibit methane emission into the hydrosphere (Table 1). At seep sites, methane partly escapes into the hydrosphere in the form of free gas. The main transport mechanism across the AOM barrier seems to be gas ebullition. Although parts of the methane may dissolve in the sediment pore water during the rise of bubbles, a major fraction may remain inaccessible to the AOM consortium and emanates into the hydrosphere. Another loophole for methane at high advective methane seeps could be a limitation of the electron acceptor. If sulfate is already depleted in the surface sediments (top 10 cm, Table 1) it may become limiting, and methane may escape the sediments by fluid flow or even diffusion.

From today's knowledge and methodology we are not able to completely reconstruct the fate of fluids or methane bubbles rising from methane seeps. There have been hydro-acoustic observations of methane flumes emanating from Hydrate Ridge showing a disappearance of methane bubbles below the ocean surface (J. Greinert, pers. comm.). It is hypothesized that a thin layer of gas hydrates forms between the gas bubble and the surrounding water, preventing

a dissolution of methane (E. Suess, pers. comm.). When the gas bubbles surpasses hydrate stability, the methane dissolves and is not any longer detectable with hydro-acoustic methods. High methane concentrations and low $\delta^{13}C$ values of methane in the bottom water above Hydrate Ridge also confirmed methane emission into the water column (K. Heeschen, unupl. data). However, there was no signal of seep methane found in the surface waters above the plumes. Thus, the amount of methane that escapes into the atmosphere from methane seeps has not been constrained yet. The water column may also represent a sink for methane due to aerobic microbial oxidation processes, which might ultimately control methane emission from seeps. In the anoxic waters of the Black Sea, anaerobic microbial consumption of methane seems to control methane emission, however, the responsible microorganisms have not been found (Reeburgh et al., 1991). Today, a satisfying calculation of global methane emission from methane seeps and its impact on atmospheric methane concentration is not possible, because realistic estimations about the worldwide distribution of methane seeps and their methane emission are not available.

1.4 Is the magnitude of AOM predictable for non-seep sites?

From AOM rates reviewed by Hinrichs and Boetius (2002) it was hypothesized in Chapter 1 of this study, that there might be a decrease in AOM rates with water depth in non-seep habitats due to a decrease in organic matter supply and methane production rates. However, this study shows that a generalization is not possible. Although Eckernförde Bay is a coastal marine sediment with very high deposition rates of organic matter, AOM peaks and areal AOM were only one third of the 800 m deep site investigated at the Chilean continental margin (Fig. 1, Table 1). High deposition of organic matter from the euphotic zone could be the reason for a locally higher methane production and consumption rate at the Chilean site, which is located in the world's most productive marine region, i.e. the upwelling region off South America. At a close-by site, in 2750 m water depth, the rates were one order of magnitude lower compared to the 800 m site, confirming the correlation of AOM with water depth when considered only for a restricted region.

However, even within the same region, AOM can vary at similar water depths pointing to more complex controlling factors: in Århus Bay, a semi-enclosed embayment of the Baltic Sea north of Eckernförde Bay, AOM rates in the sediments at 16 m water depth are one order of magnitude lower compared to the 25/28 m deep sites in Eckernförde Bay (Thomson et al., 2001). Furthermore, the AOM zone was located 125 cm deeper compared to Eckernförde

Bay. It still seems difficult to determine which factors are the best predictors of AOM rates: it could be the productivity in the euphotic zone, the water depth, the burial rate of organic matter, the methane production rates, and/or the sediment properties such as porosity and permeability, or any combination thereof.

1.5 What is the diversity of methanotrophic microorganisms at the AOM habitats?

At three sites, i.e. Hydrate Ridge (Boetius et al., 2000), Black Sea reef, and Eckernförde Bay, the microorganisms apparently mediating AOM were identified. All archaeal methanotrophs belonged to the phylogenetic group *Euryarchaeota,* which comprises also all methanogens. The specific microorganisms dominating the biomass in the different habitats belonged to different phylogenetic sub-groups within the *Euryarchaeota.* The different groups formed different morphological types of consortia (Fig. 2). Hydrate Ridge was dominated by shell-type aggregates of ANME-2 (inner core) and *Desulfococcus/Desulfosarcina* (outer shell). Eckernförde Bay was also dominated by aggregates of ANME-2, which were not directly associated with a bacterial partner. However, aggregates of SRB of the *Desulfococcus/Desulfosarcina* cluster were found in the same depth where aggregates of ANME-2 were found. The Black Sea reef was dominated by ANME-1 and bacteria of the *Desulfococcus/Desulfosarcina* cluster forming a mat-type consortium. It can be concluded that AOM can be mediated by different groups of archaea with a diversity of aggregation morphologies. Nevertheless, it remains unknown if and on which spatial scales both archaea and sulfate-reducing bacteria depend on each other in the process of AOM. It is possible that the methanotrophs have the enzymatic apparatus to mediate both AOM and sulfate reduction. It is also interesting to note that so far methanotrophic mats are only known from the Black Sea and the ANME 1 group. However, it is not understood whether this is correlated with the habitat or with a species-specific ability.

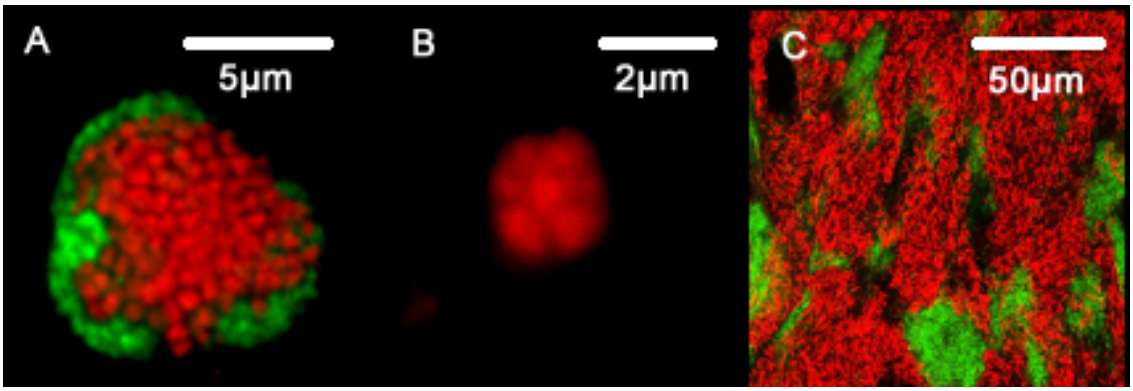

Figure 2. Three types of AOM communities: a) shell-type consortium: an aggregate with an inner core of archaeal cells of ANME-1 surrounded by an outer shell of sulfate-reducing bacteria of the *Desulfococcus/Desulfosarcina* cluster, Hydrate Ridge (Boetius et al., 2000); b) an aggregate of ANME-2 cells without bacterial partner, Eckernförde Bay (Chapter 3); c) mat-type consortium: a microbial mat dominated by ANME-1 including patches of sulfate-reducing bacteria of the *Desulfococcus/Desulfosarcina* cluster, Black Sea reef (Chapter 5). In all pictures, cells of archaea are stained red, and cells of sulfate-reducing bacteria are stained green.

2. Methodological advantages and disadvantages of AOM field measurements with radiotracers

General advantages and disadvantages of radiotracer measurements. The two major advantages of measurements with radiotracers are: (1) the possibility to measure turnover rates in environmental, i.e. undisturbed, samples, and (2) the high sensitivity of the method, enabling the detection of even very low turnover rates. A disadvantage of radiotracer measurements is that only gross rates can be determined. Without the knowledge of methane production rates and/or methane fluxes, it cannot be determined whether the environment represents a sink or a source of methane. Here, a combination of rate measurements and flux modeling from concentration profiles can help to understand the system. Modeling from concentration profiles give only net reactions in the sediment, which can lead to underestimations of true turnover rates; however, they reflect the final consequence of combined biogeochemical reactions in the sediment (Fossing et al., 2000; Jørgensen et al., 2001). In Chapter 2 we demonstrated that modeling of AOM zonation is possible even in high advective habitats revealing relative good agreements with measured rates. However, the modeled rates did not reflect the natural variability of the sediment, as mentioned above.

Difficulties of ex situ measurements. Measurements of AOM after recovery of sediment samples from greater water depths, i.e. ex situ measurements, always bear the problem of methane degassing due to decompression. The loss of methane most likely leads to an underestimation of the in situ rate as AOM depends on the methane concentration (Nauhaus et al., 2002). Furthermore, the formation of small gas bubbles, so-called foaming, disturbs the primary structure of the sediment.

Whole-core injection method. Ex situ measurements with surface sediments should be done with push-cores according to the "whole-core injection method" of Jørgensen (1978). By this method, the disturbance of the sediment structure is minimized, the sealing of the sediments against methane releases and oxygen penetration is achieved by thick rubber stoppers, and a homogenous injection into the sediment in small intervals is possible from the side through little openings filled with silicon. Especially AOM rates determined in Eckernförde Bay (Chapter 3) demonstrate that consistent replicates can be gained by whole-core injection. In surface sediments, this method should be preferred to sub-sampling with small glass tubes. Glass tubes comprise only a small volume of sediment and are not as safely sealed as the larger injection tubes. This could lead to artifacts as discussed below.

Incubations in glass tubes. When sampling very long sediment cores, e.g. gravity cores, containing dry or hard sediments, it becomes very difficult to press injection cores into the sediment. In this study, glass tubes were used to sub-sample gravity cores. The tubes were sealed with rubber stoppers at both open ends and the tracer was injected through the rubber stopper. Although rates were measured in expected AOM zones, this technique was problematic. It is difficult to close the tubes without headspace when the sediment is getting more compact. Methane can be lost into the headspace or oxygen can diffuse into the sediment. A better sealing technique would be necessary to gain good samples. It also has to be considered if AOM rates of the deeper sediment should better be determined by modeling from concentration profiles as recommended by Jørgensen et al. (2001). Modeling of pore water profiles, however, does face the same problems as radiotracer measurements when it has to rely on ex situ methane profiles.

Difficulties of measurements with ^{14}C-methane. Gaseous $^{14}CH_4$ bears the problem that it has to be dissolved in water before it can be injected homogenously. The solubility of methane in water is not very good, wherefore the specific activity of injected volumes is generally low. During this study, it was observed that stock solutions of $^{14}CH_4$ dissolved in anoxic water consistently produce small amounts of $^{14}CO_2$ by an unknown chemical reaction. This leads to poor blanks which is critical for the determination of very low AOM rates. To

minimize the error, numerous controls (3-5 as a minimum) should always be taken in parallel to measurements. In calculations, a sample should only be assigned a positive value when the dpm value of the $^{14}CO_2$ is three times the standard deviation of the controls. When the background $^{14}CO_2$ of the stock solution exceeds a certain value, e.g. 500 dpm per 15 µl, the methane has temporarily to be transferred into vials with sodium hydroxide to clean it from $^{14}CO_2$. Furthermore, processing of AOM samples incubated with $^{14}CH_4$ are very time consuming and a high number of replicates are needed to obtain a satisfying impression of a habitat. However, this method is still very important in habitats with high advective methane transport to estimate the efficiency of AOM because modeling cannot reflect the dynamics of these systems.

3. Future research questions

The first priority should be the measurement of in situ rates. This can be done by measuring AOM either at the seafloor or in samples that were recovered without any changes in pressure and temperature. It is important that decompression of the sediment is prevented until the incubation is stopped. Only under these conditions a true in situ rate can be gained. In situ sulfate reduction measurements at the seafloor were already performed with incubation chamber techniques (Greeff et al., 1998; Weber et al., 2001) and there are efforts to combine in situ sulfate reduction with AOM measurements (U. Witte, personal comm.). However, so far, no in situ measurements of AOM or methane-driven SR are available.

To understand distribution, relevance and control of AOM in a given habitat, it is also very important to obtain the following information:

- How large is the methane and sulfate turnover in characteristic biogeochemical zones of a habitat?
- How large is the methane flux from below, and the sulfate flux from above?
- How effectively is methane removed in the sediment? How does turnover compare to methane production and transport?
- What is the fate of the reaction products CO_2 and H_2S?
- Which phylogenetic groups of microorganisms mediate AOM at this location?
- What is the distribution of AOM communities and how abundant are they?
- Which and how much specific biomarkers can be found and what is their isotopic carbon signal compared to the source?

- What are the special environmental characteristics of the habitat and how are they met by the physiology of the AOM consortium?

It would further be interesting to find out if AOM is possible in other extreme marine habitats and in non-marine locations. It is currently not known if AOM is a significant process in hot environments (e.g. at methane emitting hydrothermal vents). AOM has already been confirmed for the hypersaline Mono Lake, CA (Joye et al., 1999). However, pelagic AOM communities have so far not been identified. It is unknown if AOM is occurring in sewage plants or in sulfate-free environments like rice paddies.

To understand the physiology and biochemical functioning of AOM it will be necessary to obtain AOM consortia in pure culture. Without the exclusion of other organisms from the sediment or microbial mat, physiological investigations remain difficult. Here, efforts should be made to establish pressurized flow through reactors which mimic the high flux of methane through sediments, and which allow for a constant removal of the products of AOM, i.e. CO_2 and H_2S, as in nature.

4. References

Abegg, F., Anderson, A.L. (1997). The acoustic turbid layer in muddy sediments of Eckernfoerde Bay, Western Baltic: methane concentration, saturation and bubble characteristics. Mar. Geol. 137, 137-147.

Boetius, A., Ravenschlag, K., Schubert, C.J., Rickert, D., Widdel, F., Giesecke, A., Amann, R., Jørgensen, B.B., Witte, U., Pfannkuche, O. (2000). A marine microbial consortium apparently mediating anaerobic oxidation of methane. Nature 407, 623-626.

Bohrmann, G., Greinert, J., Suess, E., Torres, M. (1998). Authigenic carbonates from the Cascadia subduction zone and their relation to gas hydrate stability. Geology 26(7), 647-650.

Bouloubassi, I., Aloisi, G., Pancost, R.D., Damsté, J.S.S., Pierre, C., Party, M.S. (2000). Lipid biomarkers in carbonate crusts from mud volcanoes of the eastern Mediterranean Ridge: Implications for methane oxidation. Goldschmidt Conference, Oxford, UK. 2000 Cambridge Publications, 5, 237-238.

Fossing, H., Ferdelman, T.G., Berg, P. (2000). Sulphate reduction and methane oxidation in continental sediments influenced by irrigation (South-East Antlantik off Namibia). Geochim. Cosmochim. Acta 64(5), 897-910.

Greeff, O., Glud, R.N., Gundersen, J., Holby, O., Jørgensen, B.B. (1998). A benthic lander for tracer studies in the sea bed: in situ measurements of sulfate reduction. Continental Shelf Research 18, 1581-1594.

Hinrichs, K.-U., Boetius, A. (2002). The anaerobic oxidation of methane: new insights in microbial ecology and biogeochemistry. In: G. Wefer, D. Billett, D. Hebbeln et al. (Eds.), Ocean Margin Systems. Springer-Verlag, Berlin, pp. 457-477.

Jørgensen, B.B. (1978). A comparison of methods for the quantification of bacterial sulphate reduction in coastal marine sediments: I. Measurements with radiotracer techniques. Geomicrobiol. J. 1(1), 11-27.

Jørgensen, B.B., Weber, A., Zopfi, J. (2001). Sulphate reduction and anaerobic methane oxidation in Black Sea sediments. Deep-Sea Res. I 48, 2097-2120.

Joye, S.B., Boetius, A., Orcutt, B.N., Montoya, J.P., Schulz, H.N., Erickson, M.J., Logo, S.K. (accepted). The anaerobic oxidation of methane and sulfate reduction in sediments from Gulf of Mexico cold seeps. Chem. Geol.

Joye, S.B., Connell, T.L., Miller, L.G., Premland, R.S., Jellison, R.S. (1999). Oxidation of ammonia and methane in an alkaline, saline lake. Limnol. Oceanogr. 44(1), 178-188.

Lein, A.Y., Ivanov, M.V., Pimenov, N.V., Gulin, M.B. (2002). Geochemical characteristics of the carbonate constructions formed during microbial oxidation of methane under anaerobic conditions. Mikrobiologiya 71(1), 89-103.

Naehr, T.H., Rodriguez, N.M., Bohrmann, G., Paull, C.K., Botz, R. (2000). 29. Methane-derived authigenic carbonates associated with gas hydrate decomposition and fluid venting above the Blake Ridge Diapir. Proceedings of the Ocean Drilling Program, Scientific Results 164, 285-300.

Nauhaus, K., Boetius, A., Krüger, M., Widdel, F. (2002). In vitro demonstration of anaerobic oxidation of methane coupled to sulphate reduction in sediment from marine gas hydrate area. Environ. Microbiol. 4(5), 298-305.

Peckmann, J., Reimer, A., Luth, U., Luth, C., Hansen, B.T., Heincke, C., Hoefs, J., Reitner, J. (2001). Methane-derived carbonates and authigenic pyrite from the northwestern Black Sea. Mar. Geol. 177, 129-150.

Reeburgh, W.S. (1996). "Soft spots" in the global methane budget. In: L. M.E. and F. R. Tabita (Eds.), Microbial Growth on C_1 Compounds. Kluwer Academic Publishers, Intercept, Andover, UK, pp. 334-342.

Reeburgh, W.S., Ward, B.B., Whalen, S.C., Sandbeck, K.A., Kilpatrick, K.A., Kerkhof, L.J. (1991). Black Sea methane geochemistry. Deep-Sea Res. I 38(2), 1189-1210.

Sahling H, Rickert D, Raymond WL, Linke P, Suess E (2002) Macrofaunal community structure and sulfide flux at gas hydrate deposits from the Cascadia convergent margin, NE Pacific. Mar Ecol Prog Ser 231:121-138

Sommer, S., Pfannkuche, O., Linke, P., Gubsch, S., Gust, G., Greinert, J., Drews, M. (2003). Methane, oxygen and nitrate fluxes in sediments hosting shallow gas hydrates at Hydrate Ridge. AGU Fall Meeting, San Francisco, CA.

Thiel, V., Peckmann, J., Richnow, H.H., Luth, U., Reitner, J., Michaelis, W. (2001). Molecular signals for anaerobic methane oxidation in Black Sea seep carbonates and microbial mat. Mar. Chem. 73, 91-112.

Thomson, T.R., Finster, K., Ramsing, N.B. (2001). Biogeochemical and molecular signatures of anaerobic methane oxidation in a marine sediment. Appl. Environ. Microbiol. 67(4), 1646-1656.

Torres, M.E., McManus, J., Hammond, D., Angelis de, M.A., Heeschen, K.U., Colbert, S.L., Tryon, M.D., Brown, K.M., Suess, E. (2002). Fluid and chemical fluxes in and out of sediments hosting methane hydrate deposits on Hydrate Ridge, OR, I: Hydrological provinces. Earth Planet. Sci. Lett. 201, 525-540.

Von Rad, U., Rösch, H., Berner, U., Geyh, M., Marching, V., Schulz, H. (1996). Authigenic carbonates derived from oxidized methane vented from the Makran accretionary prism off Pakistan. Mar. Geol. 136, 55-77.

Weber, A., Riess, W., Wenzhoefer, F., Jørgensen, B.B. (2001). Sulfate reduction in Black Sea sediments: in situ and laboratory radiotracer measurements from the shelf to 2000 m depth. Deep-Sea Res. I 48, 2073-2096.

Poster and oral presentations during my PhD study

Poster presentations

1. T. Treude, A.Boetius, K. Knittel, D. Rickert "**Anaerobic oxidation of methane above gas hydrates**", MARGINS Meeting, Kiel, Germany, October 2001

2. T. Treude, A.Boetius, K. Knittel, D. Rickert "**Anaerobic oxidation of methane above gas hydrates**", Sonne Statusseminar, Kiel, Germany, March 2002

3. T. Treude **"Eine Ehe fürs Methan"** und **"Wissenschaft auf See"**, MPI Tag der offenen Tür, Bremen, Germany, June 2002

4. T. Treude, J. Kallmeyer, P. Wintersteller, J. Niggemann **"Anaerobe Methanoxidation am chilenischen Kontinentalhang (SO156, April/Mai 2001)"**, Sonne Statusseminar, Hamburg, Germany, March 2003

5. T. Treude, A. Gieseke, K. Nauhaus, K. Knittel, A. Boetius, B.B. Joergensen, W. Michaelis **"Methanotrophic microbial mats forming reefs in the anoxic Black Sea"**, EGS-AGU-EUG Joint Assembly, Nice, France, April 2003 (no personal participation on the conference)

6. T. Treude, W. Ziebis A. Boetius, B.B. Jørgensen **"Anaerobic oxidation of methane above gas hydrates at Hydrate Ridge, Cascadia Margin",** EGS-AGU-EUG Joint Assembly, Nice, France, April 2003 (no personal participation on the conference)

Oral presentations

1. T. Treude **"Methan: Energieträger und Treibhausgas. Die Rolle der Ozeane als Regulatoren"**, 90 min, Lions Club Lehrte, Germany, April 2002

2. T. Treude **"Methan: Energieträger und Treibhausgas. Die Rolle der Ozeane als Regulatoren"**, 45 min, MPI Tag der offenen Tür, Bremen, Germany, June 2002

3. T. Treude **"Anaerobe Methanoxidation: eine mikrobielle Senke für Methan."**, 60 min, Kompaktkurs "Genese und Verbreitung von Gashydraten" für Studenten der FU Berlin, Berlin, Germany, Juni 2002

4. T. Treude, K. Nauhaus, K. Knittel, A.Gieseke, Boetius, R. Amann, B. B. Jørgensen, F. Widdel, V. Thiel, M. Blumenberg, K. Peterknecht, T. Pape, R. Seifert, W.Michaelis, J. Peckmann, N. Pimenov, M. Gulin **"Carbonate landscape in the anoxic Black Sea formed by massive mats of methane oxidizing Archaea"**, 20 min, 7th International Conference on Gas in Marine Sediments, Baku, Azerbaijan, October 2002

6. T. Treude **"Eigenschaften und Relevanz von Gashydraten"**, 90 min, Lehrerfortbildung der Geotechnologien, Meißen, Germany, November 2002

7. T. Treude, K. Nauhaus, A. Gieseke, K. Knittel, A. Boetius, B. B. Jørgensen, W. Michaelis "**Methanotrophic microbial mats forming reefs in the anoxic Black Sea**", 15 min, ASLO Meeting, Salt Lake City, UT, USA, February 2003

9. T. Treude, W. Ziebis, A. Boetius, B. B. Jørgensen **"Anaerobic oxidation of methane (AOM) above gas hydrates at Hydrate Ridge, Cascadia Margin (SO 165, July/August 2002)"**, 20 min, Sonne Statusseminar, Hamburg, Germany, March 2003

10. T. Treude **"Eigenschaften und Relevanz von Gashydraten"**, 90 min, Lehrerfortbildung der Geotechnologien, Ludwigsfelde, Germany, April 2003-12-01

11. T. Treude **"AOM above gas hydrates at Hydrate Ridge, Oregon"** and **"AOM vs. Methanogenesis in Black Sea reefs !?"**, 30 min, University of Århus, Denmark, June 2003

12. T. Treude, A. Boetius "**Researching anaerobic oxidation of methane: a co-evolution of knowledge and applied methods",** 40 min (keynote lecture), 16th International Symposium on Environmental Biogeochemistry, Aomori, Japan, September 2003

13. T. Treude, A. Boetius, K. Knittel, K. Nauhaus, M. Elvert, M. Krüger, T. Lösekann, K. Wallmann, B.B. Jørgensen, F. Widdel, R. Amann **"Anaerobic oxidation of methane at Hydrate Ridge (OR)"**, 15 min, Goldschmidt Conference, Kurashiki, Japan, September 2003

Participation on expeditions during my PhD study

1. **Hydrate Ridge**, Oregon: "Sonne" 148-1, 20.07.-03.08. 2000, Victoria - Victoria (Canada), projects: TECFLUX II/MUMM
2. **Chile**: "Sonne" 156, 18.04-14.05.2001, Valparaiso – Talcahuano (Chile), projects: PUCK/MUMM
3. **Black Sea**: "Prof. Logachev", 29.06.-23.07.2001, Constanza - Constanza (Romania), projects: GHOSTDABS/MUMM
4. **Eckernförde Bay**: "Littorina", 05./06.09.2001, 20./21.09.2001, 05./06.03.2002, Kiel (Germany), project: MUMM
5. **Hydrate Ridge**, Oregon: "Sonne" 165, 08.06.-21.08.2002, San Diego – Portland - San Francisco (USA), projects: OMEGA/LOTUS/MUMM
6. **Gulf of Mexico**: "Sonne" 174-1, 02.10.-23.10.2003, Balboa (Panama) – Corpus Christi (USA), projects: OMEGA/LOTUS/MUMM

Further publications during my PhD study

1. Treude, T., F. Janßen, U. Witte, W. Queisser (2002) **"Metabolism and decompression tolerance of scavenging lysianassoid deep-sea amphipods"** Deep-Sea Research I, 49: 1281-1289

Schlusswort und Danksagung

Schlusswort- Diese Arbeit hat mir Spaß gemacht. Ich bekam die Chance, mich in ein für mich sehr neues Feld zu begeben, der Marinen Mikrobiologie. Wenn man wie ich Meerskunde studiert hat, so wird man im Hauptstudium nur sehr peripher mit der Mikrobiologie in Kontakt gebracht. Eigentlich sind mir aus dem damaligen zweiwöchigen Praktikum "Marine Mikrobiologie", welches einen Teil des meereskundlichen Großpraktikums in Kiel darstellte, im Wesentlichen zwei Dinge im Gedächtnis geblieben: erstens, die sich ständig wiederholenden Lieblingsworte unserer Praktikumsbetreuerin: "Sofort Abfackeln!", womit sie die Sterilisation der Impföse mit Hilfe einer Bunsenbrennerflamme meinte; und zweitens, die mangelnden zoologischen Kenntnisse unseres Mikrobiologie Professors, der meine Ratte, die ich öfters mit in den Unterricht zu bringen pflegte, für einen Hamster hielt. Damals erschien mir der Gedanke, sich mit Mikroben zu beschäftigen, gänzlich unmöglich. Meine Diplomarbeit machte ich über Aasfresser in der Arabischen Tiefsee, ganz entsprechend meiner Leidenschaft für die Meereszoologie. Da ich gerne zur See fahre, nutzte ich die Gelegenheit, nach Abgabe meiner Diplomarbeit noch einmal als studentische Hilfskraft mit auf Ausfahrt zu gehen. Es ging damals zum Hydratrücken vor Oregon. Dies war meine erste Konfrontation mit Methan, wenn man mal von dem Gasherd der Gaststätte meiner Großeltern absah. Ich begann, mich für dieses weiße Eis zu interessieren, das man einfach so anzünden konnte. Zugegeben, die Sedimentproben, die wir bargen, hatten nicht gerade einen charismatischen Geruch. Aber immerhin wurden diese Methanquellen am Meeresgrund von Muscheln besiedelt. Also hatte es doch entfernt etwas mit Zoologie zu tun? Im Sommer 2000 erfuhr ich dann, dass am MPI in Bremen eine Doktorandenstelle zum Thema "Anaerobe Methanoxidation" ausgeschrieben war. Zuerst zögerte ich.....Mikrobiologie....ich? Dann hellte wieder die Begeisterung für das brennende Eis auf. Als ich Antje Boetius, die ich schon von früheren Expeditionen kannte, endlich zielsicher auf die Stelle anschrieb, schrieb sie mir zurück: "Tina, du weißt aber, dass das nichts mit Tieren zu tun hat und du ne Menge Chemie pauken musst?". Ich holte ein paar mal tief Luft und antwortete "Ja, mich interessiert das und ich will das machen!". Auch Bo Jørgensen erkannte die Herausforderung für mich, in ein neues Thema einzusteigen, aber schien relativ unbesorgt: "Viele Menschen, die hier her gekommen sind, haben sich in eine neue Materie eingearbeitet. Das ist durchaus möglich." So kam ich schließlich ans MPI und habe es bis heute nicht bereut. Meine Doktorandenzeit war eine schöne Zeit, die ich mit einer Menge Menschen verbinde, denen ich im Folgenden danken möchte.

Danksagung- Zuerst einmal danke ich natürlich Antje Boetius und Bo Barker Jørgensen für die Vergabe des Themas und das Vertrauen, das sie in mich hatten. Antje danke ich für ihre offene, herzliche Art, für ihren Humor und für ihr Wissen, das sie an mich weitergab in punkto Mikrobiologie wie auch zu allen anderen alltäglichen Dingen zum Thema "wie lebt es sich als WissenschaftlerIn". Vor allem möchte ich ihr danken, dass sie bei allem Termindruck immer noch Zeit für mich fand. Bo möchte ich ebenfalls für seine herzliche Art und für die Unterstützung meiner Arbeit in jeglicher Form sowie den guten Ratschlägen beim Verfassen der Manuskripte danken.

Als Nächstes möchte ich meinen unmittelbaren Kollegen in und um das MUMM Projekt herum danken, mit denen ich eine sehr kreative Zusammenarbeit hatte. An erster Stelle ist da Katja Nauhaus zu nennen. Katja und ich sind während unserer Doktorarbeiten zu einem echten syntrophen Konsortium zusammengewachsen. Wobei ich nicht weiß, wer methanotroph ist und wer Sulfat reduziert. Neben einer hervorragenden Zusammenarbeit ist daraus auch noch eine Freundschaft entstanden. Für weitere gute Zusammenarbeit und Unterstützung innerhalb von MUMM danke ich Imke Müller, Markus Hartmann, Martin Krüger, Katrin Knittel, Tina Lösekann, Armin Gieseke und Marcus Elvert.

Für eine gelungene wissenschaftliche Zusammenarbeit außerhalb des MUMM-Projektes danke ich Jens Kallmeyer, Jutta Niggemann, Wiebke Ziebis, Paul Wintersteller, Carsten Schubert und Klaus Wallmann sowie den Co-Autoren des Science Papers.

Für technische Unterstützung jeglicher Art im und ums Labor herum danke ich Heiko Löbner, Astrid Rohwedder, Sabine Knipp, Tomas Wilkop und Jörg Wulf. Vielen Dank an Tim Ferdelman und an das TA Büro, insbesondere an Kirsten Neumann, Swantje Lilienthal und Gabi Klockgether, für Hilfestellungen bei Problemen mit allmöglichen Geräten.

Für die technische Unterstützung und wissenschaftliche Zusammenarbeit auf meinen vielen Seereisen möchte ich mich besonders bedanken bei Fabian Jakobi, Julia Polanski, Marion Kohn, Matthew Erickson, Wolfgang Queisser, Asmus Petersen, Bernhard Bannert, Thorsten Schott, Klaus Steffen, Jens Greinert, Fritz Abegg sowie den Fahrtleitern Olaf Pfannkuche, Gerhard Bohrmann, Peter Linke, Toni Eisenhauer, Walter Michaelis und Dierk Hebbeln. In diesem Zuge sei auch herzlichst der Crew von FS "Sonne", "Professor Logachev" und "Littorina" für ihre Hilfe an Bord gedankt.

Ich danke Uwe Rabsch für die Beherbergung im Isotopenlabor am Institut für Meereskunde in Kiel. Vielen Dank an Ulrike Tietjen für ihre zuverlässige Unterstützung in punkto Flugbuchung und anderen organisatorischen Dingen. Für verschiedenste Dinge des

alltäglichen Lebens am MPI danke ich Waltraud Sundag, Bernd Stickford, Olaf Gundermann, Carsten Witt, Manfred Schlösser, Axel Krack, Volker Meyer, Paul Färber und der Verwaltung.

Für die Durchsicht meiner Arbeit danke ich Marcus Elvert, Niko Finke, Jochen Nüster, Nina Knab und Matthias Seaman.

Niko Finke danke ich für die schöne Zeit in unserem Büro, den vielen Gesprächen, die über die Arbeit hinaus gingen und für die Freundschaft, die ich gewonnen habe. Meinem Mann, Steffen Böhme, danke ich für seine Unterstützung während meiner ganzen Doktorarbeit, für seine Geduld, wenn es abends mal später wurde, für die Einsamkeit, die er ertragen hat, wenn ich auf See war und nicht zuletzt sein für sein Computer und Grafik KnowHow, das mir oft, insbesondere beim Layout dieser Arbeit, aus der Klemme geholfen hat. Meinen geliebten Eltern und meiner Großmutter danke ich für ihre Unterstützung in jeglicher Form und für die schönen Wochenenden mit ihnen. Kater Mauzi sei für die unverbesserlichen Störungen beim Schreiben gedankt, die mich auch mal ans Pausemachen erinnerten.

Vermutlich habe ich trotzdem einige Menschen vergessen. In diesem Sinne: Danke an alle, die meine Doktorandenzeit in irgendeiner Weise unterstützt und/oder verschönert haben.

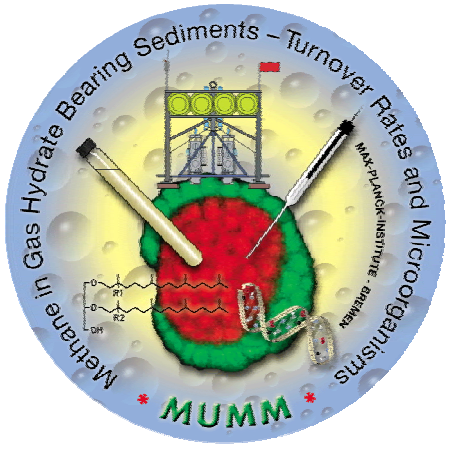

Erklärung

Hiermit versichere ich, dass ich die vorliegende Arbeit

1) ohne unerlaubte fremde Hilfe angefertigt habe,
2) keine anderen, als die von mir angegebenen Quellen und Hilfsmittel benutzt habe, und
3) die den benutzen Werken wörtlich oder inhaltlich entnommenen Stellen als solche kenntlich gemacht habe.

Bremen, den 19.12.2003

Tina Treude